Advanced separation and anaerobic digestion technologies for value-added bioproducts and biofuel from pulp and paper mill wastes.

BY

Alnour M. A. Bokhary

Faculty of Natural Resources Management

Lakehead University

Thunder By, Ontario

January 2021

Advanced separation and anaerobic digestion technologies for value-added bioproducts and biofuel from pulp and paper mill wastes.

BY

Alnour Mahmmoud Alnour Bokhary

A thesis submitted to the Faculty of Graduate Studies, Lakehead University - in the partial fulfillment of the requirements for the degree of doctor of philosophy in Forest Sciences.

Faculty of Natural Resources Management

Lakehead University

Thunder By, Ontario

January 2021

Supervisor: Dr. Baoqiang Liao

Supervisor: Dr. Mathew Leitch

Committee Member: Dr. Eltayeb Mohamedelhassan

Abstract

In the first research project, the extraction of hemicellulose from the process water and synthetic hydrolyzate using liquid-liquid extraction (LLE) was examined. Specifically, the effects of the main experimental variables (the type of solvent, hydrolyzate to solvent volume ratio, and pH) on extraction performance were explored. The tested solvents showed varying affinity and selectivity to recover hemicellulose. It was found that the hemicellulose extraction efficiency of n-hexane (71.03%) and tributyl phosphate (TBP) (72.34%) was higher than that of 1-butanol (62.36%), and toluene (67.03%) at a solvent: hydrolyzate volume ratio of 1:3. A pH value of 4.3, a phase ratio of 1:3 mL/mL, and an extraction time of 30 min were considered optimal conditions for hemicellulose extraction.

In the second study, the thermophilic submerged anaerobic membrane bioreactor (ThSAnMBR) technology was used for pulp and paper primary sludge treatment, and both biological and membrane performance were evaluated. The biological performance was studied in terms of biogas production, solids reduction, chemical and structural changes of the digestate, and permeate quality under various operating conditions. While the effect of primary sludge on the membrane performance and fouling was systematically investigated. Several experimental parameters were investigated including solids retention time (SRT) (32-55 days), hydraulic retention time (HRT) (3-8 days), organic loading rates (OLRs) (2.5-6.8 kg-COD/m^3d), temperature (50±1°C), membrane fouling and cleaning frequency. Membrane performance was evaluated by monitoring its flux and corresponding transmembrane pressure as well as changes in its chemical and physical properties resulting from operating conditions using Fourier transform infrared (FTIR), scanning electron microscopy (SEM), energy-dispersive X-ray analyzer (EDX), contact angle, and pore size measurement.

The tested conditions have shown varying biogas productivity and fouling propensity, and it can be concluded that the longer the SRT and the lower the OLR, the higher is the biogas yield. At the optimum SRT of 55 d and hydraulic retention time of 5 d, biogas yield of 153.8 m^3 biogas/ tonne mixed liquor suspended solids $(MLSS)_{removed}$ was achieved with an average methane content of 56±4. Under various OLRs, stable biogas productions were obtained, and the best results were achieved with lower OLR (2.5 kg-COD/m^3 d) and higher HRT (8d), at biogas yields of 189 L biogas/kg MLSS fed. However, it was found that the biogas production and sludge biomass degradation decrease when the organic loading rate increases, and no difference was observed in biogas production when the primary sludge was co-digested with process water under OLR of 2.5 kg-COD/m^3 d and HRT of 8 d compared to the digestion of the primary sludge alone under same conditions. The reduction ratio of the sludge biomass ranged from 28.9 to 54.9 % in this study, depending on the applied conditions. Based on the chemical and structural change analysis, the digestate contained more lignin, while the nitrogen concentration decreased with increasing

digestion time. The permeates had much-reduced metal ions concentrations, and the values for most of the elements did not vary greatly with the change in the organic loading rate. Permeate chemical oxygen demand (COD) values have fluctuated to some extent with OLRs and SRTs and ranged between 2.40±0.79 mg/L and 0.32±0.11 mg/L. In these experiments, digestate properties under different operating conditions of ThAnMBR were also evaluated.

The membrane had stable performance and that the primary sludge showed low tendencies for membrane fouling. However, the degree of fouling increases with increasing SRT, while mixed liquor suspended solids (MLSS) concentration was the predominant factor affecting membrane performance. This result indicates that OLR of less than 2.5 kg COD/m^3d, HRT of 8d, and solids retention time (SRT) of 32d should be maintained to achieve stable membrane performance. High-resolution SEM images reveal distinct differences in the pore morphology between the virgin and used membranes indicating the effect induced by the operating conditions. Fouling characterization results, using EDX, XPS, and FTIR analysis, revealed the gel layer is the predominant fouling mechanism during the treatment of primary sludge from the pulp and paper industry and accounts for most of the total membrane resistance. Overall, the primary sludge from pulp and paper mill can be treated successfully by ThSAnMBR for methane production with stable membrane performance and high treatment efficiency. However, the addition of nutrients should be considered to compensate for the lack of phosphorous and nitrogen content in pulp and paper mill sludge.

Keywords: Biogas production; thermomechanical pulping; primary sludge, anaerobic digestion; membrane bioreactor, pulp and paper mill sludge.

Acknowledgments

Foremost, I would like to express my deepest appreciation to my supervisors Dr. Baoqiang Liao and Dr. Mathew Leitch for their guidance, insightful feedback, continuous support, and encouragement. Besides my supervisors, I would like to thank my thesis committee Dr. Eltayeb Mohamedelhassan, for his constructive feedback and comments.

I would like to thank my research group at Dr. Liao's lab, Lakehead University for making this work possible through their fruitful discussion. Special thanks to Dr. Meijia Zhang who helped me with several analytical protocols.

I would like to extend my sincere thanks to Dr. Guosheng Wu for running SEM/EDX and XPS tests, and Dr. Pedram Fatehi for allowing us to use some of his lab equipment. As well, the assistance provided by Dr. Weijue Gao at Pedram Laboratory, Lakehead University for hemicellulose and lignin measurements is greatly appreciated.

I additionally want to thank the personnel at Resolute Forest Products, Paper Mill in Thunder Bay, Ontario for providing us with the primary sludge and process water.

Finally, I want to thank my family and friends for their enduring support and encouragement.

List of included papers and publications.

This dissertation is based on the following papers. The study period included two different research projects, one dealing with biogas production from thermomechanical pulp primary sludge, and the other dealing with liquid-liquid extraction technology for bioresource recovery from pulp and paper effluents. These papers are arranged according to the order in which they appear in the thesis.

I. **Bokhary**, A., Leitch, M. and Liao, B.Q., 2020. Liquid–liquid extraction technology for resource recovery: Applications, potential, and perspectives. Journal of Water Process Engineering, 101762.

II. **Bokhary**, A., Leitch, M. and Liao, B., 2021. Recent Advances in Bioconversion of Pulp and Paper Mill Sludges to Biofuels: Potentials and Constraints. Will be submitted to Biofuels, Bioproducts and Biorefining.

III. **Bokhary**, A., Leitch, M., Gao, W.J., Fatehi, P. and Liao, B.Q., 2019. Separation of hemicelluloses and lignins from synthetic hydrolyzate and thermomechanical pulp mill process water via liquid-liquid extraction. Separation and Purification Technology, 215, 508-515.

IV. **Bokhary**, A., Leitch, M. and Liao, B., 2021. Thermophilic anaerobic membrane bioreactor for pulp and paper primary sludge treatment: Effect of solids retention time on the biological performance. Submitted to Biomass & Bioenergy.

V. **Bokhary**, A., Leitch, M. and Liao, B., 2021. Thermophilic anaerobic digestion of pulp and paper primary sludge using a submerged AnMBR: Effect of solids retention time on the membrane performance. Will be submitted to Science of the Total Environment.

VI. **Bokhary**, A., Leitch, M. and Liao, B., 2021. Thermophilic anaerobic membrane bioreactor for pulp and paper primary sludge treatment: Effect of organic loading rate on the biological performance. Journal of clean technologies and environmental policy.

VII. **Bokhary**, A., Leitch, M. and Liao, B., 2021. Thermophilic submerged anaerobic membrane bioreactor for pulp and paper primary sludge treatment: Membrane performance and fouling characteristics. Will be submitted to Journal of Environmental Chemical Engineering.

Additionally, the following publications were also generated within the time frame of the PhD but not included in the thesis. They are arranged chronologically.

I. **Bokhary**, A., Maleki, E., Hong, Y., Hai, F.I. and Liao, B., 2020. Anaerobic membrane bioreactors: Basic process design and operation. In: Ngo H., Guo W., Ng H., Mannina G., Pandey A., (ed) Current Developments in Biotechnology and Bioengineering, 1st edn. Elsevier, 25-54.

II. Maleki, E., **Bokhary**, A., Leung, K. and Liao, B.Q., 2019. Long-term performance of a submerged anaerobic membrane bioreactor treating malting wastewater at room temperature (23±1° C). Journal of Environmental Chemical Engineering, 7 (4), 103269.

III. Liao[1], Y., **Bokhary**[1], A., Maleki, E. and Liao, B., 2018. A review of membrane fouling and its control in algal-related membrane processes. Bioresource Technology, 264, 343-358.

IV. Maleki, E., **Bokhary**, A. and Liao, B.Q., 2018. A review of anaerobic digestion bio-kinetics. Reviews in Environmental Science and Bio/Technology, 17 (4), 691-705.

V. **Bokhary**, A., Tikka, A., Leitch, M. and Liao, B., 2018. Membrane fouling prevention and control strategies in pulp and paper industry applications: A review. Journal of Membrane Science and Research, 4 (4), 181-197.

VI. Duncan[1], J., **Bokhary**[1], A., Fatehi, P., Kong, F., Lin, H. and Liao, B., 2017. Thermophilic membrane bioreactors: a review. Bioresource Technology, 243, 1180-1193.

Table of Contents

List of Figures

List of Tables

Chapter I

Introduction

1.1. Background

Effluents and waste streams in paper and pulp mills (PPMs) are often problematic wastes and need appropriate management. Traditionally, most waste streams are burned in recovery boilers to generate mill heat sources (e.g., black liquor and primary sludge) or are discharged into wastewater streams for aerobic biological treatment (Van Heiningen, 2006). The effluent in pulping industry has a very low heating value due to its high-water content (70-90%), thus, it should be properly dewatered before the incineration process (Kehrein et al., 2020). Also, the aerobic treatment of this waste generates a large amount of sludge that needs further treatment and disposal along with high energy consumption due to the aeration requirements. In contrast, waste streams of paper and pulp mills contain valuable compounds and are not fully explored and utilized. During the pulping processes, a substantial amount of short fibers, lignin, and hemicellulose are rejected, dispersed, or dissolved in the process water (Sundblom, 1999; Smook, 2002). While it has been reported that the yield of sludge from the paper mill is five to six times higher than that of the municipal wastewater treatment plant of the same size (Wu and Zhou, 2011). Besides, sludge from PPMs contains a high percentage of organic matter (65–97 % of volatile solids) compared to sewage sludge (59–68 % volatile solids) (Elliott and Mahmood, 2012).

The organic molecules contained in PPMs effluents and waste streams can be economically recovered into various useful biomaterials with high added value through the development of effective separation technologies, such as liquid-liquid extraction. The use of liquid-liquid extraction was considered a potential feasible technique for high purity requirements (Hassan et al. 2013). It is also a simple and clean process, plus the solvents that have been used can be easily recovered (Cruz et al. 1999). Plenty of applications for lignins and hemicelluloses have been proposed recently. For example, hemicelluloses have been found to be an excellent candidate for oxygen barrier materials in food packing, hydrogel, emulsion stabilizers for beverages (Ebringerová 2005), while lignin has found potential applications as carbon fibers, adhesive materials, activated carbon (Qiu et al. 2005). Alternatively, the potential energy can be recovered through the development of novel technologies, such as anaerobic digestion technology. Anaerobic membrane bioreactor (AnMBR) has been considered as the next generation of technology for sustainable wastewater and organic sludge management and has been successfully applied in several industrial wastewater sites around the world (Lin et al., 2012; Dvořák et al., 2016). MBR features a higher concentration of cells in the reactor and reduced generation of solid biomass (Bokhary et al., 2020). The use of the membrane ensures complete retention of the slow-growing methanogens and allows for the decoupling of SRT and HRT. This

may increase biogas yield compared to conventional processes, while providing a high permeate quality for reuse.

This research investigated the feasibility of the liquid-liquid extraction technique for hemicellulose separation and purification from thermomechanical pulp (TMP) mill process waters. The effect of the major experimental variables on hemicellulose extraction was tested, and the optimal extraction conditions were identified. While biogas production from the primary sludge of TMP was evaluated under different digestion conditions using a thermophilic submerged anaerobic membrane bioreactor (ThSAnMBR) technology.

1.2 Research objectives

This research focused on the advanced separation and anaerobic digestion technologies. More specifically, the feasibility of the liquid-liquid extraction technique for hemicellulose recovery and purification from TMP mill process water and synthetic hydrolysate was studied. The effects of various experimental variables on hemicellulose and lignin extraction were tested (e.g., hydrolysate to solvent volume ratio; extraction time; solvent concentration; PH; and solvent type), and the optimal extraction conditions were identified. In the second research project, the effect of various AnMBR operating conditions on the treatment of pulp and paper mill primary sludge (PPMPS) and biogas production were investigated. To achieve the overall goal of the second project, the following specific objectives were addressed: (1) the effect of different SRTs and HRTs on both biological and membrane performances was evaluated, (2) The optimal SRT and OLR for both biogas production and membrane operation were identified, (3) membrane fouling during PPMPS treatment was characterized, (4) up-to-date critical literature review on how the main operational parameters affect the digestion performance of primary sludge was provided.

1.3 Research novelty

The extraction of carbohydrates from an aqueous media into an immiscible organic solution using solvent extraction is still lacking in the literature, and to our best knowledge, no study has focused on the extraction of hemicelluloses from process waters of thermomechanical pulp (TMP) mills using such techniques. Also, thermophilic anaerobic membrane bioreactor (ThAnMBR) is employed for the first time to treat the primary sludge from pulp and paper mill for biogas production and solids reduction. There is no study specifically done on the primary sludge treatment from thermomechanical pulping using the anaerobic membrane bioreactor.

1.4 Thesis Structure

The dissertation is divided into eight chapters in the form of scientific manuscripts. **Chapter I** includes a general introduction about waste streams from pulp and paper industry, membrane bioreactor, and liquid-liquid extraction. **Chapter II** involves a literature review that covered the two research projects. Literature

review I summarized liquid-liquid extraction technology for resource recovery, while literature review II critically reviewed bioenergy production from pulp and paper mill sludge. **Chapter III** covered separation of hemicelluloses and lignin from synthetic hydrolysate and thermomechanical pulp mill process water via liquid-liquid extraction, **Chapter IV and V** covered the effect of solids retention times (SRTs) on biological and membrane performance during the treatment of the primary sludge, respectively. While **Chapter VI and VII** covered the influence of hydraulic retention times (HRTs) on biological and membrane performance, respectively. Finally, **Chapter VIII** includes the conclusion and recommendations.

References

[1] Bokhary, A., Maleki, E., Hong, Y., Hai, F.I., Liao, B., Anaerobic membrane bioreactors: Basic process design and operation. In: Ngo, H. H., Guo, W., Ng, H. Y., Mannina, G., Pandey, A., (Eds.), Current developments in biotechnology and bioengineering, Elsevier, Amsterdam, 2020, p. 25-54. https://doi.org/10.1016/B978-0-12-819852-0.00002-6.

[2] Ebringerová A., 2005. Structural diversity and application potential of hemicelluloses. In Macromolecular Symposia, Wiley- VCH Verlag. 232, 1-12. https://doi.org/10.1002/masy.200551401.

[3] Elliott, A., Mahmood, T., 2012. Comparison of mechanical pretreatment methods for the enhancement of anaerobic digestion of pulp and paper waste activated sludge. Water Environ. Res. 84, 497-505. https://doi.org/10.2175/106143012X13347678384602.

[4] Kehrein, P., van Loosdrecht, M., Osseweijer, P., Garfí, M., Dewulf, J. Posada, J., 2020. A critical review of resource recovery from municipal wastewater treatment plants–market supply potentials, technologies and bottlenecks. Environ. Sci. Water Res. Technol. 6, 877-910. https://doi.org/10.1039/C9EW00905A.

[5] Dvořák, L., Gómez, M., Dolina, J., Černín, A., 2016. Anaerobic membrane bioreactors—a mini review with emphasis on industrial wastewater treatment: applications, limitations and perspectives, Desalination Water Treat. 57, 19062-19076. https://doi.org/10.1080/19443994.2015.1100879.

[6] Lin, H., Gao, W., Meng, F., Liao, B.Q., Leung, K.T., Zhao, L., Chen, J., Hong, H., 2012. Membrane bioreactors for industrial wastewater treatment: a critical review. Crit. Rev. Environ. Sci. Technol. 42, 677-740. https://doi.org/10.1080/10643389.2010.526494.

[7] Qiu, X.Q., Lou, H.M., Yang, D.J., Pang, Y.X., 2005. Research progress of industrial lignin modification and its utilization as fine chemicals [J]. Fine Chemicals.

[8] Smook, G.A., 2002. Handbook for Pulp and Paper Technologists. 3rd Ed. Angus Wilde Publications Inc., Vancouver. 46–65.

[9] Sundblom, J., 1999. Mechanical pulping, papermaking science and technology. Fapet Oy Published, Helsinki, Finland.

[10] Van Heiningen., A., 2006. Converting a kraft pulp mill into an integrated forest biorefinery. Pulp and Paper Canada, 107, 38-43.

[11] Wu, F., Zhou, S., 2011. Anaerobic biohydrogen fermentation from paper mill sludge. J. Energ. Eng. 138, 1-6. https://doi.org/10.1061/(ASCE)EY.1943-7897.0000054.

Chapter II

Literature Review

1. Literature Review I

Liquid-Liquid Extraction Technology for Resource Recovery: Applications, Potential, and Perspectives

Abstract:

Biorefinery of biomass for value-added products and biofuel plays an important role in the sustainable global bioeconomy. Among various biorefinery processes and platforms, effective separation technologies are key to the economical production of value-added products and biofuel from biomass at a low cost. Amid the several separation technologies available, liquid-liquid extraction (LLE) has been shown to play a vital role in the separation and purification of bioproducts in biomass biorefining processes and has demonstrated many advantages, as compared to other separation technologies. LLE has become a potential technology for biomass biorefinery. Lab-scale and pilot-scale studies of LLE technology in biorefinery have been reported. This review focuses on the applications of LLE technologies in various processes of biomass biorefinery, including extraction and separation of biochemical materials and biofuels from aqueous mixtures and removing fermentation inhibitors from biomass hydrolysates. This review paper aims to offer an up-to-date discussion of the applications, recent progress, potential, and future research directions of LLE in biomass biorefineries. LLE technology is a promising separation technology for biomass biorefineries with a bright future.

Keywords: liquid-liquid extraction, solvent, biorefinery, recovery, separation, biomass.

---

1. Introduction

Bio-based economy, and in particular, the emergence of different biorefining strategies, is one of the central pillars of sustainable economic growth. Biorefineries can support the development of various sustainable paradigms for the bioeconomy, compared to individual processes. In respect of product diversification and the sustainability perspective, the concept of the biorefinery offers a wide range of economic, social, and environmental benefits. Biorefineries involve the processing of biomass feedstocks to produce biofuels, platform chemicals, biopolymers, other value-added biomaterials, and have the potential to introduce new bioproducts and processes (Novotny and Nuur 2013). Among the biorefinery-based industries, pulp and paper mills have now transformed themselves into a biorefinery platform to produce new materials alongside the traditional pulp products (Moshkelani et al., 2013). However, developing a bioeconomy or biorefinery process is a challenge that calls for both social and technological changes. Such a transition necessitates the adoption of various advanced separation technologies that deliver the end products in a usable form.

Bokhary, A., Leitch, M., Liao, B.Q., 2020. Liquid–liquid extraction technology for resource recovery: Applications, potential, and perspectives. Journal of Water Process Engineering. 101762.

Within this framework, several separation methods have been investigated for biomaterial, biofuel, and chemical recoveries from the aqueous effluent of biomass raw materials. Accordingly, various review papers have been published dealing with the separation technologies in biorefineries, including membrane technology (Bokhary et al., 2017), phase-change separations (Kiss et al., 2016), and adsorbent-based separations (Nguyen et al., 2017). Huang et al. (2008) reviewed the key separation technologies related to biorefining processes with some overview of extractive fermentation. Kiss et al. (2016) presented examples illustrating the impact of well-designed separation technologies on biorefining economic viability. However, no review has yet been carried out in detail to summarize the findings of the liquid-liquid extraction (LLE) or solvent extraction (SE) in biorefining processes.

Due to the need to retrieve products from more complex matrices and higher product purity requirements, LLE has been utilized in a broad range of applications to recover desirable materials or remove unwanted impurities from liquid mixtures. LLE is a mass transfer process in which a solute transfer between two immiscible liquids typically an aqueous solution and an organic liquid. The solvent usually shows a preferential affinity towards one or more of the constituents in the liquid mixture. After the two phases are brought into contact, the product of interest, usually in an aqueous solution, will begin to partition between the two phases. Then, the separated material establishes an equilibrium distribution between the immiscible solvents, after which the two phases can be separated because of their immiscibility (Bo and Jianguo 2013). LLE can be performed in a single contact batch apparatus or in a multi-stage extraction procedure, and in direct contact (using contactors), or indirect contact (using porous membranes) (Vane 2008). Sometimes, these extraction techniques are called co-current (often used to recover or remove a component from a mixture) or counter-current (a common fractionation procedure). Several factors need to be considered in the designing of an extraction process. These factors may include the selection of appropriate extractant, solvent capacity for the partitioning of the product, solvent selectivity for the target product over other constituents, extraction efficiency, and distribution coefficient, (K_D).

LLE is an old, well-established process and has been practiced in rare earth elements separation and purification (Mishra 2019; Bourgeois et al., 2020), carboxylic acids recovery and concentration (Sprakel and Schuur 2019), edible oils refining and de-acidification (Gonçalves et al., 2016). It has been extensively applied in petroleum, pharmaceutical, biochemical industries, and industrial waste treatment (Rydberg et al., 2004). In LLE, various types of solvents have been used, including physical solvents, reactive solvents, and ionic liquids (ILs). Variations in solvent properties and type have resulted in significant differences in the distribution ratios and selectivity of the extracted substances. LLE approaches have also been commercially used in the field of metallurgy and pharmaceutical fractional extractions for many decades (Kislik 2012; El-Nadi 2017), so there is a great deal of knowledge available from these areas. Therefore,

this knowledge can be transferred and applied to the recovery and purification of organic molecules from pulp and paper wastewater streams and biomass hydrolysates. In biorefinery, some portion of the biomass is utilized, while a large quantity of organic materials would be lost in the various waste streams (e.g., process water, black liquor, spent sulfite liquor, pre-hydrolysis liquor, and wastewater). These organic molecules can be recovered from waste streams and used to produce value-added materials and bioenergy.

But although the LLE is a mature separation technology, the applications of LLE in biomass biorefinery is relatively new and has become a potential separation technology for value-added products and biofuel recovery and purification. Usually, the wastewater resulting from the pulping process and biomass hydrolysis is heterogeneous (a solid/liquid mixture), containing a group of compounds like cellulose, hemicellulose lignin, and wood extractives. These compounds can be recovered from wastewater streams with polar or non-polar solvents, thus the use of LLE could be advantageous. In biomass biorefinery, LLE has been used in the recovery of hemicelluloses and monomer sugars from aqueous effluents (Aziz et al., 2008; Bokhary et al., 2019), recovery of biofuels (e.g., bioethanol, biobutanol, and 2, 3-butanediol) from fermentation broths (Minier and Coma 1981; Harvianto et al., 2018; Verma et al., 2018), and extraction of carboxylic acids from biomass hydrolysates (Um et al., 2011; Cebreiros et al., 2017). It has been utilized also in the removal of inhibitors from dilute mixtures (Tomek et al., 2015; Zautsen et al., 2009) and fractionation of lignin/lignosulphonates from Kraft and spent sulfite liquors (Jääskeläinen et al., 2017; Park et al., 2018). Different liquid-phase extraction technologies have been employed in biorefinery processes such as the selective dissolution of solid lignin (Melro et al., 2018), selective precipitation of dissolved lignin (Jääskeläinen et al., 2017), fractional precipitation of lignin (Cui et al., 2014), aqueous biphasic systems for hydroxylmethylfurfural (HMF), (Shimanouchi et al., 2013; Román-Leshkov et al., 2007), micellar extraction of enzymes (Kilikian et al., 2000), extractive fermentation of butanol/ethanol (Huang et al., 2008; Gonzalez-Penas et al., 2014), and polyethylene glycol (PEG)–salt aqueous two-phase systems (ATPS) for proteins and enzymes (Glyk et al., 2015). PEG–salt ATPS systems and ionic liquid extraction seem to be emerging efficient LLE technologies for the downstream processing of numerous biomolecules purification and fractionation, but these are still in-development technologies. Figure 2.1.1 shows a typical LLE standard extraction process of a single stage. LLE application in biorefinery processes is illustrated in Figure 2.1.2. Both standard extraction and fraction extraction of LLE designs are used in the downstream processing of biorefinery. This review paper brings together scattered data on the application of LLE in biomaterials and bioenergy separation and offers an up-to-date discussion of the recent progress and future research directions of LLE in biomass biorefineries.

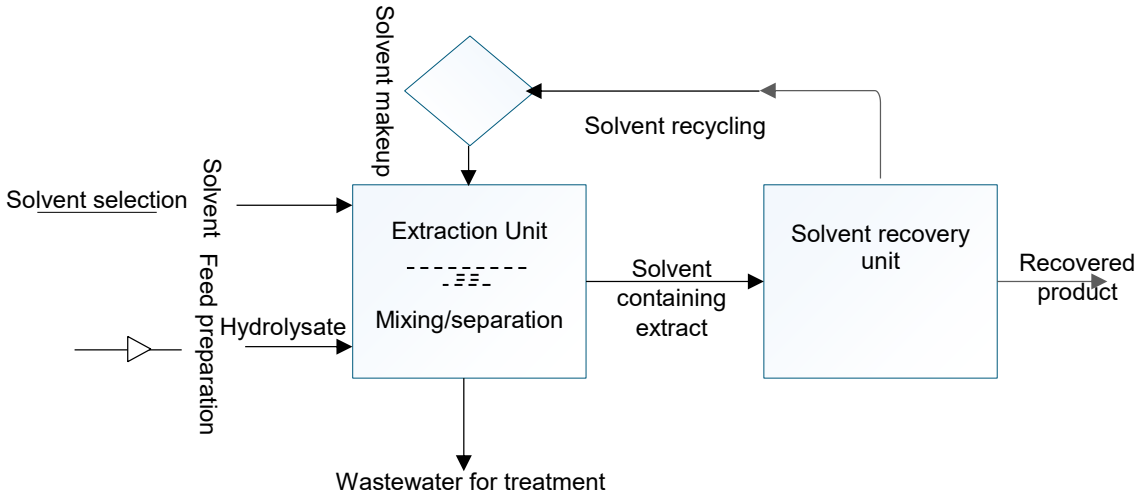

Figure 2.1.1: Typical liquid-liquid extraction unit

2. Applications of Liquid-Liquid extraction in Biomass Biorefinery

As illustrated in Figure 2.1.2, LLE has applied in biomass biorefining processes in components fractionation, product recovery and purification, inhibitors removal, biofuel production, and purification. Depending on the applied pretreatment, various product and by-product streams will be generated from the processed biomass. These streams contain valuable compounds and can be recovered or even fractionated using LLE technology. For example, lignin from black liquor and spent sulfite liquor can be fractionated by organic solvents via successive extraction based on its molar masses and solubility. The sequential solvent fractionation process can result in three or more lignin fractions (Fractions 1 - 3) using different organic solvents (SE 1-3) or one solvent with different concentrations (Figure 2.1.2). A similar approach can be used to fractionate sugar from prehydrolysis liquor (PHL) and bio-oil (scheme 3). In the second scheme of Figure 2.1.2, the microbial inhibitors can be removed from sugars rich biomass hydrolysate by a specific solvent (SE-1). Then the detoxified sugars can be fermented to produce biofuel and the resulting product can be purified using a certain solvent (SE-2). In bioethanol production, LLE can be either coupled with the fermentation process (extractive-fermentation) or proceeded as a downstream process. In the final scheme of Figure 2.1.2, the process water from biomass treatment can be first treated (SE-1and SE-2) to recover the lignin with different fractions followed by the acid hydrolysis of the resulting sugar stream to generate furfural, which subsequently can be purified by an organic solvent (SE-1). To date, most researchers have focused on laboratory-scale studies with a few works done on the pilot-scale level. Among the pilot-scale investigations, LLE has been used in enzyme recovery (Skovgaard et al., 2014), ethanol separation (Gyamerah and Glover 1996; Quijada-Maldonado et al., 2013), acetic acid extraction (Aghazadeh and Engelberth 2016; Weeranoppanant et al., 2017), and recycling of phenol from wastewater (Jiang et al., 2003). This research can lead to scalable processes when the best extractants and optimum extraction conditions have been established. The progression of LLE applications in biorefineries towards

commercial deployment is indicated by the Technology Readiness Level (TRL), as shown in Table 1-7. The following sections summarize and discuss the applications of LLE and its research progress in biomass biorefining.

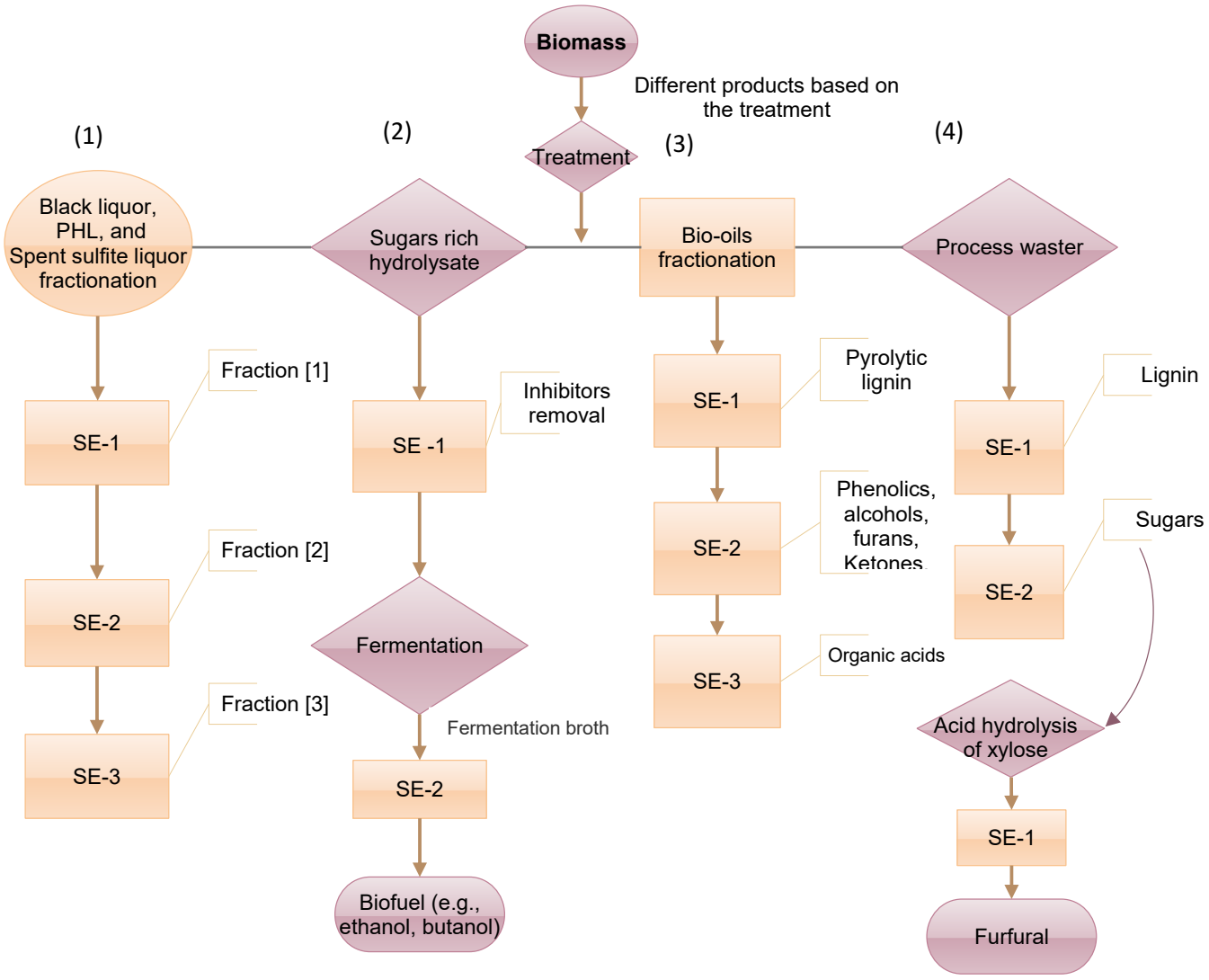

Figure 2.1.2: Application of liquid-liquid extraction in biorefinery processes

2.1. Hemicelluloses and monomer sugars recovery

During the pulp production process, the hemicelluloses and lignin are extracted from the wood chips and eventually end up in the black liquor (BL) or pre-hydrolysis liquor (PHL). Traditionally, the organic molecules dissolved in the BL and PHL will be discharged into wastewater streams as wastes and need further aerobic biological treatment. Carbohydrates (cellulose/hemicellulose) from lignocellulosic biomass are important polymers. These polymers could be separated and transformed into various chemicals of added value. Hemicelluloses are an excellent feedstock for the production of hydrogels, xylitol, furfural, oxygen barrier film in packing materials, and an emulsifier stabilizer in food, as well as a source of sugars

(xylose) that can be fermented for bioethanol production (Ajao et al., 2018; Bokhary et al., 2018). However, the separation of sugars from black liquor or pre-hydrolysis liquor remains a difficult task due to the complexity of the extracted effluents. Various separation technologies have been involved in carbohydrate extractions (e.g., membrane technology and chromatographic separation). Nonetheless, relatively few studies considered the recovery of hemicellulose, sugar alcohols (xylitol, sorbitol, and inositols), and monomeric sugars from an aqueous feed to an immiscible or nearly immiscible solvent (Table 1).

John and Shu (2004) purified monomeric sugars from hydrolysate aqueous solutions using various boronic acid extractants in a single extraction stage. Compared to other tested boronic acids, naphthalene-2-boronic acid achieved the highest extraction ratio (> 80 %). However, boronic extractants are expensive and may create a barrier to economic feasibility for large-scale applications, so cheap alternative acids would be required. Mussatto et al. (2005) studied xylitol purification using different solvents (either ethyl acetate, chloroform, and dichloromethane) in a single contact batch process. Among the solvents used, ethyl acetate seems to be a very capable extractant to purify xylitol from fermented broth without xylitol losses. Hameister and Kragl (2006) developed a method for the selective extraction of carbohydrates from aqueous effluent. They investigated several organic solvents like n-hexane, butanol, methyl tertiary-butyl ether, or toluene. It has been demonstrated that recovery rates up to 40% can be achieved in a single-stage process. Recently, we demonstrated that hemicellulose could be extracted from the wood hydrolysate in a single-stage process, using n-hexane, toluene, tributyl phosphate (TBP), and 1-butanol. N-hexane accomplished the highest selectivity, followed by toluene, a pH change in hydrolysate, resulting in varying influences contingent upon the type of employed solvents (Bokhary et al., 2019). As reported in Table 2.1.1, the selectivity coefficients ranged between 0.6 and 8.7. A higher selectivity coefficient indicates a more concentrated product stream and an improved solvent ability to favor hemicellulose over other products from the feed stream. While the reported distribution ratio was in the range of 0.27–6.7. The distribution ratio (D) indicates the ratio of hemicellulose concentration in the organic phase to its concentration in the aqueous phase at equilibrium. A higher D value implies better hemicellulose extraction and less extractant utilization. Hemicellulose extraction efficiency (%E) in the range of 22– 98 % was reported and these values demonstrate the relative quantity of hemicellulose that moved from the aqueous solution to the organic phase using a certain solvent.

In considering the influence of temperature on extraction yield, Hameister and Kragl (2006) separated carbohydrates (glucose, lactose, and galactose) from an aqueous solution at different temperatures (20, 30, and 40 °C) and found that the highest extraction rate was obtained at 40 °C. However, the temperature beyond 40 °C led to the formation of unidentified by-products (Hameister and Kragl 2006). Table 2.1.1 summarizes hemicelluloses and monomer sugars isolation from aqueous solutions. Various solvents classes

are used, pure or in mixtures. Considerable variations are observed in reported results in terms of the sugar yields, purity, and selectivity (the amount of the hemicellulose extracted compared to the quantity of unwanted by-products). These variations can be attributed to the difference between extracting agents as well as the separation procedures (single-stage or several extraction steps, under favorable environmental conditions or unoptimized separation conditions). Sometimes, a single solvent may not achieve the purity of the desired product on its own, thus, the solvent needs to be mixed with another extractant, or the extraction process demands to be repeated (1–3 times) to meet the separation requirements. Carbohydrates and some of their derivatives have shown a low solubility in organic solvents. This makes sugars extraction via solvents from aqueous effluents an expensive process, especially for large-scale operations.

Table 2.1.1: A summary of hemicelluloses and monomer sugars recovery from aqueous feeds

Raw material	Extraction conditions	Results	TRL	Ref.
Eucalyptus kraft black liquor (BL)	Solvent: ethanol in ratios ranging from 0.2-12 L ethanol/L black liquor.	The recovery rates of pentosanes and lignin were 40% and 22 %, respectively.	2	(Caperos and Villar 1990)
Oligosaccharides from plant materials	Solvent: methanol and ethanol at 20 or 50 °C.	The reported recoveries were in the range of 46 – 98%.	1	(Johansen et al., 1996)
Eucalyptus wood hydrolysates	Solvent: chloroform, ethyl acetate, diethyl ether, trichloroethylene, and hexane, at r.t. for 6 h.	Concentrations of xylitol in the range of 16.2–18 g/l were obtained.	1	(Parajó et al., 1997)
Eucalyptus wood hydrolysates (Xylitol)	Solvent: diethyl ether, at r.t. Mixed 60 min.	Xylitol concentrations in the range 40–50 g/L were reported.	2	(Diz et al., 2002)
Monosaccharides (d-glucose, d-fructose, d-galactose.	Extractant: dihydroxyphenylborane and TOMAC, n-hexane, 1-octanol, at 30 °C.	The distribution ratio of glucose, d-fructose, and d-galactose was 6.7, 1.6, and 1.9, respectively.	1	(Matsumoto et al., 2003)
Sugar model solution and hydrolysates of bagasse	Extractants: isodecyl alcohol, boronic acids, and mine Aliquat® 336. Diluents: shellsol® 2046 or Exxal® 10, at 25 °C.	Naphthalene-2-boronic acid achieved the highest extraction ratio (> 80 %).	1	(John and Shu 2004)
Synthetic solution (xylose, glucose, and fructose)	Extractants: isodecyl alcohol, 3, 5-dimethyl phenyl boronic acid, and improved Aliquat® 336. Diluent: Exxal® 10, at 25 °C.	Xylose concentrated 4 times compared to the initial feed whereas the acid-soluble lignins concentration reduced by 90%.	1	(Griffin 2005)
Xylitol from fermented hemicellulosic hydrolysate	Solvent: ethyl acetate (EA), chloroform (CF) or dichloromethane (DCM).	Xylitol concentrations in the fermented broth were 37 g/l for EA, 35.6 g/l for CF, and 36 g/l for DCM.	1	(Mussatto et al., 2005)
Synthetic aqueous solution	Extractant: trioctylmethylammonium chloride and phenylboronate, dissolved in n-hexane and 1-octanol, at 30 °C.	Glucose and xylose extractability were higher than other tested sugars (fructose, arabinose, galactose, and mannose).	1	(Matsumoto et al., 2005)
Mono- and disaccharides from aqueous media	Solvent: methyl tertiary-butyl ether, butanol, toluene, or n-hexane, at 20, 30, and 40 °C, 30/120 min.	The carbohydrate recovery rates were 40%, and the selectivities ranged from 1.3 up to 875.4.	1	(Hameister and Kragl 2006)
Xylose and glucose from aqueous solution	Extractant: naphthalene-2-boronic acid and trioctylmethylammonium chloride. Diluent: 1-octanol and n-hexane, at r.t. Stirred for 5 h at 200 rpm.	Extraction percentages of xylose and glucose were 91 and 96%, respectively.	1	(Aziz et al., 2008)
Carbohydrate complex mixtures	Solvent: isopropanol, ethanol, n-butanol, and n-propanol, at 60 -100 °C.	The highest selective extraction was reported for lactulose sugar (81 wt. %).	2	(Montañés et al., 2008)

Ionic liquid biomass liquor (glucose, xylose, and cellobiose)	Extractant: naphthalene-2-boronic acid or phenylborinic acid. Diluents: n-hexane and 1-octanol, at 25 °C.	90% of monomeric and disaccharides can be extracted from the liquor.	1	(Brennan et al., 2010)
Xylitol from fermented broth	Solvent: ethyl acetate, chloroform, or dichloromethane, at 30 °C.	The distribution ratio was 0.27 for chloroform and 0.35 for ethyl acetate. Ethyl acetate yielded 17.01 g/l of xylitol in the top phase and 48.07 g/l of xylitol in the bottom phase.	2	(Misra et al., 2011)
Thermomechanical pulp process water	Solvent: tributyl phosphate, 1-butanol, n-hexane, and toluene, at r.t. Extraction time: 30 min.	Hemicellulose extraction efficiency in the range of 62 – 72 % was reported. The average selectivity coefficients were between 0.6 and 8.7	1	(Bokhary et al., 2019)
Preservatives and artificial sweeteners	Solvent: acetone, ethanol, acetonitrile, and 2-propanol. pH: 3.	Extraction recoveries ranged between 85 and 122%.	1	(Tighrine et al., 2019)

r.t. = room temperature

2.2. Lignin recovery and fractionation

During the lignin removal (delignification process), the lignin will be separated from the cellulose fibers and released into the pre-hydrolysis liquor, black liquor, or spent sulfite liquor dependent on the treatment processes. These waste liquors are a complex mixture of lignin, other dissolved biomass substances, and inorganic molecules. The fate of these liquid waste streams either ends in the recovery boiler to recover the heat (black liquid in the Kraft pulp process) or into the wastewater streams for further treatment. Lignin can be recovered and used in the manufacture of many valuable products. For example, Kraft lignin has been considered an excellent candidate to produce carbon and composite fibers, while lignosulfonates are proposed to be employed as adhesive, surfactant, and dye dispersing agents (Fatehi and Chen 2016) or as starting feedstock for synthesizing other biomaterials such as vanillin. More recently, significant attention has been directed at the development of a bio-based economy and an environmentally sustainable paradigm for the use of this unexploited resource. However, in order to use these lignins, they should be recovered in a pure condition. Thus, several separation methods have been attempted, including precipitation at low pH values, membrane filtration, and adsorption. Among the used separation methods, LLE has also been investigated for lignin recovery from real hydrolysates and synthetic solutions. Kontturi and Sundholm (1986) studied the capacity of different solvents and long-chain aliphatic amines on lignosulfonates extraction. The reported extraction degrees were near to 100% in a single extraction stage and the lignin could be fractionated based on its molar mass in a three-step extraction process using an amine-solvent system at different concentrations. Villar et al. (1996) reported a 90% recovery of lignin from Kraft black liquor using different alcohol-calcium solutions (ethanol, methanol, and isopropanol) in a single batch extraction. The three tested alcohol-calcium systems were showed similar behaviors. Hamala et al. (1982) patented a method for the recovery of lignosulfonates from spent sulfite liquors using methyl isobutyl ketone (MIBK) as an organic solvent in a single extraction process followed by stripping. They extracted a considerable quantity of sugar-free lignosulfonates, and the reported recovery degree was 99%. Cruz et al. (1999) recovered up to 84% of lignin compounds (phenolics) under the optimal conditions of ethyl acetate

and diethyl ether in a single step at 25 or 30 °C and solvent:hydrolysate volume ratios in the range 1:1 to 1:9. Ethyl acetate showed an advantage over diethyl ether, and no significant difference in phenolic removal was observed between the single extraction stage and the second extraction stage when it was performed sequentially (Cruz et al., 1999). Recently, Stiefel et al. (2017) developed a green LLE process to transfer lignin from pretreated lignocellulosic biomass into different alkaline concentrates for further valorization. They were able to extract the lignin entirely from the organic phase of the Organo-Cat process (2017).

In recent times, solvent fractionation of lignin is being considered by many researchers for lignin valorization using a wide range of organic solvents such as acetone, butanone, diethyl ether, dioxane, dichloromethane, ethanol, ethyl acetate, hexane, isopropanol, methanol, and tetrahydrofuran (Jääskeläinen et al., 2017; Park et al., 2018; Ropponen et al., 2011; Li et al., 2012; Arshanitsa et al., 2013; Araújo et al., 2020; Dodd et al., 2014; Duval et al., 2017; Jiang et al., 2016; Passoni et al., 2016; An et al., 2017; Domínguez-Robles et al., 2018). Several solvent fractionation approaches have been used to obtain pure and more homogeneous lignins, including successive extraction and selective dissolution of solid lignins followed by fractional precipitation of lignin using anti-solvent (Jääskeläinen et al., 2017; Domínguez-Robles et al., 2018). Sequential solvent extraction is the most used approach for lignin fractionation. This approach offers an attractive way to fractionate lignin into different segments with specific properties for a wide range of potential applications. Nevertheless, this method faces some technological constraints such as the need for long extraction cascade with repeated steps and the use of toxic solvents, potentially leading to increased process costs and health and environmental problems. Solvents fractionate lignins according to their molecular weight, where low molecular weight fractions have been found to have greater solubility in the solvent than higher molecular weight fractions (Ropponen et al., 2011). The solubility of lignins in organic solvents was observed to depend on the solvent's polarity and hydrogen bonding capacity (Mörck et al., 1986). Solvents of intermediate polarity are more efficient in dissolving lignin compared to polar and non-polar solvents (Melro et al., 2018). A summary of lignin extraction and fractionation by organic solvents is presented in Table 2.1.2.

Ionic liquids-based solvents were also examined as promising green candidates to extract lignin and butanol from aqueous liquid effluents. ILs are organic salts with reduced melting points (<100 ° C) and several of them are liquid at room temperature (Simoni et al., 2010). Due to low vapor pressure, non-flammability, reduced toxicity, wide liquid temperature range, and tuneable physicochemical properties, the use of ILs have gained considerable attention as industrial solvents to replace volatile organic compounds (Simoni et al., 2010; Ha et al., 2010; Cascon et al., 2011). Also, ILs are stable over a broad range of temperatures (~ −70 °C to 400 ° C), and this can result in reduced solvent loss and make-up requirements (Simoni et al., 2010). Several types of ILs have been investigated as viable alternatives to volatile organic solvents,

including imidazolium (Pu et al., 2007; Lee et al., 2009; Fu et al., 2010; Ji et al., 2012; Sun et al., 2016), ammonium (Fu et al., 2010), phosphonium/pyrrolidinium (Glas et al., 2015), and protic ILs (Achinivu et al., 2014; Rashid et al., 2016). The aprotic ILs are most studied compared to protic ILs. Among the aprotic ILs examined, imidazolium received extensive consideration, and imidazolium acetate demonstrated significant efficacy in lignin solubility (Rashid et al., 2016). Despite its effectiveness, the use of IL technology has some disadvantages such as increased IL synthesis cost, biocompatibility problems, high viscosity, high operating temperatures, and high IL load. Deep eutectic-based systems, alternatively, are another category of solvent extraction whose lignin applications have been studied recently (Lynam et al., 2017; Soares et al., 2017; Smink et al., 2020) to overcome the drawbacks associated with ILs applications.

Table 2.1.2: Summary of lignin recovery and fractionation via organic solvents

Raw material	Extraction conditions	Results	TRL	Ref.
Spent sulfite liquor	Solvent: methyl isobutyl ketone.	The reported recovery degree was 99%.	4	(Hamala et al., 1982)
Lignosulfonates	Solvent: 1-butanol, 1, 2-dichloroethane, cyclohexane, 1-pentanol, and methyl isobutyl ketone. Stirred for 5 min at r.t.	The degrees of extraction were close to 100%.	2	(Konttur and Sundholm 1986)
Kraft black liquors	Solvent: methanol, isopropanol, ethanol, and acetone. Stirred at r.t. Settled for 1 h.	90% of the lignin was recovered.	2	(Villar et al., 1996)
Eucalyptus wood hydrolysates	Solvent: ethyl acetate and diethyl ether. Stirred at 300 rpm in the range 10–40°C, and pH 3 or 6.5.	84% of lignin-derived compounds were extracted.	1	(Cruz et al., 1999)
Spent sulfite liquor	Solvent: dicyclohexylamine, n-butanol, and diethyl ether.	81% of the lignosulfonates could be recovered using amine extraction.	1	(Ringena et al., 2005)
Hydrolyzable tannins	Solvent: petroleum ether, *n*-hexane, dichloromethane, acetone, chloroform, ethanol, methanol. Extraction time: 3 h.	The extraction yields were between 1.8–26.2%.	1	(Markom et al., 2007)
Kraft black liquor	Solvent: methane chloride, ethyl ether, n-propanol, methanol, ethanol, and dioxane.	The yield of lignin fractions was between 4.4 and 32.28 %.	2	(Yuan et al., 2009)
Kraft black liquor	Solvent: dioxane/water mixtures. A binary solvent system, Stirred at 20 °C for 1 h.	Lignin solubility was 24.75 g/kg.	1	(Evstigneev 2010)
Kraft and sulfite liquors	Solvent: Ethyl acetate	The obtained crude extracts contained 92.7 to 181.6 mg GAE/g phenolic compounds.	2	(Faustino et al., 2010)
Technical lignins	Solvent: n-propanol, dichloromethane, and methanol/ dichloromethane mixture. Stirred at r.t. for 30 min.	The yields of lignin fractions were in the range of 0.9 – 43.0 %.	2	(Gosselink et al., 2010)
Kraft black liquor	Solvent: dichloromethane, acetone, and methanol, at 23 °C, 1 h, pH: 4.	Extraction yields were 26, 86, 87%, respectively.	2	(Methacanon et al., 2010)
Kraft black liquor	Solvent: hexane, diethyl ether, methylene chloride, methanol, and dioxane, at r.t.	The yields of lignin fractions were in the range of 0.2 – 59.1 %.	2	(Wang et al., 2010)
Kraft lignin and Organosolv lignins	Solvent: diethyl ether, diethyl ether/acetone, and acetone, at r.t., contacted for 2 h.	The reported solubility was in the range of 0.2–39%. Acetone achieved the highest solubility. The yield of residual lignin was in the range of 60–76%.	2	(Ropponen et al., 2011)
Organosolv lignin	Solvent: ether, ethyl acetate, methanol, acetone, and dioxane/water, at r.t., contacted for 2 h.	The five fractions yield was 2.80, 39.85, 18.64, 23.38, and 13.30%, respectively.	1	(Li et al., 2012)
Soda lignin	Solvent: i-propanol/ethanol mixture and methanol.	The total yield of lignin after fractionation was 90.7%.	2	(Yue et al., 2012)

Technical lignins	Solvent: dichloromethane, methanol, and their mixture, at r.t., stirred for 2 h.	About 40% of the lignin was solubilized.	2	(Arshanitsa et al., 2013)
Technical lignins	Solvent: acetone/water mixtures and ethyl acetate, at 20 °C.	Yields of soluble/insoluble lignin portions were in the range of 10–>80%.	2	(Boeriu et al., 2014)
Industrial softwood Kraft lignin	Solvent: dichloromethane, n-propanol, and methanol, at r.t., contacted for 1 h.	Fractionation yields were in the range of 19–42 wt %.	2	(Dodd et al., 2014)
Softwood Kraft Lignin	Solvent: hexanes and acetone, at r.t., stirred for 2 h.	The accumulated yield of lignin was nearly 80%. Yields of polyphenolic material were ranging between 10 and 20% w/w.	2	(Cui et al., 2014)
Spent sulfite liquor	Solvent: chloroform, diethyl ether, trichloroethylene, benzene, and hexane, at r.t., contacted for 10–390 min.	The phenolic recovery (%) obtained in three sequential extraction steps was in the range of 10–50%.	2	(Llano et al., 2015)
Kraft lignin	Solvent: isopropanol, ethanol, 1-propanol, tert-butanol, methyl ethyl ketone, acetone, and ethyl acetate, at r.t., stirred for 2 h.	Yields of the soluble fraction were between 8.0 and 66.5 %.	1	(Duval et al., 2016)
Softwood kraft lignin	Solvent: tetrahydrofuran, methanol, 2-butanone, and dimethyl sulfoxide. Contacted for 8 h under vigorous magnetic stirring.	Lignin fractionation yield was between 21 and >99 %.	2	(Passoni et al., 2016)
Switchgrass and pine organosolv lignins	Solvent: acetone and mixtures of acetone/water, at r.t., stirred for 6 h.	Both organosolv lignin samples exhibited 100% solubility at 60% acetone concentration.	2	(Sadeghifar et al., 2016)
Pine kraft lignin	Solvent: 1:1 ethyl acetate/petroleum ether, ethyl acetate, and petroleum ether.	Extraction yields were 48%, 39%, 10%, and 3%, respectively.	1	(Jiang et al., 2016)
Alkali lignin	Solvent: 1-butanol, 1-propanol, 2-propanol, glycerol, ethylene glycol. Vortexing at 20 °C.	Lignin solubility of Ethylene glycol and Glycerol was 310 and 250 g/kg, respectively.	1	(Sun et al., 2016)
Enzymatic hydrolysis lignin	Solvent: dichloromethane, acetic ether, and n-butyl alcohol. Sonicated at 23 °C, 2 h.	Extraction yields were 13.42% for dichloromethane, 22.45% for acetic ether, and 15.04% for n-butyl alcohol.	1	(An et al., 2017)
Softwood kraft lignin	Solvent: ethanol, acetone, and propyleneglycol monomethyl ether, at r.t., stirred 20 min.	The reported yields were close to 100%. The solvent insoluble portions contained a high molecular weight (Mw 4300–18900 g/mol) and vice versa.	2	(Jääskeläinen et al., 2017)
Kraft lignin	Solvent: diethyl ether, chloroform, acetone, ethyl acetate, dioxane, ethanol, methanol, tetrahydrofuran, and dichloromethane, at 23 °C, sonicated in a water bath for 10 min.	Lignin solubility was in the range of 0.1–9.6 g/kg.	2	(Sameni et al., 2017)
Kraft, organosolv, and soda lignins	Solvent: acetone/water, at r.t., stirred for 60 min.	Lignin solubility was between 10 and 90 %, depending on the acetone concentration.	2	(Domínguez-Robles et al., 2018)
Milled wood lignin and organosolv lignin.	Solvent: acetone, 2-butanone, methanol, ethyl acetate, and dioxane/water, at r.t., stirred for 2 h.	Yields of lignin fractions were in the range of 3.7–49.6 %	1	(Park et al., 2018)
Kraft lignin	Solvent: ethanol-water mixtures, at r.t.	235.89 g/L lignin concentration was achieved.	1	(Goldmann et al., 2019)

Room temperature (r.t.)

2.3. Organic acids recovery

During the hydrolysis and pyrolysis of biomass materials, carboxylic acids form as by-products. These by-products are discharged in waste streams of pre-pulping extracts, lignocellulose hydrolysate, pre-hydrolysis liquor, or spent sulfite liquor. The recovery of organic acids from liquid streams or fermentation broths is

of great importance. For example, acetic acid can be used as a chemical feedstock to produce terephthalic acid, acetic anhydrides, esters, and mono-chloroacetic acid (Ahsan et al., 2012; Kim et al., 2015). Conversely, acetic acid is one of the fermentation inhibitors in bioethanol production processes, which decreases bioethanol yield via suppression of the bioethanol-producing microorganisms (Aghazadeh and Engelberth 2016). Extraction of acetic acid from biomass hydrolysates as a value-added chemical or as a fermentation inhibitor is performed by distillation, liquid membrane separation, and adsorption using ion-exchange resin (Cebreiros et al., 2017). Among the employed methods, several studies have shown that LLE can effectively isolate acetic acid from aqueous solutions (Um et al., 2011; Cebreiros et al., 2017; Kim et al., 2015; Mateo et al., 2013; Park et al., 2013; Kim et al., 2014).

Table 2.1.3 summarizes carboxylic acids extraction from aqueous streams. The distribution coefficients varied between <0.01 and 40 for acetic acid, while they ranged between 0.2 and 14.5 and 0.1 and 1.2 for formic acid and levulinic acid, respectively. The selectivity was in the range of 15 – 93 for acetic acid, while it ranged from 26 to 194 for formic acid. Many solvents were utilized to remove organic acids from aqueous effluents. Trioctyl phosphine oxide (TOPO), ethyl acetate, tri-octyl amine (TOA), triisooctylamine (TIOA), diethyl ether, and tributylphosphate (TBP) are the most applied extractants for removing acetic acid from aqueous effluents. Rasrendra et al. (2011) isolated the organic acids from an aqueous stream of pyrolysis oil in a batch extraction and continuous reaction extraction (CRE) system using a centrifugal contact separator (CCS). In batch extraction, n-octylamine (TOA) in 2-ethyl-hexanol (40 wt%) achieved an 84% recovery of acetic acid for a 1:1 phase ratio, while in CRE, the acetic acid recovery was 51% for the same solvent combination. In a single extraction stage, Um et al. (2011) recovered 76% of acetic acid with TOPO at a pH value below 3 and a volume ratio of 1:1, and it was found that the extraction efficiency was pH-dependent. Also, it was found that TOPO concentration, phase ratio, and to some extent temperature affect acetic acid extraction. TOPO has been shown to extract carboxylic acids from the aqueous streams effectively in a one-stage extraction. Besides its low solubility in water and excellent stability, TOPO forms strong complexes with carboxylic acids during the extraction process because of its high hydrogen-bond-acceptor basicity, which promotes the transfer of carboxylic acids to the extract phase (Kim et al., 2015). Ethyl acetate also has potential applications in the extraction of acetic acid, and extraction efficiency as high as 96% was reported in the literature for a one-stage batch experiment and phase ration of 1:4 (organic-to-aqueous) of the ternary system (Park et al., 2013). However, the main drawbacks of organic acids recovery from lignocellulosic hydrolysates via LLE are the use of volatile/toxic solvents and sugar losses.

Table 2.1.3: Summary of carboxylic acids recovery from aqueous systems

Product	Raw material	Extraction conditions	Results		TRL	Ref.
			K_D	E (%)		

Acetic acid	Model solutions	Solvent: TOPO and cyclohexane, at 30 °C, stirred for 2 h.	0.06 – 39.9	–	1	(Al-Mudhaf et al., 2002)
	Model solutions	Solvent: alamine-336 and 304, TBP, TOPO. Diluent: 2-ethyl-1-hexanol, diisobutyl ketone, and 2-heptanone, PH: 3.5.	–	85	1	(Katikaneni and Cheryan 2002)
	Model aqueous solution	Solvent: TOPO Cyanex® 921 and 923. Diluent: toluene, exxsol®, and octane, at 20 °C.	0.5 – 1.03	15.13	2	(Wisniewski and Pierzchalska 2005)
	Fast Pyrolysis Oil	Solvent: trioctylamine (TOA), octane, toluene, decane, at 20 °C.	10	71 – 93	1	(Mahfud et al., 2008)
	Lignocellulose hydrolysate	Solvent: 11 different solvents, at 34 °C.	<0.01– 0.89	–	2	(Zautsen et al., 2009)
	Hardwood hemicellulosic hydrolysates	Solvent: TOPO-alkane, pH 1, 70 °C, 36 min.	2.0 – 2.5	76	2	(Um et al., 2011)
	Aqueous pyrolysis oil	Solvent: TOA, 2-ethyl-hexanol, at 20 °C, stirred at 500 rpm for 6 h and settled for 2 h.	2.5	86	2	(Rasrendra et al., 2011)
	Pre-hydrolysis liquor/ aqueous model solution	Solvent: tri-octyl amine (TOA) and octanol as a diluent.	1.6/6.22	61.84/ 80.48	1	(Ahsan et al., 2012)
	Olive tree hydrolysates	Solvent: chloroform, n-hexane and ethyl acetate, pH 5.5, at r.t.	–	17	1	(Mateo et al., 2013)
	Acetic acid derived from the pre-pulping extract	Solvent: ethyl acetate, at 25 °C.	8.1	97	2	(Park et al., 2013)
	Pre-hydrolysis liquor	Solvent: triisooctylamine (TIOA) diluted with decanol, at 20 °C, pH 4.3 and 10 min.	1.6 – 3.9	62.5 – 79.5	1	(Yang et al., 2013a)
	Activated carbon pre-treated pre-hydrolysis liquor	Solvent: triisooctylamine (TIOA). Diluent: 2-ethyl-1-hexanol, at 20 °C, pH 4.5, and 10 min.	0.98 – 3.7	49.4 – 78.6	1	(Yang et al., 2013b)
	Barley straw hydrolysate	Solvent: isooctane, ethyl acetate, heptane, and hexane, at r.t., stirred 10 min.	–	33.2	1	(Kim et al., 2014)
	Acetic acid from pre-pulping extracts	Solvent: trioctylphosphine oxide (TOPO) and trialkylphosphine oxide (TAPO), at 25 °C, pH 0.5, 36 min.	4.9	83.1	2	(Kim et al., 2015)
	Spent sulfite liquor	Solvent: chloroform, diethyl ether, trichloroethylene, benzene, and hexane, settled 30 min, pH 3.6.		41.7	2	(Llano et al., 2015)
	Corn stover hydrolysate	Solvent: ethyl acetate, at r.t., stirred for 5 min, settled for 2 h.	5.7	90	5	(Aghazadeh and Engelberth 2016)
	Hydrolysates of *Eucalyptus grandis* wood chips	Solvent: ethyl acetate, pH 2.47, at r.t., stirred for 36 min.	0.7 – 1.3	82	1	(Cebreiros et al., 2017)
Formic acid	Model aqueous solution	Solvent: Organophosphine oxides Cyanex® 921 and 923. Diluent: toluene and octane at 20 °C.	0.6 – 0.84	8.43	1	(Wisniewski and Pierzchalska 2005)
	Model aqueous solution	Solvent: trioctylamine (TOA), isoamyl alcohol, 1-hexanol, 1-octanol, 1-decanol, at 25 °C.	1.2 – 14.5	53.4 – 93.6	1	(Uslu 2009)

	Aqueous pyrolysis oil	Solvent: tri-n-octylamine (TOA), 2-ethyl-hexanol, at 20 °C	10.9	92	2	(Rasrendra et al., 2011)
	Barley straw hydrolysate	Solvent: isooctane, ethyl acetate, heptane, and hexane, stirred for 10 min.		25.9	1	(Kim et al., 2014)
	pre-pulping extracts	Solvent: TAPO at 25 °C.	6.5	61.1	1	(Kim et al., 2015)
	Spent sulfite liquor	Solvent: chloroform, diethyl ether, trichloroethylene, benzene, and hexane, settled for 30 min, pH 3.6.	–	6.14	2	(Llano et al., 2015)
	Aqueous model solution	Solvent: trioctylamine (TOA), trioctylphosphine oxide (TOPO) and 4-tert-butylbenzenediol (TB) with 7 different diluents, at 25 °C.	0.2 – 2.2	–	1	(Brouwer et al., 2017)
Glycolic acid	Aqueous pyrolysis oil	Solvent: tri-n-octylamine (TOA), 2-ethyl-hexanol, at 20 °C	1.9	69	2	(Rasrendra et al., 2011)
Levulinic acid	Aqueous model solution	Solvent: trioctyl amine, TOPO and 4-tert-butylbenzenediol with 7 different diluents, at 25 °C.	0.1 – 1.2	–	1	(Brouwer et al., 2017)
	Spent sulfite liquor	Solvent: chloroform, diethyl ether, trichloroethylene, benzene, and hexane, settled for 30 min, pH 3.6.	–	36.36	2	(Llano et al., 2015)

E% = Extraction efficiency; K_D = Distribution coefficients; S = selectivity; TOPO = trioctyl phosphine oxide; TBP = tributyl phosphate.

2.4. Furfural recovery

Furfural extraction from aqueous solutions is particularly important because of the high demand for this product as a selective solvent in oil refining and as a feedstock for synthesizing other chemicals such as furfuryl alcohol (Coca and Diaz 1980). Furfural is produced by acid hydrolysis of biomass containing pentosan or its waste products. Furfural is usually separated by distillation, adsorption, and LLE. Solvent recovery of furfural from aqueous feeds is not a modern technique dating back to 1940 when proposed by Trimble and Dunlop (1940) as an alternative to azeotropic distillation. To date, several studies on LLE of furfural have been reported in the literature, and a variety of solvents were tested for its extraction. Both furfural and 5-hydroxymethylfurfural (HMF) whether reagent grade (Cabezas et al., 1988; Männ stö et al., 2016) or lignocellulosic derived furfural (Coca and Diaz 1980; Cabezas et al., 1988; Sunder 2003; Saha and Abu-Omar 2014) were investigated. Croker and Bowrey (1984) extracted furfural from aqueous effluents by different solvents (methyl isobutyl ketone, toluene, isobutyl acetate), among the tested solvents, toluene was the most effective solvent (99.9% extractability was reported at 30 °C for a one-stage batch experiment, ternary system) for the furfural removal from the aqueous solution compared with the tested solvents. Isobutyl acetate extracted 98.2 % of furfural but might be preferable than toluene due to its high solubility in furfural, reduced solubility in water (0.67% at 20 °C), and less toxicity (Croker and Bowrey 1984). Brouwer et al. (2017) also studied furfural and levulinic/formic acid recovery from aqueous effluents, where furfural was removed selectively through LLE with toluene. Methyl isobutyl ketone could

also be utilized to separate furfural (Shimanouchi et al., 2013; Zhang et al., 2013; Blumenthal et al., 2015), however, reduced furfural selectivity was observed (Brouwer et al., 2017). Table 2.1.4 shows furfural extraction from aqueous solutions. Different extractants have been used for furfural recoveries such as 2-methyl-2-butanol, toluene, isobutyl acetate, 2-ethyl-1-hexanol, and methyl isobutyl ketone (MIBK). Among the solvents used, toluene and ethyl acetate gave a satisfactory recovery. However, the ethyl acetate has a high solubility in water (7.7% by mass at 30 °C) needing a large subsequent recovery unit for ester, which may increase process costs. Generally, chlorinated hydrocarbons showed higher selectivity than alcohols due to their reduced water solubility.

Table 2.1.4: Furfural recovery from aqueous effluents

Raw material	Extraction conditions	Results	TRL	Ref.
Technical furfural	Ethyl acetate, at 25 °C.	88% of the furfural is recovered	2	(Trimble and Dunlop 1940)
Aqueous model solution	Trichloroethylene, 1,1,2-trichloroethane, perchloroethylene, and 1,2-dichloroethane, at 25°C.	1,2-dichloroethane and trichloroethylene showed the highest selectivity.	1	(Coca and Diaz 1980)
Aqueous solution	MIBK, toluene, isobutyl acetate, at 30 °C.	Toluene was shown better extractability (99.9%) compared with the tested solvents.	1	(Croker and Bowrey 1984)
Aqueous model solution	2-methyl-2-butanol, 2-ethyl-1-hexanol, at 25 °C.	High furfural selectivity and concentration were achieved, and distribution coefficients range from 2 – 13.	1	(Cabezas et al., 1988)
HMF production from Fructose - biphasic system	1-butanol, 2-butanol, 1-hexanol, toluene/2-butanol - biphasic system.	Partition coefficients range from 0.9 – 1.7, and HMF selectivity of 89% is achieved.	3	(Román-Leshkov et al., 2007)
Dehydration of fructose for HMF	MIBK - biphasic system, at 180 °C and 10 MPa, 3 min.	The yield of HMF was 84 % and its selectivity was 90 %.	1	(Shimanouchi et al., 2013)
Olive tree hydrolysates	Solvent: chloroform, n-hexane, and ethyl acetate, at r.t., pH 5.5.	Furfural removal in a percentage ranging between 74% and 94% were reported for ethyl acetate.	1	(Mateo et al., 2013)
Furfural from maple wood	MIBK, at 170 °C, 200 rpm, 80 min.	About 85.3% of the extraction yield was reported. The partition coefficient was 18.57.	1	(Zhang et al., 2013)
HMF production from Fructose - biphasic system	MIBK, 2-butanol, and 1-butanol - biphasic system, at 25 °C.	Partition coefficients of HMF were 1.3 for MIBK, 1.8 for 1-butanol, and 1.6 for 2-butanol.	1	(Blumenthal et al., 2015)
Barley straw hydrolysate	Isooctane, ethyl acetate, heptane, and hexane, at r.t., stirred for 10 min.	Furfural removal was 93.6 %, while 5-Hydroxymethylfurfural removal was 92.3%.	3	(Kim et al., 2014)
Spent sulfite liquor	Chloroform, diethyl ether, trichloroethylene, benzene, and hexane, at r.t., settled for 30 min, pH 3.6.	8.46 % of HMF and 12.5 % of furfural were recovered.	2	(Llano et al., 2015)
Aqueous model solution	4-Methyl-2-pentanone, MIBK, and 2-methyl-2-butanol, at 25 °C.	The distribution coefficient and selectivity of furfural were in the range of 4 – 12 and 15 – 80, respectively.	1	(Männistö et al., 2016)
Aqueous model solution	Trioctylamine (TOA), TOPO, and 4-tert-butylbenzenediol, with 7 different diluents, at 25 °C	Furfural distribution coefficients were in the range of 3 – 22.	1	(Brouwer et al., 2017)

Reagent grade furfural (synthetic wood hydrolysate)	MIBK, at 25 °C.	Furfural was extracted completely.	1	(Pokki et al., 2013)

Methyl isobutyl ketone (MIBK); trioctylphosphine oxide (TOPO)

2.5. Inhibitors removal

During the fermentation process, the mixture of the hydrolysis product (hydrolysate) comprises not only fermentable sugars but also contains a wide range of substances that have inhibitory consequences on the employed microorganisms. These substances may include aliphatic acids (e.g., acetic acid), furan compounds (e.g., furfural, furan aldehydes), and lignin compounds. Luo et al. (2002) identified potential fermentation inhibitors for the ethanol production that originated from the wood hydrolysate. Different inhibition mechanisms, including increasing cell maintenance energy requirements, changing intracellular pH, and osmotic pressure effect of the cell, have been reported in the literature (Luo et al., 2002; Salter and Kelt 1995). A variety of detoxification processes have been used to remove inhibitory compounds from aqueous lignocellulosic hydrolysates or reduce their effect on fermentation microorganisms, including adsorption, overliming, and membrane filtration. Among the applied methods, LLE is also used to remove fermentation inhibitors during biofuels production from biomass-derived solutions or fermentation products. The removal of inhibitors via LLE can be applied as a pre-treatment or *in situ* (Zautsen et al., 2009). The on-site process is a one-step process, which may reduce investment and operating costs. Table 2.1.5 summaries the removal of inhibitors from biomass hydrolysates and fermentation products. Many solvents are used such as oleyl alcohol (Qureshi et al., 1992), decanol, oleic acid, octane (Zautsen et al., 2009), isobutyl acetate (Roque et al., 2019), and diethyl ether, trichloroethylene (Llano et al., 2015). Extraction yields are highly dependent on the solvent type. Ketones and ethers are the common extractants used to remove phenolic compounds from aqueous solutions, while diethyl ether and ethyl acetate were utilized to extract small molecular mass phenolic fractions from biomass hydrolysate (Cruz et al., 1999). Ethyl acetate showed excellent extraction capacity for phenolic compounds (Cruz et al., 1999; Faustino et al., 2010), while oleyl alcohol has been indicated in the literature as a suitable solvent for inhibitors extraction due to its relatively low toxicity to bacterial cells. Using solvent-detoxified media, high fermentation performance can be achieved, and solubilized lignin fractions could be recovered as a value-added material (Cruz et al., 1999). However, the poor biocompatibility of the most applied solvents is the main drawback of LLE applications in removing fermentation inhibitors. Thus, solvents that have non-toxicity characteristics of fermentation cells are required.

Table 2.1.5: Inhibitors removal from lignocellulose hydrolysates and fermentation products

Raw material	Extraction conditions	inhibitor	Results	TRL	Ref.
Whey permeate	Solvent: oleyl alcohol, at 35 °C, 25 min agitation.	Acetic and butyric acids	Oleyl alcohol can reduce the concentration of acetic and butyric acids from 0.75 – 0.32 and 0.59 – 0.44, respectively.	1	(Qureshi et al., 1992)
Eucalyptus wood hydrolysates	Solvent: ethyl acetate and diethyl ether, at 10 – 40 °C, stirred at 300 rpm, pH 3 – 6.5.	Lignin-derived compounds (phenolic compounds)	84% of lignin-derived compounds have been extracted, and the antioxidant activity coefficient was 64%.	3	(Cruz et al., 1999)
Hybrid poplar hydrolysate	Solvent: chloroform and ethyl acetate, at r.t.	Lignin and sugar degradation compounds (e.g., aromatic and aliphatic aldehydes and furan compounds)	Both aromatic and aliphatic compounds are extracted.	2	(Luo et al., 2002)
Eucalyptus wood hydrolysates	Solvent: ethyl acetate.	Acetic acid, HMF, Furfural	After extraction, the concentration of inhibitors was below the inhibitory limit ((> 5 g/L) of acetic acid, (0.1 g/L) of HMF, and (0.05 g/L) of furfural).	2	(Gonzalez et al., 2004)
Lignocellulose hydrolysate	Solvent: series of alkanes and higher alcohols, at 34 °C, stirred for 4 h and settled for 2 h, pH 4.5.	Furfural, HMF, Acetic acid, Vanillin, Syringaldehyde, Coniferyl aldehyde.	Partition coefficients of furfural, HMF, acetic acid, and vanillin were in the range of 0.44 – 3.8, 0.001 – 1.3, <0.01 – 0.4, and 0.21 – 26.2, respectively.	3	(Zautsen et al., 2009)
Olive tree hydrolysates	Solvent: chloroform, n-hexane and ethyl acetate, at r.t., pH 5.5.	The phenolic compound, Acetic acid, Total furans (furfural and HMF)	Ethyl acetate reduces 34–49 % of phenolic compounds, after that chloroform (30 %), and lastly the n-hexane (14–24 %).	2	(Mateo et al., 2013)
Barley straw hydrolysate	Solvent: isooctane, ethyl acetate, heptane, and hexane, at r.t., stirred for 10 min.	Acetic acid and gallic acid	Removals of acetic acid and gallic acid were 33.2 % and 85.1 %, respectively.	2	(Kim et al., 2014)
Synthetic hydrolysates	Solvent: Hexadecane, 1-decanol, Octanol, and tetradecane, at 37 °C, stirred at 250 rpm.	4-vinyl guaiacol, Ferulic acid, P-coumaric acid, and 4-ethyl phenol	The partition coefficients for the 4-vinyl guaiacol were 33.3 for 1-octanol and 8.0 for tetradecane.	1	(Tomek et al., 2015)
Spent sulfite liquor	Solvent: chloroform, diethyl ether, trichloroethylene, benzene, and hexane, at pH 3.6, settled 30 min.	Acetic acid, HMF, Levulinic acid, Furfural, Formic acid	Diethyl ether extracted 41.7 % of acetic acid, 18.46 % of HMF, 36.36 % of levulinic acid, 12.5 % of furfural, and 6.14 % of formic acid. Chloroform removed 25.54 % of acetic acid.	2	(Llano et al., 2015)
Sugarcane bagasse hemicellulosic hydrolysate	Solvent: 1-butanol, isobutyl acetate, and MIBK, at r.t., stirred for 4 h, at 120 rpm.	Acetic acid, Phenolic compounds	MIBK extracted 85.4% of acetic acid and 69.0% of phenolics.	2	(Roque et al., 2019)
Phenol from wastewater	Extraction reagents: N-503, ABK, and QY1.	Phenol	QY1 was a better reagent for phenolic extraction from wastewater.	5	(Jiang et al., 2003)

r.t. = room temperature, MIBK = methyl isobutyl ketone.

2.6. Bio-ethanol separation

Ethanol is one of the main pillars of a biomass biorefinery. Ethanol produced from renewable biomass represents a promising raw material for the chemical industries and as a bioenergy source that can be used as a vehicle fuel in its pure form or as a mixture with gasoline. Various conversion technologies have been used for bioethanol production. Nowadays, ethanol is commonly produced by fermentation of C5 and C6 sugars by appropriate microorganisms. The second generation of bioethanol can be generated from the residual biomass, such as those in wastewater streams of the forest industry, or industrial or municipal waste

containing lignocellulosic materials. Ethanol should contain below 0.5 wt % of the water to be utilized as a vehicle fuel (Avilés Martínez et al., 2011). Traditionally, ethanol is recovered from fermentation broth by distillation. Distillation is characterized by high energy requirements and temperatures, which necessitates the need for energy-efficient alternative separation techniques. Among the tested alternatives, LLE has also been proposed as an effective means of separating ethanol by coupling fermentation and solvent extraction to reduce energy consumption and obtain enriched alcohol mixtures. Several classes of chemicals (e.g., ketones, alcohols, acetates, ethers) have been investigated as extraction agents to separate ethanol from dilute liquid effluents (Solimo et al., 1989; Arce et al., 2006; Corderí and González 2012).

Table 2.1.6 summarizes the results of ethanol recovery from dilute aqueous mixtures. Matsumura and Märkl (1984) examined 25 solvents from several classes to recover ethanol from the fermentation broth in batch experiments. Among the tested solvents, 2-ethyl-l-butanol had the highest distribution ratio of ethanol (0.83) and selectivity (103.8), followed by sec-octanol with 75 selectivity. Comparable findings have been reported by Egan et al. (1988), where 0.73 ethanol distribution coefficient and 29 separation factor (SF) was achieved by 2-ethyl-l-butanol in a batch contact. Sólimo and Zurita (1992) studied the influence of temperature (25, 35, and 45 °C) on the ethanol extraction from aqueous solutions using ternary mixtures of water + ethanol + 1, 2-dichloroethane (DE). DE achieved 94 percent extraction in batch phase separation and seems a potential candidate for ethanol extraction. The tested temperatures showed no effect on the extraction properties of DE for ethanol. Gyamerah and Glover (1996) operated a continuous fermentation pilot plant for ethanol production coupled with LLE to remove the product. Ethanol production was feasible and achievable with a glucose-containing feed of up to 45.8% (w/w) without by-product inhibition. Daugulis et al. (1991) conducted an economic assessment of the production of ethanol through fermentation and solvent extraction and concluded that the raw materials and energy needed to extract ethanol were two major costs of ethanol production. There is a vast disparity of the equilibrium distribution ratios of ethanol as well as separation factors (SFs) for the removal of EtOH from water, (Table 2.1.6). Numerically, the separation factor indicates the selectivity of the organic solvent for the ethanol over other by-products, while the ratio of ethanol concentration between the organic and aqueous phase at equilibrium is indicated by the distribution coefficient. Reported values range from 0.094 to 135.7 for ethanol distribution coefficients and within 1.86 – 34021.7 for SFs. The relatively high variability between the reported results can be attributed to the type of employed solvents and their properties (e.g., solubility, density difference, and stability) in addition to the experimental conditions. For example, solvents with low solubility in water had a large distribution coefficient of ethanol compared to solvents with large solubility in water, while the mixed solvents showed a relatively high distribution coefficient of ethanol and selectivity compared to the pure solvent (Habaki et al., 2016). Alternatively, Offeman et al. (2005a) attributed the large discrepancy between the literature sources in both the separation coefficients (α) and the distribution coefficients to two

likely causes (1) the propagation-of-errors effect resulting from the calculation of the separation factor from a small number of data and (2) differences in determining of the water content in the extract phase, which affects the separation factor as a result of division by small numbers. The investigated temperatures are in the range of 20 – 45 °C, but most of the studies were performed at room temperature (Table 2.1.6). It has been noted that solvents with large SFs usually have reduced ethanol distribution coefficients, and vice versa (Offeman et al., 2005b). Liquid-liquid extraction-coupled fermentation (extractive fermentation which removes ethanol during its production) is proven to be an effective combination for strain inhibition reduction and ethanol production improvement. Also, compared with pure solvents, mixed solvent systems had better capabilities, indicating that the mixed solvent system may have more favorable extraction characteristics than the pure solvent (Salter and Kelt 1995). For example, a mixed solvent of 2-ethyl hexanol and *m*-xylene was found to enhance the solubility of ethanol, resulting in a higher distribution coefficient with constant separation selectivity (Habaki et al., 2010). However, most organic solvents used to remove the final product are toxic or inhibitory to ethanol-producing microorganisms, so there is a need for finding benign alternatives. This problem is exacerbated by the fact that different cell types have a different response to a solvent, even under the same physiological environments (Salter and Kelt 1995). Extracting agents cause cell toxicity via two mechanisms: (1) molecular-level mechanisms (e.g., enzyme inhibition, permeability changes, protein denaturation, and membrane modifications) or (2) phase level mechanisms (nutrient extraction, cell wall disruption, and emulsions formation) (Salter and Kelt 1995). Organic solvents should, therefore, be screened exclusively based on the microorganisms of interest. To address the problem of the solvent toxicity, Matsumura and Märkl (1984) used low-density absorbent materials as a protective wall to solvent molecules under the gel beads to immobilize the yeast cells. This measure was effective in preventing the solvent toxicity, ethanol production of the protected cells remained stable even after the use of 2-octanol, the highly toxic solvent. Separating the yeasts from the solvent is also reported by Honda et al. (1986), who used the castor oil as a protective agent for yeast from solvent (o-tert-butyl phenol) toxicity.

Table 2.1.6: Ethanol separation from fermentation broths and model aqueous solutions

Raw material	Extraction conditions	Results/conclusion	TRL	Ref.
Fermentation broth of glucose	Solvent: dodecanol, at 35 °C.	The fermentation was significantly improved, and ethanol production multiplied by 5.	2	(Minier et al., 1981)
Fermentation broth of glucose	Solvent: 25 organic solvents, at 30 °C, settled for 24 h.	Among the solvent classes examined, alcohols and esters showed more potential. Ethanol distribution coefficients were between 0.58 – 0.83. Selectivity ratios were between 12.9 – 108.8	2	(Matsumura and Märkl 1984)
Ethanol from the aqueous model solution	Solvent: 31 organic solvents, at 24 °C, settled 1 – 2 h.	The reported values of distribution coefficients and SFs at 30 °C were between 0.13 – 1.3 and 4.5 – 150, respectively.	2	(Munson and King 1984)
Ethanol from dilute aqueous media	Solvent: 2-ethyl-l-butanol, at 24 °C.	The reported values of the distribution coefficient and selectivity for 2-ethyl-l-butanol were 0.94 and 14.6, respectively.	2	(Mitchell et al., 1987)

EtOH from aqueous solution	Solvent: 10 organic solvents, at 21 – 24 °C.	Ethanol distribution coefficients were between 0.13 – 0.73.	1	(Egan et al., 1988)
Ethanol from aqueous solution	Solvent: benzyl alcohol, amyl acetate, and MIBK, at 25 °C.	The selectivity of the solvents was amyl acetate > methyl isobutyl ketone > benzyl alcohol.	1	(Solimo et al., 1989)
Ethanol from aqueous solution	Solvent: 1, 2-dichloroethane, at 25, 35, and 45 °C.	The reported values of distribution coefficients and SFs at 25 °C were between 0.094 – 0.413 and 10 – 47, respectively.	2	(Sólimo and Zurita (1992)
Ethanol from fermentation broths	Solvent: *n*-dodecanol at 30 °C and pilot plant.	No by-product inhibition and ethanol production by continuous fermentation in the pilot plant and LLE of ethanol was possible.	6	(Gyamerah and Glover 1996)
Ethanol from aqueous solution	Solvent: 2-ethylhexanol, at 25 °C, 48 h.	The distribution coefficient of ethanol was between 0.5 – 2.5, and the SF was between 3 and 60. The addition of sodium chloride has improved both the distribution coefficient and selectivity.	1	(Gomis et al., 1998)
Ethanol from aqueous solution	Solvent: dibutyl ether, isoamyl acetate, isooctyl alcohol, n-butyl acetate, and dibutyl oxalate, at 20 and 40°C, Settled for 12 h.	Among the tested solvents, isoamyl acetate and isooctyl alcohol were very promising extracting agents, showing EtOH distribution ratios between 1.89 – 5.93 and 3.69 – 38, and SFs 70 and 2000, respectively.	2	(Koullas et al., 1999)
Ethanol from aqueous solution	Solvent: 1-hexanol, 1-butanol, and 1-pentanol, at 30°C.	The reported values of the distribution and selectivity coefficients were 1 – 1.3 and 2.7 – 14.18, respectively.	3	(Rahman et al., 2001)
Ethanol from aqueous solution	Solvent: 57 alcohol solvents, at 33 °C.	The distribution ratio and SF were 0.35 – 1.3 and 8.9 – 28.2, respectively.	2	(Offeman et al., 2005b)
Ethanol from aqueous solution	Solvent: 10 solvents, at 33 °C, settled for 30–45 min.	Among the used solvents, 3-ethyl-3-pentanol achieved the highest K_{DE} (0.99), while 2-ethyl-1-hexanol had the highest α (20).	2	(Offeman et al., 2005b)
Ethanol from aqueous solution	Solvent: several alcohol solvents, at 33 °C.	Among the used solvents, 1-octanol achieved the highest K_{DE} (0.716), while iso-stearyl alcohol had the highest α (34.9).	4	(Offeman et al., 2008)
Ethanol from aqueous media	Solvent: m-xylene, 1-hexanol, and 2-ethyl hexanol, at 25 °C, contacted for 48 h.	m-Xylene showed low K_{DE} and high selectivity of EtOH compared with water.	1	(Hiroaki et al., 2010)
Ethanol from fermentation broths	Phosphonium-based ionic liquids. Settling time: 12 h.	Ethanol distribution coefficients in the range of 0.31 – 0.88 and selectivity in the range of 2.0–8.4 were reported. Maximum EtOH extraction was in the range of 65–91 %.	4	(Avilés Martínez et al., 2011)
Ethanol from aqueous solution	Solvent: 3 deep eutectic solvents (DESs), at 25 °C.	The reported values of distribution coefficients were 1.78 – 135.7.	1	(Oliveira et al., 2013)
Ethanol from aqueous media	Solvent: hexane and heptane, at 25 and 35°C.	High ethanol distribution coefficient and selectivity values were achieved, and heptane has the highest values (K_{DE} 29.4 and α 34021.7) compared to hexane (K_{DE} 18.7 and α 6585.8).	2	(Rodriguez et al., 2015)
Ethanol from aqueous solution	Solvent: 4 glycerol-based deep eutectic solvents (DESs), at 25 °C.	The reported distribution ratio and SF were 0.538 – 0.811 and 4.82 – 22.14, respectively.	1	(Rodriguez et al., 2016)
Ethanol from aqueous solution	Solvent: 10 deep eutectic solvents (DESs), at 25 °C, contacted for 2 h, settled for 2 h.	The reported distribution ratio and SF were 2.09 – 123.12 and 103.33 – 31357.66, respectively.	1	(Hadj-Kali et al., 2017)
Ethanol from aqueous solution	Solvent: ethylene glycol, propane-1,3-diol, 1,4-butanediol or formamide, at 36 °C, contacted for 1 h., settled for 6 h.	The reported distribution and selectivity coefficients were 1.4 – 3.07 and 3.26 – 30.13, respectively.	1	(Jia et al., 2017)
Ethanol from aqueous solution	Solvent: [emim][Tf2N] and [hmim][Tf2N], at 10, 30 and 50 °C, contacted for 10 h, settled for 12 h.	Distribution and selectivity coefficients were 1.26 – 10.07 and 1.86 – 26.67, respectively.	1	(Cháferet al., 2018)

Ethanol from aqueous solution	Solvent: n-dodecane, at 30 °C.	In a single-stage, n-dodecane extracted ethanol completely leaving the pure water in the aqueous phase.	3	(Jesús and Juan 2018)

K_{DE} = ethanol distribution coefficient; α = separation factor

2.7. Butanol purification

Butanol is traditionally produced by the ABE (acetone-butanol-ethanol) process from biomass using batch or continuous fermentation processes. LLE can be coupled with the fermentation process (extractive fermentation) or performed after the fermentation step (external) to separate the butanol from the fermentation broths. Due to the low inhibition of the product and improved BuOH productivity, the extractive fermentation process is more suitable for separating butanol from fermentation broths over external solvent extraction. Several solvents have been tested to determine their selectivity to butanol and biological compatibility with fermented organisms, including oleyl alcohol (Gonzalez-Penas et al., 2014) (decanol (Bankar et al., 2012), tri-butyl phosphate (TBP) (Evanko et al., 2013), 2-butyl-1-octanol (Gonzalez-Penas et al., 2014), and decanol-oleyl alcohol mixture. Table 2.1.7 summarizes distribution coefficients and selectivity of butanol for selected solvents. There is a wide variation in the values of the distribution coefficient even for a single solvent between the different studies. For example, oleyl alcohol (OA) showed varied distribution coefficient values among the reported results; and this could be due to the differences in its chemical purity. For instance, Verma et al. (2018) used OA with ≥99% chemical purity and reported a distribution coefficient for OA in the range of 59.0 – 218. Whereas Cascon et al. (2011) utilized OA with ca.60% purity and achieved a 3.32 distribution coefficient. Among the employed solvents, oleyl alcohol is studied extensively and displays good biological compatibility and distribution coefficients. Compared to oleyl alcohol, decanol and mesitylene have shown higher distribution coefficients for butanol, however, they are toxic to fermented cells. It has been observed that separating agents with a high distribution factor of BuOH were toxic to fermentation microorganisms, therefore, possible solutions are to find more green solvents or identify more tolerant cells. Figure 2.1.3 shows the extraction of biofuel via liquid fluid - combined with the conventional partitioned wall columns configuration.

Ionic liquids (ILs) have recently gained a lot of interest as alternatives to organic solvents to recover butanol from aqueous solutions. Table 2.1.8 summarizes distribution coefficients and selectivity of butanol for selected ionic liquids. Selectivity and distribution coefficients of butanol varied greatly among the employed ILS. The reported distribution coefficients were in the range of 1.1 – 903, while the selectivity ranged from 12.2 to 2138.2. These variations can be attributed to the differences in ILs chemical and physical properties. From this Table, it can be concluded that butanol can be recovered effectively, and high selectivity and distribution coefficients can be achieved. Various ILs were investigated. Ha et al. (2010) used imidazolium-based ionic liquids and reported a distribution coefficient of 1.94, selectivity of 132, and extraction efficiency of 74% at 323.15 K. Extraction efficiency and selectivity of butanol were dependent

on the polarity of the ILs. Simoni et al. (2010) achieved selectivities in the range of 30 – 300, and [hmim][eFAP] was considered a good solvent for 1-butanol extraction. Biobutanol recovery with [TOAMNaph] has been reported to require 73% less energy compared to conventional distillation (Garcia-Chavez et al., 2012)

Table 2.1.7: Distribution coefficient for butanol and water (D_{BuOH} and DH_2O) and the selectivity of butanol/water separation for selected solvents.

Product	Solvent	Initial conc.	Temp. (°C)	BuOH org	H_2O org	BuOH aq	H_2O aq	D_{BuOH}	D H_2O	Selectivity	Ref.
BuOH	Oleyl alcohol	2 wt %	37	–	–	–	–	3.4	–	192	(Roffler et al., 1988)
BuOH	Hexane	2 wt %	37	–	–	–	–	0.5	–	2700	(Groot et al., 1990)
	Heptanol	2 wt %	37	–	–	–	–	11	–	180	
	Octanol	2 wt %	37	–	–	–	–	10	–	130	
	Dibutyl adipate	2 wt %	37	–	–	–	–	2.5	–	2	
	Decane	2 wt %	37	–	–	–	–	0.3	–	4300	
	Sesame oil	2 wt %	37	–	–	–	–	0.3	–	220	
BuOH	Oleyl alcohol	2 wt %	r.t.	–	–	–	–	3.32	–	–	(Cascon et al. 2011)
i-BuOH	Butyl acetate,	0.7 wt %	25	0.83	1.3	0.34	99.7	2.5	0.013	187	(Evanko et al., 2013)
	Tri-butyl phosphate	1.4 wt %	25	1.2	7.1	0.22	99.8	5.4	0.071	76	
	2-Heptanone	1.0 wt %	25	1.15	1.7	0.44	99.2	2.6	0.017	155	
	Decanol	0.8 wt %	25	1.11	3.8	0.30	99.7	3.8	0.038	99	
	Octane	–	24	2.5	0.076	4.6	95.4	0.543	0.0008	650	
	Gasoline	–	24	0.38	0.08	0.58	99.4	0.66	0.0008	800	
BuOH	Octane	–	24	2.5	0.07	4.6	95.4	0.55	0.0008	650	
BuOH	Oleyl alcohol	10.6 g/L	36	–	–	–	–	4.57		294.7	(Gonzalez-Penas et al., 2014)
	2-butyl-1-octanol	10.6 g/L	36	–	–	–	–	6.76		644.8	
	Diisobutyl adipate	10.6 g/L	36	–	–	–	–	2.6		834.1	
	Silicon oil	10.6 g/L	36	–	–	–	–	0.59		3161.9	
	Pomace oil	10.6 g/L	36					0.62		577.6	
1-BuOH	Mesitylene	2 wt %	25	0.254	0.008	0.012	0.988	21.3	–	2591.2	(Verma et al., 2018)
	Mesitylene	2 wt %	25	0.529	0.098	0.013	0.987	39.5	–	398.9	
	Oleyl alcohol	2 wt %	25	0.218	0.035	0.001	0.997	218.0	–	6932.6	
	Oleyl alcohol	2 wt %	25	0.118	0.066	0.002	0.997	59.0	–	777.1	

r.t. room temperature.

Table 2.1.8: Butanol extraction performance results for selected ionic liquids

Product	Ionic Liquids	Initial conc.	Temp. (°C)	BuOH org	H_2O org	BuOH aq	H_2O aq	D $_{BuOH}$	D $_{H_2O}$	Selectivity	Ref.
1-BuOH	[hmim][Tf2N]	5 wt %	22	–	–	–	–	6	0.0666	90	(Simoni et al., 2010)
	[HOhmim][Tf2N]	5 wt %	22	–	–	–	–	1.5	0.0375	40	
	[hmim][eFAP]	5 wt %	22	–	–	–	–	5	–	300	
1-BuOH	[Omim][Tf2N]	6 wt %	25	–	–	–	–	1.372	0.018	78.9	(Ha et al., 2010)
	[Omim][BF4]	6 wt %	25	–	–	–	–	2.183	0.179	12.2	
	[Hmim][Tf2N]	6 wt %	25	–	–	–	–	1.253	0.019	66.11	
BuOH	[THA][DHSS]	2 wt %	r.t.	–	–	–	–	7.99	–	–	(Cascon et al., 2011)
	[Ph3t][DCN]	2 wt %	r.t.	–	–	–	–	7.49	–	–	
1-BuOH	TOAMNaph	1 wt %	25	0.0095	0.0765	0.0005	0.9996	21	0.08	274	(Garcia-Chavez et al., 2012)
	[HMIMNTf2]	1 wt %	25	0.0056	0.0092	0.0050	0.9950	1.11	0.01	120	
	[TDAMCH]	1 wt %	25	0.0075	0.0650	0.0009	0.9991	8.49	0.07	130	
1-BuOH	[HMIM][TCB]	–	35	0.067–0.487	0.502–0.560	0.002–0.019	0.981–0.997	25.6–33.5	0.512–0.562	45.9–66.5	(Domańska and Królikowski 2012)
	[DMIM][TCB]	–	35	0.29–0.48	0.23–0.52	0.01–0.02	0.98–0.99	24–48	0.23–0.525	45.2–137.9	
	[P14,6,6,6][TCB]	–	35	0.127–0.60	0.140–0.522	0.001–0.018	0.982–0.997	50–903	0.143–0.554	26.6–127	
1-BuOH	[DMIM][TCB]	2 wt %	25	–	–	–	–	3.27	–	104	(Pitner et al., 2013)
	[OMIM][TCB]	1 wt %	25	–	–	–	–	3.7	–	97	
1-BuOH	[TDTHP][Phosph]	–	25	0.151–0.724	0.156–0.228	0.0004–0.038	0.962–0.9996	18.9–377.8	0.162–0.228	80.18–2138.16	(Rabari and Banerjee 2013)
n-BuOH	[BMIM][Tf2N]	3 wt %	30	–	–	–	–	1.435	0.0211	79.86	(Kubiczek et al., 2016)
	[Hmim][PF6]	3 wt %	30	–	–	–	–	1.10	0.0244	54.58	
	[Bmp][Tf2N]	3 wt %	30	–	–	–	–	1.17	0.0193	73.94	
1-BuOH	[HMIM]FEP	2 wt %	25	–	–	–	–	176.8	–	360	(Dezhang et al., 2019)

D = Distribution coefficient

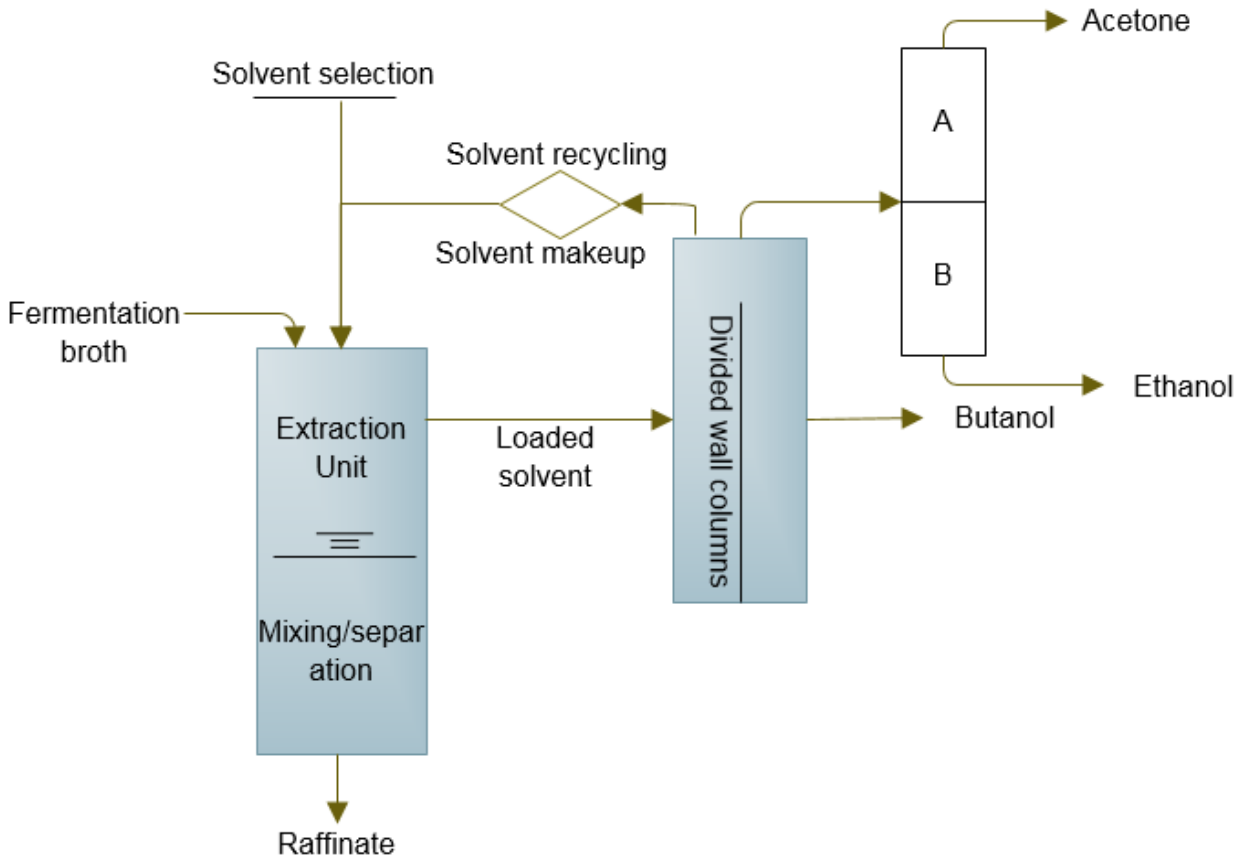

Figure 2.1.3: LLE extraction-combined with conventional divided wall columns configuration.

2.8. 2,3-Butanediol recovery

2,3-Butanediol (2,3-BDO) is generated by biomass fermentation and is applied as an additive for fuel, lubricant, or feedstock for chemical production. Different classes of solvents (alcohols, phenolics, ester, chlorinated, ketone, ether, etc.) and ionic liquids were examined for LLE of 2,3-BDO from aqueous streams. Table 2.1.9 displays distribution coefficients and SFs of 2,3-butanediol for selected solvents. Oeyl alcohol (Harvianto et al., 2018; Khayati et al., 2009; Birajdar et al., 2014), 2-methyl-2-BuOH, 3-methyl-1-BuOH, 1-BuOH (Birajdar et al., 2014; Wu et al., 2008) isobutanol (Wu et al., 2012), 2-ethyl-1-hexanol (Gilani et al., 2006), tributylphosphate (TBP), 2- sec butyl-phenol (Birajdar et al., 2015), dodecanol, and ILs such as tetraoctylammonium 2-methyl-1-naphthoate (TOA MNaph) (Garcia-Chavez et al., 2012) were investigated comprehensively as extractants. A purity of 99% was obtained using n- butanol, cyclohexanol, and TBP (Birajdar et al., 2015). Distribution factors were reported in the range of 0.32 to 6.5, while the SF ranged from 2.01 to 421.9. Oleyl alcohol appears to be the most suitable solvent for 2,3-BDO extraction. It is characterized by a higher distribution coefficient (0.06–6.5) and selectivity (7.24–421.9) for 2,3-BDO than other solvents. Also, 2- sec butyl phenol, 2-ethyl-1-hexanol, and 1-butanol have shown a potential capacity for 2,3-BDO recovery.

Table 2.1.9: Distribution coefficients and separation factors of 2,3-butanediol for selected solvents at different temperatures

Solvent	Temperature (°C)	Distribution coefficient (K_d)	Separation factor (α)	Ref.
2-(2-Butyl)phenol	25	1.20	4.23	(Birajdar et al., 2015)
tri (n-butyl) phosphate (TNBP)	25	0.32	3.43	Birajdar et al., 2015)
Cyclohexyl Alcohol	25	0.90	2.80	Birajdar et al., 2015)
n- butanol	25	1.60	2.01	Birajdar et al., 2015)
1-butanol	25	0.72–0.88	1.5–2.95	Wu et al., 2008
	25	1.60	–	(Birajdar et al., 2014)
Isobutanol	25	1.45–1.60	2.27–2.92	(Wu et al., 2012)
1-pentanol	25	0.55–0.76	2.58–4.13	(Jeong et al., 2018)
	45	0.82–1.01	2.65–5.09	
2-ethyl-1-hexanol	27	1.26–1.81	1.99–20.1	(Gilani et al., 2006)
	25	0.25	–	(Birajdar et al., 2014)
Methyl-2-pentanol	25	0.35–0.54	3.56–4.68	(Yim et al., 2019)
	35	0.4–0.65	3.57–6.84	
Oleyl alcohol	27	2.66–6.52	2–420	(Khayati et al., 2009)
	25	0.06	–	(Birajdar et al., 2014)

3. Challenges and opportunities

Biorefinery demands several new routes of separation technology in downstream processing in order to be economically viable. LLE plays a vital role in downstream treatment but faces many challenges. Several factors influence LLE's performance in the bioprocesses and biomaterials application. Based on this review, these challenges represent in the high consumption of potential toxic solvent, high solvent costs, poor solvent biocompatibility, product loss, environmental pollution, difficult/costly solvent regeneration, and solvent choice. Table 2.1.10 displays some challenges of LLE in biorefining processes and discusses the possible solutions. These challenges are discussed in some details in this section, while the opportunities offered by LLE in biorefinery processes are also outlined.

Table 2.1.10: Challenges of liquid-liquid extraction in biorefining processes and the possible solutions.

Process	Challenge	Cause	Possible solution
Bioenergy and biomaterials	Solvent selection	Choosing the right solvent for a particular biomass biorefining process is a difficult task, as a combination of several factors must be considered.	Conducting preliminary screening tests for solvents with the use of the media and strain of interest could be more realistic. However, a solvent selection guide can be used to prepare a tentative list of solvents that will be utilized for further screening.
Bioenergy (bioethanol, biobutanol, 2,3-Butanediol)	Solvent biocompatibility	Poor biocompatibility of the most applied solvents with the used microorganisms	Solvents that have no or reduced toxicity effect on fermentation cells need to be developed. Organic solvents need to be screened exclusively based on the microorganisms of interest using computer-assisted models. Using a protective wall (e.g., membrane) (Matsumura and Märkl 1984) or another agent (Honda et al., 1986) to prevent cells from contacting with solvent was also shown its effectiveness. Alternatively, the use of microorganisms that could tolerate the toxicity of the solvent and its inhibitory effect can address the problem but are calling for further research.
Biomaterials (Lignin, Sugars, Furfural)**, bioenergy (**bioethanol, biobutanol, 2,3-Butanediol)	Solvent recovery	Most of the solvent recovery approaches (e.g., evaporation, and distillation) are energy-intensive. Also, due to thermal stability issues of some substances (e.g., lactic acid, sugars), thermal regeneration is not recommended which necessitates the application of alternative approaches like back-extraction (Kiss et al., 2016). Some solvents (e.g., ethyl acetate) are partially soluble in aqueous solutions (McPartland et al., 2012), thus their use may increase the problem.	Due to the reduced energy demand, solvent-resistant nanofiltration (NF), as a new technology, could provide a more cost-effective solvent recovery mean (Welton 2015). However, the problems related to membrane fouling and the cost of membrane replacement must be tackled to make schemes involving membranes more attractive.
Biomaterials (Lignin, Sugars, Furfural), **inhibitors removal**	Products losses	Several biomass-derived compounds are characterized by reduced volatility and increased thermal sensitivity (Nguyen et al., 2017).	A low-temperature processing condition is required.
Bioenergy (bioethanol, biobutanol, 2,3-Butanediol)	Solvent toxicity	The use of conventional volatile/toxic solvents, as the most common employed solvents, have been classified as problematic or hazardous (Prat et al., 2017).	The development of alternative green solvents is needed to replace the use of volatile and toxic organic compounds.
Biomaterials (Lignin, Sugars, Furfural), **bioenergy (**bioethanol, biobutanol, 2,3-Butanediol)	Solvent costs	The current market value of organic solvents is high. Also, a dilute concentration of the product (s) of interest requires a large volume of solvent coupled with high energy consumption.	Finding more effective extracting agents that enable less usage of solvent is required.
Lignin fractionation	Time-consuming	Some processes such as lignin fractionation involve several treatment steps (successive extraction). It is therefore not only time-consuming but also complicates the whole process.	An intensified process coupled with an effective solvent could solve this problem and reduce the downstream processing steps.
Hydrolysates and fermentation broths	Mass transfer issues	Phase separation problem: due to a complex hydrolysate (many dissolved solid substances), the high viscosity of fermentation broths, and low solubility of carbohydrates in organic solvents.	Carbohydrates extraction can be facilitated by a carrier addition like primary amines (Hameister and Kragl 2006).
A downstream process of LLE	Scaling up challenges	The high current market value of the extractant agents and the cost of the subsequent solvent recovery process make the scaling of LLE problematic.	Developing cheap extractants and effective solvent recovery processes are needed.
Bioenergy and biomaterials	Personal safety and environmental footprint	Most of the commonly employed solvents have toxicity, affecting not only the microorganisms but also the operators, and the environment.	The development of green eco-friendliness solvents is needed.

Solvent selection: Selection of a suitable separating agent is the backbone of the process where it can significantly affect the outcome of the operation but choosing the right solvent for a particular biomass biorefining process is a difficult task, as a combination of several factors must be considered. These factors may include solvent capacity for the partitioning of the product of interest and solvent's selectivity for the targeted solute over other components (Offeman et al., 2005b; McPartland et al., 2012). The selection of this or that solvent depends mainly on the characteristic of the solute of interest, solvent properties, and the extraction methodology. Thus, to perform the LLE process, it is necessary to know the underlying principles governing extraction technique, such as solute properties (e.g., solubility, molecular weight, and acid dissociation), distribution coefficient, and extraction selectivity. As a rule of thumb, the two employed solvents should be immiscible, and the extractant must have good chemical stability, rapid phase separation, reduced solubility in the raffinate phase, and low harmfulness for the operator and the environment (Offeman et al., 2008). Since it may be very difficult to find a solvent that can meet all these requirements, therefore, it is necessary to find a compromise. Also, conducting preliminary screening tests for solvents with the use of the media and strain of interest could be more realistic. Selection of the right diluent is necessary as the diluent is required to improve the extraction selectivity (Yang et al., 2013), increase the density variance amongst the phases, and reduce the viscosity of the solvent (Rydberg et al., 2004).

In the literature, various methods have been developed to assist with solvents selection such as the use of solvent descriptive guides, screening techniques, database lookups, and predictive models. Recently, Syngenta developed an interactive tool with a browser-type interface using R software to aid in solvent selection (Piccione et al., 2019). They believe this tool is a steppingstone towards designing an experiment in chemical process development. AstraZeneca also developed an interactive tool to facilitate the selection of solvents and this tool is currently available and in active use by the scientists at AstraZeneca (Diorazio et al., 2016). With this tool, users can assess solvents based on chemical reactivity, physical properties, and safety/health/environmental (SHE) impact, serving the generic needs of the process. However, this guide categorized a reduced number of solvents and, therefore, should be expanded to include larger data sets. Likewise, other companies have developed their guides like Sanofi's solvent selection guide, which ranked solvents based on SHE facilitating green (bio-derived) solvents selection (Prat et al., 2015), and GSK's solvent selection guide, which embeds sustainability rules and physical properties into the solvent selection (Henderson et al., 2011). On the other hand, several product-related screening studies exist. Offeman et al. (2005a) and Koullas et al. (1999) screened several organic solvents to generate solvent candidates for ethanol recovery. Whereas Shen and Lehn (2020) applied a conductor-like screening model for real solvents to improve the separation efficacy of lignin-derived monomers. In the same respect, Kwok et al. (2020) used several screening classes (performance, hazards/environment, cost/availability, and process economics) to provide metrics for 30 solvents from multiple molecular functional groups. Among the

investigated solvent, 1-methylpiperazine emerged as a potential candidate for lignin separation. In the future, solvents selection approaches would be more useful if they used automated data processing tools, which could result in reliable and efficient solvent selection.

Solvent toxicity: Some solvents such as chloroform, diethyl ether, and dichloromethane are highly toxic to both the operator and the environment, making solvent extraction an unacceptable means in many industrial applications. Prat et al. (2015) ranked the common solvents as recommended, problematic, hazardous, and highly hazardous. Most common solvents have been classified as problematic or hazardous. Thus, solvent loss during the materials or solvent recovery can generate problematic waste by-products that need to be managed in an environmentally safe manner, which increases the cost of the extraction process (the cost of waste treatment). Therefore, research is needed to find safer and environmentally friendly solvents to replace the use of volatile organic compounds. To address these problems, recently significant progress has been made in the transition towards more sustainable solvent alternatives, and a wide range of green solvents have been developed or proposed. Clarke et al. (2018) recently reviewed the major sustainable organic solvents in use today (e.g., ionic liquids, deep eutectic, and renewable solvents), considering technical, economic, and environmental aspects. This review proposed several sustainable solvents that can be derived from plant biomass within integrated bio-refining processes. This area may open up interesting new avenues for further research and industrial considerations.

Solvent biocompatibility: Some biorefinery processes involve bioactive organisms (e.g., ethanol, butanol, and 2,3-butanediol -producing microorganisms) or biocatalysts, which may be exposed to solvents used in one form or another. Thus, the potential extraction agent should be biocompatible with the employed microorganisms, or the use of organisms that could tolerate the toxicity of the solvent and its inhibitory effect. A further investigation into the latter option to combine with a solvent process is an area of interest. Solvent toxicity can lead to reduced product yield and productivity. In finding a benign solvent, Offeman et al. (2008) carried out screening tests for ethanol extraction with different alcohol solvents, investigated the performance of extractants and their noxiousness to yeast. They found that solvents containing twelve or fewer carbon had an inhibitor and toxic effect on yeast, while those with fourteen or more carbon are not toxic. In terms of low toxicity, oleyl alcohol appears to be the best choice for extraction processes that involve microorganisms because it combines a good SF with low toxicity.

Solvent recovery: Regeneration of the used solvent and minimization of solvent losses must be considered in process design to reduce process costs, as solvent expenses are a significant contributor to the increased cost of the process. Distillation under low pressure, flash vaporization, back extraction, and hot water washing are common methods of solvent regeneration (Kim et al., 1999). However, using these methods may result in losses of solvents as well as being expensive due to increased energy demand. For instance,

vaporization of the organic solvent has the disadvantage of relatively high-energy demand, as well as reagents of solvent extraction, are usually not designed for elevated temperature applications, and different decomposition mechanisms may be initiated at high temperature, which may make the solvent unsuitable for reuse. Similarly, solvent recovery by distillation requires protective measures to avoid any undesirable reactions, which may lead to losses of the solvent. Also, distillation entails the use of VOCs and needs a lot of energy, leading to various health and environmental problems. Due to the reduced energy demand, solvent-resistant nanofiltration (NF), as a new technology, could provide a more cost-effective solvent recovery mean (Welton 2015; Rundquist and Pink 2012). It has been reported that the nanofiltration membrane as an in situ solvent recovery process can reduce the solvent consumption to nearly zero while removing 98% of the impurities (Kim et al., 2014). Generally, membrane technologies are characterized by excellent fractionation/separation capacity and reduced energy requirements, which may further expand LLE applications in the future. However, membrane fouling could be the major shortcoming of applying this technology in solvent recovery in biomass biorefinery (Bokhary et al., 2018). In the same respect, Zhu et al. (2015) fabricated high-performance graphene-modified absorbents by agile thermal reduction of graphene oxide on melamine foam skeletons to separate organic solvents from water. It believes that this technique is capable to effectively recycle organic solvents and that the cost-effective manufacturing method allows for a scaling up of the process. Instead, various techniques are used to improve the phase separation and ultimately maintain the properties of the solvent as well as facilitate the solvent recovery from the solute, such as adjusting the operating conditions of the process (e.g., pH, temperature, phase ratio).

Products recovery and losses: Recovering products from organic phases remains a major challenge for LLE as a downstream process and requires the synthesis of more selective solvents. In many cases the losses of the product have been reported, for example, Llano et al. (2015) reported 1.4 g/l sugar losses (0.72 %) during phenolic compound extraction from spent sulfite liquor. Several similar reports have been stated about the loss of sugar during the removal of fermentation inhibitors. To overcome these limitations, some researchers have developed methods to recover products extracted from the organic phase. For example, Stiefel et al. (2017) indicated that lignin can be transferred from the organic phase to alkaline solutions (NaOH) of different concentrations for further use. It has been reported that at pH values of 13 and 14, lignin can be extracted almost completely from the organic phase, however, this process leads to changes in the molecular structure of the lignin besides NaOH is very corrosive. Other methods were also used, such as evaporation of an organic solvent (Viell et al., 2013), stripping off the lignin (Hamala et al., 1982), and precipitation of lignin with an anti-solvent followed by drying (De Wild et al., 2012). However, these methods have been characterized by higher energy demand and higher costs of anti-solvent. On the other

hand, extensive literature discussions are currently obtainable on improving solvent selection as previously discussed, which would contribute significantly to reducing product loss.

Costs: The current solvent market, high equipment costs, product separation from the extractant, and subsequent solvent recovery process can make LLE application expensive and a fairly complex process. Hence, the cost of LLE application should be carefully considered when design LLE processes for biomass biorefinery products recovery and purification, particularly for low-value products (relative to the prices of metals). The design of low-cost, low solubility in water, and high separation efficiency solvents and processes call for further studies. In this regard, Radient Technologies Inc. (Edmonton, Canada) has developed Microwave Assisted Processing (MAP™) technology and they design demonstration plants to extract natural products. This technology has been reported to feature lower solvent and energy use as well as increased product selectivity and purity with ease of commercial scalability and lower capital costs. Aghazadeh and Engelberth (2016) conducted a techno-economic analysis on the effect of fermentation inhibition (acetic acid) removal from corn stover hydrolysate by LLE on total revenues from a commercial-scale bioethanol plant with a processing capacity of 61 million gallons per year. This study indicated that the extraction column cost accounted for less than 1% of the total cost of the biorefinery equipment, while the annual solvent purchase cost is about 5.9% of the total operating cost of the plant, but removing the inhibitor can improve ethanol production by 11-14%.

Figure 2.1.4 shows the applications of LLE in biomass biorefinery processes. Among the solvent application opportunities in biorefinery, LLE is preferred in separating products with similar volatilities (e.g., organic acid in water), products forming azeotropes (e.g., ethanol-water), and products that are thermo-sensitive (e.g., natural antioxidants). The diluted streams of biorefinery usually require expensive separation schemes for concentration (e.g., distillation), which are very energy-intensive. Here, the use of LLE can be economically advantageous, in part because the solvent does not need large amounts of energy or costly equipment, especially when a non-volatile solvent is used, which enables the subsequent solvent recovery (Rodriguez et al., 2015). On the other hand, conventional distillation cannot remove a homogeneous azeotrope, and extractive or azeotropic distillation processes involve high pressures or high temperatures and, thus, they entail high energy consumption; in this case, a LLE could also be the preferred method. Also, LLE can be the preferred method for butanol separation from ABE fermentation broths due to its reduced butanol concentration and increased hydrophobicity, which makes it less miscible with water than ethanol (Huanget al., 2014). Another area that holds particular potential in biorefining is the separation of thermo-sensitive materials like large organic molecules, phenolic compounds, and fermentation products. LLE is typically performed at low temperatures so that there is the advantage of reducing the loss

of thermally sensitive products. Also, mild process conditions may lead to rather low energy requirements and reduced solvent vaporization (Bo and Jianguo 2013).

Recently integrated LLE hybrid processes are proposed to minimize energy consumption and carbon dioxide emissions (Zhao et al., 2018) while maximizing the product purity (Avilés Martínez et al., 2011). Avilé Martínez et al. (2011) proposed a hybrid system of LLE and extractive distillation (ED) to reduce energy usage and total costs for the purification step in the bioethanol production process. While Zhao et al. (2018) investigated hybrid processes of LLE/heterogeneous azeotropic distillation (HAD) and LLE/ED to separate a blend of propylene glycol, methyl ether, and water. Both LLE-HAD and LLE-ED demonstrated good economic and environmental capabilities compared with the traditional processes, achieving reductions of 40.24% and 34.18% in total annual cost and 45.37% and 43.95% in CO_2 emissions, respectively. Conversely, Chen et al. (2015) reported better economics (reduced operating and annual costs) for the LLE-ED process compared to LLE-HAD when they studied the separation of pyridine and water using the n-propyl format or diisopropyl ether as solvents.

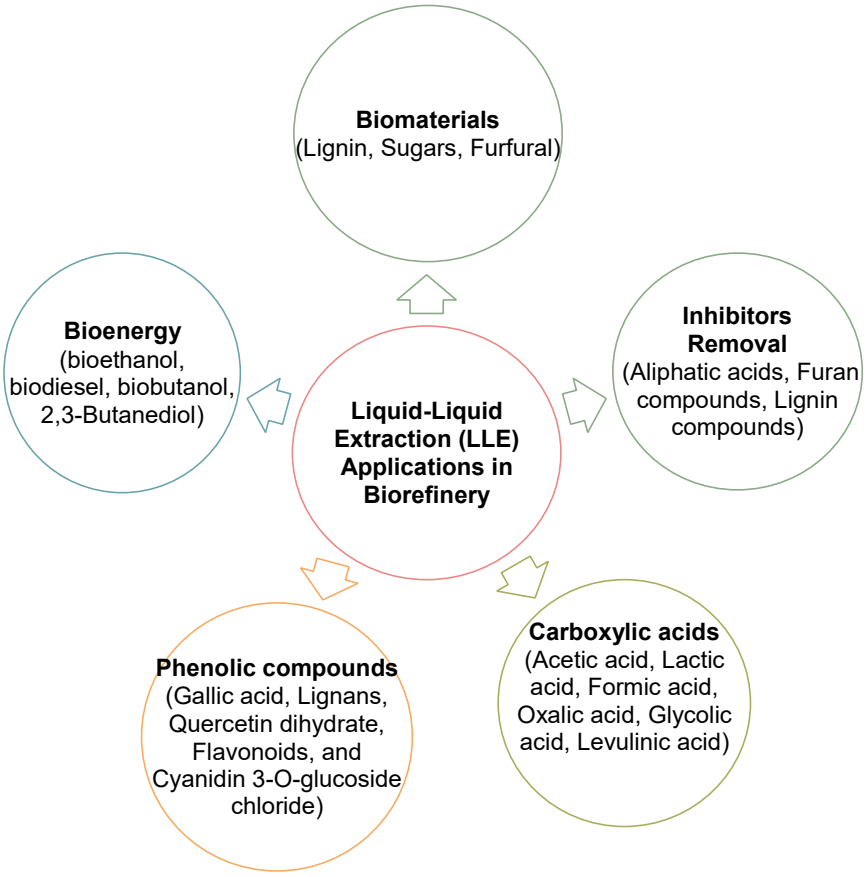

Figure 2.1.4: Liquid-Liquid applications in biorefinery

4. Conclusions and future perspectives

In biomass biorefining processes, the applicability of various solvent classes as extracting agents has been widely studied to fractionate, separate, and purify a variety of useful bioproducts or remove unwanted materials. In the present review, perspectives on LLE applications in biorefineries are presented, and future research directions are identified. Numerous types of extractants show promise in recovery, separation, or purification of bioproducts from aqueous streams. Although LLE is employed in different biorefining processes and has shown great potential, several challenges still exist and need to be overcome and equally, there are many opportunities for future development. The employed solvents must meet several requirements in order to be in line with the concept of biorefinery, such as low toxicity, high selectivity, excellent biocompatibility, reduced product losses, and fast degree and rate of de-mixing. However, most of the commonly employed solvents have toxicity, affecting not only the microorganisms but also the operators and the environment, thus developing a sustainable green LLE process is required. Also, computer-assisted screening studies are needed not only to identify solvents that are more bio-compatible but also to provide maximum extraction efficiency and make biorefinery processes economically viable. Moreover, the current market value of the extractant agents and the cost of the subsequent solvent recovery process have hindered the scaling-up of LLE as a downstream process. Thus, one possible solution would be to find cheap extractants or offset these costs by developing cost-effective techniques of solvent recovery. Finally, techno-economic analyses of LLE applications under the biorefinery concept are needed to determine its economic feasibility.

Acknowledgements

This research was financially supported by the Ontario Graduate Scholarship (OGS) and Natural Sciences and Engineering Research Council of Canada (NSERC).

References

[1] Novotny, M., Nuur, C., 2013. The transformation of pulp and paper industries: the role of local networks and institutions, Int. J. Innovation and Regional Development. 5, 41–57. https://EconPapers.repec.org/RePEc:ids:ijirde:v:5:y:2013:i:1:p:41-57.

[2] Moshkelani, M., Marinova, M., Perrier, M., Paris, J., 2013. The forest biorefinery and its implementation in the pulp and paper industry: Energy overview, Appl. Therm. Eng. 50, 1427–1436. https://doi.org/10.1016/j.applthermaleng.2011.12.038.

[3] Bokhary, A., Liao, B., Cui, L., Lin, H., 2017. A Review of Membrane Technology for Integrated Forest Biorefinery, J. Membr. Sci. Res. 3, 120–141. https://doi.org/10.22079/JMSR.2016.22839.

[4] Kiss, A.A., Lange, J.P., Schuur, B., Brilman, D.W.F., van der Ham, A.G., Kersten, S.R., 2016. Separation technology–Making a difference in biorefineries, Biomass Bioenerg. 95, 296–309. https://doi.org/10.1016/j.biombioe.2016.05.021.

[5] Nguyen, H., DeJaco, R.F., Mittal, N., Siepmann, J.I., Tsapatsis, M., Snyder, M.A., Fan, W., Saha, B., Vlachos, D.G., 2017. A review of biorefinery separations for bioproduct production via thermocatalytic processing, Annu. Rev. Chem. Biomol. Eng. 8, 115–137. https://doi.org/10.1146/annurev-chembioeng-060816-101303.

[6] Huang, H.J., Ramaswamy, S., Tschirner, U.W., Ramarao, B.V., 2008. A review of separation technologies in current and future biorefineries, Sep. Purif. Technol. 62, 1–21. https://doi.org/10.1016/j.seppur.2007.12.011.

[7] Bo, H., Jianguo, Z., 2013. Liquid-Liquid Extraction (LLE), in: S. Ramaswamy, H.J. Huang, B.V. Ramarao (Eds.), Separation and purification technologies in biorefineries, John Wiley & Sons, Ltd., Oxford, U.K., 2013, 61–78.

[8] Vane, L.M., 2008. Separation technologies for the recovery and dehydration of alcohols from fermentation broths. Biofuels, Bioproducts and Biorefining, 2, 553–588. https://doi.org/10.1002/bbb.108.

[9] Mishra, S., 2019. Comprehensive outlook for liquid-liquid separation of rare earth elements, in: A. Akcil (Eds.), Critical and rare earth elements: Recovery from secondary resources, CRC Press, 165 – 188.

[10] Bourgeois, D., El Maangar, A., Dourdain, S., 2020. Importance of weak interactions in the formulation of organic phases for efficient L/L extraction of metals, Curr. Opin. Colloid Interface Sci. 46, 36–51. https://doi.org/10.1016/j.cocis.2020.03.004.

[11] Sprakel, L.M.J., Schuur, B., 2019. Solvent developments for liquid-liquid extraction of carboxylic acids in perspective, Sep. Purif. Technol. 211, 935–957. https://doi.org/10.1016/j.seppur.2018.10.023.

[12] Gonçalves, C.B., Rodrigues, C.E., Marcon, E.C., Meirelles, A.J., 2016. Deacidification of palm oil by solvent extraction, Sep. Purif. Technol. 160, 106–111. https://doi.org/10.1016/j.seppur.2016.01.016.

[13] Rydberg, J., Michael, C., Claude, M., Gregory, R. C., 2004. Solvent extraction principles and practice revised and expanded, second ed., CRC press, Taylor & Francis Group.

[14] El-Nadi, Y.A., 2017. Solvent extraction and its applications on ore processing and recovery of metals: classical approach, Sep. Purif. Rev. 46, 195–215. https://doi.org/10.1080/15422119.2016.1240085.

[15] Kislik, V.S., 2012. Solvent extraction: classical and novel approaches. Elsevier.

[16] Aziz, H.A., Kamaruddin, A.H., Bakar, M.A., 2008. Process optimization studies on solvent extraction with naphthalene-2-boronic acid ion-pairing with trioctylmethylammonium chloride in sugar purification using design of experiments, Sep. Purif. Technol. 60, 190–197. https://doi.org/10.1016/j.seppur.2007.08.011.

[17] Bokhary, A., Leitch, M., Gao, W.J., Fatehi, P., Liao, B.Q., 2019. Separation of hemicelluloses and lignins from synthetic hydrolyzate and thermomechanical pulp mill process water via liquid-liquid extraction, Sep. Purif. Technol. 215, 508–515. https://doi.org/10.1016/j.seppur.2019.01.041.

[18] Minier, M., Coma, G., 1981. Production of ethanol by coupling fermentation and solvent extraction, Biotechnol. Lett. 3, 405–408. https://doi.org/10.1007/BF01134098.

[19] Harvianto, G.R., Haider, J., Hong, J., Long, N.V.D., Shim, J.J., Cho, M.H., Kim, W.K., Lee, M., 2018. Purification of 2, 3-butanediol from fermentation broth: process development and techno-economic analysis, Biotechnol. Biofuels. 11, 1–16. https://doi.org/10.1186/s13068-018-1013-3.

[20] Verma, R., Dehury, P., Bharti, A., Banerjee, T., 2018. Liquid-liquid extraction, COSMO-SAC predictions and process flow sheeting of 1-butanol enhancement using mesitylene and oleyl alcohol, J. Mol. Liq. 265, 824–839. https://doi.org/10.1016/j.molliq.2018.06.088.

[21] Um, B.H., Friedman, B., van Walsum, G.P., 2011. Conditioning hardwood-derived pre-pulping extracts for use in fermentation through removal and recovery of acetic acid using trioctylphosphine oxide (TOPO), Holzforschung. 65, 51–58. https://doi.org/10.1515/hf.2010.115.

[22] Cebreiros, F., Guigou, M.D., Cabrera, M.N., 2017. Integrated forest biorefineries: recovery of acetic acid as a by-product from eucalyptus wood hemicellulosic hydrolysates by solvent extraction, Ind. Crop. Prod. 109, 101–108. https://doi.org/10.1016/j.indcrop.2017.08.012.

[23] Tomek, K.J., Saldarriaga, C.R.C., Velasquez, F.P.C., Liu, T., Hodge, D.B., Whitehead, T.A., 2015. Removal and upgrading of lignocellulosic fermentation inhibitors by in situ biocatalysis and liquid- liquid extraction, Biotechnol. Bioeng. 112, 627–632. https://doi.org/10.1002/bit.25473.

[24] Zautsen, R.R.M., Maugeri- Filho, F., Vaz- Rossell, C.E., Straathof, A.J.J., Van der Wielen, L.A.M., De Bont, J.A.M., 2009. Liquid–liquid extraction of fermentation inhibiting compounds in lignocellulose hydrolysate, Biotechnol. Bioeng. 102, 1354-1360. https://doi.org/10.1002/bit.22189.

[25] Jääskeläinen, A.S., Liitiä, T., Mikkelson, A., Tamminen, T., 2017. Aqueous organic solvent fractionation as means to improve lignin homogeneity and purity. Ind. Crop. Prod. 103, 51–58. https://doi.org/10.1016/j.indcrop.2017.03.039.

[26] Park, S.Y., Kim, J.Y., Youn, H.J., Choi, J.W., 2018. Fractionation of lignin macromolecules by sequential organic solvents systems and their characterization for further valuable applications, Int. J. Biol. Macromol. 106, 793–802. https://doi.org/10.1016/j.ijbiomac.2017.08.069.

[27] Melro, E., Alves, L., Antunes, F.E., Medronho, B., 2018. A brief overview on lignin dissolution. J. Mol. Liq. 265, 578–584. https://doi.org/10.1016/j.molliq.2018.06.021.

[28] Cui, C., Sun, R., Argyropoulos, D.S., 2014. Fractional precipitation of softwood kraft lignin: isolation of narrow fractions common to a variety of lignins, ACS Sustain. Chem. Eng. 2, 959–968. https://doi.org/10.1021/sc400545d.

[29] Shimanouchi, T., Kataoka, Y., Yasukawa, M., Ono, T., Kimura, Y., 2013. Simplified model for extraction of 5-hydroxymethylfurfural from fructose: use of water/oil biphasic system under high temperature and pressure conditions, Solvent. Extr. Res. Dev. Japan. 20, 205–212. https://doi.org/10.15261/serdj.20.205.

[30] Román-Leshkov, Y., Barrett, C.J., Liu, Z.Y., Dumesic, J.A., 2007. Production of dimethylfuran for liquid fuels from biomass-derived carbohydrates, Nature, 447, 982–985. DOI: 10.1038/nature05923.

[31] Kilikian, B.V., Bastazin, M.R., Minami, N.M., Gonçalves, E.M.R., Junior, A.P., 2000.Liquid-liquid extraction by reversed micelles in biotechnological processes, Braz. J. Chem. Eng. 17, 29–38. https://doi.org/10.1590/S0104-66322000000100003.

[32] Gonzalez-Penas, H., Lu-Chau, T.A., Moreira, M.T., Lema, J.M., 2014. Solvent screening methodology for in situ ABE extractive fermentation, Appl. Microbiol. Biotechnol. 98, 5915–5924. https://doi.org/10.1007/s00253-014-5634-6.

[33] Glyk, A., Scheper, T., Beutel, S., 2015. PEG–salt aqueous two-phase systems: an attractive and versatile liquid–liquid extraction technology for the downstream processing of proteins and enzymes, Appl. Microbiol. Biotechnol. 99, 6599–6616. https://doi.org/10.1007/s00253-015-6779-7.

[34] Skovgaard, P.A., Christensen, B.H., Felby, C., Jørgensen, H., 2014. Recovery of cellulase activity after ethanol stripping in a novel pilot-scale unit, J. Ind. Microbiol. Biot. 41, 637–646. https://doi.org/10.1007/s10295-014-1413-8.

[35] Gyamerah, M., Glover, J., 1996. Production of ethanol by continuous fermentation and liquid–liquid extraction, J. Chem. Technol. Biotechnol. 66, 145–152. https://doi.org/10.1002/(SICI)1097-4660(199606)66:2<145::AID-JCTB484>3.0.CO;2-2.

[36] Quijada-Maldonado, E., Aelmans, T.A.M., Meindersma, G.D., de Haan, A.B., 2013. Pilot plant validation of a rate-based extractive distillation model for water–ethanol separation with the ionic liquid [emim][DCA] as solvent, Chem. Eng. J. 223, 287–297. https://doi.org/10.1016/j.cej.2013.02.111.

[37] Aghazadeh, M., Engelberth, A.S., 2016. Techno- economic analysis for incorporating a liquid–liquid extraction system to remove acetic acid into a proposed commercial scale biorefinery, Biotechnol. Prog. 32, 971–977. https://doi.org/10.1002/btpr.2325.

[38] Weeranoppanant, N., Adamo, A., Saparbaiuly, G., Rose, E., Fleury, C., Schenkel, B., Jensen, K.F., 2017. Design of multistage counter-current liquid–liquid extraction for small-scale applications, Ind. Eng. Chem. Res. 56, 4095–4103. https://doi.org/10.1021/acs.iecr.7b00434.

[39] Jiang, H., Tang, Y., Guo, Q.X., 2003. Separation and recycle of phenol from wastewater by liquid–liquid extraction, Sep. Sci. Technol. 38, 2579–2596. https://doi.org/10.1081/SS-120022289.

[40] Ajao, O., Marinova, M., Savadogo, O., Paris, J., 2018. Hemicellulose based integrated forest biorefineries: Implementation strategies, Ind. Crop. Prod. 126, 250–260. https://doi.org/10.1016/j.indcrop.2018.10.025.

[41] Bokhary, A., Maleki, E., Liao, B., 2018. Ultrafiltration for hemicelluloses recovery and purification from thermomechanical pulp mill process waters, Desalin. Water Treat. 118, 103–112. https://doi.org/doi: 10.5004/dwt.2018.22641.

[42] John Griffin, G., Shu, L., 2004. Solvent extraction and purification of sugars from hemicellulose hydrolysates using boronic acid carriers, J. Chem. Technol. Biotechnol. 79, 505–511. https://doi.org/10.1002/jctb.1013.

[43] Mussatto, S.I., Santos, J.C., Ricardo Filho, W.C., Silva, S.S., 2005. Purification of xylitol from fermented hemicellulosic hydrolyzate using liquid–liquid extraction and precipitation techniques, Biotechnol. Lett. 27, 1113–1115. https://doi.org/10.1007/s10529-005-8458-8.

[44] Hameister, D., Kragl, K., 2006. Selective recovery of carbohydrates from aqueous solution facilitated by a carrier, Eng Life Sci. 6, 187–192. https://doi.org/10.1002/elsc.200620906.

[45] Caperos, A., Villar, J.C., 1990. New chemical, and biochemical integrated treatment for the valorization of extractives, carbohydrates and lignin from paper mills and forest exploitation waste into fine aromatic chemicals, surfactants and polymers, Final report, contract MAlD-OOOl-E (A) INIAEU.

[46] Johansen, H.N., Glitsø, V., Bach Knudsen, K.E., 1996. Influence of extraction solvent and temperature on the quantitative determination of oligosaccharides from plant materials by high-performance liquid chromatography, J. Agric. Food Chem. 44, 1470–1474. https://doi.org/10.1021/jf950482b.

[47] Parajó, J.C., Domínguez, H., Domínguez, J.M., 1997. Xylitol production from Eucalyptus wood hydrolysates extracted with organic solvents, Process Biochem. 32, 599–604. https://doi.org/10.1016/S0032-9592(97)00016-2.

[48] Diz, J., Cruz, J.M., Domínguez, H., Parajó, J.C., 2002. Xylitol production from eucalyptus wood hydrolysates in low-cost fermentation media, Food Technol. Biotech. 40, 191–198. https://hrcak.srce.hr/178461.

[49] Matsumoto, M., Tanaka, T., Kondo, K., 2003. Selective separation of d-glucose by solvent extraction with ion-pair extractant, J. Ion Exch. 14, 341–344. https://doi.org/10.5182/jaie.14.Supplement_341.

[50] Griffin, G.J., 2005. Purification and Concentration of Xylose and Glucose from Neutralized Bagasse Hydrolysates Using 3, 5- Dimethylphenylboronic Acid and Modified Aliquat 336 as Coextractants, Sep. Sci. Technol. 40, 2337–2351. https://doi.org/10.1080/01496390500202522.

[51] Matsumoto, M., Ueba, K., Kondo, K., 2005. Separation of sugar by solvent extraction with phenylboronic acid and trioctylmethylammonium chloride, Sep. Purif. Technol. 43, 269–274. https://doi.org/10.1016/j.seppur.2004.11.010.

[52] Montañés, F., Corzo, N., Olano, A., Reglero, G., Ibáñez, E., Fornari, T., 2008. Selective fractionation of carbohydrate complex mixtures by supercritical extraction with CO2 and different co-solvents, J Supercrit Fluid. 45, 189–194. https://doi.org/10.1016/j.supflu.2007.08.012.

[53] Brennan, T.C., Datta, S., Blanch, H.W., Simmons, B.A., Holmes, B.M., 2010. Recovery of sugars from ionic liquid biomass liquor by solvent extraction, Bio. Energy Res. 3, 123–133. https://doi.org/10.1007/s12155-010-9091-5.

[54] Misra, S., Gupta, P., Raghuwanshi, S., Dutt, K., Saxena, R.K., 2011. Comparative study on different strategies involved for xylitol purification from culture media fermented by Candida tropicalis, Sep. Purif. Technol. 78, 266–273. https://doi.org/10.1016/j.seppur.2011.02.018.

[55] Tighrine, A., Amir, Y., Alfaro, P., Mamou, M., Nerín, C., 2019. Simultaneous extraction and analysis of preservatives and artificial sweeteners in juices by salting out liquid-liquid extraction method prior to ultra-high-performance liquid chromatography, Food Chem. 277, 586–594. https://doi.org/10.1016/j.foodchem.2018.10.107.

[56] Fatehi, P., Chen, J., 2016. Extraction of technical lignins from pulping spent liquors, challenges and opportunities, In: Z. Fang, Jr. R. Smith (Eds.), Production of biofuels and chemicals from lignin, Springer, Singapore, 2016, 35–54. https://doi.org/10.1007/978-981-10-1965-4_2.

[57] Kontturi, A.K., Sundholm, G., 1986. The extraction and fractionation of lignosulfonates with long chain aliphatic amines, Extraction. 40, 121–125. https://doi.org/10.3891/acta.chem.scand.40a-0121.

[58] Villar, J.C., Caperos, A., Garcia-Ochoa, F., 1996. Precipitation of kraft black liquors by alcohol-calcium solutions, Sep. Sci. Technol. 31, 1721–1739. https://doi.org/10.1080/01496399608000722.

[59] Hamala, S.L., Koivunen, S.T., Kontturi, A.K., Sarkkinen, V.J., Tampella Oy AB, 1982. Process for recovering lignosulfonates from spent sulfite liquor, U.S. Patent US4336189A.

[60] Cruz, J.M., Domínguez, J.M., Domínguez, H., Parajó, J.C., 1999. Solvent extraction of hemicellulosic wood hydrolysates: a procedure useful for obtaining both detoxified fermentation media and polyphenols with antioxidant activity, Food Chem. 67, 147–153. https://doi.org/10.1016/S0308-8146(99)00106-5.

[61] Stiefel, S., Di Marino, D., Eggert, A., Kühnrich, I.R., Schmidt, M., Grande, P.M., Leitner, W., Jupke, A., Wessling, M., 2017. Liquid/liquid extraction of biomass-derived lignin from lignocellulosic pretreatments, Green Chem. 19, 93–97. 10.1039/C6GC02270G.

[62] Ropponen, J., Räsänen, L., Rovio, S., Ohra-Aho, T., Liitiä, T., Mikkonen, H., Van De Pas, D., Tamminen, T., 2011. Solvent extraction as a means of preparing homogeneous lignin fractions, Holzforschung. 65, 543–549. https://doi.org/10.1515/hf.2011.089.

[63] Li, M.F., Sun, S.N., Xu, F., Sun, R.C., 2012. Sequential solvent fractionation of heterogeneous bamboo organosolv lignin for value-added application, Sep. Purif. Technol. 101, 18–25. https://doi.org/10.1016/j.seppur.2012.09.013.

[64] Arshanitsa, A., Ponomarenko, J., Dizhbite, T., Andersone, A., Gosselink, R.J., van der Putten, J., Lauberts, M., Telysheva, G., 2013. Fractionation of technical lignins as a tool for improvement of their antioxidant properties, J. Anal. Appl. Pyrol. 103, 78–85. https://doi.org/10.1016/j.jaap.2012.12.023.

[65] Araújo, L.C.P., Yamaji, F.M., Lima, V.H., Botaro, V.R., 2020. Kraft lignin fractionation by organic solvents: Correlation between molar mass and higher heating value, Bioresour. Technol. 314, 123757. https://doi.org/10.1016/j.biortech.2020.123757.

[66] Dodd, A.P., Kadla, J.F., Straus, S.K., 2014. Characterization of fractions obtained from two industrial softwood kraft lignins, ACS Sustain. Chem. Eng. 3, 103–110. https://doi.org/10.1021/sc500601b.

[67] Duval, A., Vilaplana, F., Crestini, C., Lawoko, M., 2016. Solvent screening for the fractionation of industrial kraft lignin, Holzforschung. 70, 11–20. https://doi.org/10.1515/hf-2014-0346.

[68] Jiang, X., Savithri, D., Du, X., Pawar, S., Jameel, H., Chang, H.M., Zhou, X., 2017. Fractionation and characterization of kraft lignin by sequential precipitation with various organic solvents, ACS Sustain. Chem. Eng. 5, 835–842. https://doi.org/10.1021/acssuschemeng.6b02174.

[69] Passoni, V., Scarica, C., Levi, M., Turri, S., Griffini, G., 2016. Fractionation of industrial softwood kraft lignin: Solvent selection as a tool for tailored material properties. ACS Sustain. Chem. Eng. 4, 2232–2242. https://doi.org/10.1021/acssuschemeng.5b01722.

[70] An, L., Wang, G., Jia, H., Liu, C., Sui, W., Si, C., 2017. Fractionation of enzymatic hydrolysis lignin by sequential extraction for enhancing antioxidant performance. Int. J. Biol. Macromol. 99, 6742017.681. https://doi.org/10.1016/j.ijbiomac.2017.03.015.

[71] Domínguez-Robles, J., Tamminen, T., Liitiä, T., Peresin, M.S., Rodríguez, A., Jääskeläinen, A.S., 2018. Aqueous acetone fractionation of kraft, organosolv and soda lignins, Int. J. Biol. Macromol. 106, 979–987. https://doi.org/10.1016/j.ijbiomac.2017.08.102.

[72] Mörck, R., Yoshida, H., Kringstad, K.P., Hatakeyama, H., 1986. Fractionation of kraft lignin by successive extraction with organic solvents. 1. Functional groups (13) C-NMR-spectra and molecular weight distributions, Holzforschung (Germany, FR). 40, 51–54. doi: 10.1515/hfsg.1986.40.1.51.

[73] Simoni, L.D., Chapeaux, A., Brennecke, J.F., Stadtherr, M.A., 2010. Extraction of biofuels and biofeedstocks from aqueous solutions using ionic liquids, Comput. Chem. Eng. 34, 1406–1412. https://doi.org/10.1016/j.compchemeng.2010.02.020.

[74] Ha, S.H., Mai, N.L., Koo, Y.M., 2010. Butanol recovery from aqueous solution into ionic liquids by liquid–liquid extraction, Process Biochem. 45, 1899–1903. https://doi.org/10.1016/j.procbio.2010.03.030.

[75] Cascon, H.R., Choudhari, S.K., Nisola, G.M., Vivas, E.L., Lee, D.J., Chung, W.J., 2011. Partitioning of butanol and other fermentation broth components in phosphonium and ammonium-based ionic liquids and their toxicity to solventogenic clostridia, Sep. Purif. Technol. 78, 164–174. https://doi.org/10.1016/j.seppur.2011.01.041.

[76] Pu, Y., Jiang, N., Ragauskas, A.J., 2007. Ionic liquid as a green solvent for lignin, J. Wood Chem. Technol. 27, 23–33. https://doi.org/10.1080/02773810701282330.

[77] Lee, S.H., Doherty, T.V., Linhardt, R.J., Dordick, J.S., 2009. Ionic liquid- mediated selective extraction of lignin from wood leading to enhanced enzymatic cellulose hydrolysis, Biotechnol. Bioeng. 102, 1368–1376. https://doi.org/10.1002/bit.22179.

[78] Fu, D., Mazza, G., Tamaki, Y., 2010. Lignin extraction from straw by ionic liquids and enzymatic hydrolysis of the cellulosic residues, J. Agric. Food Chem. 58, 2915–2922. https://doi.org/10.1021/jf903616y.

[79] Ji, W., Ding, Z., Liu, J., Song, Q., Xia, X., Gao, H., Wang, H., Gu, W., 2012. Mechanism of lignin dissolution and regeneration in ionic liquid, Energy Fuels. 26, 6393–6403. https://doi.org/10.1021/ef301231a.

[80] Sun, J., Dutta, T., Parthasarathi, R., Kim, K.H., Tolic, N., Chu, R.K., Isern, N.G., Cort, J.R., Simmons, B.A., Singh, S., 2016. Rapid room temperature solubilization and depolymerization of polymeric lignin at high loadings, Green Chem. 18, 6012–6020. https://doi.org/10.1039/c6gc02258h.

[81] Glas, D., Van Doorslaer, C., Depuydt, D., Liebner, F., Rosenau, T., Binnemans, K., De Vos, D.E., 2015. Lignin solubility in non- imidazolium ionic liquids, J. Chem. Technol. Biotechnol. 90, 1821–1826. https://doi.org/10.1002/jctb.4492.

[82] Achinivu, E.C., Howard, R.M., Li, G., Gracz, H., Henderson, W.A., 2014. Lignin extraction from biomass with protic ionic liquids, Green Chem. 16, 1114–1119. DOI: 10.1039/C3GC42306A.

[83] Rashid, T., Kait, C.F., Regupathi, I., Murugesan, T., 2016. Dissolution of kraft lignin using protic ionic liquids and characterization, Ind. Crop. Prod. 84, 284–293. https://doi.org/10.1016/j.indcrop.2016.02.017.

[84] Lynam, J.G., Kumar, N., Wong, M.J., 2017. Deep eutectic solvents' ability to solubilize lignin, cellulose, and hemicellulose; thermal stability; and density, Bioresour. Technol. 238, 684–689. https://doi.org/10.1016/j.biortech.2017.04.079.

[85] Soares, B., Tavares, D.J., Amaral, J.L., Silvestre, A.J., Freire, C.S., Coutinho, J.A., 2017. Enhanced solubility of lignin monomeric model compounds and technical lignins in aqueous solutions of deep eutectic solvents, ACS Sustain. Chem. Eng. 5, 4056–4065. https://doi.org/10.1021/acssuschemeng.7b00053.

[86] Smink, D., Kersten, S.R., Schuur, B., 2020. Recovery of lignin from deep eutectic solvents by liquid-liquid extraction, Sep. Purif. Technol. 235, 116127. https://doi.org/10.1016/j.seppur.2019.116127.

[87] Ringena, O., Saake, B., Lehnen, R., 2005. Isolation and fractionation of lignosulfonates by amine extraction and ultrafiltration: A comparative study, Holzforschung, 59, 405–412. DOI: https://doi.org/10.1515/HF.2005.066.

[88] Markom, M., Hasan, M., Daud, W.R.W., Singh, H., Jahim, J.M., 2007. Extraction of hydrolysable tannins from Phyllanthus niruri Linn: Effects of solvents and extraction methods, Sep. Purif. Technol. 52, 487–496. https://doi.org/10.1016/j.seppur.2006.06.003.

[89] Yuan, T.Q., He, J., Xu, F., Sun, R.C., 2009. Fractionation and physico-chemical analysis of degraded lignins from the black liquor of Eucalyptus pellita KP-AQ pulping, Polym. Degrad. Stabil. 94, 1142–1150. https://doi.org/10.1016/j.polymdegradstab.2009.03.019.

[90] Evstigneev, E.I., 2010. Specific features of lignin dissolution in aqueous and aqueous-organic media, Russ. J. Appl. Chem. 83, 509–513. https://doi.org/10.1134/S1070427210030250.

[91] Faustino, H., Gil, N., Baptista, C., Duarte, A.P., 2010. Antioxidant activity of lignin phenolic compounds extracted from kraft and sulphite black liquors, Molecules. 15, 9308–9322. https://doi.org/10.3390/molecules15129308.

[92] Gosselink, R.J., van Dam, J.E., de Jong, E., Scott, E.L., Sanders, J.P., Li, J., Gellerstedt, G., 2010. Fractionation, analysis, and PCA modeling of properties of four technical lignins for prediction of their application potential in binders, Holzforschung. 64, 193–200. DOI: https://doi.org/10.1515/hf.2010.023.

[93] Methacanon, P., Weerawatsophon, U., Thainthongdee, M., Lekpittaya, P., 2010. Optimum conditions for selective separation of kraft lignin, Kasetsart J. Nat. Sci., 44, 680–690.

[94] Wang, K., Xu, F., Sun, R., 2010. Molecular characteristics of kraft-AQ pulping lignin fractionated by sequential organic solvent extraction, Int. J. Mol. Sci. 11, 2988–3001. https://doi.org/10.3390/ijms11082988.

[95] Yue, X., Chen, F., Zhou, X., He, G., 2012. Preparation and characterization of poly (vinyl chloride) polyblends with fractionated lignin, Int. J. Polym. Mater. 61, 214–228. https://doi.org/10.1080/00914037.2011.574659.

[96] Boeriu, C.G., Fiţigău, F.I., Gosselink, R.J., Frissen, A.E., Stoutjesdijk, J., Peter, F., 2014. Fractionation of five technical lignins by selective extraction in green solvents and characterisation of isolated fractions. Ind. Crop. Prod. 62, 481–490. https://doi.org/10.1016/j.indcrop.2014.09.019.

[97] Llano, T., Alexandri, M., Koutinas, A., Gardeli, C.H.R., Papapostolou, H., Coz, A., Quijorna, N., Andres, A., Komaitis, M., 2015. Liquid–liquid extraction of phenolic compounds from spent sulphite liquor, Waste biomass valorization, 6, 1149–1159. https://doi.org/10.1007/s12649-015-9425-9.

[98] Sadeghifar, H., Wells, T., Le, R.K., Sadeghifar, F., Yuan, J.S., Jonas Ragauskas, A., 2016. Fractionation of organosolv lignin using acetone: water and properties of the obtained fractions, ACS Sustain. Chem. Eng. 5, 580–587. https://doi.org/10.1021/acssuschemeng.6b01955.

[99] Sameni, J., Krigstin, S., Sain, M., 2017. Solubility of lignin and acetylated lignin in organic solvents, BioResources, 12, 1548–1565.

[100] Goldmann, W.M., Ahola, J., Mikola, M., Tanskanen, J., 2019. Solubility and fractionation of Indulin AT kraft lignin in ethanol-water media, Sep. Purif. Technol. 209, 826–832. https://doi.org/10.1016/j.seppur.2018.06.054.

[101] Ahsan, L., Jahan, M.S., Liu, H., Ni, Y., 2012. Recovery of acetic acid from pre-hydrolysis liquor of the Kraft based dissolving pulp production process by reactive extraction with tri-octyl amine (TOA) and octanol. J. For, Journal of Science & Technology for Forest Products and Processes. 2, 38–43.

[102] Kim, S.J., Kwon, H.S., Kim, G.H., Um, B.H., 2015. Green liquor extraction of hemicellulosic fractions and subsequent organic acid recovery from the extracts using liquid–liquid extraction, Ind. Crop. Prod. 67, 395–402. https://doi.org/10.1016/j.indcrop.2015.01.040.

[103] Mateo, S., Roberto, I.C., Sánchez, S., Moya, A.J., 2013. Detoxification of hemicellulosic hydrolyzate from olive tree pruning residue, Ind. Crop. Prod. 49, 196–203. https://doi.org/10.1016/j.indcrop.2013.04.046.

[104] Park, S.J., Moon, J.K., Um, B.H., 2013. Evaluation of the efficiency of solvent systems to remove acetic acid derived from pre-pulping extraction, J. Korean Wood Sci. Technol. 41, 447–455. http://dx.doi.org/DOI:10.5658/WOOD.2013.41.5.447.

[105] Kim, S.B., Yoo, H.Y., Kim, J.S., Kim, S.W., 2014. The hydrolysate of barley straw containing inhibitors can be used to produce cephalosporin C by solvent extraction using ethyl acetate, Process Biochem. 49, 2203–2206. https://doi.org/10.1016/j.procbio.2014.10.007.

[106] Rasrendra, C.B., Girisuta, B., Van de Bovenkamp, H.H., Winkelman, J.G.M., Leijenhorst, E.J., Venderbosch, R.H., Windt, M., Meier, D., Heeres, H.J., 2011. Recovery of acetic acid from an aqueous pyrolysis oil phase by reactive extraction using tri-n-octylamine, Chem. Eng. J. 176, 244–252. https://doi.org/10.1016/j.cej.2011.08.082.

[107] Al-Mudhaf, H.F., Hegazi, M.F., Abu-Shady, A.I., 2002. Partition data of acetic acid between aqueous NaCl solutions and trioctylphosphine oxide in cyclohexane diluent, Sep. Purif. Technol. 27, 41–50. https://doi.org/10.1016/S1383-5866(01)00192-7.

[108] Katikaneni, S.P., Cheryan, M., 2002. Purification of fermentation-derived acetic acid by liquid− liquid extraction and esterification, Ind. Eng. Chem. Res. 41, 2745–2752. https://doi.org/10.1021/ie010825x.

[109] Wisniewski, M., Pierzchalska, M., 2005. Recovery of carboxylic acids C1-C3 with organophosphine oxide solvating extractants, J. Chem. Technol. Biotechnol. 80, 1425–1430. https://doi.org/10.1002/jctb.1348.

[110] Mahfud, F.H., Van Geel, F.P., Venderbosch, R.H., Heeres, H.J., 2008. Acetic acid recovery from fast pyrolysis oil. An exploratory study on liquid-liquid reactive extraction using aliphatic tertiary amines, Sep. Sci. Technol. 43 (2008) 3056–3074. https://doi.org/10.1080/01496390802222509.

[111] Yang, G., Jahan, M.S., Ahsan, L., Ni, Y., 2013a. Influence of the diluent on the extraction of acetic acid from the prehydrolysis liquor of kraft based dissolving pulp production process by tertiary amine, Sep. Purif. Technol. 120, 341–345. https://doi.org/10.1016/j.seppur.2013.10.004.

[112] Yang, G., Jahan, M.S., Ahsan, L., Zheng, L., Ni, Y., 2013b. Recovery of acetic acid from pre-hydrolysis liquor of hardwood kraft-based dissolving pulp production process by reactive extraction with Triisooctylamine, Bioresour. Technol. 138, 253–258. https://doi.org/10.1016/j.biortech.2013.03.164.

[113] Uslu, H., 2009. Reactive extraction of formic acid by using tri octyl amine (TOA), Sep. Sci. Technol. 44, 1784–1798. https://doi.org/10.1080/01496390902775893.

[114] Brouwer, T., Blahusiak, M., Babic, K., Schuur, B., 2017. Reactive extraction and recovery of levulinic acid, formic acid and furfural from aqueous solutions containing sulphuric acid, Sep. Purif. Technol. 185, 186–195. https://doi.org/10.1016/j.seppur.2017.05.036.

[115] Coca, J., Diaz, R., 1980. Extraction of furfural from aqueous solutions with chlorinated hydrocarbons, J. Chem. Eng. Data. 25, 80–83. https://doi.org/10.1021/je60084a023.

[116] Trimble, F., Dunlop, A.P., 1940. Recovery of furfural from aqueous solutions, Ind. Eng. Chem. Anal. Ed. 12, 721–722. https://doi.org/10.1021/ac50152a005.

[117] Cabezas, J.L., Barcena, L.A., Coca, J., Cockrem, M., 1988. Extraction of furfural from aqueous solutions using alcohols, J. Chem. Eng. Data. 33, 435–437. https://doi.org/10.1021/je00054a014.

[118] Männistö, M., Pokki, J.P., Creati, A., Voisin, A., Zaitseva, A., Alopaeus, V., 2016. Ternary and binary LLE measurements for solvent (4-methyl-2-pentanone and 2-methyl-2-butanol) + furfural+ water between 298 and 401 K, J. Chem. Eng. Data. 61, 903–911. DOI: 10.1021/acs.jced.5b00738.

[119] Sunder, M.S., Prasad, D.H.L., 2003. Phase equilibria of water+ furfural and dichloromethane+ n-hexane. J. Chem. Eng. Data. 48, 221-223. https://doi.org/10.1021/je020053r.

[120] Saha, B., Abu-Omar, M.M., 2014. Advances in 5-hydroxymethylfurfural production from biomass in biphasic solvents, Green Chem. 16, 24–38. DOI: 10.1039/C3GC41324A.

[121] Croker, J.R., Bowrey, R.G., 1984. Liquid extraction of furfural from aqueous solution. Industrial & engineering chemistry fundamentals, 23, 480–484.

[122] Zhang, T., Kumar, R., Wyman, C.E., 2013. Enhanced yields of furfural and other products by simultaneous solvent extraction during thermochemical treatment of cellulosic biomass, Rsc Adv. 3, 9809–9819. DOI: 10.1039/C3RA41857J.

[123] Blumenthal, L.C., Jens, C.M., Ulbrich, J., Schwering, F., Langrehr, V., Turek, T., Kunz, U., Leonhard, K., Palkovits, R., 2016. Systematic identification of solvents optimal for the extraction of 5-hydroxymethylfurfural from aqueous reactive solutions, ACS Sustain. Chem. Eng. 4, 228–235. https://doi.org/10.1021/acssuschemeng.5b01036.

[124] Pokki, J.P., Männistö, M., Alopaeus, V., 2018. Separation of furfural and acetic acid with liquid-liquid-extraction and distillation in biorefinery systems: Simulations and laboratory experiments, Chem. Eng. 69, 2283–9216. https://doi.org/10.3303/CET1869004.

[125] Luo, C., Brink, D.L., Blanch, H.W., 2002. Identification of potential fermentation inhibitors in conversion of hybrid poplar hydrolyzate to ethanol, Biomass Bioenerg. 22, 125–138. https://doi.org/10.1016/S0961-9534(01)00061-7.

[126] Salter, G.J., Kelt, D.B., 1995. Solvent selection for whole cell biotransformations in organic media, Crit. Rev. Biotechnol. 15, 139–177. https://doi.org/10.3109/07388559509147404.

[127] Qureshi, N., Maddox, I.S., Friedl, A., 1992. Application of continuous substrate feeding to the ABE fermentation: relief of product inhibition using extraction, perstraction, stripping, and pervaporation, Biotechnol. Prog. 8, 382–390. https://doi.org/10.1021/bp00017a002.

[128] Roque, L.R., Morgado, G.P., Nascimento, V.M., Ienczak, J.L., Rabelo, S.C., 2019. Liquid-liquid extraction: A promising alternative for inhibitors removing of pentoses fermentation, Fuel, 242, 775–787. https://doi.org/10.1016/j.fuel.2018.12.130.

[129] Gonzalez, J., Cruz, J.M., Domınguez, H., Parajó, J.C., 2004. Production of antioxidants from Eucalyptus globulus wood by solvent extraction of hemicellulose hydrolysates, Food Chem. 84, 243–251. https://doi.org/10.1016/S0308-8146(03)00208-5.

[130] Avilé Martínez, A., Saucedo-Luna, J., Segovia-Hernandez, J.G., Hernandez, S., Gomez-Castro, F.I., Castro-Montoya, A.J., 2011. Dehydration of bioethanol by hybrid process liquid–liquid extraction/extractive distillation, Ind. Eng. Chem. Res. 51, 5847–5855. https://doi.org/10.1021/ie200932g.

[131] Solimo, H.N., Martinez, H.E., Riggio, R., 1989. Liquid-liquid extraction of ethanol from aqueous solutions with amyl acetate, benzyl alcohol, and methyl isobutyl ketone at 298.15 K, J. Chem. Eng. Data. 34, 176–179. https://doi.org/10.1021/je00056a008.

[132] Arce, A., Rodríguez, H., Soto, A., 2006. Effect of anion fluorination in 1-ethyl-3-methylimidazolium as solvent for the liquid extraction of ethanol from ethyl tert-butyl ether, Fluid Phase Equilibr. 242, 164–168. https://doi.org/10.1016/j.fluid.2006.01.008.

[133] Corderí, S., González, B., 2012. Ethanol extraction from its azeotropic mixture with hexane employing different ionic liquids as solvents, J. Chem. Thermodyn. 55, 138–143. https://doi.org/10.1016/j.jct.2012.06.028.

[134] Matsumura, M., Märkl, H., 1984. Application of solvent extraction to ethanol fermentation, Appl. Microbiol. Biotechnol. 20, 371–377. https://doi.org/10.1007/BF00261937.

[135] Egan, B.Z., Lee, D.D., McWhirter, D.A., 1988. Solvent extraction and recovery of ethanol from aqueous solutions, Ind. Eng. Chem. Res. 27, 1330–1332. https://doi.org/10.1021/ie00079a038.

[136] Sólimo, H.N., Zurita, J.L., 1992. Influence of temperature on the liquid-to-liquid extraction of ethanol from (water+ ethanol+ 1, 2-dichloroethane), Can. J. Chem. 70, 2310–2313. https://doi.org/10.1139/v92-291.

[137] Daugulis, A.J., Axford, D.B., McLellan, P.J., 1991. The economics of ethanol production by extractive fermentation, Can. J. Chem. Eng. 69, 488–497. https://doi.org/10.1002/cjce.5450690213.

[138] Habaki, H., Hu, H., Egashira, R., 2016. Liquid–liquid equilibrium extraction of ethanol with mixed solvent for bioethanol concentration, Chin. J. Chem. Eng. 24, 253–258. https://doi.org/10.1016/j.cjche.2015.07.022.

[139] Offeman, R.D., Stephenson, S.K., Robertson, G.H., Orts, W.J., 2005. Solvent extraction of ethanol from aqueous solutions. I. Screening methodology for solvents, Ind. Eng. Chem. Res. 44, 6789–6796. https://doi.org/10.1021/ie0500319.

[140] Offeman, R.D., Stephenson, S.K., Robertson, G.H., Orts, W.J., 2005. Solvent extraction of ethanol from aqueous solutions. II. Linear, branched, and ring-containing alcohol solvents, Ind. Eng. Chem. Res. 44, 6797–6803. https://doi.org/10.1021/ie0500321.

[141] Habaki, H., Tabata, O., Kawasaki, J., Egashira, R., 2010. Extraction equilibrium of ethanol for bioethanol production—solvent selection and liquid-liquid equilibrium measurement, J. Jpn. Petrol. Inst. 53, 135–143. https://doi.org/10.1627/jpi.53.135.

[142] Honda, H., Taya, M., Kobayashi, T., 1986. Ethanol fermentation associated with solvent extraction using immobilized growing cells of Saccharomyces cerevisiae and its lactose-fermentable fusant, J. Chem. Eng. Jpn. 19, 268–273. https://doi.org/10.1252/jcej.19.268.

[143] Munson, C.L., King, C.J., 1984. Factors influencing solvent selection for extraction of ethanol from aqueous solutions, Ind. Eng. Chem. Process Des. Dev. 23, 109–115. https://doi.org/10.1021/i200024a018.

[144] Mitchell, R.J., Arrowsmith, A., Ashton, N., 1987. Mixed solvent systems for recovery of ethanol from dilute aqueous solution by liquid–liquid extraction, Biotechnol. Bioeng. 30, 348–351. https://doi.org/10.1002/bit.260300304.

[145] Gomis, V., Ruiz, F., Boluda, N., Saquete, M.D., 1998. Salt effects in extraction of ethanol from aqueous solution: 2-ethylhexanol+ sodium chloride as the solvent, Ind. Eng. Chem. Res. 37, 599–603. https://doi.org/10.1021/ie970372p.

[146] Koullas, D.P., Umealu, O.S., Koukios, E.G., 1999. Solvent selection for the extraction of ethanol from aqueous solutions, Sep. Sci. Technol. 34. 2153–2163. https://doi.org/10.1081/SS-100100762.

[147] Rahman, M.A., Rahman, M.S., Nabi, M.N., 2001. Extraction of ethanol from aqueous solution by solvent extraction-liquid-liquid equilibrium of ethanol-water-1-butanol, ethanol-water-1-pentanol and ethanol water-1-hexanol systems, Indian J. Chem. Technol. 8, 385–389. http://nopr.niscair.res.in/handle/123456789/22933.

[148] Offeman, R.D., Stephenson, S.K., Franqui, D., Cline, J.L., Robertson, G.H., Orts, W.J., 2008. Extraction of ethanol with higher alcohol solvents and their toxicity to yeast, Sep. Purif. Technol. 63, 444–451. https://doi.org/10.1016/j.seppur.2008.06.005.

[149] Hiroaki, H., Osamu, T., Junjiro, K., Ryuichi, E., 2010. Extraction equilibrium of ethanol for bioethanol production-solvent selection and liquid-liquid equilibrium measurement, J. Jpn. Petrol. Inst. 53, 135–143. https://doi.org/10.1627/jpi.53.135.

[150] Oliveira, F.S., Pereiro, A.B., Rebelo, L.P., Marrucho, I.M., 2013. Deep eutectic solvents as extraction media for azeotropic mixtures, Green Chem. 15, 1326–1330. DOI: 10.1039/C3GC37030E.

[151] Rodriguez, N.R., Molina, B.S., Kroon, M.C., 2015. Aliphatic+ ethanol separation via liquid–liquid extraction using low transition temperature mixtures as extracting agents, Fluid Phase Equilibr. 394, 71–82. https://doi.org/10.1016/j.fluid.2015.03.017.

[152] Rodriguez, N.R., Ferre Guell, J., Kroon, M.C., 2016. Glycerol-based deep eutectic solvents as extractants for the separation of MEK and ethanol via liquid–liquid extraction, J. Chem. Eng. Data. 61, 865–872. https://doi.org/10.1021/acs.jced.5b00717.

[153] Hadj-Kali, M.K., Hizaddin, H.F., Wazeer, I., Mulyono, S., Hashim, M.A., 2017. Liquid-liquid separation of azeotropic mixtures of ethanol/alkanes using deep eutectic solvents: COSMO-RS prediction and experimental validation, Fluid Phase Equilibr. 448, 105–115. https://doi.org/10.1016/j.fluid.2017.05.021.

[154] Jia, B., Xin, K., Yang, T., Yu, J., Yu, Y., Li, Q., 2017. Measurement and thermodynamic modeling of ternary (liquid+ liquid) equilibrium for extraction of ethanol from diethoxymethane solution with different solvents, J. Chem. Thermodyn. 111, 1-6. https://doi.org/10.1016/j.jct.2017.03.014.

[155] Cháfer, A., de la Torre, J., Loras, S., Montón, J.B., 2018. Study of liquid–liquid extraction of ethanol+ water azeotropic mixtures using two imidazolium-based ionic liquids, J. Chem. Thermodyn. 118, 92–99. https://doi.org/10.1016/j.jct.2017.11.006.

[156] Jesús, M-P. J., Juan, G. S-H., 2018. Alternative Schemes for the Purification of Bioethanol: A Comparative Study, Recent. Adv. Petrochem Sci. 4, 1–9. DOI: 10.19080/RAPSCI.2018.04.555631.

[157] Bankar, S.B., Survase, S.A., Singhal, R.S., Granström, T., 2012. Continuous two stage acetone–butanol–ethanol fermentation with integrated solvent removal using *Clostridium acetobutylicum* B 5313, Bioresour. Technol. 106, 110–116. https://doi.org/10.1016/j.biortech.2011.12.005.

[158] Evanko, W.A., Eyal, A.M., Glassner, D.A., Miao, F., Aristidou, A.A., Evans, K., Gruber, P.R., Hawkins, A.C., Meinhold, P., Feldman, R.M.R., Gunawardena, U., 2013. Recovery of higher alcohols from dilute aqueous solutions, U.S. Patent Application US20130059370A1.

[159] Garcia-Chavez, L.Y., Garsia, C.M., Schuur, B., de Haan, A.B., 2012. Biobutanol recovery using nonfluorinated task-specific ionic liquids, Ind. Eng. Chem. Res. 51, 8293–8301. https://doi.org/10.1021/ie201855h.

[160] Roffler, R., Blanch, H.W., Wilke, C.R., 1998. In situ extractive fermentation of acetone and butanol, Biotechnol. Bioeng. 31, 135–143. https://doi.org/10.1002/bit.260310207.

[161] Groot, W.J., Soedjak, H.S., Donck, P.B., Van der Lans, R.G.J.M., Luyben, K.C.A., 1990. Timmer, J.M.K., 1990. Butanol recovery from fermentations by liquid-liquid extraction and membrane solvent extraction, Bioprocess Eng. 5, 203–216. https://doi.org/10.1007/BF00376227.

[162] Domańska, U., Królikowski, M., 2012. Extraction of butan-1-ol from water with ionic liquids at T= 308.15 K, J. Chem. Thermodyn. 53, 108–113. https://doi.org/10.1016/j.jct.2012.04.017.

[163] Pitner, W.R., Schulte, M., Górak, A., Santangelo, F., Wentink, A.E., 2013. Use of ionic liquids with tetracyanoborate anions as a solvents for extraction of alcohols from aqueous solutions. U.S. Patent US8455703B2.

[164] Rabari, D., Banerjee, T., 2013. Biobutanol and n-propanol recovery using a low density phosphonium based ionic liquid at T= 298.15 K and p= 1 atm, Fluid Phase Equilibr. 355, 26–33. https://doi.org/10.1016/j.fluid.2013.06.047.

[165] Kubiczek, A., Kamiński, W., Górak, A., 2016. Modeling of single-and multi-stage extraction in the system of water, acetone, butanol, ethanol and ionic liquid, Fluid Phase Equilibr. 425, 365–373. https://doi.org/10.1016/j.fluid.2016.05.023.

[166] Dezhang, S., Huisheng, F., Feng, X., Wenxiu, L., Zhigang, Z., 2019. Feasibility of ionic liquid as extractant for bio-butanol extraction: Experiment and simulation, Sep. Purif. Technol. 215, 287–298. https://doi.org/10.1016/j.seppur.2018.12.074.

[167] Khayati, G., Pahlavanzadeh, H., Vasheghani-Farahani, E., Ghaemi, N., 2009. (Liquid+ liquid) phase equilibria for (water+ 2, 3-butanediol+ oleyl alcohol) at T=(300.2, 307.2, and 314.2) K, J. Chem. Thermodyn. 41, 150–154. https://doi.org/10.1016/j.jct.2008.10.004.

[168] Birajdar, S.D., Padmanabhan, S., Rajagopalan, S., 2014. Rapid solvent screening using thermodynamic models for recovery of 2, 3-butanediol from fermentation by liquid–liquid extraction, J. Chem. Eng. Data. 59, 2456–2463. https://doi.org/10.1021/je500196e.

[169] Wu, Y.Y., Zhu, J.W., Chen, K., Wu, B., Fang, J., Shen, Y.L., 2008. Liquid–liquid equilibria of water+ 2, 3-butanediol+ 1-butanol at T= 298.15 K, T= 308.15 K and T= 318.15 K, Fluid Phase Equilibr. 265, 1–6. https://doi.org/10.1016/j.fluid.2007.12.003.

[170] Wu, Y.Y., Pan, D.T., Zhu, J.W., Chen, K., Wu, B., Ji, L.J., 2012. 2012. Liquid–liquid equilibria of water+ 2, 3-butanediol+ isobutanol at several temperatures, Fluid Phase Equilibr. 325, 100–104. https://doi.org/10.1016/j.fluid.2012.04.018.

[171] Gilani, H.G., Khiati, G., Haghi, A.K., 2006. Liquid–liquid equilibria of (water+ 2, 3-butanediol+ 2-ethyl-1-hexanol) at several temperatures, Fluid Phase Equilibr. 247, 199–204. https://doi.org/10.1016/j.fluid.2006.06.025.

[172] Birajdar, S.D., Padmanabhan, S., Rajagopalan, S., 2015. Repulsive effect of salt on solvent extraction of 2, 3- butanediol from aqueous fermentation solution, J. Chem. Technol. Biotechnol. 90 , 1455–1462. https://doi.org/10.1002/jctb.4450.

[173] Jeong, A.Y., Cho, J.A., Kim, Y., Cho, H.K., Choi, K.Y., Lim, J.S., 2018. Liquid-liquid equilibria for water+ 2, 3-butanediol+ 1-pentanol ternary system at different temperatures of 298.2, 308.2, and 318.2 K, Korean J. Chem. Eng. 35, 1328–1334. https://doi.org/10.1007/s11814-018-0036-6.

[174] Yim, J.H., Park, K.W., Lim, J.S., Choi, K.Y., 2019. Liquid–liquid equilibrium measurements for the ternary system of water/2, 3-butanediol/4-methyl-2-pentanol at various temperatures, J. Chem. Eng. Data. 64, 3882–3888. https://doi.org/10.1021/acs.jced.9b00290.

[175] Welton, T., 2015. Solvents and sustainable chemistry. Proceedings of the Royal Society A471: Mathematical, Physical and Engineering Sciences, 47, 1–26. https://doi.org/10.1098/rspa.2015.0502.

[176] McPartland, T.J., Patil, R.A., Malone, M.F., Roberts, S.C., 2012. Liquid–liquid extraction for recovery of paclitaxel from plant cell culture: solvent evaluation and use of extractants for partitioning and selectivity, Biotechnol. Prog. 28, 990–997. https://doi.org/10.1002/btpr.1562.

[177] Prat, D., Wells, A., Hayler, J., Sneddon, H., McElroy, C.R., Abou-Shehada, S., Dunn, P.J., 2015. CHEM21 selection guide of classical-and less classical-solvents, Green Chem. 18, 288-296. DOI: 10.1039/C5GC01008J.

[178] Piccione, P.M., Baumeister, J., Salvesen, T., Grosjean, C., Flores, Y., Groelly, E., Murudi, V., Shyadligeri, A., Lobanova, O., Lothschu¨z, C., 2019. Solvent selection methods and tool, Org. Process Res. Dev. 23, 998–1016. https://doi.org/10.1021/acs.oprd.9b00065.

[179] Diorazio, L.J., Hose, D.R. Adlington, N.K., 2016. Toward a more holistic framework for solvent selection, Org. Process Res. Dev. 20, 760–773. https://doi.org/10.1021/acs.oprd.6b00015.

[180] Henderson, R.K., Jiménez-González, C., Constable, D.J., Alston, S.R., Inglis, G.G., Fisher, G., Sherwood, J., Binks, S.P., Curzons, A.D., 2011. Expanding GSK's solvent selection guide–embedding sustainability into solvent selection starting at medicinal chemistry, Green Chem. 13, 854–862. https://doi.org/10.1039/C0GC00918K.

[181] Shen, Z., Van Lehn, R.C., 2020. Solvent selection for the separation of lignin-derived monomers using the conductor-like screening model for real solvents, Ind. Eng. Chem. Res. 59, 7755–7764. https://doi.org/10.1021/acs.iecr.9b06086.

[182] Kwok, T.T., Bright, J.R., Vora, S.R., Chrisandina, N.J., Luettgen, C.O., Realff, M.J., Bommarius, A.S., 2020. Solvent selection for lignin value prior to pulping, ChemSusChem, 13, 267–273. https://doi.org/10.1002/cssc.201901518.

[183] Clarke, C.J., Tu, W.C., Levers, O., Brohl, A., Hallett, J.P., 2018. Green and sustainable solvents in chemical processes, Chem. Rev. 118, 747–800. https://doi.org/10.1021/acs.chemrev.7b00571.

[184] Kim, J.K., Iannotti, E.L., Bajpai, R., 1999. Extractive recovery of products from fermentation broths, Biotechnol. Bioprocess Eng. 4, 1–11. https://doi.org/10.1007/BF02931905.

[185] Rundquist, E.M., Pink, C.J., Livingston, A.G., 2012. Organic solvent nanofiltration: a potential alternative to distillation for solvent recovery from crystallisation mother liquors, Green Chem. 14, 2197–2205. https://doi.org/10.1039/C2GC35216H.

[186] Kim, J.F., Szekely, G., Schaepertoens, M., Valtcheva, I.B., Jimenez-Solomon, M.F., Livingston, A.G., 2014. In situ solvent recovery by organic solvent nanofiltration. ACS Sustain. Chem. Eng. 2, 2371–2379. https://doi.org/10.1021/sc5004083.

[187] Bokhary, A., Tikka, A., Leitch, M., Liao, B., 2018. Membrane fouling prevention and control strategies in pulp and paper industry applications: A review, J. Membr. Sci. Res. 4, 181–197. https://doi.org/10.22079/JMSR.2018.83337.1185.

[188] Zhu, H., Chen, D., An, W., Li, N., Xu, Q., Li, H., He, J., Lu, J., 2015. A robust and cost- effective superhydrophobic graphene foam for efficient oil and organic solvent recovery, Small. 11, 5222–5229. https://doi.org/10.1002/smll.201501004.

[189] Viell, J., Harwardt, A., Seiler, J., Marquardt, W., 2013. Is biomass fractionation by Organosolv-like processes economically viable? A conceptual design study, Bioresour. Technol. 150, 89–97. https://doi.org/10.1016/j.biortech.2013.09.078.

[190] De Wild, P.J., Huijgen, W.J.J., Heeres, H.J., 2012. Pyrolysis of wheat straw-derived organosolv lignin, J. Anal. Appl. Pyrolysis, 93, 95–103. https://doi.org/10.1016/j.jaap.2011.10.002.

[191] Huang, H.J., Ramaswamy, S., Liu, Y., 2014. Separation and purification of biobutanol during bioconversion of biomass, Sep. Purif. Technol. 132, 513–540. https://doi.org/10.1016/j.seppur.2014.06.013.

[192] Zhao, T., Geng, X., Qi, P., Zhu, Z., Gao, J., Wang, Y., 2018. Optimization of liquid–liquid extraction combined with either heterogeneous azeotropic distillation or extractive distillation processes to reduce energy consumption and carbon dioxide emissions, Chem. Eng. Res. Des. 132, 399–408. https://doi.org/10.1016/j.cherd.2018.01.037.

[193] Chen, Y.C., Li, K.L., Chen, C.L., Chien, I.L., 2015. Design and control of a hybrid extraction–distillation system for the separation of pyridine and water, Ind. Eng. Chem. Res. 54 (2015) 7715–7727. https://doi.org/10.1021/acs.iecr.5b01671.

2. Literature Review II

Recent Advances in Bioconversion of Pulp and Paper Mill Sludges to Biofuels: Potentials and Constraints

Abstract

Due to stringent environmental regulations and depletion of fossil fuel resources, the need for renewable materials and clean energy has increased, which created an opportunity to exploit pulp and paper mill sludge (PPMS) as feedstock to produce renewable biofuels. PPMS represents a large part of the industrial waste and contains a high portion of the organic matter that can be used as a substrate for biofuel production. However, this waste stream poses unique challenges when exposed to anaerobic digestion (AD) and fermentation processes (FPs) because of its unique recalcitrant characteristics. In this review, we discuss AD and FPs of PPMS, along with the PPMS availability and suitability for bioconversion processes. AD and FPs are reliable and effective technologies for bioenergy recovery and sludge stabilization. All these studies were in the lab-scale and pilot-scale level and no full-scale application has been reported yet. Based on this review, the main limiting factors for the use of PPMS as a biofuel substrate on a large scale are the long residence times, the nutrient/soluble substances deficiency problems, and lignin inhibition effects. Thereby, a wide range of pre-treatments ranging from simple mechanical grinding to sophisticated treatments has been used aiming at breaking down the recalcitrant properties of the sludge substrate. Co-digestion with other non-paper mill substrates was also applied to compensate for nutrient deficiencies or reducing the inhibition effects. But to this day, PPMS-related studies regarding pre-treatment methods and their simplicity and effectiveness remain essential as they might help in upgrading energy-rich PPMS from environmentally polluting waste to a valuable resource suitable for biofuels production.

Keywords: Biofuel, Paper sludge, Anaerobic digestion, Fermentation, Biogas, Bioethanol, Biohydrogen

1. Introduction

The pulp and paper (P&P) industry generates large quantities of sludge waste of various kinds, contingent upon the fibers liberating processes (pulping) and subsequent wastewater treatment technologies. The resulting sludge features high chemical oxygen demand (COD) and contains suspended solids (i.e., fibers), sulfur compounds, fatty acids, lignin, and hemicelluloses (Kolbl et al., 2017). Thus, it should be treated and disposed of per higher waste treatment standards and established environmental commandments that are pertaining to effluent quality to prevent potential ecosystem damages. Typical management practices for this sludge are landfilling, and incineration and as such represent a considerable financial burden to the P&P industry due to high capital costs of transportation and the energy needed to remove large quantities of water prior to incineration (Stoica et al., 2009). Reportedly, sludge management consumes up to 60% of the total wastewater treatment facility budget (Elliott and Mahmood, 2012; Park et al., 2012). In addition to high costs, these traditional management methods were characterized by air pollution problems (e.g., incineration), leachate related issues, and public opposition (e.g., landfilling).

On the other hand, pulp and paper mills sludge (PPMS) contains valuable and underexploited compounds (85 to 95% volatile organic matter) which are a potential source of bioenergy production. As for the main organic components, the PPMS contains cellulose, hemicellulose, and lignin as a wood-based material, in addition to inorganic substances for the primary sludge (PS) and secondary sludge (SS) (microorganism sludge) from the biological wastewater treatment systems. The proportions of these substances depend on the type of sludge (e.g., primary sludge (PS), waste activated sludge (WAS), de-inking paper sludge)

(Monte et al., 2009). Most of the sludge molecules are precious feedstock in some industries, and within the spirit of the circular economy, great efforts have been made for utilizing them. PPMS also contains some valuable nutrients that could be recovered and used. Burning or disposing of these wastes results in resource loss, not to mention gaseous emissions and water pollution (Bayr et al., 2013; Hazarika and Khwairakpam, 2018). Thus, the conversion of these wastes into valuable value-added materials or bioenergy would be beneficial for forest industries to reduce the cost of waste management and increase their market competitiveness. Figure 2.2.1 shows possible routes for biofuels production from PPMS.

Biomass waste valorizations have become the most acceptable alternative to disposal and incineration methods. Several strategies and technologies, including pyrolysis, gasification, liquefaction, and hydrothermal processes have evolved to convert sludge waste into value-added products and biofuels. In recent years, advanced biochemical conversion technologies (anaerobic digestion for biomethane production, fermentation for bioethanol, and biohydrogen production) have received increasing attention for improved bioenergy production. Anaerobic digestion (AD) and fermentation processes (FPs) upgrade PPMS from environmentally polluted waste to valuable resources that can be utilized as feedstock for renewable biofuel production. Industrial adoption of these technologies has the benefit of energy recovery, volume reduction, and greenhouse gas alleviation compared to conventional processes that dispose of or burn biomass wastes. Pulp and paper mills are interested in adopting and integrating waste-to-bioenergy conversion technologies into their system operations to reduce their environmental footprint while creating economic values. Different design and configuration of fermentation/digestion technologies are used worldwide for sludge valorization, and numerous pre-treatment methods have been applied to boost bioenergy production as well as improve the economics of the process. Both laboratory and pilot-scale investigations were performed to explore the suitability of the AD and FPs for PPMS treatment.

AD and FPs have been described as potential technologies to meet the present and future requirements of renewable energy. Recent advances in higher mass reduction, increased biogas production, and reduced hydraulic retention times (HRTs) make the AD technology attractive to the P&P industry. ScienceDirect was used to identify the PPMS digestion-related articles. From the late 1990s to date, publications on the AD of PPMS have increased significantly (Saha et al., 2011; Bayr and Rintala, 2012; Hagelqvist, 2013; Priadi et al., 2014; Kinnunen et al., 2015; Ekstrand et al., 2016; Lopes et al., 2018; Takizawa et al., 2018; Alexander and Grant, 2018). The marked increase in the number of published papers began in 2008, but the last five years have witnessed a major jump. Of the studies published between 1995 and 2020, 45% of them were disseminated between 2016 and 2020. It is the authors' opinion that the recession of 2008 has forced the P&P industry to seek diversified returns to boost its profitability, which motivated the research to explore PPMS as a biofuel substrate. Also, a remarkable scientific interest was shown in the fermentation

of paper sludge for bioethanol and biohydrogen production, and several studies have been performed (Dwiarti et al., 2012; Lin et al., 2013; Robus, 2013; Chen et al., 2014; Gurram et al., 2015; Moreau et al., 2015; Robus et al., 2016; Mendes et al., 2017; Gogoi et al., 2018).

However, bioconversion of PPMS is not adequately discussed in the published review papers as it usually would be included with other wastes, for example, municipal sewage sludge and wastewaters. There are limited structured and specified reviews of this literature to assess the viability of PPMS for AD and FPs as well as highlight the gaps in the peer-reviewed literature. To this end, the reviews of Elliott and Mahmood (2007), Meyer and Edwards (2014), and Veluchamy and Kalamdhad, (2017) provided a useful insight into the effect of pre-treatments on AD of PPMS. A paper mill sludge-related review is needed because building up a complete picture could help to identify the practical interventions required to increase the efficiency of bioconversion pathways of PPMS. The objective of this review is to offer an up-to-date, detailed discussion of the recent developments, potentials, and constraints of bioconversion of PPMS to biogas, biohydrogen, biobutanol, and bioethanol. This review highlights the role that AD technology and FPs plays in PPMS biovalorization and biofuel generation. This paper also describes the composition, availability, and suitability of PPMS for bioconversion processes. It is anticipated that this review will serve as a useful literature source for researchers interested in the bioconversion of sludge to biofuels.

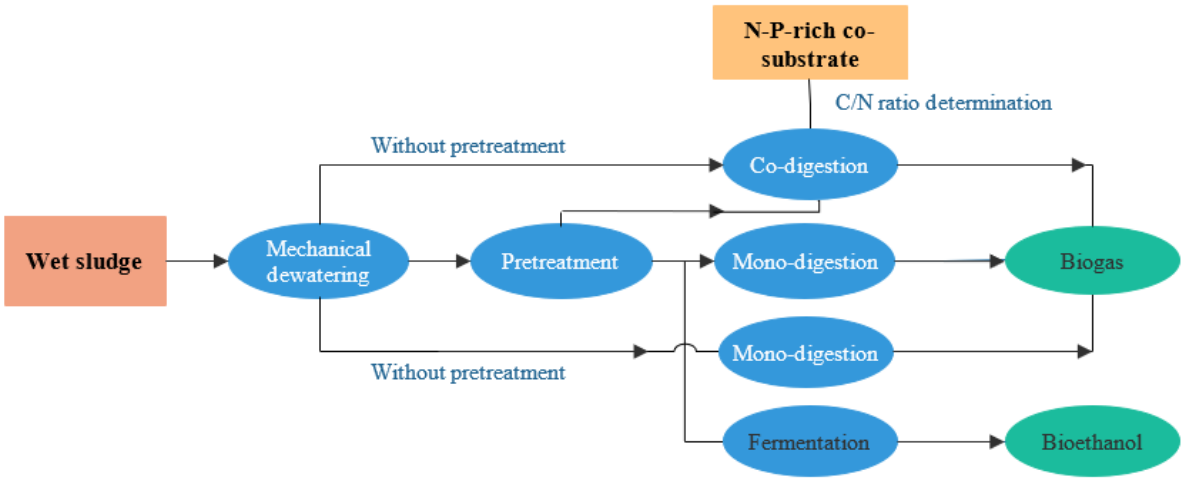

Figure 2.2.1: Potential pathways for biofuels production from pulp and paper sludge.

2. Composition and availability of PPMS

Various pulping methods are used to convert wood chips into individual fibers (pulp) including mechanical pulping, thermomechanical pulping, chemical pulping, chemo-mechanical pulping, and chemo-thermomechanical pulp. It has been reported that more than 7745 mills are currently in operation worldwide and producing about 192 Mt of pulp (Veluchamy and Kalamdhad, 2017). During the pulping processes, a

substantial amount of short fibers, lignin, and hemicellulose are rejected and dispersed or dissolved in the process water. It has been estimated that every tone of recovered fiber produces between 40–50 kg (dry weight) of the sludge of various kinds, about 70 percent of which are PS and 30 percent SS (Bajpai, 2015). It represents roughly 4.3 percent of the final product and increases to 20–40 percent in recycled paper mills (Ochoa de Alda, 2008). Table 2.2.1 summarizes the quantities of sludge production in selected countries. It has been reported that the yield of sludge from the paper mill is five to six times higher than that of the municipal wastewater treatment plant of the same size (Wu and Zhou, 2011). Global production of PPMS is projected to increase over the next 50 years between 48 and 86% above the current level (Mabee and Roy 2003). PPMS are available all year round all over the globe. During the pulping process, process water is discharged into the primary clarifier stream for physical treatment (either sedimentation or flotation), producing a large amount of PS after the dewatering process. In the case of the papermaking process, large quantities of wastewater are produced, requiring treatment by a primary and secondary clarifier, which yields secondary sludge (SS) or waste activated sludge (WAS) or as it is called bio-sludge (Fig. 2.2.2).

There is a vast disparity between the components of PS and SS, depending on the pulping process and the processed feedstock. Primary clarifier sludge comprises of cellulose, hemicelluloses, lignin, ash, extractives, and papermaking fillers, while SS contains primarily bacterial cells, cell-decay materials, and lignin precipitate (Bayr and Rintala, 2012; Park et al., 2012). Table 2.2.2 presents the lignocellulosic compositions of PPMS produced from different P&P mills. During pulping and papermaking processes, different chemicals are used; the fate of these chemical residuals also ends in sludge streams. Paper sludge should be treated to meet the environmental regulations before being released into the environment. Acceptably treating these wastes places a heavy burden on the P&P industry. Bio-sludge is usually burned with PS in the fluidized bed recovery boiler or disposed of in a landfill. Due to landfill restrictions by environmental regulatory authorities, combustion became the most common treatment practice to reduce the amounts of PS, and SS. However, P&P sludge has a very low heating value and can cause boiler failures, so it is necessary to obtain the dry content of the sludge as high as possible before the burning process. On the other hand, PS is an excellent source of biofuels because of its high carbohydrate content, and bioenergy recovery from PPMS has become a highly acceptable alternative to conventional management practices (e.g., disposal and incineration) in both scientific research and practice.

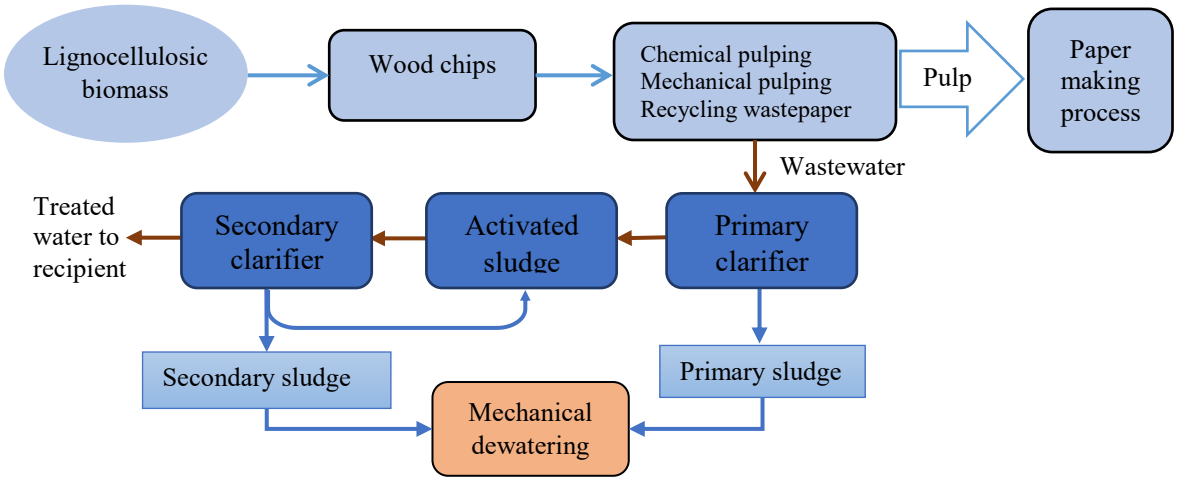

Figure 2.2.2: Pulping and water treatment processes in mills using activated sludge system

Table 2.2.1: Estimates of PPMS production in selected countries

Country	**Estimated sludge generation** (dry metric tons)	**Reference**
Canada	7.1 million	(Geng et al., 2007)
Colombia	70,000 – 110,000	(Madrid and Quintero, 2011)
China	12 million	(Dwiarti et al., 2012)
Europe	11 million	(Monte et al., 2009)
Hungary	50,000	(Kádár et al., 2004)
Italy	600,000	(Fava et al., 2010)
Japan	3.18 million	(Jeong et al., 2016)
Portugal	350 000	(Mendes et al., 2017)
UK	2 million	(Dwiarti et al., 2012)
USA	8 million	(Dwiarti et al., 2012)
South Africa	500 000	(Boshoff et al., 2016)

3. Suitability of PPMS as feedstock for bioconversion processes

PPMS has a very low heating value due to its high water content (70–90%) and can cause boiler failures, so it is necessary to obtain the dry content of the sludge as high as possible before the burning process. For this reason, PPMS is considered a biofuel of poor quality in the incineration and gasification processes. In contrast, substrates with large water content, reduced amounts of inorganic materials, and amiable to hydrolysis are ideal for AD and FPs. Further, the sludge from PPMs contains a high percentage of organic matter (65–97 % of volatile solids) compared to sewage sludge (59–68 % volatile solids) (Elliott and Mahmood, 2012). Besides the volatile fraction, PPMS contains 3.3–7.7 % nitrogen and 0.5–2.8 % phosphorus, based on the total solids compared to 2.4–5.0 % nitrogen and 0.7– 5.0 % phosphorus in the municipal sewage sludge (Elliott and Mahmood, 2007). The energy contained in these organic matters could be converted to high-quality biofuels in the form of biomethane, hydrogen, and ethanol, and the released nutrients from the AD process (residual digestates) could be utilized as biofertilizer in forest lands or can be recirculated to the aerobic activated sludge system (Karlsson et al., 2011) or used as a bioethanol

substrate. The high content of the volatile organic substances can also make PPMS more amenable to pre-treatment technologies.

Although PPMS has many appropriate physical and chemical properties, the AD of this waste sludge has some challenges that should be addressed so that it can be further valorized. These constraints might include low soluble COD, long residence time, and weak buffering capacity. Fortunately, there are several success stories of PS co-digestion with a complementary substrate. As reported in the literature, the poor buffering capacity and the modest fraction of N content in the lignocellulosic substrate can be compensated by mixing it with another substrate (e.g., municipal sewage sludge, pig manure, or cow dung) to maintain a variety of anaerobic microbes for good methanogenesis. Also, many successful pre-treatment approaches have been established to tackle the issues of low soluble COD and long HRTs (Table 2.2.5). Co-digestion of two streams aims to supplement N deficiency from the complementary substrate and reduce the inhibition effects, in addition to adding readily biodegradable COD and alkalinity (Parameswaran and Rittmann, 2012). Although many wastes could be used in the joint digestion with paper sludge, the co-digested candidate must be available in large quantities at adjacent locations and has appropriate physicochemical properties.

Table 2.2.2: Lignocellulosic components of pulp and paper mill sludges (PPMS) (% weight) (Kamali et al., 2016; Faubert et al., 2016; Lopes et al. 2018).

Sludge type	Lignocellulosic components (%) dry weight			Volatile matter (%)	Fixed carbon (wt %)	Total organic matter (wt%)	pH
	Cellulose	Hemicellulose	Lignin				
Primary sludge from Kraft pulp mill (virgin wood)	33 – 81	12 – 17	5 – 27	43 –77	7 – 12	91.3	6.2 – 6.9
Secondary sludge from Kraft pulp mill	15 – 31	0 – 5	23 – 30	38 – 56	4 – 8	37.2	7.3 – 8.5
Mixed PS+SS	45 – 48		15 – 22	77 – 82	13 – 18	64	3.8 – 8
De-inking paper sludge	52 – 63	14 – 22	17 – 24	43 – 63	10 – 23	50.2	7 – 9

4. Anaerobic digestion of PPMS for biogas production

4.1. Overview

AD as a process of converting organic matter into biogas by different consortia of microorganisms is an ancient technique. In addition to energy recovery, the AD has many other benefits represented in the reduced sludge volume, reduced pathogenic potential, and good sludge stabilization (Park et al., 2012). Today, AD techniques have been expanded to treat a wide range of organic wastes (municipal, agricultural, and industrial). Among other biomass types, PPMS were similarly used as feedstock for biogas generation (Puhakka et al., 1988; Puhakka et al., 1992; Park et al., 2012). Anaerobic conversion of organic matter to biogas involves three major steps: hydrolysis, acidogenesis (fermentation), and methanogenesis (Yunqin et

al., 2009). In the first step, certain bacteria hydrolyze carbohydrates and proteins into soluble compounds that can be digested further by other bacteria. While the second bacterial group (acidogenic bacteria) converts the produced sugars and fatty/amino acids to fermentation products, including CO_2, H_2, NH_3, and organic acids (e.g., acetate and formate). Finally, methanogenic archaea convert these products to methane. Besides methane, the produced biogas contains carbon dioxide and other gases such as N_2, oxygen as well as trace gases (e.g., H_2S, NH_3, and H) depending on digestion conditions.

Considering integrated forest biorefinery concepts, AD technology has been adopted in the P&P industry for the treatment of wastes. Anaerobic treatment of waste sludges has many benefits, the energy enclosed in the organic matters can be transformed to biomethane, and the produced bioenergy can be used straight as a fuel for heat generation or can be upgraded to high-value industrial biochemicals (e.g., methanol) (Bokhary et al., 2020). It has also been reported that AD of the waste activated sludge of paper mills can decrease solid wastes by 30-70% (Elliott and Mahmood, 2007). Along with biofuel yield, the nutrients contained in the anaerobic digestates might be exploited as a fertilizer or topsoil improvement (Karlsson et al., 2011). Furthermore, on-site sludge digestion provides another financial advantage for mills due to zero or lower waste sludge transportation costs (Hagelqvist, 2013). However, these substrates are not readily biodegradable. Therefore, pretreatment technologies, including physical, biological, chemical, and physicochemical were used to increase P&P sludge biodegradability and their methane yields through sludge solubilization.

Both mesophilic and thermophilic AD of paper sludge was used at the laboratory and pilot-scale levels (Table 2.2.5), but as far as we know, there is no full-scale AD plant installation in the P&P industry. This can be attributed to the high capital and operating costs of AD system installation as well as reduced degradation efficiency coupled with long HRTs. The process of mesophilic digestion is extensively applied compared to the thermophilic one, mostly because of reduced energy needs and increased process stability. In contrast, thermophilic AD is described by improved biochemical reactions, higher microorganisms' growth rate, and increased pathogen destruction (Elliott and Mahmood, 2007). Operating under thermophilic conditions allows raising the organic loading rates with the possibility of higher degradation capacity and excellent COD removal efficiency. Various types of bioreactors and configurations, whether simple batch or semi-continuous/continuous, one-stage or multi-stage, and one-phase or multi-phase, were employed (Bokhary et al., 2020). However, batches and semi-continuous bioreactor configurations are the norms in PPMS digestion (Table 2.2.5). Amongst the high-rate anaerobic bioreactors, anaerobic membrane bioreactors (AnMBR), up-flow anaerobic sludge blanket reactor (UASB), anaerobic filters (AFs), have been employed to process the PPM effluents. Several parameters influence AD processes such as

temperature, pH, organic loading rate (OLR), carbon/nitrogen ratio (C/N), hydraulic retention time (HRT), mixing (agitation), and inhibition and toxicity.

4.2 Anaerobic biodegradation improvement

In most cases, the hydrolysis and optimal C/N ratio are the rate-limiting issues during the AD of biomass waste rich in organic matters. During hydrolysis, the walls of microbial cells rupture, and the extracellular polymeric material decomposes, releasing easily degradable organic substances for anaerobic microorganisms. This is rarely the case in the treatment of PPMS due to the recalcitrant nature of its organic and inorganic constituents. To overcome these problems, different treatment approaches have been developed to make the pulp mill sludge a better source of methane, including pre-treatment techniques and co-digestion with other wastes. In the following section, commonly applied pre-treatment methods (chemical, physical, and biological) and co-digestion with other feedstocks to improve the productivity and total production of biogas are discussed.

4.2.1 Pre-treatment techniques

Pre-treatment technologies such as heating with ultrasonic, impact grinding, or addition of enzymes, were used to solubilize the paper sludge to reduce sludge HRTs, improve degradation efficiency, and increase the rate and production of biogas. Based on the nature of their work, pretreatment approaches could be classified into physical, biological, and chemical bases, but also combinations of these methods such as thermo-chemical processes are used. The following section describes some of the commonly used pretreatment techniques, along with some of their benefits and drawbacks (Table 2.2.3).

4.2.1.1. Chemical pre-treatment

Chemical pre-treatment has been used to increase PPMS accessibility to microorganisms using acid or base (e.g., NaOH, KOH) of different concentrations under different operating conditions.

4.2.1.1.1. Alkali and acidic pre-treatment

Alkali pre-treatment was used by several researchers (Heo et al., 2003; Yunqin et al., 2009; Wood et al., 2009; Park et al., 2012). These studies have shown that alkali pre-treatment increases biogas productivity from paper sludge substrates because it solubilizes lignin, which allows more access to other components such as cellulose and hemicellulose. Alkali pre-treatment also leads to swollen of the sludge and softening of the structure and can convert most of the macromolecule of paper sludge to monomers that are easily digestible by microorganisms. Park et al. (2012) reported increased solubility of about 3-14 times for TS, VS, and COD of pulp sludge compared to untreated sludge, but they did not notice any increase in gas production. The non-increase in biogas production can be partly due to the production of inhibitory compounds. Yunqin et al. (2009) pre-treated PPMS by NaOH before the AD at an HRT of 42 days and 37

°C, in laboratory-scale experiments. They achieved 83% COD solubility and 0.32 m^3CH_4/kg $VS_{removal}$ methane yield, which is higher than the control by183%, under the optimal pre-treatment condition of 8 g NaOH/100 g TS_{sludge}. NaOH is mostly utilized compared with other chemical substances such as potassium hydroxide and calcium hydroxide owing to increased COD solubility (Heo et al., 2003). Compared to thermal and sonication methods, alkali pretreatment is more efficient in dissolving proteins and carbohydrates in PPMS. However, alkali and acid pre-treatments are considered economically unattractive because of rising costs. Also, high doses of sodium hydroxide may inhibit microorganisms' activity and affect metabolic processes. Alkali pre-treatment was combined with ultrasound for improved sludge degradation (Park et al., 2012). This combination has resulted in a better sludge solubility and enhanced the AD performance, as compared to either treatment alone (Park et al., 2012), where the utilization of NaOH has weakened the walls of microbial cells, making them vulnerable to sonication analysis (Elliott and Mahmood, 2007). For more detailed information on the impact of alkali pretreatment on sludge see, e.g., Elliott and Mahmood, (2007).

4.2.1.2. Physical pre-treatment

4.2.1.2.1. Thermal pre-treatment

Thermal pre-treatment has been developed to solubilize biomass solids by disrupting the lignocellulosic complexes and cellular matter resulting in enhanced sludge bio-digestibility and biogas production. Thermal pre-treatment efficacy varies with the applied temperature and pre-treatment contact period, which in turn depends on the properties of sludge and the ratio of PS to SS.

4.2.1.2.1.1. Microwave pre-treatment

As one of the thermal pre-treatment methods, microwave (MW) pre-treatment of sludge from the forest industry was proposed and tested to improve sludge dewaterability and solubilization. Both kitchen and industrial MW type were studied whether below or above boiling temperatures. Saha et al. (2011) used an industrial MW unit and studied a wide range of temperatures (50–175°C). They reported a 90% increase in specific CH_4 yields of MW pre-treated WAS (at 175°C), compared to untreated sludge after 21 days of digestion under mesophilic conditions. The authors recommended heating rates between 1.4–4.5 °C/min and a temperature range of 50–175 °C for paper mill SS solubilization. Tyagi, et al. (2014) inspected the effects of alkali-enhanced MW on the solubilization of PPM waste-activated sludge. They achieved volatile suspended solids (VSS) and COD solubilization of 66 and 78%, respectively, with biogas production 6.3 % higher than the control. Microwave radiation was effective in sludge degradation as well as enhancing hydrolysis, leading to increased production of biogas (Saha et al., 2011; Tyagi et al., 2014). However, there is a lack of information on the impacts of MW irradiation on pulp mill SS and PS compared to municipal

biosolids. The authors argue that microwave is not economical due to the high energy inputs and small methane yields of P&P sludge.

4.2.1.2.1.2. Hydrothermal

Hydrothermal pre-treatment is applied to enhance the solubility of COD and the biological conversion potential of P&P mill SS. Bayr et al. (2013) pre-treated paper mill SS by hydrothermal and observed high COD solubilization and increased biogas yield. SCOD concentrations were increased more than nine times after hydrothermal pre-treatment, and the increase in methane yield was 31%. These results are consistent with those reported in the hydrothermal pre-treatment of pulp mill SS by Wood et al. (2009). SCOD concentrations were increased six times under hydrothermal pre-treatment (170 °C for one h), and the increase in biogas yield from the Kraft mills SS in batch experiments was 280%, and from sulfite pulping, SS was 50% under mesophilic environment (Wood et al., 2009). Thermal pre-treatment of SS from ammonium sulfite and Kraft mill reduced VSS by approximately 30% (Wood et al., 2009). Studies on pre-treatment of PPM sludge by hydrothermal are limited, thus, more investigations would be of interest.

4.2.1.2.2. Mechanical pre-treatment

Mechanical pre-treatment is used to improve the specific surface areas and readiness of sludge substrate for microorganisms, and thus to boost the biogas yield. Several researchers have studied the effect of pre-mechanical processing on PPMS digestibility.

4.2.1.2.2.1. Ultrasonic pre-treatment

Ultrasound pre-treatment, which involves the use of high-frequency sound waves resulting by a pulsing probe, has been used to disrupt the microbial cell walls and enhance biogas production of PPM biological sludge (Wood et al., 2009; Karlsson et al., 2011; Saha et al., 2011; Elliott and Mahmood, 2012). The main purpose of using the ultrasound pre-treatment is to breakdown the membrane of the microbial cells and release the intercellular organic matter in the bulk mixture of the AD. However, there is limited information and no consensus on the effect of sonication on sludges disintegration and cell membrane rupturing. For example, Wood et al. (2009) noted no significant effect for ultrasonication on biogas yield from sulfite and Kraft mills SS. Similar findings were also stated by Karlsson et al. (2011) during biogas production after ultrasound pre-treatment of SS, originating from two P&P mills (Kraft and chemi-thermomechanical pulp (CTMP)). Contrary to the research findings of Wood et al. (2009) and Karlsson et al. (2011), an increase of 51% and 28% in CH_4 yields using ultrasonic-pre-treated SS from bleached chemi-thermomechanical pulp mill (BCTMP) has been achieved in batch investigations under both mesophilic and thermophilic conditions, respectively (Saha et al., 2011). The slight effect of sonication on the paper sludge can be due to the breakage of the sludge floc and the thinning of the microbial cell wall. The variation in the reported

results could be due to the use of different sonication time and intensity, as well as the variability of sludges sources. Overall, ultrasound pre-treatment may be somewhat appropriate for biological sludge but not for primary sludge.

4.2.1.2.2.2. Liquid shear/ High-pressure homogenizer

The high-pressure homogenization (HPH) process, which uses a sudden pressure change to decompose the bacterial cells of SS before AD, has been applied to boost PPMS digestibility and reduce the sludge volume. HPH uses sharp velocity gradients and cavitation to effectively solubilize sludge solids and release cellular components (Elliott and Mahmood, 2012). A few researchers have assessed the impact of HPH on PPM sludge (bio-sludge) digestibility. Saha et al. (2011) pre-treated SS by an HPH (12,000 psi) to shorten HRT and increase biogas yield, followed by a batch AD process. After the pre-treatments, COD/TCOD increased by 70%, while the methane yield increased by 80%. The energy input during the homogenization of SS was 4000 kJ/kgTS corresponding to a total solid of 2.5%. Whereas Elliott and Mahmood (2012) noted that the HPH digester operated at a 3-day mean SRT generated 7% more biogas compared to the control. This pre-treatment features higher power consumption requirements; therefore, it is difficult to scale it up to a commercial level.

4.2.1.3. Biological pre-treatment

The effect of the hydrolytic enzyme (Karlsson et al., 2011; Mshandete et al., 2005) and mushroom compost extract (Yunqin et al., 2010) on methane production potentials were investigated and reported in the literature. Biological pre-treatments have shown clear effects on the production of biogas in the subsequent Ad of PPM secondary sludge. Mshandete et al. (2005) noted that 9 hours of enzymatic treatment of sisal pulp before AD yielded 26% more methane than the control. Yunqin et al. (2010) reported a 134 % higher methane yield for mushroom compost extract (MCE) treated PPMS than untreated PPMS. The active MCE was more efficient in terms of degradation than inactive MCE. Karlsson et al. (2011) examined the effect of hydrolytic enzyme treatment on biogas yield from sludge originated from the chemi-thermomechanical pulp (CTMP) in the CSTR experiments, but no effect was observed on sludge digestibility in viable ranges of enzyme inputs. Different hydrolytic enzymes are used such as cellulases, proteases, xylanases, lipases, pectinases, and amylases (Table 2.2.3). Based on the reported studies, biological pre-treatments have a positive effect on the solubility of the substrate. However, to ensure the efficacy of the biological pre-treatments, further investigations are needed to better elucidate their effect on AD of PPM sludge.

4.2.1.4. Summary

A wide range of pre-treatments ranging from simple mechanical grinding to sophisticated treatments is available for PPMS solubilization or disintegration, and some of them have proved their effectiveness. However, most of the studies were focused on the pre-treatment of sewage sludges from municipal

wastewater treatments, compared with relatively few studies that were concerned with PPMS manipulation by various pre-treatments. Generally, when the substrate type/composition and pre-treatment method/condition are properly matched, the feedstock becomes more easily accessible to anaerobic degradation, resulting in improved biogas production. However, this is not often the case; some pre-treatment methods have increased the rate of substrate decomposition but have not increased the productivity of biogas. On the other hand, despite different pre-treatment methods are used, it is difficult to evaluate which ones are cost-effective. There is a near-total lack of a systematic comparison and cost-benefit analysis of pre-treatment methods used in the preprocessing of PPMS prior to AD. Also, costs are not often included in research papers, thus the economic viability remains unclear. It is, therefore, worthwhile to include pre-treatment costs in the conducted studies.

Table 2.2.3: Summary of pre-treatment methods of pulp and paper mill sludges for biodegradation improvement

Pre-treatment type	Sludge type	Digestion conditions	Pre-treatment and operational conditions	Advantages	Disadvantages	Reference
Chemical	Waste activated sludge	–	Alkali (NaOH, 45 mequiv. /L, 25–55 °C, 4 h)	The solubility of COD ↑ (28%–38%)	Chemical cost and neutralization requirement before digestion	(Heo et al., 2003)
	Waste activated sludge	Mesophilic	Alkali (NaOH, KOH, $Mg(OH)_2$, 130 °C)	The fraction of the soluble COD↑ VS reduction↑ by 30%	Toxicity of Na^+, and corrosion	(Kim et al., 2003)
	Secondary sludge from ammonium sulfite and Kraft mill	Mesophilic	Alkali (NaOH, 60 min, pH 12, 140 °C)	Soluble COD↑ Biogas production↑	It generates inhibitory compounds	(Wood et al., 2009)
	P&P sludge/ Monosodium glutamate waste liquor	Mesophilic	Alkali (NaOH, 6 hr, pH 7.7 and 8.7) Dosage (4, 8, and 16 g NaOH/100 g TS_{sludge})	Soluble COD concentration (83%) ↑ Methane yield ↑	High dosage of NaOH causes microorganisms toxicity, corrosion	(Yunqin et al., 2009)
	Secondary sludge from BCTMP[a] and TMP[b] (thickened)	Mesophilic	Alkali (NaOH, 120 min, pH 8.3 and 8.8)	–	No improvement was noticed in biogas yield. pH↑→ inhibition↑ Salt build-up↑ High cost	(Park et al., 2012)
	Kraft and paper mill waste activated sludge	Thermophilic	Alkali (NaOH, pH 12)	Soluble COD↑	pH↑→ inhibition↑ Salt build-up↑ High cost	(Bayr et al., 2013)
	Kraft and paper mill waste activated sludge	Thermophilic	Nitric acid (HNO_3 (0.48 g/g VS), pH 3, 24 h)	TS↑	Ammonia inhibition↑ Biogas production ↓ → lower than the control.	(Bayr et al., 2013)
	Waste activated sludge from P&P mill	Mesophilic	Alkali (30-240 min, pH 9, 12.5)	Biogas production↑	pH↑→ inhibition↑ Salt build-up↑ High cost	(Tyagi, et al., 2014)
Thermal	BCTMP[a] pulp mill waste activated sludge	Mesophilic	Microwave (2450MHz, 1250W, 50-175 °C)	Specific methane yields ↑	High energy inputs	(Saha et al., 2011)
	Waste activated sludge from P&P mill	Mesophilic	Microwave (50-175°C, 30-438s, 1200 W, 2.45 GHz)	tCOD and VSS[d] solubilization↑ 33% and 39%, respectively	Deteriorated the sludge dewaterability	(Tyagi, et al., 2014)
	Kraft and paper mill waste activated sludge	Thermophilic	Hydrothermal (150 °C, 10 min and 70 °C, 40 min)	Soluble COD concentration↑ Methane yield ↑	High energy costs Hemicellulose content↓	(Bayr et al., 2013)
	Sulfite mills secondary sludge	Mesophilic	Hydrothermal (170 °C, 60 min)	Soluble COD concentration↑	High energy inputs	(Wood et al., 2009)

				Sludge biodegradability↑ Biogas yield ↑		
	CTMP[c] and kraft pulp activated sludge	Mesophilic	Thermal 70 and 140 °C	Pre-treatment at 140 °C had a positive effect on biogas yield	Pre-treatment at 70 °C did not improve the biogas yield.	(Granström and Montelius, 2014)
Mechanical	Secondary sludge from ammonium sulfite and Kraft mill	Mesophilic	Ultrasound (20kHz, 1 W/mL sonication intensity, 30 min)	–	High energy demand. No improved was observed in biogas yield	(Wood et al., 2009)
	BCTMP pulp mill waste activated sludge	Thermophilic	Ultrasound (20kHz, 400W, 15-90 min)	Biogas production↑ Digestate↓	High energy demand. Generated soluble non-biodegradable compounds	(Saha et al., 2011)
	Waste activated sludge from mechanical pulp mill	Mesophilic	Ultrasound (20 kHz, 1.6 kWh/kg TSS)	Digestion rate ↑	High energy demand. Ultrasound has a very low effect only suitable for biological sludge and not the PS.	(Elliott and Mahmood, 2012)
	Secondary sludge from BCTMPb and TMP (thickened)	Mesophilic	Ultrasound (40 kHz, 80 min)	The soluble TS↑, VS↑, and COD↑	No improvement was noticed in biogas yield. Sludge dewaterability was reduced	(Park et al., 2012)
	Waste activated sludge from P&P mill	Mesophilic	Ultrasound (2, 3, 5, 15 and 30 Wh L^{-1})	--	No discernible effect was noticed on methane production potential	(Karlsson et al., 2011)
	Waste activated sludge from P&P mill	Mesophilic	Ultrasound (15-60 min, 40 kHz, 500 W)	tCOD and VSS solubilization↑ 58% and 37%, respectively	High energy demand. Ultrasound has a very low effect only suitable for biological sludge and not the PS.	(Tyagi, et al., 2014)
	Kraft and paper mill waste activated sludge	Thermophilic	Ultrasound (45 kHz, 30 min)	A slight increase (6%) in methane yield.	High energy demand. Did not improve the methane yields significantly.	(Bayr et al., 2013)
	Waste activated sludge from mechanical pulp mill	Mesophilic	Mechanical shear (high shear mixing at 1500 rmp)	sCOD↑	High energy demand	(Elliott and Mahmood, 2012)
	Waste activated sludge from mechanical pulp mill	Mesophilic	High-pressure homogenization	Methane production↑ Soluble COD↑ TSS↓	Higher power consumption requirements	(Elliott and Mahmood, 2012)
Biological	Dehydrated paper pulp sludge	Mesophilic	Enzyme (5 different brands)	Substrate degradation↑ Methane concentration↑ Faster degradation rate	Process instability was observed	(Kolbl et al., 2017)
	Kraft and paper mill waste activated sludge	Thermophilic	Enzymes (a mixture of Accelerases, 70 mg/gVS)	Substrate degradation↑ Methane concentration↑ Soluble COD↑	No significant increase in methane yields was noticed when enzymes were used alone.	(Bayr et al., 2013)
	P&P mill secondary sludge	Mesophilic	Mushroom compost extract (250 A.U./gVS_{sludge}) Aerobically, 37°C, 4h	sCOD↑ The concentration VSS↓ Methane yield↑	Inactive MCE was not effective as the active one.	(Yunqin et al., 2010)
	Paper Sludge	Mesophilic	Rumen fluid, 37°C, 6 h	Methane production↑ Substrate degradation↑ Dissolved COD↑	–	(Takizawa et al., 2018)
	P&P bio-sludge		Enzymes (different brands)	Biogas yield↑ by 26%		(Bonilla et al., 2018)
	Waste activated sludge from CTMP mill	Mesophilic	Enzymes (a mixture of cellulases, proteases and lipases)	–	No positive effects were noticed on methane production potential	(Karlsson et al., 2011)
Hybrid pre-treatment						
Thermo-chemical	Activated sludge from P&P mill	Mesophilic	MW–alkali pH 12, 175 °C	tCOD and VSS solubilization↑ 78% and 66%, respectively	Inhibition of AD activity under harsh thermal–alkali treatment conditions.	(Tyagi, et al., 2014)
	Activated sludge from P&P mill	Mesophilic	US–alkali pH 12+60 min	tCOD and VSS solubilization↑ 66% and 49%, respectively. The biogas generation↑ by 47% over the control	Deteriorated the sludge dewaterability	(Tyagi, et al., 2014)

Chemical-mechanical	Secondary sludge from BCTMP[b] and TMP[b] (thickened)	Mesophilic	Alkaline and Ultrasound (40 kHz, 80 min) and Alkali (NaOH, 120 min, pH 8.3 and 8.8)	The soluble TS, VS, and COD increased 3-14 times over non-treated sludge.	Biogas production has not been significantly improved. Reduced the dewaterability of sludges	Park et al., (2012)

[a]BCTMP: bleached chemi-thermomechanical pulp; [b]TMP: thermomechanical pulp; CTMP[c]: chemi-thermomechanical pulp, [d]VSS: volatile suspended solids.

4.2.2. Co-digestion of PPMS and non-mill substrates

Among the energy recovery scenarios, co-digestion of PPMS with a nutrient-rich solid waste is used by several researchers to enhance the performance of AD and methane production (Poggi-Varaldo et al., 1997; Mshandete et al., 2004; Chen et al., 2013; Lin et al., 2013; Hagelqvist and Granström, 2016). Co-digestion of mixture feedstocks has the benefit of accomplishing the desired carbon/nitrogen ratio (C/N) and enhancing the nutrient content of the AD. Anaerobic digestion tends to be unsuccessful when a single, readily biodegradable organic matter source (e.g., PS) is used as the sole substrate without nutrients and buffering agents' addition (Lin et al., 2012). Numerous wastes contain excellent buffer-capacity and high nutritional contents, which can be exploited in the in co-digestion with P&P sludge. Optimizing C/N ratio through joint digestion with a complementary substrate increases not only the production of biogas but also reduces the concentration of toxic ammonia. This practice has been applied by Poggi-Varaldo et al. (1997), who co-digested a mixture of paper sludge and municipal solid waste and reported improved biogas yield (increased by 48%) under thermophilic condition. Similarly, Hagelqvist, (2013) co-digested P&P sludge with sewage sludge and achieved 84 $NmlCH_4/gVS_{added}$ of methane production compared to 53 $NmlCH_4/gVS_{added}$ for SS alone under the mesophilic condition for 19 days. Co-digestion of food wastes, pig manure, monosodium glutamate liquor, or cow manure with PPS are other examples to improve PPMS digestibility (Ofoefule et al., 2010; Chen et al., 2013; Lin et al., 2013). Lin et al. (2011) treated paper mill sludge and monosodium glutamate liquid (which have a high nitrogen content) in a batch process and reached organic removal efficiency in the range of 25 – 32.2% and biogas production of 200 $mlCH_4/gVS_{added}$. In another study, Lin et al. (2013) co-digested PPMS and food waste (FW) for the co-production of methane and hydrogen and achieved 432 ml/g VS_{fed} production of methane and 64.5 ml/g VS_{fed} hydrogen under sludge/FW ration of 1:1VS. The combined digestion of PPM sludge with other substrates could enhance not only methane productivity (energy recovery) but also organic matter degradation (Table 2.2.4). However, significant differences were observed in methane production due to the difference in types and sources of co-substrates. As a rule of thumb, the choice of the co-substrate should depend on the co-substrate availability and in a nearby location, reduced cost, and high nitrogen content, as well as the content of macro and micronutrients.

Table 2.2.4: Summary of pulp and paper mill sludges co-digestion with other substrates (non-paper mill sludge)

Sludge type	Experimental setup	Digestion conditions	Biogas production (ml CH_4/g VS_{added})	Percentage increase in CH4 yield	Reference
Paper sludge and municipal solid waste	Lab-scale	35 and 55 °C, pH 8, ORL (4.5 and 8.2 g VS/kg.d).	–	48%	(Poggi-Varaldo et al., 1997)
Sisal pulp and fish wastes	Batch	1 L digester, 27 °C,	0.62[b]	93.75%	(Mshandete et al., 2004)
Algal sludge and wastepaper	Bench-scale	4L digester, HRT 10 day, 35 °C, pH 6.5, C/N 18.	100 – 140	104%	(Yen and Brune, 2007)
Paper waste and cow dung	Lab-scale	50L digester, HRT 45 day, 26 – 43 °C, pH 7.5	6.23 – 9.34[b]	50%	(Ofoefule et al., 2010)
Paper mill sludge and monosodium glutamate liquor	Bench-scale	10L digester, 37 °C, pH 6.0–8.0	200	–	(Lin et al., 2011)
Paper sludge and food waste	Lab-scale	0.7L digester, 37 °C, pH 5.8–8.4	123 – 256	70.6%	(Lin et al., 2012)
Paper sludge and pig waste	Batch BMP[a]	1 and 3L digesters, HRT 35 day, 37 °C, pH 6.8–7.6	–	78.6%	(Parameswaran and Rittmann, 2012)
Paper tube and glue sodium silicate/glue polyvinyl alcohol	Lab-scale	10 L digester, HRT 20 – 25 day, 55 °C, pH 7.0	268 – 403	50%	(Teghammar et al., 2012)
P&P sludge with pig manure	Lab-scale	2 L reactor, 50°C, SRT 10 days,	71.58 – 83.54	–	(Chen et al., 2013)
P&P sludge and sewage sludge	Batch wise	0.25 L digesters, HRT 19 day, 38/40 °C, pH 7.9 and 7.6	53 – 84	58.5%	(Hagelqvist, 2013)
Pulp & paper sludge and food waste	Lab-scale	0.8 L digesters, 55 °C, pH 7.0	432.3	–	(Lin et al., 2013)
Rice straw and paper mill sludge	BMP[a]	1 L, 35 °C	330	–	(Mussoline et al., 2013)
Paper sludge and cow manure	Lab-scale	15 L bioreactor,	269	105.55%	(Priadi et al., 2014)
Secondary paper and pulp sludge and natural zeolite	Lab-scale	5 L, 30 °C	183	10%	(Huiliñir et al., 2014)
Sewage sludge and sugar beet pulp lixiviation	Lab-scale	0.130 L, 35/ 55°C, pH 6.6 –7.7	28.2 – 544.4	–	(Montañés et al., 2015)
Ground rice straw and cow manure	Lab-scale	2.5 L reactor, 37 °C, C/N 24	380	–	(Li et al., 2015)
P&P mill sludge with manure and grass silage	Lab-scale	0.5 L reactor, 38 °C, pH 7.1–7.6,	50	–	(Hagelqvist and Granström, 2016)
Cassava pulp with pig manure	Lab-scale	7 L reactor, 31°C, pH 7.2–7.8, C/N 35	130 – 380	–	(Glanpracha and Annachhatre, 2016)
Sewage sludge and paper pulp reject	BMP[a]	1 L, 35 °C,	157 – 368	134.4%	(Xie et al., 2017)
Wastepaper and macroalgae	BMP[a]	0.5 L reactor, 37 °C, pH 6.95,	185 – 386	33%	(Rodriguez et al., (2018)

[a]BMP = Biochemical methane potential assay; [b] = m^3CH_4/kg VS_{added}

4.3.Anaerobic digestion of primary sludge

Several researchers investigated paper sludges as a substrate for biogas production of both primary and secondary sludge types and their mixture with or without pre-treatment. However, the reported results of AD of PS are limited, and PS exploitation as a biogas substrate is still in the investigation stage (Fein and Patel, 1998; Jokela et al., 1997; Bayr and Rintala, 2012; Veluchamy et al., 2017). The methane potential of the PS varied considerably depending on the mill production process (pulping type) and reactor configuration/digestion conditions. Jokela et al. (1997) achieved biomethane production of 45 m^3 CH_4/tVS_{added} for the PS from a thermomechanical pulp mill (TMP) in the batch test. While, Bayr and Rintala (2012) reported a biogas yield of 210–230 m^3 CH_4/tVS_{added} for the PS from a bleached kraft P&P mill in batch experiments, which is several times higher than those reported by Jokela et al. (1997) for the primary sludge from TMP. This suggests that PS from kraft pulping is a more potential substrate for biogas production than the PS from TMP, due to better decomposition by chemical cooking. In the TMP, the wood chips are steam heated and mechanically refined, thus the resulting sludge requires pre-treatment to make its holocellulose more amenable to the anaerobic degradation. In a recent study, Veluchamy et al. (2017) used a PS of Kraft pulping mill and reported methane potential of 264.5 $mLCH_4/g$ of $VSd_{egraded}$ in biochemical methane potential (BMP) experiments. Based on the literature, the reported studies were conducted at relatively long (HRTs) hydraulic retention times 15–60 days and low (OLRs) organic loading rates 1–2.5 gVS/m^3d (Table 2.2.5). Investigation studies under shorter HRTs and higher OLRs would be interesting and noteworthy. Also, the adoption of an anaerobic membrane reactor (AnMBR) that decouples HRT and SRT can achieve a significant decrease in HRT and reactor sizes. Unlike the SS, PS has greater energy potential due to the higher fiber content and produces methane gas two to three times greater than the SS in both mesophilic and thermophilic conditions. However, PS suffers from nutrient deficiency problems (relatively low in 6– 0% nitrogen and 2–5% phosphorous), and therefore, nutrients must be added to improve the nutrient content needed for the growth of anaerobic microorganisms.

On the other hand, other PPM sludges, like deinking sludge from waste paper recycling, paper tube sludge, and sedimented paper fiber were investigated for methane production (Ogun et al., 2015; Steffen et al., 2017; Amare et al., 2019), and their methane generation is poorer or comparable to the PS. The methane production for sedimented paper fiber was 201 mL/g VS, COD_{fed}, and is comparable to PS. Whereas, the methane potential for the deinking sludge ranged between 105–159 mL/g VS, COD_{fed} (Table 2.2.5)

4.4. Anaerobic digestion of secondary sludge

Compared to PS, the biogas production of waste activated sludge (WAS) from various pulp processes has been extensively investigated (Puhakka et al., 1992; Karlsson et al., 2011; Bayr and Rintala, 2012). Secondary sludge is a highly biodegradable substrate; microbial cells and cell-decay materials its main

components. Its characteristics vary with raw materials used and the pulping process, as well as the wastewater treatment system (Bayr et al., 2013). Thus, methane yield as low as 50 m^3/t VS_{added} was reported for bleached Kraft PPM WAS, and as high as 230 m^3/t VS_{added} was reported for bleached chemi-thermomechanical pulping (CTMP) (Table 2.2.5). OLRs in the range of 1.5–5.2 kgCOD/m3/d and HRTs in the range of 8–42 d was investigated in the literature, as can be seen in Table 2.2.5. Puhakka et al. (1992) studied kraft PPM waste sludge (WAS) in a pilot-scale process, under mesophilic conditions for 21 months and reported biogas yields of 0.360 m^3/kg VS_{added}, and the content of the methane was 56–57%. In this study, a 40% reduction in sludge volume was achieved, and the sludge OLR of 2.2 kg/m^3 d was suggested for high process performance. Karlsson et al. (2011) studied biomethane production possibilities of WAS from the six pulping facilities in batch treatments at 35 °C and reported biogas production 90–197 m^3/t VS_{added} for TMP sludge, 159 m^3/t VS_{added} for the sulfite PPM sludge, and, 145 m^3/t VS_{added} for the kraft PPM sludge, and 97–200 m^3/t VS_{added} for chemi-thermomechanical and kraft PPM sludges. From these results, it seems that there is not much difference in the average biogas productivity between the P&P mill processes. Also, the biogas yield from SS is to some extent lower than PS. This can be explained by the fact that the organic matter in SS is partially degraded in the aerobic activated sludge process, and contains lignin, which is poorly biodegradable plus sulfur-containing substances. Also, lignin was found to cause an inhibitory effect on microorganisms.

4.5. Co-digestion of primary and secondary sludge

The synergistic influences of co-digestion of PS and SS from P&P industry have been investigated by many researchers (Puhakka et al., 1988; Bayr and Rintala, 2012). Biogas yields in the range of 50 – 170 m^3CH4/tVS_{added} were observed (Table 2.2.5). Puhakka et al. (1988) investigated AD of a mixture of PS/SS from a CTMP mill under both mesophilic and thermophilic conditions in flow reactor experiments, and they reported higher biogas yields (0.09 $m^3/kgVSS_{added}$) under mesophilic (35°C) conditions than thermophilic (55°C) conditions (0.05 $m^3/kgVSS_{added}$) at an OLR of 2.5 kg VSS/m^3d and HRT of 15 days. The authors attributed these results to the stability of the mesophilic digestion process. In another study, Yunqin et al. (2009) achieved a biomethane yield of 0.32 m^3CH_4/kg $VS_{removed}$ under mesophilic conditions. Bayr and Rintala (2012) examined the co-digestion of PS and SS at a ratio of 3:2 (VS basis) under thermophilic conditions in CSTR, and they achieved biomethane yields of 150–170 m^3CH4/tVS_{fed} under OLR of 1 kgVS/m^3d and HRTs of 25–31d; this was resulted in VS removal between 25 and 40 % and (Bayr and Rintala, 2012). This indicates that the removal efficiency of the organic matter is not high resulting in an anaerobic rich digestate. This digestate needs further biovalorization via its conversion to biofuel or another value-added material. On the other hand, Bayr and Rintala (2012) observed no difference in the biogas yield between the digestion of the PS alone and the co-digestion of the PS/SS. This shows that there is no point in co-digesting PS with SS. PS should be digested separately from SS and followed by a

bioethanol production from the resulting waste (digestate). Alternatively, PPM sludges are preferably co-digested with non-mill substrates; this would be useful not only to offset the nutrients shortage/balance C/N ratio but also to reduce inhibitory substances.

4.6. PPM sludges vs other substrates

Figure 2.2.3 compares the potential of biogas recovery from the AD of PPM sludges and selected non-mill substrates. A wide range of organic substrates has been anaerobically digested. The substrate content of sugars, fats, and proteins, as well as the ratio of C/N, governs its potential and quality for energy production (Dobre et al., 2014). Sometimes, co-digestion is performed to balance the content of substrates. Compared with the selected substrates, P&P primary sludge considers a promising energy source, most likely due to its preprocessed biomass and high cellulose content. It yields biogas in the range of 210 – 260 $m^3_{Biogas}/t_{substrate}$ (Table 2.2.5). However, food grease is the most attractive substrate compared to PS, and its methane potential is more than 300 $m^3/t_{substrate}$ as shown in Fig. 2.2.3, which is much higher than all other feedstocks reported. Based on this review, it is worth noting that the PS produced from the chemical pulping has more energy potential compared to the thermomechanical pulping sludge. This difference can be explained by the difference in the pulping conditions. Despite its potential for energy production, the reported results for anaerobic digestion of PS are somewhat rare compared to SS. The composition of biogas differs slightly among the reported substrates despite the differences in the energy potential. The methane content for residues of agriculture and energy crops ranged between 52 and 56% (Das and Mondal, 2016), while the methane content for animal manures ranges from 55 – 65% %. Sources of substrates for AD vary, but they must meet certain criteria to be feasible energy sources.

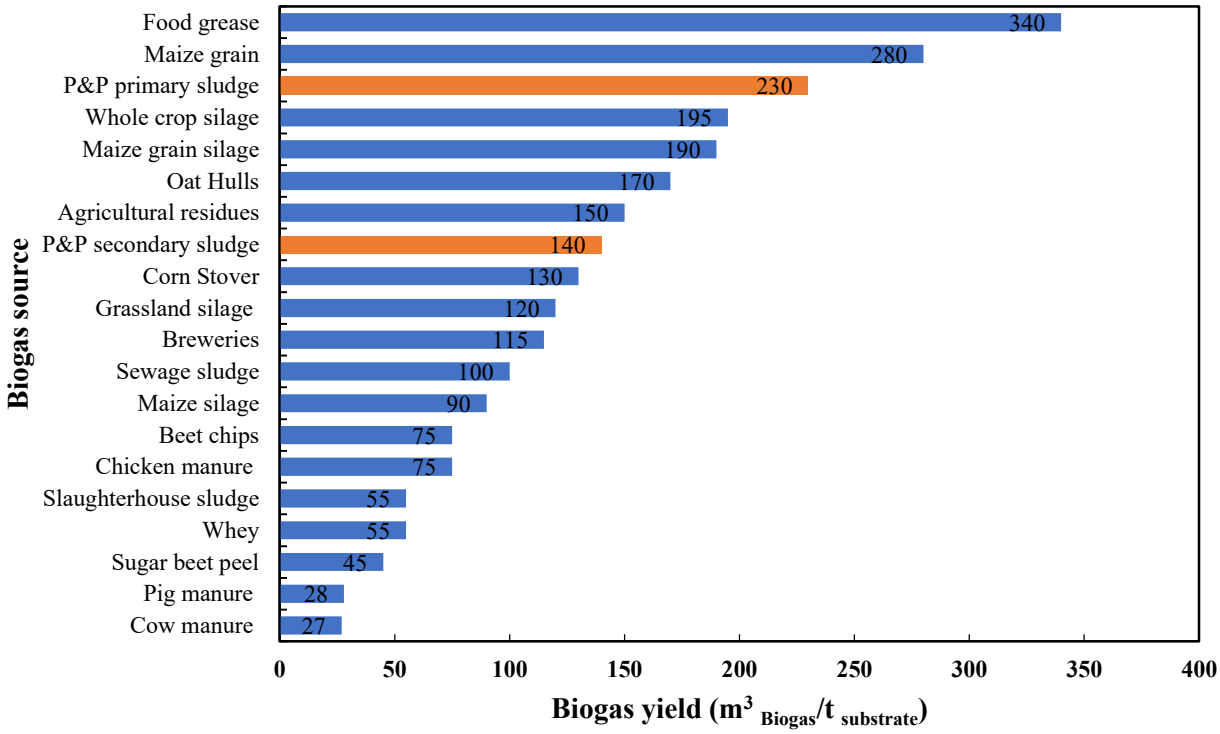

Figure 2.2.3: Potential of PPM sludge for biogas production compared with other selected non-mill substrates (Weiland, 2000; Hamilton, 2012; Kythreotou et al., 2012).

4.7. Summary

Table 2.2.5 summarizes the anaerobic digestion of PPM sludges. Compared with the non-mill substrate, PPM sludge is a promising feedstock for biogas production. All PPM sludge types and their mixture as well as their co-digestion with non-mill substrates were investigated for biogas production. Organic loading rates in the range of 1–7 kgCOD/m^3/d and hydraulic retention times in the range of 4–72 days, were examined under both mesophilic and thermophilic temperatures. Of the reported studies, 7 studies were performed in thermophilic conditions and only two studies at ambient temperature, while the remaining work was done under mesophilic conditions. However, most studies were conducted at the laboratory level using BMP with few studies at the pilot level and no industrial-scale implementation. Although the AD is practiced largely in the municipal sector; it has not gained much popularity in the forest industry for solid organic waste treatment at a full-scale level due to long retention times (30–60 day) and low efficiency of total degradation rates (30–50%) of dry organic solids. From microorganisms' performance point of view, paper mill activated sludge is technically more suitable for AD compared to primary sludge. However, PS can potentially be a better substrate for biogas production than bio-sludge if an appropriate treatment method is developed. In the literature, several pre-treatment techniques based on chemical, physical, and biological principles have been tested in attempts to break down the PPMS- recalcitrant characteristics and make it

amenable to anaerobic microorganisms. Also, combinations of these pre-treatments such as thermochemical processes are applied. However, there is still a need to conduct PPMS-related systematic studies (methodological comparison and cost-benefit analysis) of possible pre-treatment technologies. Above all, the economic viability of PPM sludge depends not only on the effectiveness of the pre-treatment method but also on the price of the biogas produced and valorization of the digestate.

Table 2.2.5: Anaerobic digestion of pulp and paper mill sludges

Type of sludge	Experimental setup	Optimal temperature (°C)	pH	Retention time (days)	OLR kgCOD/m^3/d	Working volume (L)	Specific methane yield (mL/g VS, COD_{fed})	CH_4 content (%)	VS removal (%)	TCOD removal (%)	Reference
Primary and secondary sludge from pp mill	BMP assay[a]	37	7.7– 8.7	40	–[k]	0.7	0.32[h]	–	–	83–93[g]	(Yunqin et al., 2009)
Secondary sludge from ammonium sulfite mill	BMP assay	35	7	34	–	0.16	200 ± 0.01	70	15 ± 7[i]	42 ± 2	(Wood et al., 2009)
Secondary sludge from Kraft mill	BMP assay	35	7	34	–	0.16	45	70	27 ± 2[i]	6 ± 0.5	(Wood et al., 2009)
Secondary sludge from BCTMP mill	BMP assay	37	7.4–8.6	42	–	0.7	230	–	33–44	56–71	(Yunqin et al., 2010)
Secondary sludge from BCTMP[b] + 10% monosodium glutamate	Semi-continuous fed reactor	37±2	5.3–7.8	8–27	1.5–5.0	2	0.434[h]	–	47–61	–	(Yunqin et al., 2011)
Paper sludge and food waste	Fed-batch lab-scale process	37	5.8–8.4	8–55	–	0.7	123–256	–		73 – 93	(Lin et al., 2012)
Mixed PS and secondary sludge from BCTMP mill	BMP assay	55	–	21	1.98	2, 3.5	50 – 95	–	9–21	12 – 20	(Saha et al., 2011)
Mixed PS and secondary sludge from BCTMP mill	BMP assay	35	–	21	1.7	2, 2.5	55 –75	–	10–24	12 –58	(Saha et al., 2011)
Paper sludge and pig waste	Batch-BMP	37	6.8–7.6	35	–	1	0.14[j]	60	–	54	(Parameswaran and Rittmann, 2012)
Secondary sludge from BCTMP and TMP[c] (thickened)	BMP assay	36±1	74–7.6	28	–	0.25	320	–	–	–	(Park et al., 2012)
Primary sludge	Semi-continuous fed reactor	55	6.5–8.2	16–32	1–2	4	210 – 230	–	30–40	–	(Bayr and Rintala, 2012)
Secondary sludge	Semi-continuous fed reactor	55	6.5–8.2	25–31	1	4	50 – 100	–	29–32	–	(Bayr and Rintala, 2012)
Co-digestion of primary and secondary sludge	Semi-continuous fed lab-scale reactor	55	6.6–8.2	25–31	1–1.4	4	150 – 170	–	25–32	–	(Bayr and Rintala, 2012)
Secondary sludge from a mechanical pulp mill	Bench-scale reactor	37	6.8–7.5	20	2.2 – 16.6	5	73 – 91	65	9 – 58	60	(Elliott and Mahmood, 2012)
Secondary sludge from TMP, CTMP, Sulphite, DIP[d], and Kraft	Semi-continuous lab-scale reactors	37	7.3– 7.8	20	1.2 – 3.3	4	100 – 200	56	–	–	(Karlsson et al., 2011)
Paper tube and glue sodium silicate/glue polyvinyl alcohol	BMP assay	55	7.0	20–25	1.6–2	10	268 – 403	70	–	–	(Teghammar et al., 2012)
Secondary sludge from kraft mill and paper mill	BMP assay	23 ± 1	7	20–23	–	0.118	108±5–131±5	–	–	–	(Bayr et al., 2013)
Secondary sludge from P&P industry	BMP assay	38/40	7.9/7.6	19	1.5	0.25/0.5	53 – 84	–	–	–	(Hagelqvist, 2013)
Pulp & paper sludge and food waste	Lab-scale	55	7.0	–	–	0.8	432	–	–	71–87[g]	(Lin et al., 2013)

Sludge from CTMP mill	BMP assay	35	–	19	–	0.5	223 – 359	44 – 65	–	–	(Granström and Montelius, 2014)
Sludge from P&P industry	Bench-scale reactor	29 – 32.5	6.2–7.3	–	–	15	14.7	–	–	–	(Priadi et al., 2014)
Secondary sludge from P&P mill	BMP assay	35	6.9–7.2	20–14	0.5–2.2	0.06	70 –78	56 – 63	9–10	–	(Kinnunen et al., 2015)
Secondary sludge from P&P mill	Semi-continuous lab-scale reactor	35	7.0–7.2	10	1.6–1.9	5	138	63	25	–	(Kinnunen et al., 2015)
Deinking sludge from wastepaper recycling	BMP assay	–	–	23	–	1	90 – 115	–	–	–	(Ogun et al., 2015)
Deinking sludge from wastepaper recycling	CSTRs[e]	–	–	50–72	–	10	134	–	–	–	(Ogun et al., 2015)
Co-digestion of primary and secondary sludge from kraft pulp mill	CSTRs	37	–	4	0.5 – 4	4	230 ± 10	–	59	–	(Ekstrand et al., 2016)
P&P mill sludge	Bench-scale	37±2	6.1–7.5	50	–	1	429.19	–	–	–	(Lin et al., 2017)
Paper mill sludge	BMP assay	35	–	–	–	2	49 – 66	–	–	–	(Song et al., 2017)
Primary sludge from kraft pulp mill with food	BMP assay	30 – 38	6.8– 7.8	40	–	1	264.5	–	–	–	(Veluchamy and Kalamdhad, 2017)
Deinking Sludge	BMP assay	37±2	7.4	21	–	0.6	118 – 280.4	–	–	–	(Steffen et al., 2017)
Kraft pulp mill sludge	BMP assay	55	7.4	20	–	0. 275	46.9	–	–	–	(Lopes et al., 2018)
Paper sludge (pretreated and control)	BMP assay	37	7 – 7.7	20	–	0.8	231.3 – 67.9	–	–	–	(Takizawa et al., 2018)
Sedimented paper fiber	CSTR	37	7	60	2.5	5.0–5.3	201±18	45–57	–	–	(Chatterjee et al., 2018)
Sedimented paper fiber	BMP assay	35	7 – 8.1	–	–	1	250	–	61–65	66–84	(Kokko et al., 2018)
P&P secondary sludge	BMP assay	37	–	20	–	0.5	267	–	–	–	(Sethupathy and Sivashanmugam, 2018)
P&P biosludge	BMP assay	37	7 – 7.5	–	–	0.160	160 – 200	70–80	–	–	(Bonilla et al., 2018)
Recycled P&P sludge	CSTR	37	6.8–7.6	–	0.5 – 3	1	159	–	77	–	(Bakraoui et al., 2019)

[a]BMP = Biochemical methane potential; [b]BCTMP = Bleached chemi-thermo-mechanical pulp ; [c]TMP = thermomechanical pulp; [d]DIP = deinked pulp; [e] CSTR = continuously stirred tank reactors; [f]KgTS $m^{-3}d^{-1}$; [g]Soluble COD; [h]m^3 $CH_4/kgVS_{removed}$; [i]VSS removal; [j]L CH4/L-day; [k]– indicates value not found or not reported.

5. Fermentation of PPMS for biofuel production

5.1. Overview

The production of biofuels from PPM sludges via fermentation processes follows the same multiple steps that are used in the production of biofuels from lignocellulosic biomass. However, due to its preprocessed fiber during the pulping, PPM sludge does not need the initial preparation steps that include cleaning and milling, which utilize a large amount of energy. The common steps in the production process involve pre-treatment, hydrolysis, saccharification, and product recovery and purification. Several pre-treatment methods (physical, biological, or chemical methods) are used to improve the hydrolysis efficiency by reducing cellulose crystallinity and removing lignin. PPM sludge may require mild pre-treatment because its delignified fibers are amenable to enzymatic hydrolysis compared to the virgin lignocellulosic biomass. In contrast, pre-treatment of lignocellulose may generate microbial inhibition products such as furfural, acetic acid, phenolic compounds, which require a proper detoxification process. These degradation products, however, can be recovered and valorized as value-added biomaterials. Adsorption, neutralization, extraction, and evaporation are the most applied detoxification strategies (Branco et al., 2019). Enzymatic hydrolysis is the second important step in the process and encompasses the conversion of the carbohydrates (cellulose/hemicellulose) into monosaccharides. It can be accomplished either by enzymes or acids, but enzymatic hydrolysis is highly compatible with the fermentation microorganisms coupled with reduced energy consumption. Following the hydrolysis, fermentable monomers are converted into biofuels. Various fermentation configurations are used. Separate hydrolysis and fermentation (SHF), simultaneous saccharification and fermentation (SSF), and simultaneous saccharification and co-fermentation (SSCF) are the main configurations utilized in the production of bioethanol and biobutanol from PPM sludges (Silva et al., 2017). Whereas, photo-fermentation, dark-fermentation, sequential dark- and photo-fermentation are used in the production of biohydrogen (Liu et al., 2019). Biofuels are produced at very low concentrations, so they must be concentrated and purified. Distillation and adsorption using zeolite molecular sieves are the used methods for biofuels recovery followed by a dehydration step. Recent developments in the production of bioethanol, biohydrogen, and biobutanol from PPM sludges are discussed in detail in the following sections.

Although pre-treatments aim to facilitate the access of organic matter to microorganisms, all pre-treatments used in anaerobic digestion of PPM sludge are concerned only with secondary sludge (Table 2.2.3). Thus, it is difficult to generalize or use them in the production of ethanol and butanol. Also. Although some studies reported the importance of pre-treatment during the production of ethanol from PPM sludge due to paper sludge high susceptibility to enzymatic hydrolysis, pre-treatment could greatly improve the ethanol yield. However, it should be mild and reliable pre-treatment and not like that used for virgin lignocellulosic

treatment nor waste activated sludge. Yamashita et al. (2010) applied a combined pre-treatment of mechanical grinding for a relatively short period (2 min) followed by chemical swelling (1h) using H3PO4. This sequential pre-treatment increased the hydrolysis yield by 70% and the subsequent ethanol yield by 33%. The ethanol conversion rate was 81.5% for treated sludge with a productivity of 1.27 g/L/h compared to 54.3% and 0.424 g/L/h for untreated samples. In another study, Gurram et al. (2015) reported a 25% increase in the hydrolysis yield (g glucose/g cellulose) after paper mill sludge was pre-treated by hydrogen peroxide, with improved ethanol yield, productivity. Kang et al. (2011) de-ashed paper sludge by floatation and screening (using CO_2 and 100-mesh screen); despite this fractionation process increases ethanol yield by 10%, it is associated with glucan and xylan losses.

5.2. Bioethanol

Ethanol is one of the most widely used liquid biofuels and represents an alternative to petroleum-derived fuels in many countries, especially those that have no access to crude oil resources. Ethanol can be used as a fuel in regular combustion engines in its pure form or can be mixed with gasoline. Bioethanol has a higher compression ratio, and lower evaporation loss than gasoline but has low energy density and water miscibility problems (Mejía-Barajas et al., 2018). When ethanol is mixed with gasoline, greenhouse gas emissions can be significantly reduced by better combustion and reduced carbon dioxide emissions. Recently, several biomass feedstocks and various conversion technologies have been used for bioethanol production. Among feedstocks used, paper sludge to ethanol is gaining more attention in recent times due to its excellent dispersed structure, low cost, and high carbohydrate content. Incorporating fiber sludge in a mill-based biorefinery could provide a way to diversify products and make more efficient use of raw materials from pulp mills. Although ethanol can be produced industrially via the acid-catalyzed hydration of ethylene (Al-Azkawi et al., 2019), FPs, using glucose or xylose sugars, are the most used bioconversion methods for sustainable ethanol production.

As mentioned before, biotransformation of PPMS to ethanol usually involve multiple steps that include pre-treatment of sludge materials, hydrolysis (acidic or enzymatic), fermentation process, distillation, and waste treatment (e.g., anaerobic digestion process). Figure 2.2.4 shows the simplified diagram of the bioethanol production process from PPM sludge. The first step in the conversion of PS to ethanol is the pre-treatment of sludge materials, in which the sludge is conditioned to make cellulosic materials amenable to enzymatic hydrolysis. Since woody materials are pre-processed in the pulping step, the resulting sludge may need mild pre-treatment or may not need it. Various studies indicated that ethanol could be produced from paper sludge without pretreatment through simultaneous saccharification and fermentation (SSF), and higher ethanol yield could be obtained (Dwiarti et al., 2012). Also, due to associated costs and inhibitors generation, severe pre-treatment should be avoided. The next step comprises hydrolysis of PS cellulose and

hemicellulose to monomer sugars (glucose, xylose), followed by fermentation through different configurations. Fermentation can be done in a separate or combined process (separate hydrolysis and fermentation (SHF), SSF, or simultaneous saccharification and co-fermentation (SSCF). SSF has been considered as the major option because it usually results in improved hydrolysis rates and shorter residence times. Finally, ethanol is recovered from the fermenting effluent by the distillation process, and the resulting solid byproducts can be treated anaerobically to generate biogas.

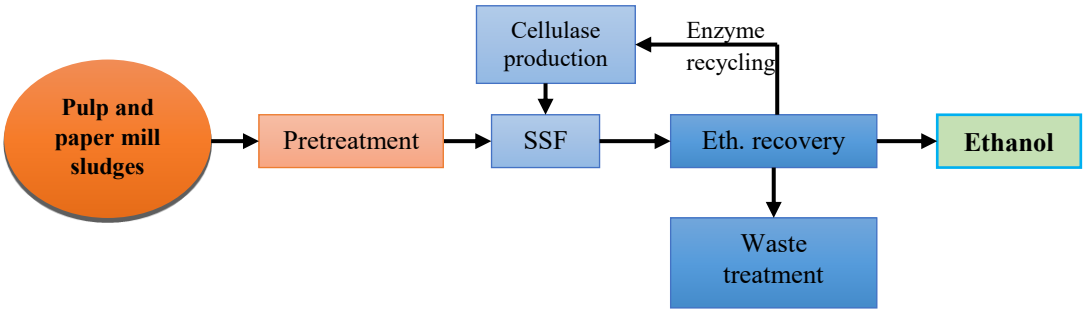

Figure 2.2.4: Flow diagram of the bioethanol production process and enzyme recovery

Table 2.2.6 summarizes the studies that investigated bioethanol production from P&P mill sludges. These studies focused on the use of primary or recycled paper sludge, which has high carbohydrate content. Both SHF and SSF are studied. As aforementioned, SSF is mostly favored over SHF and is operated in a batch, fed-batch, or semi-continuous mode. In contrast, SHF, which involves hydrolysis of the cellulose followed by fermentation of glucose, provides optimal conditions for both steps because they occur in separate reactors, but it has enzymes inhibition problem. Kang et al. (2011) achieved ethanol concentrations of up to 60 g/L treating de-ashed paper sludge by saccharification and fermentation process. SSF is a cost-effective process for the conversion of PS to alcohol. However, despite the economic advantage of SSF over separate SHF, the main issue with SSF is the difference between the cellulase and the fermenting microorganism optimal temperature (Kádár et al., 2004). Hence, the use of thermotolerant yeast strains is recommended. The tested fermentation temperature is between 25 and 42 °C, depending on the employed microorganisms, and the hydrolysis temperature is about 50 °C. Different enzymes are used for the hydrolysis of paper sludge, but the most applied are cellulases and celluclast. The cost of producing the enzyme showed a significant impact on the efficacy of ethanol production from paper sludge. It has been estimated that the cost of cellulases represents around 20% of the total cost of the production process (Gurram et al., 2015). More research endeavors are needed to minimize the cost of cellulose synthesis and optimize the cellulase loading dose to the extent that it does not affect sugar yield. *K. marxianus, S. cerevisiae, P. stipitis, Z. mobilis, T. accharolyticum* are the most employed microorganisms in the FPS (Table 2.2.6). Compared with other microorganisms, *S. cerevisiae* excels in all properties except for the

fermentation of the pentose sugars. The pH value tested in the reported studies ranges from 4.4 to 6.5, and pH 5 is considered optimal for FPs. Based on this review, PPM sludge is a promising substrate for bioethanol production due to its good dispersed structure and easy enzymatic hydrolysis. However, the high content of ash and impurities are the main challenges of converting paper sludge into ethanol, as it reduces the cellulose loading capacity in the bioreactor and changes the pH of the sludge. Thus, a pre-treatment step is required to remove ash and modify the pH before enzymatic hydrolysis (Kang et al., 2011; Wang et al., 2011). Most of the research done on ethanol production from PPMs sludge was at the laboratory level with few studies at the pilot scale and no reports for full-scale fermentation plant. Thus, the transformation from lab-scale component to pilot and full scale is required.

Table 2.2.6: Bioethanol production from pulp and paper mill sludges

Sludge type	Process mode	Reactor volume (ml)	Fermentation			Employed microorganism	Substrate loading (g/L)	Ethanol conc. (g/L)	Ethanol yields %	Productivity (g/L/h)	Reference
			Temp. (°C)	pH	Time (h)						
Recycled paper sludge	Batch SSF	250	30–42	5	40	*K. marxianus* ATCC 36907	180–190	32–35	50	0.52	(Lark et al., 1997)
Recycled paper sludge	Fed-batch SSF	250	42	4.8	72	*K. marxianus* CECT 10875	50/75	8.2–17.7	53.7–80.3	–	(Ballesteros et al., 2002)
Bleached paper sludge	Batch & semi-continuous SSF	800	36	4.5	96	*S. cerevisiae* D5A	82/120	42.16±3.58	46.6	–	(Fan et al., 2003)
Corrugated cardboard and paper sludge	Fed-batch SSF and non-isothermal SSF	750	30/40	4.4 –5.3	96	*K. marxianus* Y01070	188	17	58–41	0.49–0.62	(Kádár et al., 2004)
Primary sludge	Batch & semi-continuous SSF	250	37	–	96	*S. cerevisiae* D5A	60	>40	49.4	–	(Fan et al., 2007)
Fiber sludge	Batch	55	30	5.5	12	*S.cerevisiae*	2.0	–	–	–	(Sjöde et al., 2007)
Recycled paper sludge	Fed-batch SHF	500	30	5.5	179	*P. stipitis* CBS5773	75	19.6	54	0.33	(Marques et al., 2008)
Recycled paper sludge	Fed-batch SSF	500	30	5.5	48	*P. stipitis* CBS5773	75	18.6	51	0.39	
Paper sludge	Repeated fed-batch SSF	500	30	5.5	48	Z. mobilis NBRC 13756	200	5.32–17.86	47.8	0.111–0.372	(Yamashita et al., 2008)
Paper sludge	Batch & Fed-batch, SSCF	100	37	5.5	48	*S. cerevisiae* RWB222	62.4/24.5 25/36/50	14	–	–	(Zhang et al., 2009)
Wastepaper sludge	Batch SSF	250	37	5.8	96	*S. cerevisiae* D5A	31.9	–	65	–	(Shao et al., 2009)
Recycled paper sludge	Fed-batch SSF	100	37	4.8	48	*S. cerevisiae* ATCC 200062	30	25.5/32.6	75–81	0.14	(Kang et al., 2010)
Recycled paper sludge	Fed-batch SSCF	100	37	6	24	*E. coli* ATCC 55124	30	45/42	68	0.16	
Wastepaper sludge	Fed-batch SSCF	900	37	5.5	16–20	*Z. mobilis* 8b	170	36.6	60.7	0.31	(Zhang and Lynd, 2010)
Wastepaper sludge	Batch SSCF	900	30	5.5	24–36	*S. cerevisiae* RWB222	170	40	68.5	0.39	
Primary sludge	Fed-batch SSCF	100	37	–	24	*E. coli* ATCC 55124	154	60	70	0.50	(Kang et al., 2011)
Primary sludge	Fed-batch SSF	100	37	–	12/24/48	*S. cerevisiae* ATCC 200062	231	47.8	70	0.40	
Recycled paper sludge	Batch SHF	250	38	4.5	48	*K. marxianus* ATCC 36907	30/90	12.2	51	–	(Madrid and Quintero, 2011)
Recycled paper sludge	Batch SSF	250	38	4.5	72	*K. marxianus* ATCC 36907	30/90	40	50–59	–	
Paper sludge	Batch SHF	250	33	–	24	*S. cerevisiae* GIM-2	40.8	9.5	56.3	0.59	(Peng and Chen, 2011)
Primary clarifier sludge	Fed-batch SSF	500	42	4	–	*S. cerevisiae* TJ14	15	40	66.3	–	(Prasetyo et al., 2011)

Paper sludge	Batch SHF	50	25 – 37	3.5 – 6.5	72	*S. cerevisiae/P. stipitis* SHY07-1	110	14.18	49	1.2	(Zhu et al., 2011)
Paper sludge	Batch SSF	250	37	5.2	96	*S. cerevisiae* TJ14	–	11.3–11.8	50	–	(Dwiarti et al., 2012)
Pulp & paper sludge	Batch SSF	360/600	40	4.5/6	60–72	*S. cerevisiae CICC 1001*	–	42.5	–	–	(Lin et al., 2012)
Paper sludge	Fed-batch SSF	500	37	–	168	*S. cerevisiae* MH1000 and D5A	20	47.7–57.3	84.6	–	(Robus, 2013)
Sulfate and sulfite fiber sludge	Fed-batch SSF	750	30	5.2	48	*S. cerevisiae*	–	45.6/64.7	51.1/42.3	–	(Cavka et al., 2014)
Primary sludge	Batch	–	51	5.8	68	*T. saccharolyticum* strain MO1442	100	4.2–4.3	–	–	(Chen et al., 2014)
Primary sludge	Batch/SHF	100	30	5	12	*S. cerevisiae P. stipites* DSM 3651	46	10.5	0.39	0.14	(Mendes et al., 2014)
Paper mills sludge	Batch	350	37	5	9	FermPro™	–	24.9–30	94.5–95.7	1.73–3.28	(Gurram et al., 2015)
Paper sludge	Fed-batch SSF	100	37	4–6	180	*S. cerevisiae* MH1000	20	34.2–45.5	66.9–78.2	0.23	(Boshoff et al., 2016)
Recycled paper sludge	–	–	30	4.8	–	*S. cerevisiae* PE-2	8	4 – 7	–	1.16	(Gomes et al., 2016)
Paper sludge	Batch SSF and Fed-batch SSF	100	35	–	168	*S. Cerevisiae MH1000*	20	57.31/47.72	85.34–94.07	0.40	(Robus et al., 2016)
Primary sludge and Unbleached Pulp	Batch SSF	100	38/42	4.5–5.5	24	*S. cerevisiae* ATCC 26602	25/50	9.0–22.7	48.9–49.4	0.46–0.94	(Mendes et al., 2017)
Primary sludge and Unbleached Pulp	Batch SSF	100	38/42	4.5–5	24	*K. marxianus* NCYC 1426	25/50	6.1–20.7	39.1–46.4	0.57–2.75	
Primary sludge and Unbleached Pulp	Fed-batch	100	38/42	4.5–5.5	6–168	*S. cerevisiae* ATCC 26602 *K. marxianus* NCYC 1426	100/200	13.6–40.7	18.8–80.0	0.17–3.83	
Recycled paper sludge	Batch SHF and SSF	100	30	5/4.4	72/84	*S. cerevisiae* PE-2	16/98	6.3/7.8	45.8/55.7	0.47–0.52	(Schroeder et al., 2017)
Recycled paper sludge	Batch		35	4.8	25	*S. cerevisiae* CA11	8	20.28–25.86	–	–	(Gomes et al., 2018)
Paper mill sludge	–	100	37	6.8	48	*C. sporogenes* NCIM 2337	–	15	–	0.116–0.559	(Gogoi et al., 2018)

5.3.Biohydrogen

PPMS has been treated through supercritical water technologies and fermentation processes to produce biohydrogen. Hydrogen can be utilized in numerous domains due to its high energy density (Wu and Zhou, 2011; Liu et al., 2019). Since it produces only water upon combustion, it can be one potential alternative to fossil fuel energy. In this section, hydrogen production via biological processes is discussed. Few researchers examined PPMS as a possible waste for hydrogen production via FPs (Kádár et al., 2003, 2004; Valdez-Vazquez et al., 2005; Wu and Zhou, 2011; Lin et al., 2013; Moreau et al., 2015; Farghaly et al., 2016; Vaez et al., 2017). Table 2.2.7 summarizes the performance of biological processes for hydrogen production from PPM sludge. Different processes have been developed to boost biohydrogen production and enhance its practicality and economic feasibility, whether in light-dependent or dark fermentation processes. Compared to photo-fermentation, dark-fermentation was gained more attention due to process simplicity, less energy input, and stable microorganisms' performance. However, photo-fermentation is characterized by the complete conversion of organic compounds into hydrogen and high yield. Dark fermentation is sometimes combined with photo-fermentation in a two-stage process to improve the hydrogen yield. In dark fermentation, both thermophilic (Kádár et al., 2003) and extreme thermophilic (Kádár et al., 2004) processes have been tested. The hydrogen yield varied between 50 and 94% of the theoretical maximum in Kádár et al.'s (2004) work, and the highest volumetric hydrogen generation rate was 5 to 6 mmol/(L·h) (Kádár et al., 2004). The lower biohydrogen yields can be attributed to the intricacy of the paper sludge content and inhibitor effect. Kádár et al. (2003) tested thermophilic bacteria (*Thermotoga elfii* and *Caldicellulosiruptor saccharolyticus*) for biohydrogen production. Both were able to produce hydrogen; however, the inhibition effect was more noticeable in *C. saccharolyticus* than *T. elfii*. Moreau et al. (2015) used *C. thermocellum* DSMZ for hydrogen production from the PS of a recycled paper mill. *C. thermocellum* was able to hydrolyze PPMS, and they obtained 11.20 mole H_2/m^3 after 60 h of fermentation. Wu and Zhou (2011) fermented paper mill sludge pretreated by ultrasonic and achieved a hydrogen yield of 620.8 mLH_2/g COD under an OLR of 3 g COD/L/d, a sludge reaction time of 32 h, and at 36.5°C. PPMS seems a viable substrate for biohydrogen production; however, pre-treatment is needed to improve its biodegradability and hydrogen production yields. Biological production of biohydrogen from PS is so far in its initial stages and needs further developments regarding fermented microorganisms, pre-treatment, and process design optimization to boost the hydrogen yield and reduce its total production cost.

Table 2.2.7: Performance of biological processes for hydrogen production from PPMS

Sludge type	Process conditions					Maximum yield of H_2	Reference
	Experimental setup	Working volume (L)	SRT (h)	T °C	pH		
Paper sludge hydrolysate	[a]F. assays	0.03	72	65	7.2	27 mmol/g	(Kádár et al., 2003)
Paper sludge hydrolysate	F. assays	0.03	24	70	7.2	20.5 – 21.6 mmol/g	(Kádár et al., 2003)
Paper sludge hydrolysate	Batch anaerobic reactor	2	24	70	6.4	87.3 – 129.5 mmol/g	(Kádár et al., 2004)
Thickened paper mill sludge		2.6	32	36	5.5	620.8 ml/g	(Wu and Zhou, 2011)
Pulp & paper sludge	Batch reactor	0.8	–	37	5.5	64.48 mL/g	(Lin et al., 2013)
Primary sludge from recycled paper mill	F. assays	0.1	60	60	5.8	11.20 mol/m^3	(Moreau et al., 2015)
Paperboard mill Sludge	Batch reactor	6	–	35	5	5.29 mmol/g	(Farghaly et al., 2016)
Paper mill sludge	F. assays	0.06	49	37–55	5–7	38.8 mL/g	(Vaez and Zilouei, 2020)

[a]F. assays = fermentation essays

5.4. Biobutanol

PPM sludge was investigated as a substrate for the production of biobutanol via ABE (acetone, butanol, and ethanol) fermentation. Biobutanol has versatile applications but is commonly used as an alternative biofuel to ethanol and biodiesel because butanol has around 30% more energy than ethanol and is neither hygroscopic nor corrosive (Benali et al., 2019). SSF (simultaneous saccharification and fermentation) with Clostridium species is the commonly utilized approach, as Clostridium species can catabolize both hexoses and pentoses sugars (Guan et al., 2018). Butanol production from the sludge fiber is still in its research phase. Most of the sludge related studies were carried out at the laboratory scale (Guan et al., 2016; Gogoi et al., 2018) with no reported studies at the pilot and full-scale levels. Kraft paper mill sludge can be fermented without pre-treatment or detoxification but requires partial ash removal, as ash has been found to inhibit enzymatic hydrolysis (Guan et al., 2016). On the other hand, it was found that ash has a positive effect on the fermentation process due to the buffering effect of $CaCO_3$. Guan et al. (2016) studied the digestibility of de-ashed PPM sludge using SSF and reported butanol concentration of 5.3–10.2 g/L with a yield of 0.13 g/g under a substrate loading of 6.3–7.4 wt% and enzyme loading from 10–15 FPU. Gogoi et al. (2018) fermented alkali pre-treated paper mill sludge and reported a total ABE yield of 0.559 g/L for 15 % concentration of alkali pretreated sludge. Guan et al. (2018) studied butanol production from hemicellulose pre-hydrolysate using SSF and the detoxified substrate produced 9.3 g/L butanol per a total

of 15.3 g/L ABE solvent. However, the fermentation of the untreated substrate was inhibited by phenolic compounds.

Alternatively, co-valorization of PPM sludge and non-mill substrates was investigated. Cao et al. (2020) co-fermented PPM sludge and corn steep liquor (CSL) for n-butanol production using *Clostridium tyrobutyricum*. They achieved 16.5 g/L butanol with a yield of 0.26 g/g from PPM sludge and 5% CSL, via SHF. They indicated that CSL provides both nitrogen source and lactic acid that can be converted by *C. tyrobutyricum* to biobutanol. Compared with mono-fermentation, co-fermentation seems more promising, where butanol concentration leveled around 10g/L for mono-fermentation and 16.5 g/L for co-fermentation with better butanol yield as well.

Paper sludge is amenable to enzymatic hydrolysis and no need for pre-treatment; however, inhibitory effects of phenolic compounds and high downstream recovery cost are the main obstacles to the technical and economic viability of biobutanol processes. Therefore, developing effective detoxification and downstream recovery methods coupled with techno-economic studies are the possible ways that could lead to its industrial commercialization.

6. Potentials and constraints

PPM sludges hold considerable potential for bioconversion to biofuels. However, despite the very promising potentials of PPMs sludge, and successful pilot-scale projects have already been implemented, these technologies have not yet been fully marketed, and numerous challenges require to be tackled to increase the process's performance further and move from the component level to the full-scale application. Currently, the anaerobic bioreactor facilities at pulp mills are mainly used to treat wastewater rich in soluble substances rather than biosolid waste like primary and secondary sludges due to the long residence times (30–60 days) and large reactor volume required to treat slowly digestible organic materials of the sludges. The overall bioconversion efficacy of dry organic solids was estimated to be between 30–50% (Yunqin et al., 2009). The limiting step of anaerobic digestion of PP primary and secondary sludge is the hydrolysis of the biopolymers from biomass and sludge into monomers before bioconversion of monomers into biomethane and biohydrogen (Chen et al., 2020). Recently, enzymatic hydrolysis technologies have received much attention in recent years in improving the hydrolysis of secondary sludge (Ding et al., 2018) and lignocellulosic biomass (Xu et al., 2019). Pilot-scale testing of the use of enzymatic hydrolysis technologies in anaerobic digestion of secondary sludge (Ding et al., 2018) and hydrolysis of lignocellulosic materials (Ding et al., 2018; Xu et al., 2019) have been conducted. Although the results are promising, further studies to develop new enzymes, improve the enzymatic hydrolysis efficiency, reduce the cost of energy, and recover and reuse enzymes are essential for full-scale applications (Liu et al., 2019). Recently,

different practical pre-treatment approaches were developed to break the inherent recalcitrant characteristics of lignocellulosic materials (Xu et al., 2019). Converting this complex lignocellulosic material (cellulose and hemicellulose) into monosaccharide is the key to biofuels generation, whether it is methane or ethanol. The surplus heat normally available in P&P mills can supply energy for pre-treatment as well as for the bioconversion processes (Bayr et al., 2013). The pre-treatment approaches enhance the accessibility of lignocellulosic contents via several mechanisms, such as the breakdown of covalent bonds amid the lignocellulosic constituents (cellulose, hemicelluloses, and lignin), lignin depolymerization, the reduction of cellulose crystallinity, and the dissolving of hemicelluloses (Veluchamy and Kalamdhad, 2017). In most reported studies of bioconversion, monosaccharides are considered biodegradable, while lignin content is non-biodegradable and inhibits the microbial performance, which entails the detoxification regime. The low biodegradability of lignin can be attributed in part to its phenylpropanoid subunits, which make the enzymatic hydrolysis of lignin difficult (Bayr and Rintala, 2012). Cellulose removal of 70 - 73% was reported in semi-continuously co-digestion of primary and SS under thermophilic conditions (Bayr and Rintala, 2012). Compared to microcrystalline structures of cellulose, hemicellulose it is more accessible.

In anaerobic digestion, PPMs sludges as substrates for biogas production have nutrients deficiency problems and lignin inhibition effects. The lack of nitrogen content in PPMS can result in ammonia defect for microbial growth and low buffering capacity, thereby low methane yields. Due to these limitations, PPMS demands to be co-digested with N- and P-rich substrates such as municipal sewage sludge, and there is sufficient knowledge to digest municipal sludge as a substrate already in place. Alternatively, we argue that most studies of AD of PPM sludges are carried out using biochemical methane potential. Currently, various high-rate AD bioreactors exist such as AnMBR, UASB, anaerobic filters (AFs). These reactors can be customized and specifically tailored for PPM sludge treatment (solid-state AD). Solid-state AD requires enhancement in different areas to operate successfully. Figure 2.2.5 illustrates the proposed Triad of the improved biogas production from PPM sludge. The strategic components of Triad would include the sludge pre-treatment, reactor configuration, and co-digestion. Matching of pre-treatment method and the co-digested substrate with the targeted paper sludge can achieve the desired biofuel yields. Different actions should – or can be taken – in the configuration of the digester, sludge pre-treatment, and co-digestion levels, to promote the production of final biofuel. For making greater benefit of paper sludge, this triad should be considered, developed, and implemented during the bioconversion process.

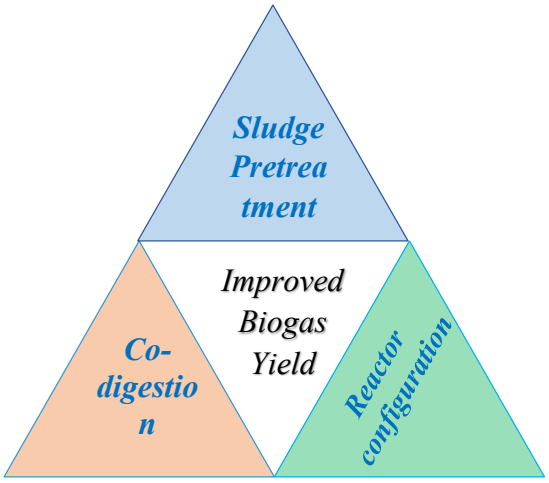

Figure 2.2.5: Proposed triad for improved biogas yield from PPM sludge.

Figure 6 shows a proposed anaerobic membrane bioreactor (AnMBR) process for biogas (biomethane) production from primary sludge. AnMBR could be a promising technology for the AD of PPM sludge. The main advantages of the MBR are a higher cell concentration in the reactor because the use of membrane ensures complete retention of slow-growing methanogens, along with reduced biosolid mass for disposal and decoupling the SRT and HRT. This results in increased biogas productivity compared to conventional processes, while also providing a high permeate quality and improved operational control. The main challenge for a conventional AD of PPM sludge is the very long residence time (20-30 days). However, decoupling the HRT and SRT in an AnMBR can achieve a significant reduction in reactor volumes, thereby reducing capital costs. To date, as a new technology, no study has demonstrated using AnMBRs for paper sludge treatment. However, there have been several successful experiments using organic sludge as AD substrates. For instance, Pileggi and Parker (2017) compared the performance of a pilot-scale AnMBR and a conventional anaerobic digester when treated raw mixed sludges from two water resource recovery plants. Compared to conventional AD, AnMBR achieved a significant decrease in volatile solids along with increased methane production (an average of 38% increase) and a stable process operation was attained at temperatures ranging from 25 to 55 °C. Similarly, Yu et al. (2016) reported enhanced sludge reduction and improved methane production for a submerged anaerobic dynamic membrane bioreactor (AnDMBR) treating waste activated sludge compared to conventional AD. In another study, Meabe et al. (2013) examined the performance of AnMBR when treating a sewage sludge under both mesophilic (35 °C) and thermophilic (55 °C) conditions. They were able to successfully operate the system at a high organic loading rate (6.4 gCOD/L·d at 55 °C, and 4.6 gCOD/L·d at 35 °C), indicating a substantial reduction in digester volume compared to conventional processes. As these cases very clearly demonstrate, AnMBRs have a better performance than conventional systems. Thus, it would be interesting to explore AnMBR technology for PPMS treatment and investigate its ability in terms of biogas yield and total energy conversion. In this

proposed process, PS can be continuously fed to the membrane reactor, and membrane filtration can be incorporated into the bioreactor to separate microorganisms from the treated paper sludge (Fig. 2.2.6). However, a proper membrane fouling control strategy needs to be adopted during the operation of this process.

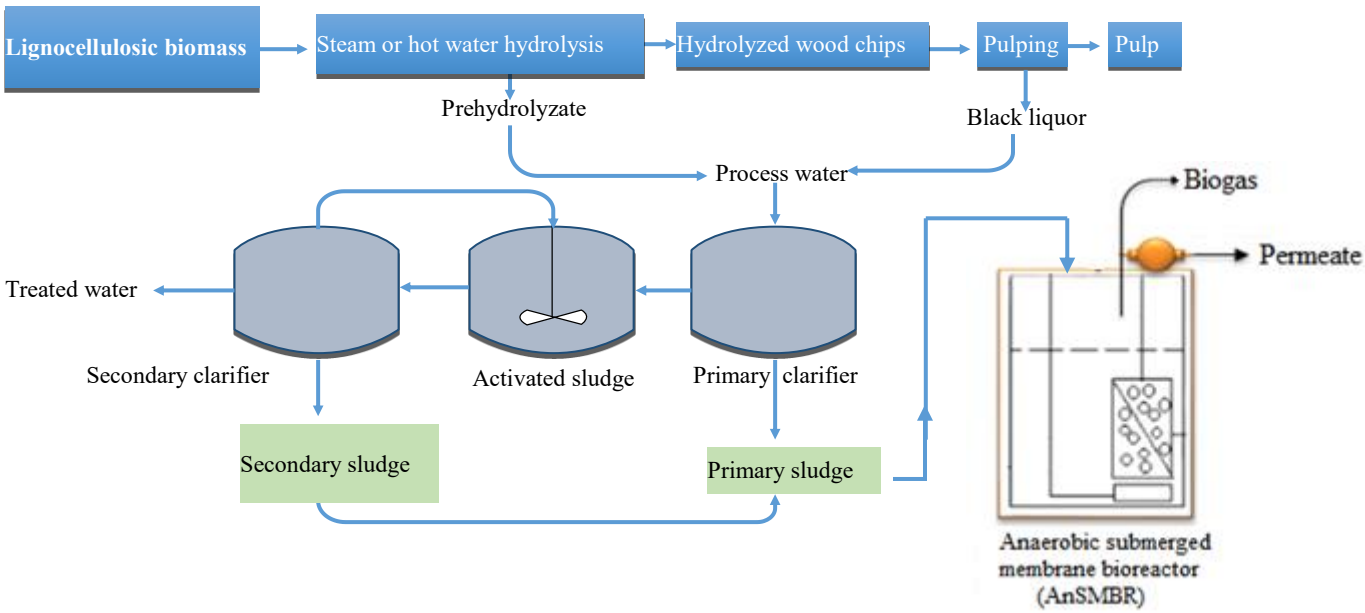

Figure 2.2.6: Proposed AnMBR for methane production and sludge management in the pulp and paper mill.

As described in this paper, a considerable bioethanol yield can be attained without sludge pre-treatment. But each employed technology possesses unique abilities and constraints. Table 2.2.8 summarizes the advantages and shortcomings of the bioconversion processes. In terms of process consolidation and improved ethanol production, SSF considers promising (e.g., low enzyme loading, a higher concentration of produced ethanol, and a reduced inhibitory effect) among the employed methods. However, there are still some areas that need further development to increase the overall ethanol yield. For example, the operating temperature and pH are neither ideal for hydrolysis nor fermentation microorganisms. Therefore, the development of microorganisms that can withstand such conditions is required. Also, due to the presence of biomass degradation products, an effective detoxification process needs to be developed. Furthermore, PPMS typically contains very high ash content (e.g., in de-inking sludge). During sludge fermentation, this ash not only limits the content of sugars in the hydrolysates but also reduces enzyme activity due to enzyme adsorption (Kang et al., 2010). Therefore, sludge de-ashing before FP is required by applying an appropriate de-ashing step. Overall, the techno-economic analysis demands to be done in detail to determine the feasibility of the entire process.

On the other hand, H_2 can be produced from PPM sludge, but the generation rate is unsatisfactory. Biogas generation from PPM sludge is much higher than producing hydrogen from the same substrate. Hence, more improvement in both biological and technological aspects is needed for improved hydrogen yield. One of the drawbacks of state-of-the-art fermentation technologies like photo-fermentation is the high energy demand and the high capital cost associated with photo-bioreactors. Here, a hybrid process that combines the advantages of both dark-fermentation and photo-fermentation should be developed not only to boost the H_2 yield but also to reduce the total cost of the process. Sludge-to -biobutanol is also considered but it is still in the first stage of the research. Based on what has been achieved so far, co-fermentation showed more potential compared with the mono-fermentation.

An overview of the PPM sludge biovalorization approach is demonstrated in Figure 2.2.7. This approach aims to integrate biofuels conversion methods within the established pulping processes. Developing a holistic biorefinery process can result in lower energy and investment costs, compared to conventional independent biorefineries. To ensure a high conversion rate of PPM sludge, PPM sludge can be used as a biogas production substrate with or without pre-treatment and the resulting digestate can be further fermented to produce bioethanol. AD waste fibers (digestate) have been reported to have better enzymatic degradability compared to pre-treated lignocellulosic biomass (Yue et al., 2010). Alternatively, the PPM primary sludge can be fermented first for bioethanol or biobutanol generation followed by the AD process of the resulting waste. For reducing the overall operating costs, a process is being developed to recycle the costly enzyme and microbial culture. This integrated approach of the simultaneous production of biogas and bioethanol can bring some marketing potential in the future, but the economics of this concept needs to be studied unequivocally to know its economic feasibility, which can be measured using economic modeling techniques that are based on the financial data and cash flows.

7. Economic and environmental perspectives

From an economic point of view, wastewater sludge treatment was found to cost about 50-350 US$/ton in Australia or 165-550 US$/ton in Europe, and total handling charges were found to reach above 10 billion USD per annum in 2013 (Zhang et al., 2017). This indicates high handling fees for the sludge and the necessity of finding alternative solutions that reduce these costs and environmental burdens. Waste to biofuels option can cut down environmental burdens and generate revenue for pulp mills. However, a techno-economic evaluation is required to determine an economically viable bioconversion process (e.g., in terms of energy requirements and operating costs) among other available alternatives. Although extensive research has been conducted on PPMS bioconversion, most of the previously published studies are limited to process performance and operating parameters optimization. Of the few studies that included techno-economic analysis, Fan and Lynd (2007) examined the profitability of a paper mill with a capacity

of 50 dry tons per day and found that the plant was generating positive cash flow with an internal rate of return (IRR) exceeding 15%. They consider the negative cost of sludge, the possibility of using the existing plant infrastructure, and the lack of pre-treatment being the main important assets of the economic viability of producing bioethanol from PPMS at a small scale. Aksoy et al. (2011) studied the economic feasibility of four scenarios of biorefinery technologies including two different woody biomass gasification processes, SSF of paper sludge to ethanol, and direct incineration of woody biomass for power generation. Among these processes, only the SSF and direct spouted bed (DSB) gasification processes were economically feasible with more than 80 and 22.5% IRR, respectively. Compared to the IRR for DSB, the IRR for SSF was significantly higher, indicating the higher rate of return which would be expected from ethanol production from PPMS in an integrated bio-refining approach. Chen et al. (2014) conducted an economic evaluation to convert different pulp and paper sludges (fractionated for ash removal and non-fractionated) into bioethanol. They found fractionated virgin paper mills sludge more profitable (99.8% probability of business success) due to the reduced capital and operating costs with a net present value of $ 11.4 million compared to recycled paper mills. The payback period was found to be only 4.4 years, with a high internal rate of return (IRR of 28%), at a minimum ethanol revenue of $ 0.32 per liter. Robus et al. (2016) reported a payback period of lesser than three years with an IRR value higher than 25%, which is lower than the payback period and IRR obtained by Chen et al. (2014).

In terms of the economic viability of biogas production from PPMS, Larsson et al. (2015) performed a techno-economic assessment and reported that an average Nordic Kraft pulp mill with an annual pulp output of 327,000 air dry tons can produce 26 - 27 GWh LBG per year from the primary and secondary sludges and Kraft evaporator condensate with an average biogas production of 80 kWh per air dry ton, and about 6700 Nm^3 per day, equivalent to 7600 liters of diesel. In contrast to these findings, however, AnMBR could be a more feasible technology with a positive energy operation over conventional anaerobic digestion (CAD) system. In a comparison of CAD and AnMBR energy balance, Pileggi and Parker (2017) observed a positive energy balance for AnMBR over CAD under ambient, mesophilic, and thermophilic operating conditions with the potential of full-scale applications. The evidence presented here supports the findings of Yu et al. (2016), who conducted energy balance analysis and reported improved energy efficiency for the AnDMBR system with a 37.3% reduction in net energy demand compared to CAD. There would therefore seem to be a clear benefit to use AnMBR in the treatment of PPMS. Alternatively, the obvious noteworthy benefit to pulp mills is that biogas/bioethanol production plant can be integrated with existing mill streams that can remove the cost of sludge disposal and eliminate the impact of the environmental pollution.

In terms of environmental performance, few studies have addressed the environmental burdens related to the production of biofuels from PPMS, although many modern tools and methodologies such as life cycle assessment (LCA) are available, which are used to assess the potential environmental impact of a given product throughout its entire life cycle. Sebastião et al. (2016) conducted a life cycle assessment of bioethanol production from PPMS and all impacts were attributed to enzymatic hydrolysis and neutralization of $CaCO_3$ contributing up to 85% to the total environmental burdens. The impact of the later can be decreased by reducing the amount of hydrochloric acid used in the neutralization step, while the impact of the former can be minimized through the use of a light pre-treatment before hydrolysis. From a wide LCA perspective, the environmental impacts resulting from a novel biogas production system could consider negligible (Yasar et al., 2017). In general, carbon emissions from biofuel generation and utilization can be balanced by its displacement for fossil fuel and waste management, since fossil fuel releases large quantities of CO_2, SO_2, and phosphorous compounds compared to renewable energy.

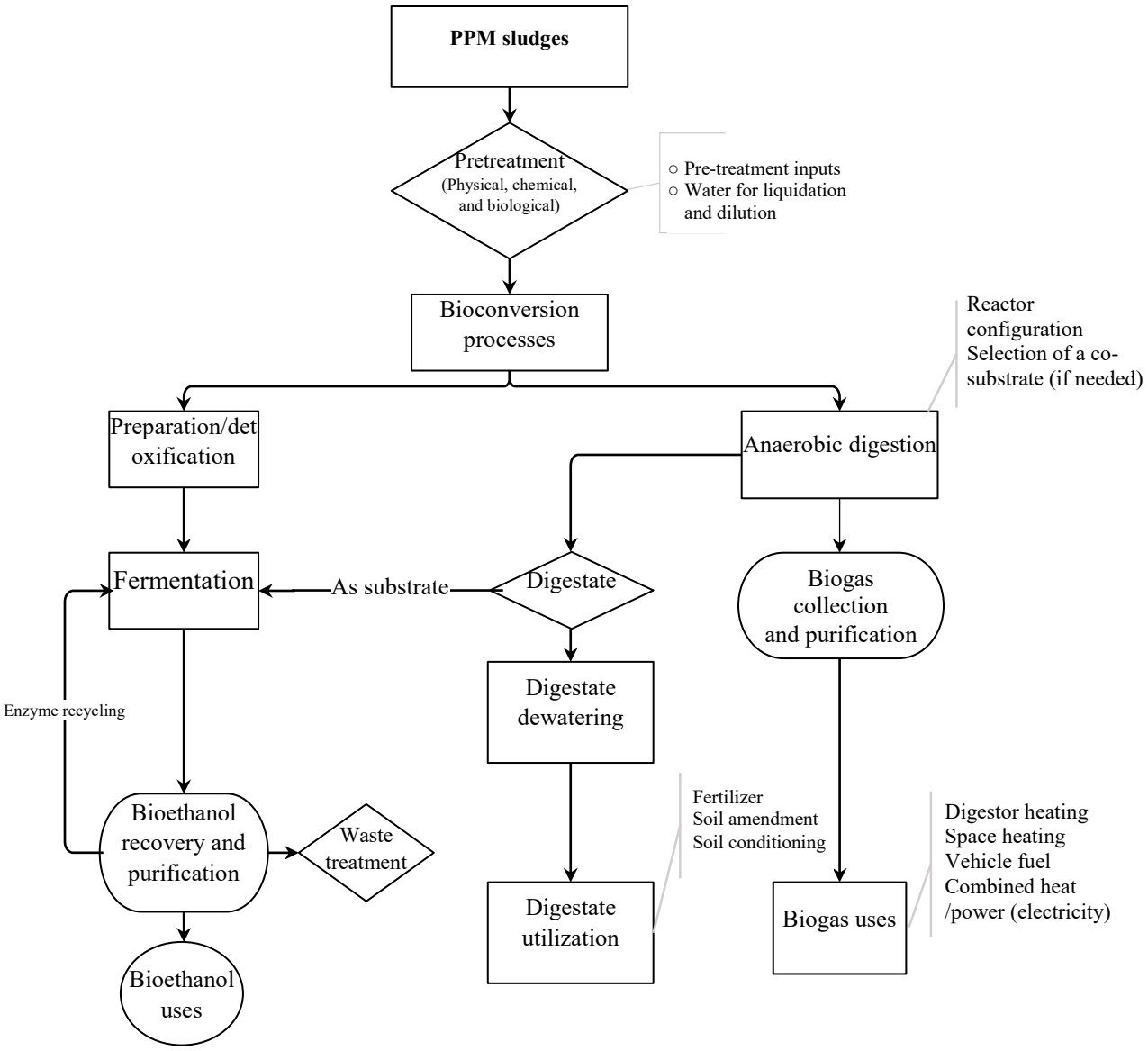

Figure 2.2.7: A proposed integrated approach for the utilization of PPM sludge as a biofuel substrate.

Table 2.2.8: Advantages and disadvantages of biochemical conversion processes

Biochemical conversion route	Process	Advantages	Disadvantages	Reference
Anaerobic digestion	Anaerobic digester	⬧ Minimizing GHG ⬧ Environmentally friendly technology ⬧ Providing energy-rich biogas ⬧ Producing digestate that can be reused ⬧ Destroying pathogenic organisms ⬧ Reducing the sludge disposal problems ⬧ Recovery of the valuable materials ⬧ No sludge dewaterability required. ⬧ Low chemical consumption	⬧ The biological process in AD takes several days, weeks, or months (long residence time) due to the slow metabolic process. ⬧ The initial start-up of the AD process needs a long time. ⬧ Paper sludge may need a pre-treatment that could be expensive. ⬧ The problem of shock loading and foaming. ⬧ The problem of a thick layer formation in the top of the reactor	(Veluchamy and Kalamdhad, 2017; Bayr and Rintala, 2012)
Fermentation	Simultaneous Saccharification and Fermentation (SSF)	⬧ Cost-effective process, as requires lesser amounts of enzymes. ⬧ Shorter operating time ⬧ A higher concentration of produced ethanol. ⬧ Improved hydrolysis ⬧ A decreased inhibitory effect on cellulase ⬧ Decreased enzyme loading	⬧ Temperature and pH are neither ideals for hydrolysis nor fermentation microorganisms. ⬧ Inhibition of cellulase by produced ethanol	(Silva et al., 2017; Zhang et al., 2009; Kádár et al., 2004)
	Separate Hydrolysis and Fermentation (SHF)	⬧ Optimal operation conditions due to two separate units of hydrolysis and fermentation ⬧ Opportunity for fermentation in continuous mode with cell recycles. ⬧ Possibility of recycling and reusing of fermentation yeast in the process	⬧ Longer processing time because of separated units ⬧ Lower ethanol yields due to the inhibition of cellulose by produced ethanol and released sugars (cellobiose and glucose). ⬧ Higher contamination risk ⬧ Higher capital cost (two reactors) ⬧ Inhibition of enzymatic hydrolysis by sugars	(Silva et al., 2017; Dwiarti et al., 2012; Zhang et al., 2009)
	Simultaneous Saccharification and Cofermentation (SSCF)	⬧ Lower capital cost due to co-fermentation of pentoses and hexoses with simultaneous enzymatic hydrolysis ⬧ Lesser inhibitory effect resulting from the continuous removal of the final product of enzymatic hydrolysis. ⬧ Higher ethanol productivity and yield compared to SHF	⬧ The optimum temperature discrepancies between saccharolytic enzymes and fermentation microbes ⬧ Ethanol inhibits the enzymes. ⬧ Co-fermentation of xylose can be less viable because of the high concentration of glucose, compared to the SHF.	(Silva et al., 2017; Jin et al., 2012)
	Dark fermentation	⬧ Simple process design and light is not needed. ⬧ Stable performance for hydrogen-producing bacteria ⬧ Uses a wide range of substrate sources. ⬧ Less energy inputs	⬧ CO_2 emission ⬧ Energy conversion efficiency is relatively low. ⬧ Residual COD production about 70% of the substances remains in the substrate	(Liu et al., 2019; Lin et al., 2013)
	Photo-fermentation	⬧ Excellent conversion rate nearly complete conversion of organic acid. ⬧ More productive than dark fermentation ⬧ High hydrogen content	⬧ Requires enough light and controlled conditions. ⬧ Inhibition possibility ⬧ The higher cost of the reactor and high energy demand ⬧ Sensitive to oxygen	(Liu et al., 2019; Moreau et al., 2015)

8. The future of bioconversion of PPM sludge and development

Waste-to-bioenergy or value-added bioproducts have been increasingly considered in numerous pulp and paper mills around the world. The P&P industry needs to use advanced waste processing technologies to boost its profitability and competitiveness in the current deteriorating P&P markets and minimize environmental impact. Hence, the bioconversion of PPM sludge to biofuels has a bright future in terms of research interest and industrial commercialization. On the other hand, as second-generation biofuels, their global market is expected to surpass the market for the first generation of biofuels due to the use of inedible raw materials (Aditiya et al., 2016). Also, bioconversion technologies are favorable due to their reduced environmental footprint and require no sludge dewatering, where sludge dewatering represents a considerable economic burden to the pulping industry. These technologies can be considered as long-term solutions for PPMS valorization compared to currently available conventional processes because they can simultaneously serve as methods of waste management and resource recovery. However, in the current situation, biotransformation technologies require further development to target more efficient yield, reduced production cost, and minimal environmental impacts. In the future, dedicated pre-treatment methods, novel reactor configurations, and biogas upgrading processes such as CO_2 removal should be investigated and developed. Regarding bioethanol production, usually, both hexose and pentose sugars exist in the fiber hydrolysate, thus, ethanol-producing microorganisms capable of converting both sugars should be developed taking advantage of the genome-editing technology. Several compounds have an inhibitory effect during biovalorization of PPM sludges, in consequence, proper detoxification processes capable of extracting inhibitor materials and economically acceptable should be developed. In the foreseeable future, a financially viable and socially acceptable biorefinery system must be developed for three reasons: 1) to effectively recover energy from PPM waste, 2) to reduce the financial burden of sludge management, and 3) to solve long-term waste management challenge in the pulping industry.

Bioconversion of PPM sludge for various products needs to compete with the physical and chemical conversion of PPM sludge for different types of products, such as activated carbon, brick materials, fertilizers, and soil amendment, etc. (Vieira et al., 2016; Nasr et al., 2017; Simão et al., 2018). The advantage of bioconversion is the lower energy consumption but its distinct disadvantage is the longer reaction time and larger bioreactor sizes. Thus, to improve the competitiveness of bioconversion technologies of PPM sludge, novel process development with a target of reducing reaction time and thus reducing capital and production costs is highly desirable.

9. Conclusion

Based on this review, PPM sludge has good potential as a source of energy. The energy trapped in the organic material can be transferred to biofuels via both anaerobic and fermentation technologies. These technologies also can be integrated into established pulping processes, which result in lower energy and investment costs, compared to conventional independent biorefineries. Despite the constraints, AD of PS, SS, and co-digestion of them with non-mill substrates showed great potential. In contrast, digesting PS alone or co-digesting it with SS showed no difference in biogas yield, thus, it would be preferable to digest PS separately from SS, followed by bioethanol production from the resulting cellulose-rich digestate. However, although the high-rate reactors like UASB, AFs, and AnMBR were developed a long time ago and represent roughly 50% of all industrial reactors, most of the digestion studies were performed using BMP assay. Adopting such systems to convert PPM sludge into biofuels is worthwhile. Also, the PPM sludge is characterized by a lack of nutrients, whose deficiency limits the microbial growth which in turn reduces the ultimate possible OLR, thus, co-digestion with a non-mill substrate could be of great benefit. Moreover, the PPM sludge contains reduced soluble substances so the biovalorization processes require long residence times. Consequently, PPM sludge must be converted to monosaccharides by pre-treatment. To achieve this, a wide range of pre-treatments have been developed, ranging from simple mechanical grinding to chemical hydrolyzation. PPM sludge-to-ethanol seems feasible, but more work is needed to increase its low concentration and facilitate its downstream recovery process. As well, most of the research was done at the laboratory level, thus, the transformation from lab-scale component to pilot and full scale is required. Current research also shows that the exploration for the utilization of PPM sludges as a substrate for the production of bio-hydrogen and biobutanol is still in the early stages, and further developments regarding fermented microorganisms, pre-treatment, and process design optimization are needed. Overall, there is good potential for the bio-valorization of PPM sludge as a bioenergy source taking advantage of on-site equipment of the P&P facility and developing a holistic biorefinery process.

Conflict of interest

The authors declare no conflict of interest.

Acknowledgment

The authors gratefully acknowledge the financial support for their research programs from the (OGS) Ontario Graduate Scholarship and (NSERC) the Natural Sciences and Engineering Research Council of Canada.

References

[1] Aditiya, H.B., Mahlia, T.M.I., Chong, W.T., Nur, H., Sebayang, A.H., 2016. Second generation bioethanol production: A critical review. Renew. Sust. Energ. Rev. 66, 631-653. https://doi.org/10.1016/j.rser.2016.07.015.

[2] Aksoy, B., Cullinan, H., Webster, D., Gue, K., Sukumaran, S., Eden, M., Sammons, N., 2011. Woody biomass and mill waste utilization opportunities in Alabama: Transportation cost minimization, optimum facility location, economic feasibility, and impact. Environ. Prog. Sustain. Energy. 30, 720-732. https://doi.org/10.1002/ep.10501.

[3] Al- Azkawi, A., Elliston, A., Al- Bahry, S., Sivakumar, N., 2019. Waste paper to bioethanol: Current and future prospective. Biofuel Bioprod. Biorefin. 13,1106-1118. https://doi.org/10.1002/bbb.1983.

[4] Alexander, F., Grant, D., 2018. Evaluating the effect of enzymatic pretreatment on the anaerobic digestibility of pulp and paper biosludge. Biotechnol. Rep. 17, 77-85. https://doi.org/10.1016/j.btre.2017.12.009.

[5] Amare, D.E., Ogun, M.K. Körner, I., 2019. Anaerobic treatment of deinking sludge: Methane production and organic matter degradation. Waste manag. 85, 417-424. https://doi.org/10.1016/j.wasman.2018.12.046.

[6] Bajpai, P., 2015. Management of pulp and paper mill waste. Springer International Publishing.

[7] Bakraoui, M., Karouach, F., Ouhammou, B., Aggour, M., Essamri, A., El Bari, H., 2019. Kinetics study of the methane production from experimental recycled pulp and paper sludge by CSTR technology. J. Mater. Cycles Waste Manag. 21, 1426–1436. https://doi.org/10.1007/s10163-019-00894-6.

[8] Ballesteros, M., Oliva, J.M., Manzanares, P., Negro, M.J., Ballesteros, I., 2002. Ethanol production from paper material using a simultaneous saccharification and fermentation system in a fed-batch basis. World J. Microbiol. Biotechnol.18, 559-561. https://doi.org/10.1023/A:1016378326762.

[9] Bayr, S., Kaparaju, P., Rintala, J., 2013. Screening pretreatment methods to enhance thermophilic anaerobic digestion of pulp and paper mill wastewater treatment secondary sludge. Chem. Eng. J. 223, 479-486. https://doi.org/10.1016/j.cej.2013.02.119.

[10] Bayr, S., Rintala, J., 2012. Thermophilic anaerobic digestion of pulp and paper mill primary sludge and co-digestion of primary and secondary sludge. Water Res. 46, 4713-4720. https://doi.org/10.1016/j.watres.2012.06.033.

[11] Benali, M., Ajao, O., El Mehdi, N., Restrepo, A.M., Fradj, N., Boumghar, Y., 2019. Acetone–Butanol–Ethanol Production from Eastern Canadian Yellow Birch and Screening of Isopropanol–Butanol–Ethanol-Producing Strains. Ind. Biotechnol. 15,188-201. https://doi.org/10.1089/ind.2019.0002.

[12] Bokhary, A., Maleki, E., Hong, Y., Hai, F.I., Liao, B., 2020. Anaerobic membrane bioreactors: Basic process design and operation. In: Ngo, H., H., Guo, W., Ng, H., Y., Mannina, G., Pandey A. (Eds.), Current Developments in Biotechnology and Bioengineering. Elsevier. pp. 25-54.

[13] Bonilla, S., Choolaei, Z., Meyer, T., Edwards, E.A., Yakunin, A.F., Allen, D.G., 2018. Evaluating the effect of enzymatic pretreatment on the anaerobic digestibility of pulp and paper biosludge. Biotechnol. Rep. 17, 77-85. https://doi.org/10.1016/j.btre.2017.12.009.

[14] Boshoff, S., Gottumukkala, L.D., van Rensburg, E., Görgens, J., 2016. Paper sludge (PS) to bioethanol: Evaluation of virgin and recycle mill sludge for low enzyme, high-solids fermentation. Bioresour. Technol. 203, 103-111. https://doi.org/10.1016/j.biortech.2015.12.028.

[15] Branco, R.H., Serafim, L.S., Xavier, A.M., 2019. Second generation bioethanol production: on the use of pulp and paper industry wastes as feedstock. Fermentation, 5, 4. https://doi.org/10.3390/fermentation5010004.

[16] Cao, X., Chen, Z., Liang, L., Guo, L., Jiang, Z., Tang, F., Yun, Y., Wang, Y., 2020. Co-valorization of paper mill sludge and corn steep liquor for enhanced n-butanol production with Clostridium tyrobutyricum Δcat1: adhE2. Bioresour. Technol. 296,122347. https://doi.org/10.1016/j.biortech.2019.122347.

[17] Cavka, A., Alriksson, B., Rose, S.H., Van Zyl, W.H., Jönsson, L.J., 2014. Production of cellulosic ethanol and enzyme from waste fiber sludge using SSF, recycling of hydrolytic enzymes and yeast, and recombinant cellulase-producing Aspergillus niger. J. Ind. Microbiol. Biotechnol. 41, 1191-1200. https://doi.org/10.1007/s10295-014-1457-9.

[18] Chatterjee, P., Lahtinen, L., Kokko, M., Rintala, J., 2018. Remediation of sedimented fiber originating from pulp and paper industry: Laboratory scale anaerobic reactor studies and ideas of scaling up. Water Res. 143, 209-217. https://doi.org/10.1016/j.watres.2018.06.054.

[19] Chen JH, Lin CC, Wang KS., 2013. Potential of Methane Production by Thermophilic Anaerobic Co-Digestion of Pulp and Paper Sludge with Pig Manure. J. Biobased Mater. Bioenergy 7:300–4. https://doi.org/10.1166/jbmb.2013.1327.

[20] Chen, H., Han, Q., Daniel, K., Venditti, R., Jameel, H., 2014. Conversion of industrial paper sludge to ethanol: Fractionation of sludge and its impact. Appl. Biochem. Biotechnol. 174, 2096-2113. https://doi.org/10.1007/s12010-014-1083-z.

[21] Chen, H., Venditti, R., Gonzalez, R., Phillips, R., Jameel, H., Park, S., 2014. Economic evaluation of the conversion of industrial paper sludge to ethanol. Energy Econ. 44, 281-290. https://doi.org/10.1016/j.eneco.2014.04.018.

[22] Chen, Z., Li, W., Qin, W., Sun, C., Wang, J. Wen, X., 2020. Long-term performance and microbial community characteristics of pilot-scale anaerobic reactors for thermal hydrolyzed sludge digestion

under mesophilic and thermophilic conditions. Sci. Total Environ. Article in press. 142940. https://doi.org/10.1016/j.scitotenv.2020.142940.

[23] Das, A., Mondal, C., 2016. Biogas production from Co-digestion of substrates: A Review. Int. Res. J. Environment Sci. 5, 49-57.

[24] Ding, H.H., Chang, S. Liu, Y., 2017. Biological hydrolysis pretreatment on secondary sludge: Enhancement of anaerobic digestion and mechanism study. Bioresour. Technol. 244, 989-995. https://doi.org/10.1016/j.biortech.2017.08.064.

[25] Dobre, P., Nicolae, F., Matei, F., 2014. Main factors affecting biogas production-an overview. Rom. Biotech. Lett. 19, 9283-9296.

[26] Dwiarti, L., Boonchird, C., Harashima, S., Park, E.Y., 2012. Simultaneous saccharification and fermentation of paper sludge without pretreatment using cellulase from Acremonium cellulolyticus and thermotolerant Saccharomyces cerevisiae. Biomass Bioenergy. 42, 114-122. https://doi.org/10.1016/j.biombioe.2012.02.019.

[27] Ekstrand, E.M., Karlsson, M., Truong, X.B., Björn, A., Karlsson, A., Svensson, B.H., Ejlertsson, J., 2016. High-rate anaerobic co-digestion of kraft mill fibre sludge and activated sludge by CSTRs with sludge recirculation. Waste Manag. 56, 166-172. https://doi.org/10.1016/j.wasman.2016.06.034.

[28] Elliott, A., Mahmood, T., 2007. Pretreatment technologies for advancing anaerobic digestion of pulp and paper biotreatment residues. Water Res. 41, 4273-4286. https://doi.org/10.1016/j.watres.2007.06.017.

[29] Elliott, A., Mahmood, T., 2012. Comparison of mechanical pretreatment methods for the enhancement of anaerobic digestion of pulp and paper waste activated sludge. Water Environ. Res. 84, 497-505. https://doi.org/10.2175/106143012X13347678384602.

[30] Fan, Z., Lynd, L.R., 2007. Conversion of paper sludge to ethanol, II: process design and economic analysis. Bioprocess Biosyst. Eng. 30, 35-45. https://doi.org/10.1007/s00449-006-0092-x.

[31] Fan, Z., South, C., Lyford, K., Munsie, J., van Walsum, P., Lynd, L.R., 2003. Conversion of paper sludge to ethanol in a semicontinuous solids-fed reactor. Bioprocess Biosyst. Eng. 26, 93-101. https://doi.org/10.1007/s00449-003-0337-x.

[32] Farghaly, A., Tawfik, A., Danial, A., 2016. Inoculation of paperboard mill sludge versus mixed culture bacteria for hydrogen production from paperboard mill wastewater. Environ. Sci. Pollut. Res. 23, 3834-3846. https://doi.org/10.1007/s11356-015-5652-7.

[33] Faubert, P., Barnabé, S., Bouchard, S., Côté, R., Villeneuve, C., 2016. Pulp and paper mill sludge management practices: What are the challenges to assess the impacts on greenhouse gas

emissions?. Resour. Conserv. Recycl. 108, 107-133. https://doi.org/10.1016/j.resconrec.2016.01.007.

[34] Fava, G., Ruello, M.L. Corinaldesi, V., 2010. Paper mill sludge ash as supplementary cementitious material. J Mater. Civil. Eng. 23, 772-776.

[35] Fein, J.E., Patel, G.B., Cook, C.R., 1989. Anaerobic digestion of Kraft Mill primary sludge. In TAPPI environmental conference proceedings, Orlando, 143-148.

[36] Geng, X., Zhang, S.Y. Deng, J., 2007. Characteristics of paper mill sludge and its utilization for the manufacture of medium density fiberboard. Wood. Fiber. Sci. 39, 345-351.

[37] Glanpracha, N., Annachhatre, A.P., 2016. Anaerobic co-digestion of cyanide containing cassava pulp with pig manure. Bioresour. Technol. 214, 112-121. https://doi.org/10.1016/j.biortech.2016.04.079.

[38] Gogoi H, Nirosha V, Jayakumar A, Prabhu K, Maitra M, Panjanathan R., 2018. Paper mill sludge as a renewable substrate for the production of acetone-butanol-ethanol using Clostridium sporogenes NCIM 2337. Energy Sources, Part A: Recovery, Utilization, and Environmental Effects. 40, 39-44. https://doi.org/10.1080/15567036.2017.1405107.

[39] Gomes, D., Domingues, L., Gama, M., 2016. Valorizing recycled paper sludge by a bioethanol production process with cellulase recycling. Bioresour. Technol., 216, 637-644. https://doi.org/10.1016/j.biortech.2016.06.004.

[40] Gomes, D., Gama, M., Domingues, L., 2018. Determinants on an efficient cellulase recycling process for the production of bioethanol from recycled paper sludge under high solid loadings. Biotechnol. Biofuels. 11, 1-12. https://doi.org/10.1186/s13068-018-1103-2.

[41] Granström, K.M., Montelius, J., 2014. Pre-treatment to enhance biogas yield from pulp and paper mill sludge. J. Chem. Chem. Eng. 8, 825-833.

[42] Guan W, Shi S, Tu M, Lee YY. 2016. Acetone-butanol-ethanol production from Kraft paper mill sludge by simultaneous saccharification and fermentation. Bioresour Technol. 200, 713-721. https://doi.org/10.1016/j.biortech.2015.10.102.

[43] Guan, W., Xu, G., Duan, J., Shi, S., 2018. Acetone–Butanol–Ethanol production from fermentation of hot-water-extracted hemicellulose hydrolysate of pulping woods. Ind. Eng. Chem. Res. 57, 775-783. https://doi.org/10.1021/acs.iecr.7b03953.

[44] Gurram, R.N., Al-Shannag, M., Lecher, N.J., Duncan, S.M., Singsaas, E.L., Alkasrawi, M., 2015. Bioconversion of paper mill sludge to bioethanol in the presence of accelerants or hydrogen peroxide pretreatment. Bioresour. Technol., 192, 529-539. https://doi.org/10.1016/j.biortech.2015.06.010.

[45] Hagelqvist, A., 2013. Batchwise mesophilic anaerobic co-digestion of secondary sludge from pulp and paper industry and municipal sewage sludge. Waste Manag. 33, 820-824. https://doi.org/10.1016/j.wasman.2012.11.002.

[46] Hagelqvist, A., Granström, K., 2016. Co-digestion of manure with grass silage and pulp and paper mill sludge using nutrient additions. Environ. Technol. 37, 2113-2123. https://doi.org/10.1080/09593330.2016.1142000.

[47] Hamilton, D., 2012. Anaerobic digestion of animal manures: methane production potential of waste materials. Oklahoma State University. https://hdl.handle.net/11244/49650.

[48] Hazarika, J. Khwairakpam, M., 2018. Evaluation of biodegradation feasibility through rotary drum composting recalcitrant primary paper mill sludge. Waste Manag. 76, 275-283. https://doi.org/10.1016/j.wasman.2018.03.044.

[49] Heo, N.H., Park, S.C., Lee, J.S., Kang, H., 2003. Solubilization of waste activated sludge by alkaline pretreatment and biochemical methane potential (BMP) tests for anaerobic co-digestion of municipal organic waste. Water Sci. Technol. 48, 211-219. https://doi.org/10.2166/wst.2003.0471.

[50] Huiliñir, C., Quintriqueo, A., Antileo, C., Montalvo, S., 2014. Methane production from secondary paper and pulp sludge: Effect of natural zeolite and modeling. Chem. Enzg. J. 257, 131-137. https://doi.org/10.1016/j.cej.2014.07.058.

[51] Jeong, J.H., Takaoka, M., Ichiura, H., Oshita, K. Fujimori, T., 2016. Evaluation of metals in the residue of paper sludge after recovery of pulp components using an ionic liquid. J. Mater. Cycles. Waste. 18, 215-221. https://doi.org/10.1007/s10163-015-0391-x.

[52] Jin, M., Gunawan, C., Balan, V., Lau, M.W., Dale, B.E., 2012. Simultaneous saccharification and co-fermentation (SSCF) of AFEX TM pretreated corn stover for ethanol production using commercial enzymes and Saccharomyces cerevisiae 424A (LNH-ST). Bioresour. Technol. 110, 587-594. https://doi.org/10.1016/j.biortech.2012.01.150.

[53] Jokela, J., Rintala, J., Oikari, A., Reinikainen, O., Mutka, K., Nyrönen, T., 1997. Aerobic composting and anaerobic digestion of pulp and paper mill sludges. Water Sci. Technol. 36, 181-188. https://doi.org/10.1016/S0273-1223(97)00680-X.

[54] Kádár Z., De Vrije T., Budde M.A.W., Szengyel Z., Réczey K., Claassen P.A.M. 2003. Hydrogen Production from Paper Sludge Hydrolysate. In: Davison B.H., Lee J.W., Finkelstein M., McMillan J.D. (Eds.), Biotechnology for Fuels and Chemicals. Appl. Biochem. Biotechnol. Humana Press, Totowa, NJ, pp. 557-566. https://doi.org/10.1007/978-1-4612-0057-4_46.

[55] Kádár, Z., Szengyel, Z., Réczey, K., 2004. Simultaneous saccharification and fermentation (SSF) of industrial wastes for the production of ethanol. Ind. Crops. Prod., 20, 103-110. https://doi.org/10.1016/j.indcrop.2003.12.015.

[56] Kamali, M., Gameiro, T., Costa, M.E.V., Capela, I., 2016. Anaerobic digestion of pulp and paper mill wastes–An overview of the developments and improvement opportunities. Chem. Eng. J. 298, pp.162-182. https://doi.org/10.1016/j.cej.2016.03.119.

[57] Kang, L., Wang, W., Lee, Y.Y. 2010. Bioconversion of kraft paper mill sludges to ethanol by SSF and SSCF. Appl. Biochem. Biotechnol., 161, 53-66. https://doi.org/10.1007/s12010-009-8893-4.

[58] Kang, L., Wang, W., Pallapolu, V.R., Lee, Y.Y., 2011. Enhanced ethanol production from de-ashed paper sludge by simultaneous saccharification and fermentation and simultaneous saccharification and co-fermentation. BioResources, 6, 3791-3808.

[59] Karlsson, A., Truong, X.B., Gustavsson, J., Svensson, B.H., Nilsson, F., Ejlertsson, J., 2011. Anaerobic treatment of activated sludge from Swedish pulp and paper mills–biogas production potential and limitations. Environ. Technol. 32, 1559-1571. https://doi.org/10.1080/09593330.2010.543932.

[60] Kim, J., Park, C., Kim, T.H., Lee, M., Kim, S., Kim, S.W., Lee, J., 2003. Effects of various pretreatments for enhanced anaerobic digestion with waste activated sludge. J. Biosci. Bioeng. 95, 271-275. https://doi.org/10.1016/S1389-1723(03)80028-2.

[61] Kinnunen, V., Ylä-Outinen, A., Rintala, J., 2015. Mesophilic anaerobic digestion of pulp and paper industry biosludge–long-term reactor performance and effects of thermal pretreatment. Water Res. 87, 105-111. https://doi.org/10.1016/j.watres.2015.08.053.

[62] Kokko, M., Koskue, V., Rintala, J., 2018. Anaerobic digestion of 30− 100-year-old boreal lake sedimented fibre from the pulp industry: Extrapolating methane production potential to a practical scale. Water Res. 133, 218-226. https://doi.org/10.1016/j.watres.2018.01.041.

[63] Kolbl, S., Forte-Tavčer, P., Stres, B., 2017. Potential for valorization of dehydrated paper pulp sludge for biogas production: addition of selected hydrolytic enzymes in semi-continuous anaerobic digestion assays. Energy, 126, 326-334. https://doi.org/10.1016/j.energy.2017.03.050.

[64] Kythreotou, N., Tassou, S.A., Florides, G., 2012. An assessment of the biomass potential of Cyprus for energy production. Energy, 47, 253-261. https://doi.org/10.1016/j.energy.2012.09.023.

[65] Lark, N., Xia, Y., Qin, C.G., Gong, C.S., Tsao, G.T., 1997. Production of ethanol from recycled paper sludge using cellulase and yeast, Kluveromyces marxianus. Biomass Bioenergy. 12, 135-143. https://doi.org/10.1016/S0961-9534(96)00069-4.

[66] Larsson, M., Jansson, M., Grönkvist, S., Alvfors, P., 2015. Techno-economic assessment of anaerobic digestion in a typical Kraft pulp mill to produce biomethane for the road transport sector. J. Clean. Prod. 104, 460-467. https://doi.org/10.1016/j.jclepro.2015.05.054.

[67] Li, D., Liu, S., Mi, L., Li, Z., Yuan, Y., Yan, Z., Liu, X., 2015. Effects of feedstock ratio and organic loading rate on the anaerobic mesophilic co-digestion of rice straw and pig manure. Bioresour. Technol. 187, 120-127. https://doi.org/10.1016/j.biortech.2015.04.033.

[68] Li, W., Siddhu, M.A.H., Amin, F.R., He, Y., Zhang, R., Liu, G., Chen, C., 2018. Methane production through anaerobic co-digestion of sheep dung and waste paper. Energy Convers. Manag. 156, 279-287. https://doi.org/10.1016/j.enconman.2018.06.099.

[69] Lin, Y., Liang, J., Zeng, C., Wang, D., Lin, H., 2017. Anaerobic digestion of pulp and paper mill sludge pretreated by microbial consortium OEM1 with simultaneous degradation of lignocellulose and chlorophenols. Renew. Energy. 108, 108-115. https://doi.org/10.1016/j.renene.2017.02.049.

[70] Lin, Y., Wang, D., Li, Q., Xiao, M., 2011. Mesophilic batch anaerobic co-digestion of pulp and paper sludge and monosodium glutamate waste liquor for methane production in a bench-scale digester. Bioresour. Technol. 102, 3673-3678. https://doi.org/10.1016/j.biortech.2010.10.114.

[71] Lin, Y., Wang, D., Liang, J., Li, G., 2012. Mesophilic anaerobic co-digestion of pulp and paper sludge and food waste for methane production in a fed-batch basis. Environ. Technol. 33, 2627-2633. https://doi.org/10.1080/09593330.2012.673012.

[72] Lin, Y., Wu, S., Wang, D., 2013. Hydrogen-methane production from pulp & paper sludge and food waste by mesophilic–thermophilic anaerobic co-digestion. Int. J. Hydrog. Energy. 38, 15055-15062. https://doi.org/10.1016/j.ijhydene.2012.01.051.

[73] Liu, G., Wang, K., Li, X., Ma, L., Ma, X. Chen, H., 2019. Enhancement of excess sludge hydrolysis and decomposition with different lysozyme dosage. J. Hazard. Mater. 366, 395-401. https://doi.org/10.1016/j.jhazmat.2018.12.002.

[74] Liu, Y., Lin, R., Man, Y., Ren, J., 2019. Recent developments of hydrogen production from sewage sludge by biological and thermochemical process. Int. J. Hydrog. Energy. 44, 19676-19697. https://doi.org/10.1016/j.ijhydene.2019.06.044.

[75] Lopes, A.D.C.P., Silva, C.M., Rosa, A.P., de Ávila Rodrigues, F., 2018. Biogas production from thermophilic anaerobic digestion of kraft pulp mill sludge. Renew. Energy. 124, 40-49. https://doi.org/10.1016/j.renene.2017.08.044.

[76] Mabee, W., Roy, D.N., 2003. Modeling the role of papermill sludge in the organic carbon cycle of paper products. Environ. Rev. 11, 1-16. https://doi.org/10.1139/a03-001.

[77] Madrid, L., Quintero Diaz, J.C., 2011. Ethanol production from paper sludge using Kluyveromyces marxianus. Dyna, 78, 185-191.

[78] Marques, S., Alves, L., Roseiro, J.C., Gírio, F.M., 2008. Conversion of recycled paper sludge to ethanol by SHF and SSF using Pichia stipitis. Biomass Bioenergy. 32, 400-406. https://doi.org/10.1016/j.biombioe.2007.10.011.

[79] Meabe, E., Déléris, S., Soroa, S., Sancho, L., 2013. Performance of anaerobic membrane bioreactor for sewage sludge treatment: Mesophilic and thermophilic processes. J. Membr. Sci. 446, 26-33. https://doi.org/10.1016/j.memsci.2013.06.018.

[80] Mejía-Barajas, J.A., Alvarez-Navarrete, M., Saavedra-Molina, A., Campos-García, J., Valenzuela-Vázquez, U., Amaya-Delgado, L., Arellano-Plaza, M., 2018. Second-Generation Bioethanol Production through a Simultaneous Saccharification-Fermentation Process Using *Kluyveromyces Marxianus* Thermotolerant Yeast: In: Ebubekir Y., Abdülkerim G., Murat E. (Eds.), Special Topics in Renewable Energy Systems. IntechOpen. London, UK, pp.21-49. https://doi.org/ 10.5772/intechopen.78052.

[81] Mendes, C.V., Rocha, J.M., Carvalho, M.G.V., 2014. Valorization of residual streams from pulp and paper mills: pretreatment and bioconversion of primary sludge to bioethanol. Ind. Eng. Chem. Res. 53, 19398-19404. https://doi.org/10.1021/ie503021y.

[82] Mendes, C.V.T., Rocha, J.M.D.S., de Menezes, F.F., Carvalho, M.D.G.V.S., 2017. Batch and fed-batch simultaneous saccharification and fermentation of primary sludge from pulp and paper mills. Environ. Technol. 38, 1498-1506. https://doi.org/10.1080/09593330.2016.1235230.

[83] Meyer, T., Edwards, E.A., 2014. Anaerobic digestion of pulp and paper mill wastewater and sludge. Water Res. 65, 321-349. https://doi.org/10.1016/j.watres.2014.07.022.

[84] Montañés, R., Solera, R., Pérez, M., 2015. Anaerobic co-digestion of sewage sludge and sugar beet pulp lixiviation in batch reactors: Effect of temperature. Bioresour. Technol. 180, 177-184. https://doi.org/10.1016/j.biortech.2014.12.056.

[85] Monte, M.C., Fuente, E., Blanco, A., Negro, C., 2009. Waste management from pulp and paper production in the European Union. Waste Manag. 29, 293-308. https://doi.org/10.1016/j.wasman.2008.02.002.

[86] Moreau, A., Montplaisir, D., Sparling, R., Barnabé, S., 2015. Hydrogen, ethanol and cellulase production from pulp and paper primary sludge by fermentation with Clostridium thermocellum. Biomass Bioenergy. 72, 256-262. https://doi.org/10.1016/j.biombioe.2014.10.028.

[87] Mshandete, A., Björnsson, L., Kivaisi, A.K., Rubindamayugi, S.T., Mattiasson, B., 2005. Enhancement of anaerobic batch digestion of sisal pulp waste by mesophilic aerobic pre-treatment. Water Res. 39, 1569-1575. https://doi.org/10.1016/j.watres.2004.11.037.

[88] Mshandete, A., Kivaisi, A., Rubindamayugi, M., Mattiasson, B., 2004. Anaerobic batch co-digestion of sisal pulp and fish wastes. Bioresour. Technol. 95, 19-24. https://doi.org/10.1016/j.biortech.2004.01.011.

[89] Mussoline, W., Esposito, G., Lens, P., Spagni, A., Giordano, A., 2013. Enhanced methane production from rice straw co-digested with anaerobic sludge from pulp and paper mill treatment process. Bioresour. Technol. 148,135-143. https://doi.org/10.1016/j.biortech.2013.08.107.

[90] Nasr, J.B., Hamdi, N. Elhalouani, F., 2017. Characterization of activated carbon Prepared from sludge paper for methylene blue adsorption. Mater. Environ. Sci. 8, 1960-1967.

[91] Ochoa de Alda, J.A.O., 2008. Feasibility of recycling pulp and paper mill sludge in the paper and board industries. Resour. Conserv. Recycl., 52, 965-972. https://doi.org/10.1016/j.resconrec.2008.02.005.

[92] Ofoefule, A.U., Nwankwo, J.I., Ibeto, C.N., 2010. Biogas Production from Paper Waste and its blend with Cow dung. Adv. Appl. Sci. Res. 1, 1-8.

[93] Ogun, M.K., Amare, D.E., Badri, A., Körner, I. 2015. Treatment of deinking sludge from wastepaper recycling by anaerobic digestion. Ramiran 2015– 16th International Conference. Rural-Urban Symbiosis, Hamburg, Germany. 649-653

[94] Parameswaran, P., Rittmann, B.E., 2012. Feasibility of anaerobic co-digestion of pig waste and paper sludge. Bioresour. Technol. 124, 163-168. https://doi.org/10.1016/j.biortech.2012.07.116.

[95] Park, N.D., Helle, S.S., Thring, R.W., 2012. Combined alkaline and ultrasound pre-treatment of thickened pulp mill waste activated sludge for improved anaerobic digestion. Biomass Bioenergy. 46, 750-756. https://doi.org/10.1016/j.biombioe.2012.05.014.

[96] Peng, L., Chen, Y., 2011. Conversion of paper sludge to ethanol by separate hydrolysis and fermentation (SHF) using Saccharomyces cerevisiae. Biomass Bioenergy. 35, 1600-1606. https://doi.org/10.1016/j.biombioe.2011.01.059.

[97] Pileggi, V., Parker, W.J., 2017. AnMBR digestion of mixed WRRF sludges: Impact of digester loading and temperature. J. Water Process. Eng. 19, 74-80. https://doi.org/10.1016/j.jwpe.2017.07.011.

[98] Poggi-Varaldo, H.M., Valdés, L., Esparza-Garcia, F., Fernández-Villagómez, G., 1997. Solid substrate anaerobic co-digestion of paper mill sludge, biosolids, and municipal solid waste. Water Sci. Technol. 35, 197-204. https://doi.org/10.1016/S0273-1223(96)00957-2.

[99] Prasetyo, J., Naruse, K., Kato, T., Boonchird, C., Harashima, S., Park, E.Y., 2011. Bioconversion of paper sludge to biofuel by simultaneous saccharification and fermentation using a cellulase of paper

sludge origin and thermotolerant Saccharomyces cerevisiae TJ14. Biotechnol. Biofuels, 4, 1-13. https://doi.org/10.1186/1754-6834-4-35.

[100] Priadi, C., Wulandari, D., Rahmatika, I., Moersidik, S.S., 2014. Biogas production in the anaerobic digestion of paper sludge. APCBEE procedia, 9, 65-69. https://doi.org/10.1016/j.apcbee.2014.01.012.

[101] Puhakka, J.A., Alavakeri, M., Shieh, W.K., 1992. Anaerobic treatment of kraft pulp-mill waste activated-sludge: gas production and solids reduction. Bioresour. Technol. 39, 61-68. https://doi.org/10.1016/0960-8524(92)90057-5.

[102] Puhakka, J.A., Viitasaari, M.A., Latola, P.K., Määttä, R.K., 1988. Effect of temperature on anaerobic digestion of pulp and paper industry wastewater sludges. Water Sci. Technol. 20, 193-201. https://doi.org/10.2166/wst.1988.0022.

[103] Robus, C.L., Gottumukkala, L.D., van Rensburg, E., Görgens, J.F., 2016. Feasible process development and techno-economic evaluation of paper sludge to bioethanol conversion: South African paper mills scenario. Renew. Energy. 92, 333-345. https://doi.org/10.1016/j.renene.2016.02.017.

[104] Robus, C.L.L. 2013. Production of bioethanol from paper sludge using simultaneous saccharification and fermentation. Master dissertation, Stellenbosch: Stellenbosch University. http://hdl.handle.net/10019.1/80251.

[105] Rodriguez, C., Alaswad, A., El-Hassan, Z., Olabi, A.G., 2018. Waste paper and macroalgae co-digestion effect on methane production. Energy, 154, 119-125. https://doi.org/10.1016/j.energy.2018.04.115.

[106] Saha, M., Eskicioglu, C., Marin, J., 2011. Microwave, ultrasonic and chemo-mechanical pre-treatments for enhancing methane potential of pulp mill wastewater treatment sludge. Bioresour. Technol. 102, 7815-7826. https://doi.org/10.1016/j.biortech.2011.06.053.

[107] Schroeder, B.G., Zanoni, P.R.S., Magalhães, W.L.E., Hansel, F.A., Tavares, L.B.B., 2017. Evaluation of biotechnological processes to obtain ethanol from recycled paper sludge. J. Mater. Cycles. Waste Manages., 19, 463-472. https://doi.org/10.1007/s10163-015-0445-0.

[108] Sebastião, D., Gonçalves, M.S., Marques, S., Fonseca, C., Gírio, F., Oliveira, A.C., Matos, C.T., 2016. Life cycle assessment of advanced bioethanol production from pulp and paper sludge. Bioresour. Technol. 208, 100-109. https://doi.org/10.1016/j.biortech.2016.02.049.

[109] Sethupathy, A., Sivashanmugam, P., 2018. Enhancing biomethane potential of pulp and paper sludge through disperser mediated polyhydroxyalkanoates. Energy Convers. Manag. 173, 179-186. https://doi.org/10.1016/j.enconman.2018.07.076.

[110] Shao, X., Lynd, L., Wyman, C. 2009. Kinetic modeling of cellulosic biomass to ethanol via simultaneous saccharification and fermentation: Part II. Experimental validation using waste paper sludge and anticipation of CFD analysis. Biotechnol. Bioeng. 102, 66-72. https://doi.org/10.1002/bit.22047.

[111] Silva Zanoni, P.R., Esteves Magalhaes, W.L., Helm, C.V., de Lima, E.A., Ballod Tavares, L.B., Kestur, S.G., 2017. Review of ethanol production based on paper sludge: processes and prospects. Environ. Eng. Manag. J. 16, 1227-1248. http://eemj.eu/index.php/EEMJ/article/view/3280.

[112] Simão, L., Hotza, D., Raupp-Pereira, F., Labrincha, J.A. Montedo, O.R.K., 2018. Wastes from pulp and paper mills-a review of generation and recycling alternatives. Cerâmica. 64 443-453. https://doi.org/10.1590/0366-69132018643712414.

[113] Sjöde, A., Alriksson, B., Jönsson, L.J., Nilvebrant, N.O. 2007. The potential in bioethanol production from waste fiber sludges in pulp mill-based biorefineries. Appl. Biochem. Biotechnol. 37, 327–337. https://doi.org/10.1007/s12010-007-9062-2.

[114] Song, X.D., Chen, D.Z., Zhang, J., Dai, X.H., Qi, Y.Y., 2017. Anaerobic digestion combined pyrolysis for paper mill sludge disposal and its influence on char characteristics. J. Mater. Cycles Waste Manag. 19, 332-341. https://doi.org/10.1007/s10163-015-0428-1.

[115] Steffen, F., Janzon, R., Wenig, F., Saake, B. 2017. Valorization of waste streams from deinked pulp mills through anaerobic digestion of deinking sludge. BioResources, 12, 4547-4566.

[116] Stoica, A., Sandberg, M., Holby, O., 2009. Energy use and recovery strategies within wastewater treatment and sludge handling at pulp and paper mills. Bioresour. Technol. 100, 3497-3505. https://doi.org/10.1016/j.biortech.2009.02.041.

[117] Takizawa, S., Baba, Y., Tada, C., Fukuda, Y., Nakai, Y., 2018. Pretreatment with rumen fluid improves methane production in the anaerobic digestion of paper sludge. Waste Manag. 78, 379-384. https://doi.org/10.1016/j.wasman.2018.05.046.

[118] Teghammar, A., Castillo, M.D.P., Ascue, J., Niklasson, C., Sárvári Horváth, I., 2012. Improved anaerobic digestion by the addition of paper tube residuals: pretreatment, stabilizing, and synergetic effects. Energy Fuels, 27, 277-284. https://doi.org/10.1021/ef301633x.

[119] Tyagi, V.K., Lo, S.L., Rajpal, A., 2014. Chemically coupled microwave and ultrasonic pre-hydrolysis of pulp and paper mill waste-activated sludge: effect on sludge solubilisation and anaerobic digestion. Environ. Sci. Pollut. Res. 21, 6205-6217. https://doi.org/10.1007/s11356-013-2426-y.

[120] Vaez, E., Taherdanak, M., Zilouei, H. 2017. Dark hydrogen fermentation from paper mill effluent (PME): The influence of substrate concentration and hydrolysis. Environ. Energy Econ. Res. 1, 163-170. https://doi.org/10.22097/EEER.2017.47243.

[121] Vaez, E., Zilouei, H., 2020. Towards the development of biofuel production from paper mill effluent. Renew. Energy. 146, 1408-1415. https://doi.org/10.1016/j.renene.2019.07.059.

[122] Valdez-Vazquez, I., Sparling, R., Risbey, D., Rinderknecht-Seijas, N., and Poggi-Varaldo, H.M. 2005. Hydrogen generation via anaerobic fermentation of paper mill wastes. Bioresour. Technol., 96, 1907-1913. https://doi.org/10.1016/j.biortech.2005.01.036.

[123] Veluchamy, C., Kalamdhad, A.S., 2017. Biochemical methane potential test for pulp and paper mill sludge with different food/microorganisms ratios and its kinetics. Int. Biodeterior. Biodegr. 117, 197-204. https://doi.org/10.1016/j.ibiod.2017.01.005.

[124] Veluchamy, C., Kalamdhad, A.S., 2017. Influence of pretreatment techniques on anaerobic digestion of pulp and paper mill sludge: A review. Bioresour. Technol. 245, 1206-1219. https://doi.org/10.1016/j.biortech.2017.08.179.

[125] Vieira, C.M.F., Pinheiro, R.M., Rodriguez, R.J.S., Candido, V.S. Monteiro, S.N., 2016. Clay bricks added with effluent sludge from paper industry: Technical, economical and environmental benefits. Appl. Clay Sci. 132, 753-759. https://doi.org/10.1016/j.clay.2016.07.001.

[126] Weiland, P., 2000. Anaerobic waste digestion in Germany–Status and recent developments. Biodegradation, 11, 415-421. https://doi.org/10.1023/A:1011621520390.

[127] Wood, N., Tran, H., Master, E., 2009. Pretreatment of pulp mill secondary sludge for high-rate anaerobic conversion to biogas. Bioresour. Technol. 100, 5729-5735. https://doi.org/10.1016/j.biortech.2009.06.062.

[128] Wu, F., Zhou, S. 2011. Anaerobic biohydrogen fermentation from paper mill sludge. J. Energ Eng., 138, 1-6. https://doi.org/10.1061/(ASCE)EY.1943-7897.0000054.

[129] Xie, S., Wickham, R., Nghiem, L.D., 2017. Synergistic effect from anaerobic co-digestion of sewage sludge and organic wastes. Int. Biodeterior. Biodegr. 116, 191-197. https://doi.org/10.1016/j.ibiod.2016.10.037.

[130] Xu, N., Liu, S., Xin, F., Jia, H., Xu, J., Jiang, M. Dong, W., 2019. Biomethane production from lignocellulose: biomass recalcitrance and its impacts on anaerobic digestion. Front. Bioeng. Biotechnol. 7, 191. https://doi.org/10.3389/fbioe.2019.00191.

[131] Yamashita, Y., Kurosumi, A., Sasaki, C., Nakamura, Y. 2008. Ethanol production from paper sludge by immobilized Zymomonas mobilis. Biochem. Eng. J. 42, 314-319. https://doi.org/10.1016/j.bej.2008.07.013.

[132] Yamashita, Y., Sasaki, C., Nakamura, Y., 2010. Development of efficient system for ethanol production from paper sludge pretreated by ball milling, phosphoric acid. Carbohydr. Polym. 79, 250-254. https://doi.org/10.1016/j.carbpol.2009.07.054.

[133] Yasar, A., Rasheed, R., Tabinda, A.B., Tahir, A., Sarwar, F., 2017. Life cycle assessment of a medium commercial scale biogas plant and nutritional assessment of effluent slurry. Renew. Sust. Energ. Rev. 67, 364-371. https://doi.org/10.1016/j.rser.2016.09.026.

[134] Yen, H.W., Brune, D.E., 2007. Anaerobic co-digestion of algal sludge and waste paper to produce methane. Bioresour. Technol. 98, 130-134. https://doi.org/10.1016/j.biortech.2005.11.010.

[135] Yu, H., Wang, Z., Wu, Z., Zhu, C., 2016. Enhanced waste activated sludge digestion using a submerged anaerobic dynamic membrane bioreactor: performance, sludge characteristics and microbial community. Sci. Rep. 6, 20111. https://doi.org/10.1038/srep20111.

[136] Yue, Z., Teater, C., Liu, Y., MacLellan, J., Liao, W., 2010. A sustainable pathway of cellulosic ethanol production integrating anaerobic digestion with biorefining. Biotechnol. Bioeng. 105, 1031-1039. https://doi.org/10.1002/bit.22627.

[137] Yunqin L., Wang, D., Li, Q., Huang, L., 2011. Kinetic study of mesophilic anaerobic digestion of pulp & paper sludge. Biomass Bioenergy. 35, 4862-4867. https://doi.org/10.1016/j.biombioe.2011.10.001.

[138] Yunqin, L., Dehan, W., Lishang, W., 2010. Biological pretreatment enhances biogas production in the anaerobic digestion of pulp and paper sludge. Waste Manag. Res. 28, 800-810. https://doi.org/10.1177/0734242X09358734.

[139] Yunqin. L., Wang, D., Wu, S., Wang, C., 2009. Alkali pretreatment enhances biogas production in the anaerobic digestion of pulp and paper sludge. J. Hazard. Mater. 170, 366-373. https://doi.org/10.1016/j.jhazmat.2009.04.086.

[140] Zhang, J., Lynd, L.R. 2010. Ethanol production from paper sludge by simultaneous saccharification and co- fermentation using recombinant xylose- fermenting microorganisms. Biotechnol. Bioeng. 107, 235-244. https://doi.org/10.1002/bit.22811.

[141] Zhang, J., Shao, X., Lynd, L.R. 2009. Simultaneous saccharification and co- fermentation of paper sludge to ethanol by Saccharomyces cerevisiae RWB222. Part II: Investigation of discrepancies between predicted and observed performance at high solids concentration. Biotechnol. Bioeng. 104, 932-938. https://doi.org/10.1002/bit.22465.

[142] Zhang, Q., Hu, J., Lee, D.J., Chang, Y., Lee, Y.J., 2017. Sludge treatment: Current research trends. Bioresour. Technol. 243, 1159-1172. https://doi.org/10.1016/j.biortech.2017.07.070.

[143] Zhu, M.J., Zhu, Z.S., Li, X.H., 2011. Bioconversion of paper sludge with low cellulosic content to ethanol by separate hydrolysis and fermentation. Afr. J. Biotechnol. 10, 15072-15083. https://doi.org/10.5897/AJB11.1644.

Chapter III

Separation of Hemicelluloses and Lignins from Synthetic Hydrolyzate and Thermomechanical Pulp Mill Process Water via Liquid-Liquid Extraction

Abstract:

The separation of hemicelluloses from thermomechanical pulping (TMP) process water is of particular interest because it yields a biopolymer suitable for various value-added biomaterials production and reduces the organic loading on the water treatment facility. However, during the TMP process, hemicellulose is released in the process water at relatively low concentrations that are difficult to recover by many methods efficiently. Liquid-liquid extraction (LLE) has been deemed as a potentially viable separation technique in modern industrial processes for valuable materials recovery and undesirable impurities removal. In this work, the extraction of hemicellulose from the process water and synthetic hydrolyzate using LLE was investigated. In particular, the effects of the major experimental variables (the type of solvent, hydrolyzate to solvent volume ratio, and pH) on extraction performance were explored. The tested solvents have shown varying affinity and selectivity for the recovery of hemicellulose. It was found that the hemicellulose extraction efficiency of n-hexane (71.03%) and tributyl phosphate (TBP) (72.34%) was higher than that of 1-butanol (62.36%), and toluene (67.03%) at a solvent: hydrolyzate volume ratio of 1:3. Although TBP showed a high degree of hemicellulose extraction (72.34), it was characterized by a low selectivity coefficient, while n-hexane achieved the highest selectivity. The average selectivity coefficients of n-hexane were 7.3, 5.1, and 8.7 followed by toluene 2.7, 2.7, and 2.9 for pH values of 9.5, 7, and 4.3, respectively. Changing the pH of the hydrolyzate has resulted in varying effects depending on the type of the solvent used. The optimum extraction pH, phase ratio, and extraction time were at 4.3, 1:3 mL/mL and 30 min, respectively.

Keywords: solvent; liquid-liquid extraction; hemicellulose; process water; value-added products.

---

1. Introduction

Due to environmental concerns and sustainability, renewable resources have become the most promising feedstock for many modern industrial societies. Natural polymers such as hemicellulose and lignin are well known biodegradable materials, and progressively being viewed as viable alternatives to some currently used materials for many applications. These polymers can economically be recovered and then converted into different high value-added biomaterials. Currently, lignin can be used as activated carbon, dispersants, carbon fibers, and sorbents (Pye 2008; He et al., 2012; Norgren and Edlund 2014; Bokhary et al., 2017). While hemicellulose can be used directly in polymeric form for novel industrial applications such as biopolymers, hydrogels, and xylan derivatives compounds (Saha 2003; Fišerová and Opálená 2012). Alternatively, hemicellulose can be fermented into biofuels after hydrolysis process (chemical or enzymatic) that hydrolyzes the hemicellulose oligomers into simple sugars (monosaccharides, especially xylose), and different fermentation processes have been developed to convert hemicellulose sugars to biofuel ethanol (Saha 2003; Ji et al., 2011).

Bokhary, A., Leitch, M., Gao, W.J., Fatehi, P. and Liao, B.Q., 2019. Separation of hemicelluloses and lignins from synthetic hydrolyzate and thermomechanical pulp mill process water via liquid-liquid extraction. Separation and Purification Technology, 215, 508-515.

However, efficient fractionation of lignocellulosic biomass components represents one of the major barriers to the effective utilization of such renewable resources (Hongzhang and Liying 2007).

In the literature, a number of separation processes have been investigated for sugars and lignin isolation from the aqueous solution (feed), e.g., membrane filtration process (Bokhary et al., 2017), precipitation process (Mussatto et al., 2007). Precipitation and membrane filtration often have relatively low selectivity, and therefore, further purification steps may be required. In addition, membrane processes often have a fouling problem, which requires very expensive cleaning regimes. Further, the low concentration of dissolved materials in the TMP mills process water may also hinder their separation by many of the conventional methods. More recently, a chromatographic separation technique is another alternative way used for sugar separation, although it is a complex process (Matsumoto et al., 2005). Also, other processes based on the chemical affinity of sugars have been proposed, e.g., liquid-liquid extraction (Cruz et al., 1999; Hameister and Kragl 2006), ion exchange membrane (Ouahid et al., 1996), liquid membrane (Luccio et al., 2000), and absorption (Olajire 2010; Liu et al., 2011).

Solvent extraction (SX), which involves the mixing of two immiscible or partially miscible liquids and subsequent separation, may overcome the limitations encountered in the aforementioned methods. The use of solvent extraction has been deemed as a feasible method in many industrial processes for valuable compounds recovery or undesirable impurities removal (Hassan et al., 2013). SX is a simple, clean, and fast process (Mussatto et al., 2005), and it is easy to recover the used solvents (Cruz et al., 1999), as well as high purity can be achieved (Hassan et al., 2013). However, many factors should be considered in evaluating the use of potential solvents for a particular extraction process such as the capacity for partitioning of product, affinity or selectivity for the target product over other constituents, and miscibility with the aqueous phase or feed phase (McPartland et al., 2012) in addition they should be environmentally-friendly. Usually, the more polar the solvent, the higher is the degree of extraction (Kontturi and Sundholm 1986). On the other hand, to reduce process costs, recycling of the used solvent must be considered in process design. The primary task of an extractor is to find optimal conditions for mass transfer between the two phases. In some cases, the capacity of the solvent can be enhanced by adding one or more extractants to the solvent phase. Other factors such as the solvent type and its concentration, hydrolyzate concentration, and pH of the aqueous stream also influence the selectivity and partitioning coefficient (Lisec et al., 2012; Martins et al., 2012; Li et al., 2012; Djas and Henczka 2018).

In the literature, sparse studies examined the extraction of lignocellulosic materials from an aqueous media into an immiscible organic solution. John et al. (2004) used boronic acid extractants to purify and concentrate sugars present in hemicellulose hydrolyzates. In this study, the concentration of xylose was increased more than seven times from the original hydrolyzate concentration, while reducing the

concentration of the acid-soluble lignin by more than 90%. Mussatto et al. (2005) purified xylitol from fermented hemicelluloses hydrolyzate using either ethyl acetate, chloroform, or dichloromethane. Ethyl acetate achieved high xylitol purification without losses. Hameister and Kragl (2006) studied the recovery of mono- and disaccharides from aqueous media using butanol, methyl tertiary-butyl ether (MTBE), and n-hexane and achieved 40 recovery percent. Cruz et al. (1999) extracted 84% of lignin-derived compounds when they studied the removal of the phenolic compounds derived from Eucalyptus hydrolyzates using ethyl acetate and diethyl ether. Organic solvents and amines have demonstrated high extraction efficiency for lignosulfonates (Kontturi and Sundholm 1986). Typical issues of extraction with amine-based solvents are the difficulty of complete removal of the amine from the extracted material, as well as foaming and emulsification problems (Ringena et al., 2005). In the studies mentioned above, several organic solvents have been tested, some of which have demonstrated excellent capacities to extract a wide range of non-polar to polar compounds. Although some organic solvents have shown significant extraction levels, the amount of organic solvent utilized in conventional SX is considerably large (Birajdar et al., 2015). Added to this, some solvents such as dichloromethane are carcinogenic, and the recent trends have been to refrain from the use of such solvents in downstream processes.

Although some studies have examined the extraction of hemicellulose and lignin from the lignocellulosic hydrolyzate into immiscible organic solutions; and technically it has been found that these materials can be extracted and purified (John et al., 2004; Matsumoto et al., 2005; Aziz et al., 2008). To the best of our knowledge, no study has focused on the extraction of hemicelluloses from process water of thermomechanical pulp mills using such techniques. The present study aims to evaluate the feasibility of liquid-liquid extraction technique for hemicellulose separation from the process water of a thermomechanical pulp mill and synthetic hydrolyzate in a single batch. The performance (selectivity coefficient, hemicellulose extraction percent, partition coefficient, and extraction time) of the different solvents namely: 1-butanol, toluene, TBP and n-hexane under various operational conditions were assessed.

2. Materials and methods

2.1. Chemicals and process water

The chemicals used in this study were xylan (Alfa Chemistry, Protheragen Inc., USA,) and lignin (low sulfonate content) (Sigma-Aldrich, Canada Co.). The materials used in this work are a synthetic hydrolyzate and process water from a Canadian thermomechanical pulp mill. The synthetic hydrolyzate was prepared as a simulation of the original TMP hydrolyzate with respect to concentrations. The process water received from the mill was stored in a cold room at 4 C° to prevent hemicellulose degradation. TMP process water used in this study contains 0.75±0.133 g/L hemicellulose and 1.94±0.21 g/L lignin, and physical-chemical characteristics of TMP process water were detailed in Bokhary et al. (2018). After a dilute-acid hydrolysis

process of samples, polysaccharide turned into monosaccharide sugars in the form of galactose (0.478±052 g/L), arabinose (0.074±034 g/L), rhamnose (0.007±003 g/L), glucose (0.063±002 g/L), xylose (0.012±0.001 g/L), and mannose (0.114±0.013 g/L). The solid content in the TMP hydrolyzate was 3.3±0.14 g/L, and pH was 4.3±0.121. The average molecular masses of hemicellulose and lignin fractions in both thermomechanical pulp pill process water and synthetic hydrolyzate are given in Table 3.1. The extraction efficiency of hemicelluloses dissolved in the TMP process stream can be affected by the molecular mass fractions and the concentration of hemicelluloses in the process water.

The solvents, tributyl phosphate (TBP), 1-butanol, n-hexane, and toluene, were supplied by Sigma-Aldrich Canada Co., as analytical grade reagents and used as obtained without any further purification. Kerosene is also supplied by Sigma-Aldrich and employed as a diluent, and the ratio of diluent to solvent range 20/80, 40/60, and 50/50 (v/v %) was tested. Process water and synthetic solution were extracted, in duplicate, with (1) 1-butanol (2) toluene (3) TBP and (4) n-hexane under a variety of operational conditions (extraction time, solvent types and concentrations, process water to solvent volume ratio, and pH).

Table 3.1: The molecular mass distribution of hemicellulose and lignin in thermomechanical pulp pill process water and synthetic hydrolyzate

Fraction	TMP Process Water		Synthetic Hydrolyzate	
	Hemicellulose	**Lignin**	**Xylan**	**Lignin**
Number-average molecular weight (M_n) (kDa)	0.708	1.096	0.170	1.324
Weight-average molecular weight (M_w) (kDa)	3.806	1.851	0.236	2.370
Molecular mass range (kDa)	0.711 – 3.876	1.063 – 1.891	0.170 – 0.239	1.117 – 2.500
Polydispersity index	5.35	1.7	1.385	1.8

2.2. Equipment and extraction experiments

A batch extraction was performed for hemicellulose extraction. Solvent: hydrolyzate volume ratios in the range 1:1 to 1:6 were studied. The organic phase and aqueous phase were mixed in a beaker for 5 min at room temperature (24°) using a magnetic stirrer (300 rpm) and then charged in 250–500mL separating funnels as required, followed by 30 min waiting to reach the equilibrium state at 24 °C for separating of two phases (the aqueous layer from the organic layer). The aqueous model solution (synthetic hydrolyzate) was prepared by dissolving xylan and lignin in deionized water. The pH of the synthetic hydrolyzate was 9.3 and adjusted later at neutral and acidic with a small amount of HCL, or at alkaline values (with NaOH), and the pH of process water was 4.3 and adjusted later as required using NaOH. The extracting solvent was prepared by mixing kerosene in 1-butanol, toluene, TBP, or n-hexane. The diluent was used to improve the

extraction power of the extractant by providing specific interaction and solvation (Yang et al., 2013). After phase separation, the bottom being the raffinate phase and the top being the extract phase, samples from each phase were collected and analyzed immediately for sugar and lignin concentrations. Aqueous phases from extraction were used to determine residual lignin (by UV absorbance readings) and sugars (by Dionex ICS-5000 Ion Chromatography System). All experiments were performed in duplicate, and the average values were calculated.

2.3. Analytical methods

2.3.1. Hemicelluloses

Hemicelluloses quantification of TMP process water and synthetic hydrolyzate was measured by a Dionex ICS-5000 Ion Chromatography System (Thermo Fisher Scientific, Canada). This system was equipped with a CarboPac™ PA1 column and an electrochemical detector (ED) (Dionex-300, Dionex Corporation, Canada). Deionized water was utilized to generate an eluent with a flow rate of 1 mL/min, while NaOH with concentrations of 0.2 M and 0.5 M was used as a supporting electrolyte with a flow rate of 1 mL/min. The column temperature was set at 30 °C. Before the sugar measurement, polysaccharide of TMP hydrolyzate was converted to a monosaccharide, using a standardized method of dilute acid hydrolysis. Samples were hydrolyzed by adding 5ml of 4% (w/w) H_2SO_4 and oil bathed at 121°C for 120 min (Hakke S45, Instruments, Inc., Portsmouth, N.H., USA) as described in the literature (Liu et al., 2011). Then the monomeric sugars were analyzed via an ion chromatography system, and the total of these monosaccharides represents the concentration of sugar in the analyzed sample.

2.3.2. Lignin

For lignin content measurement, photometric measurements were performed using a GENESYS™ 10S UV-Vis Spectrophotometer at a wavelength of 280 nm according to Tappi UM 250. Before measuring light absorption, the samples were diluted using DI water, and the dilution factor was included in the final calculations. Also, the pH of each sample was adjusted (between7–8) with 0.025 M sodium hydroxide or 0.1 M HCl as required before the measurements for stabilizing the lignin network. At that point, the total lignin content was determined. It should be taken into consideration that when measuring the lignin content, pectin degradation products also have strong UV absorbance at 280 nm, and therefore the presence of these compounds can lead to an overestimation of the lignin concentration (Krawczyk et al., 2013).

2.3.3. Molecular mass distribution of hemicellulose and lignin

The molecular weight distribution of hemicellulose and lignin in feed samples were determined using a gel permeation chromatography (GPC) (Viscotek GPCmax, Malvern, UK), as described by Bokhary et al. (2018). GPC is equipped with multi-detectors that apply a 0.1 mol/liter sodium nitrate solution as eluent and solvent with a flow rate of 0.7 ml/min. Before measuring the molecular mass distribution, the samples were filtered using a 0.20-micron nylon filter to remove particles and suspended matter and prevent GPC

column clogging, and then the permeate solutions were used to determine the molecular weight. The columns of PolyAnalytic PAA206 and PAA203 were used in the analysis, and the column temperature was 35 °C. The UV detector, detecting at 280 nm wavelength, was used to determine the molecular weight of the lignin, and the refractive index detector (RI) was used to measure the molecular weight of hemicellulose, using polyethylene oxide (PEO) as standard.

2.3.4. Calculation

The concentration of hemicellulose in the extract phase was determined by mass balance, as shown in Eq. (1).

$$[Hemi]_{org} = \frac{([\text{hemi}]_{aq} * V_{aq})_{initial} - ([\text{hemi}]_{aq} * V_{aq})_{raffinate}}{(V_{org})_{aq}} \quad [1]$$

Where V_{aq} is the volume of the aqueous phase (mL), and V_{org} is the volume of the organic phase (mL).

The single-stage fractional recovery of hemicellulose is defined as the mass of hemicellulose recovered in the extract phase divided by the mass of hemicellulose initially present in the aqueous phase:

$$\text{Recovery } (\%) = \frac{([\text{hemi}]_{org} * V_{org})_{aq}}{([\text{hemi}]_{aq} * V_{aq})_{initial}} x100\% \quad [2]$$

The equilibrium distribution coefficient (K_D) was defined by the ratio of the Hemicellulose mass fraction of the organic phase ($[\text{hemi}]_{org} * V_{org}$) to that of raffinate phase ($[\text{hemi}]_{aq} * V_{aq}$), at the given stable condition (equilibrium). K_D is a measure of the difference in solubility of the compound in these two phases. Thus, large values for K_D are desirable since less solvent is required for a given degree of extraction. The K_D is defined in Eq. [3].

$$K_D = \frac{([\text{hemi}]_{org} * V_{org})}{([\text{hemi}]_{aq} * V_{aq})} \quad [3]$$

Where [Hemi] is hemicellulose concentration; subscript "org" denotes the hemicellulose concentration extracted from the aqueous phase in the organic phase, and subscript "aq" denotes the hemicellulose concentration remaining in the aqueous phase.

Extraction percent is a more common term used to express extraction efficiency, which can be measured by the equilibrium constant for the target solute's partitioning between the aqueous and organic phase. In this study, percentage extraction is defined as the percentage of hemicellulose removed from the aqueous phase into the organic phase in one extraction step, as shown in Eq.

$$Extraction\ \% = \left(\frac{[\text{hemi}]_{initial} - [\text{hemi}]_{final}}{[\text{hemi}]_{initial}}\right) x100 \quad [4]$$

Selectivity is a key parameter of the LLE technique, and for a single-stage extraction process can be defined as the amount of the desired product extracted compared to the amount of an unwanted by-product. The selectivity coefficient provides an indication of the solvent's ability to favor a particular solute over another from the feed stream and depends largely upon the properties of the diluent–solvent. In this study, the selectivity coefficient was defined as a ratio of the overall extraction coefficients of hemicellulose and lignin at the given stable condition (equilibrium):

$$Selectivity = \frac{K_{M_1}(hemi)}{K_{M_2}(lignin)} \quad [5]$$

where subscripts ($K_{M_1\,(\text{hemi})}$) and ($K_{M_2\,(\text{lignin})}$) refer to the hemicellulose distribution coefficient and lignin distribution coefficient at the given stable condition (equilibrium).

3. Results and Discussion

3.1. Extraction equilibrium

In this study, attempts were made to study the feasibility of SX technique for hemicelluloses recovery from process water of a thermomechanical pulp mill. The optimum conditions of extraction, represented in the solvents types, process water to solvent volume ratio, pH, and duration of the treatment, were investigated. The phase behavior of the hydrolyzate, when extracted with a suitable extracted solvent, is governed by the solvent's capacity to extract hemicellulose preferentially from the hydrolyzate. Extraction time is also a significant parameter for the feasibility of the extraction process, as prolonged operation times are not recommended for industrial applications. A typical method to obtain information about this capability and extraction times is by developing phase-equilibrium data for the process (Kislik 2012; Sheabarand and Neeman 1988). In the first part of the experiments, extraction equilibrium was established for the xylan-lignin-water (as a synthetic hydrolyzate). While 1-butanol, n-hexane, TBP, and toluene were used as solvents at room temperature (24 °C), to obtain preliminary information on the maximum hemicellulose extraction percent regarding extraction time in a single step. A series of equilibrium extraction experiments were performed using solvent: hydrolyzate volume ratios in the range of 1:1 to 1:6. Under all tested operating conditions, extraction equilibrium was reached in a few minutes, regardless of the solvent: hydrolyzate volume ratios used, as shown in Figure 3. 1–3. However, slight differences were observed in the extraction time of TBP; its extraction time was a little bit longer compared to others. Also, with respect to the concentration of lignin in the raffinate phase, a slight difference was observed in the pH value of 4.3 compared with neutral pH (Figure 3. 2–3). This result can be ascribed to the change that may occur in the solubilization characteristics of the lignin in the aqueous phase by modifying the distribution of the charge over the lignin surface. Another possible cause of the change in lignin concentration in the raffinate phase is the precipitation of the lignin at low pH. However, this change is not much pronounced for 1-butanol;

this can partly be explained by the solubility differences between the solvents used, where the solubility of 1-butanol in water is (7.45 % wt) (at 25-30 °C) compared to its counterparts TBP (0.039 % wt), n-hexane (0.00123 % wt), and toluene (0.0515 % wt). Contact times between 30 to 40 minutes were deemed sufficient and were selected for subsequent experiments because the final equilibrium point was reached at this period of time and no more extraction was possible. These results correlate the results obtained by Cruz et al. (1999) for systems of phenolic compounds -water- diethyl ether, but it should be noted that the extraction process depends on the characteristics and type of extracted biomass. In the present study, after equilibrium was established for the model solution, the original hydrolyzate was tested, and 1-butanol, n-hexane, TBP, and toluene were employed as solvents and kerosene as the diluent.

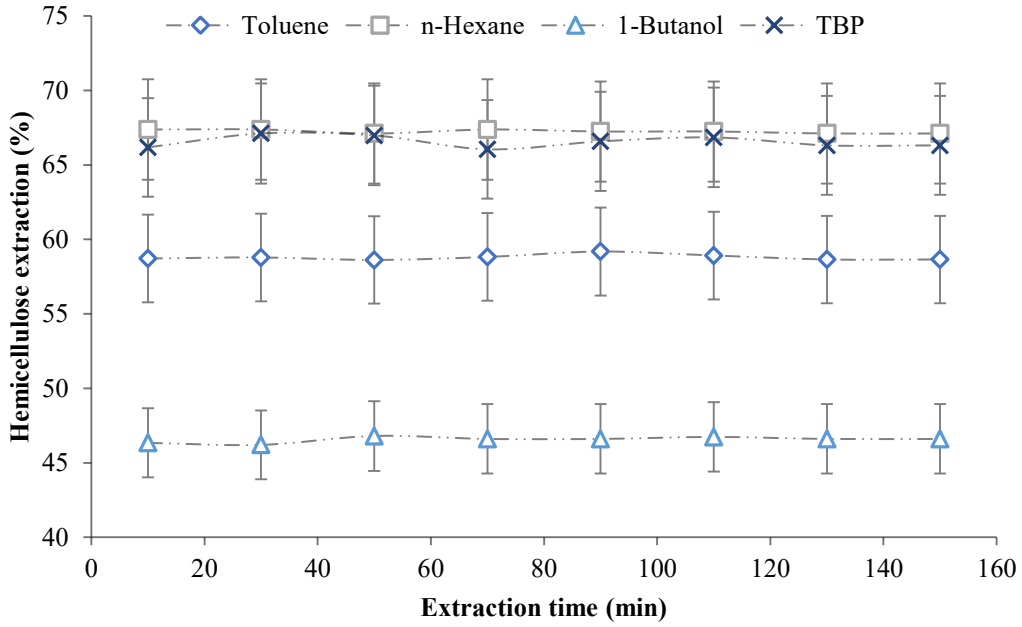

Figure 3.1: Effects of extraction time and solvent types on the hemicellulose extraction percent. Operational conditions: solvent/ diluent (50/50); solvent/hydrolyzate ratio 1:1; pH 7; room temperature 24°C; synthetic hydrolyzate. Each data point indicates the average value of the measured samples.

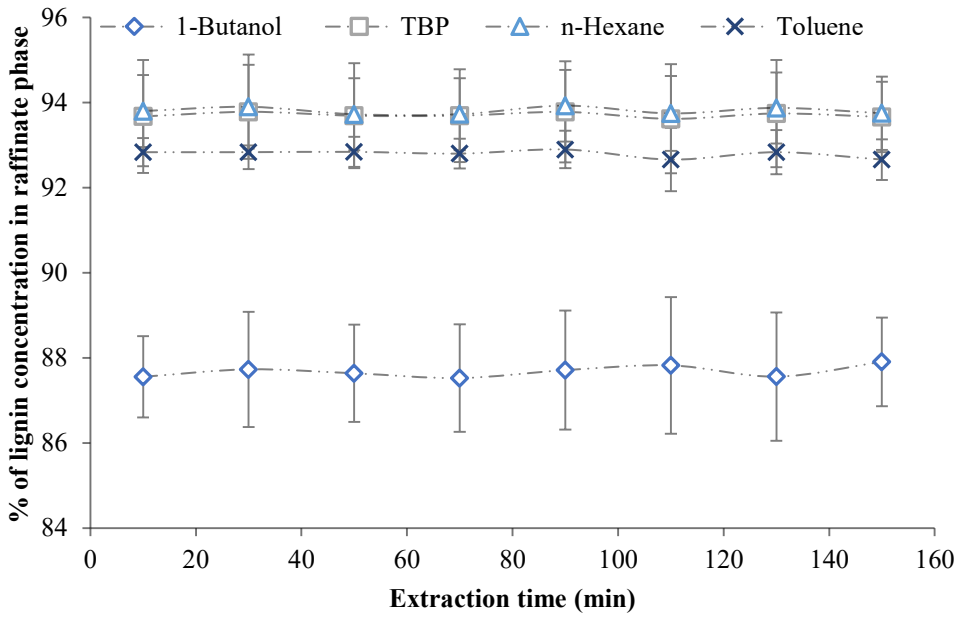

Figure 3.2: Effects of extraction time and solvent types on the extraction percent. Operational conditions: solvent/ diluent (50/50); solvent/hydrolyzate ratio 1:1; pH 7; room temperature 24°C; synthetic hydrolyzate. Each data point indicates the average value of the measured samples.

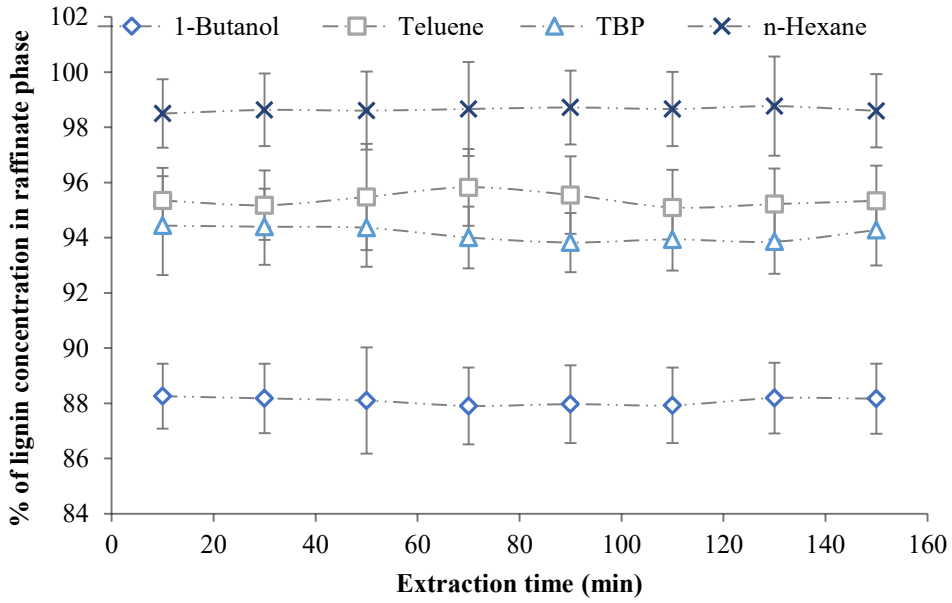

Figure 3.3: Effects of extraction time and solvent types on the extraction percent. Operational conditions: solvent/diluent (50/50); solvent/hydrolyzate ratio 1:1; pH 4.3; room temperature 24°C; synthetic hydrolyzate. Each data point indicates the average value of the measured samples.

3.2. Hemicellulose partitioning and selectivity

The extraction potentials of TBP, toluene, n-hexane, and 1-butanol for hemicellulose were compared. Solvents vary greatly in chemical and physical properties that affect their performance in the extraction of

hemicellulose. Accordingly, the hemicellulose distribution coefficient (K_D) showed some variation among the tested solvents. The variation in K_D can be attributed to the diversity in solvent properties because some organic solvents react directly with the treated compounds and extract them without the need for any additional extractant, while others do not. Also, K_D, of the extracted solute, is roughly equal to the ratio of its solubility in each phase (organic and aqueous). Thus, compounds that are slightly soluble in water but are highly soluble in organic solvents, they can be usably extracted for further valorization. Hemicellulose partitioning was between 0.8 and 2.5 for n-hexane and between 0.6 and 1.9 for toluene. Whereas, a partition coefficient of hemicellulose in the range of 0.6 to 1.6 and 1.2 to 2.6 was obtained in 1-butanol and TBP, respectively. These values indicate the extent to which hemicellulose and lignin can be partitioned into solvents in the single extraction process, and largely dependent on the solubility of hemicellulose and lignin. Consequently, the hemicellulose selectivity coefficient varied significantly among the tested solvents. However, n-hexane and toluene have shown a better affinity for hemicellulose over lignin. The average selectivity coefficients of n-hexane for hemicellulose over lignin was 7.3, 5.1, and 8.7 for pH values of 9.5, 7, and 4.3, respectively; while the average selectivity coefficient of toluene was 2.7, 2.7, and 2.9 for pH values of 9.5, 7, and 4.3, respectively. These solvents have also indicated low miscibility in aqueous solutions. The selectivity coefficient of n-hexane and toluene was statistically higher than a value of one. Using n-hexane in an SX process operating with multiple stages, a significant increase in the ratio of hemicellulose to lignin in the extract stream can be expected. Therefore, further studies on hemicellulose extraction in a multi-step system followed by hemicellulose stripping from the loaded organic phase and quantifying the sugars after their recovery from the strip solution via evaporation, or distillation or precipitation are recommended because the industrial-scale extraction typically involves more than one extraction stage and is usually performed on a continuous mode.

Other TBP and 1-butanol solvents exhibited a more limited ability to favor hemicellulose over lignin regarding selectivity coefficient (Fig. 3. 4 and 5). Tributyl phosphate and 1-butanol have average selectivity coefficients of 1.5, 1.2, and 0.8 for pH values of 9.5, 7, and 4.3, and 1.4, 1, and 1.3 for pH values of 9.5, 7, and 4.3, respectively. TBP favors extraction of both hemicellulose and lignin, which has resulted in an extract stream with an increased concentration of lignin and hemicellulose. Hence, if TBP would be used in the hemicellulose extraction from TMP hydrolyzate, it may complicate subsequent processes. Also, TBP is not a common industrial solvent and is, therefore, more expensive than the traditional solvents. This may constitute a barrier to economic viability. Whereas, 1-butanol showed a low extraction and selectivity level coupled with a water solubility issue. Therefore, the lack of selectivity for TBP and 1-butanol and miscibility concerns of 1-butanol may reduce the interest in their use for an improved liquid-liquid extraction process.

On the other hand, the target hemicelluloses are not freely available in the feed stream due to lignin-carbohydrate complexes (LCCs). These complexes can reduce the yield of hemicellulose in the extract phase and influencing the extraction efficiency. Thus, cleavage of lignin-carbohydrate complexes prior to the solvent extraction would be required to increase the yield and purity of hemicellulose. These complexes can be due to covalent linkages, hydrogen bonding, and carbon-carbon linkage between the lignin and hemicellulose. These intermolecular interactions can be affected by factors such as temperature and pH, and depend on the properties of the raw material.

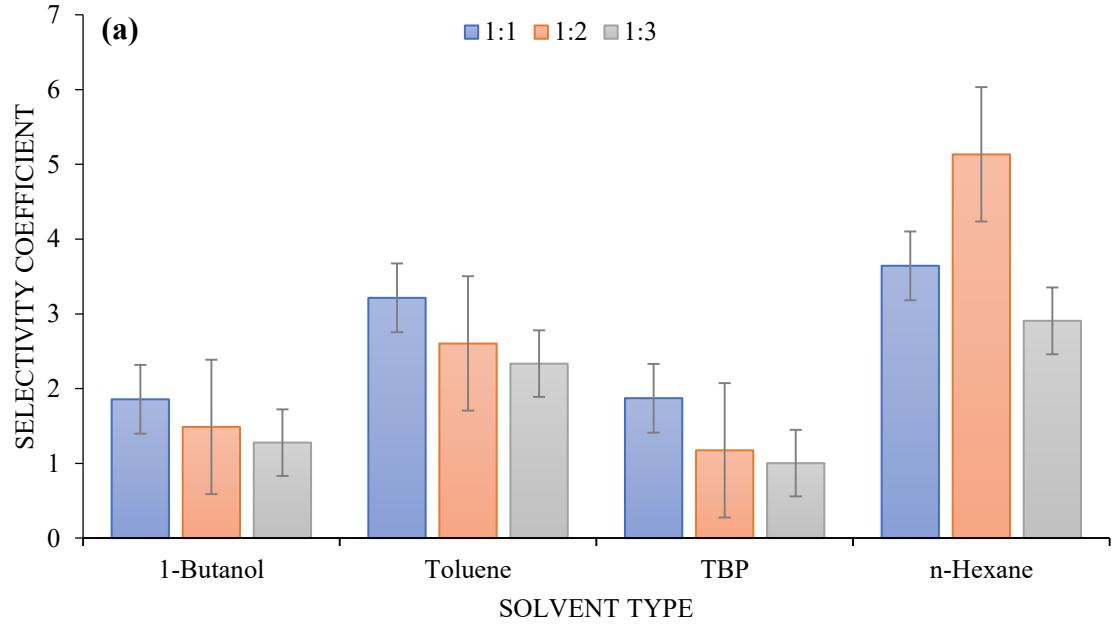

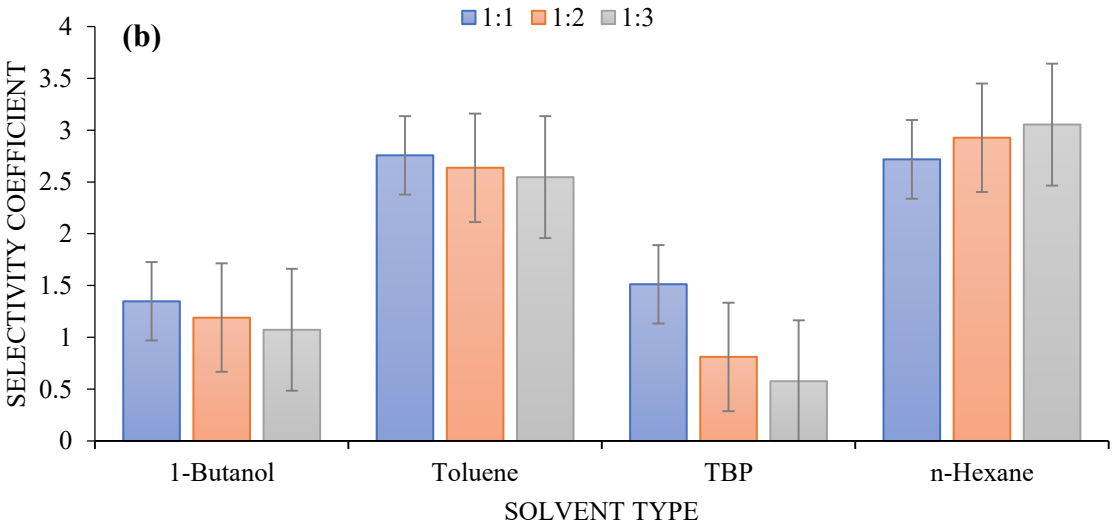

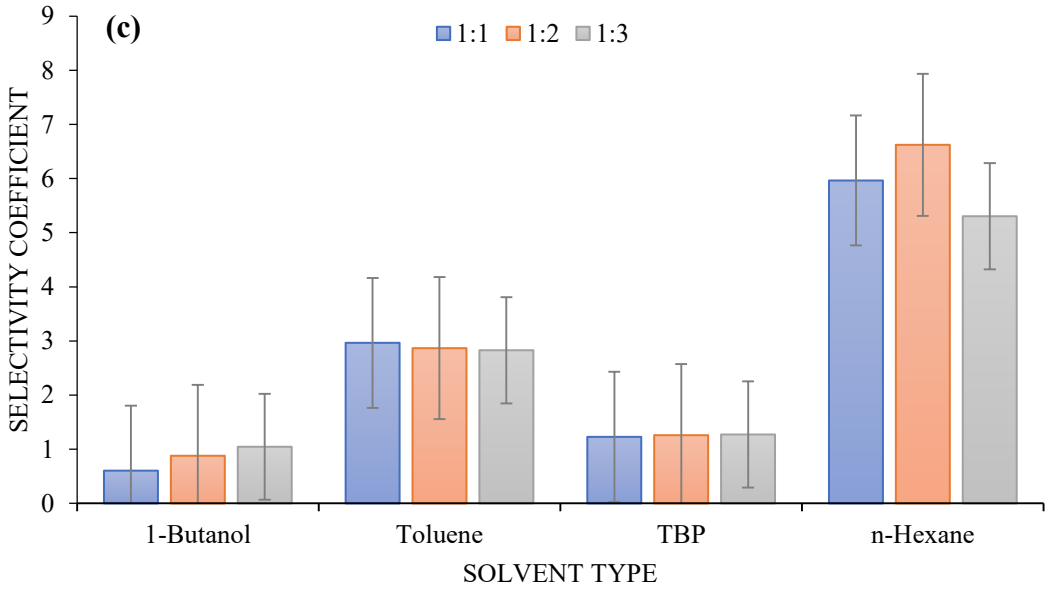

Figure 3.4: Selectivity coefficient for hemicellulose from process water at pH values of 9.5 (Fig. **a**), 7.0 (Fig. **b**), and 4.3(Fig. **c**), as the function of solvent types. Note extraction conditions: solvent: hydrolyzate volume ratio (1:1–1:3), room temperature, and contact time=30min. Each data point indicates the average value of the measured samples.

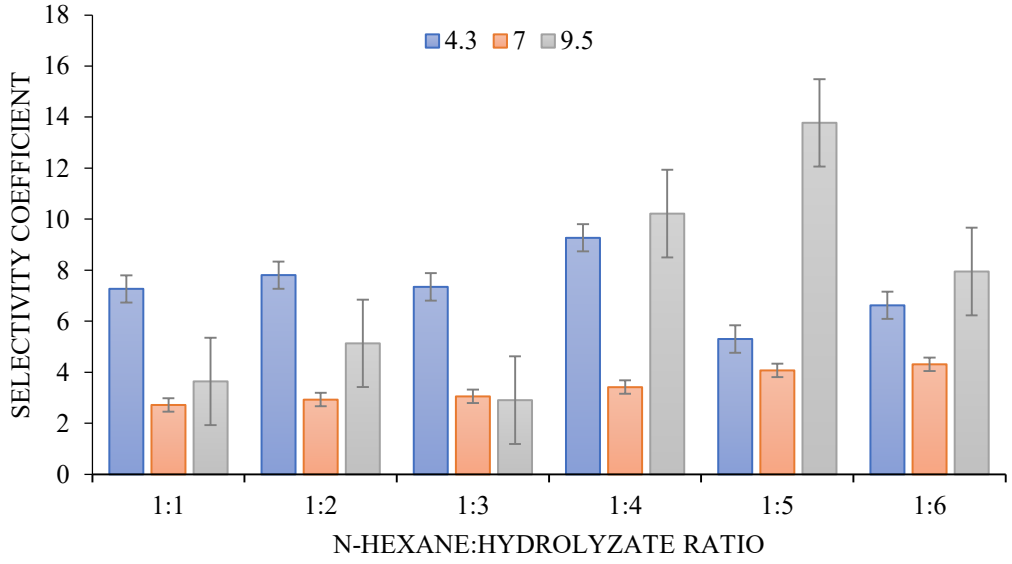

Figure 3.5: Selectivity coefficient of n-hexane for hemicellulose over lignin from process water as a function of pH values. Note: extraction conditions: pH 4.3, 7, and 9.5, room temperature, and contact time=30min. Each data point indicates the average value of the measured samples.

3.3. Hemicellulose extraction and influence of phase ratio

Figure 3. 6 (a–c) show the extraction efficiency of the different solvents for hemicellulose. A reasonable amount of hemicellulose can be extracted from hydrolyzate solutions containing concentrations of hemicellulose as low as 0.75±0.133 g/L using n-hexane and TBP as the extracting solvents. It should be noted that solvent concentration affects extraction percent of all tested solvents, except n-hexane is not showing any extraction differences whether a diluent was added or not. Solvent/ diluent volume (50/50) was best for toluene, TBP, and 1-butanol. From Fig. 3. 6 (a–c), it is evident that TBP extracts a considerable amount of the hemicelluloses. However, although TBP showed a high degree of extraction (Fig. 3. 6 (a–c)), its selectivity was low (Fig. 3. 4 and 5), this can be attributed to the fact that lignin and hemicellulose were extracted together in the organic phase. From Fig. 3. 6 (a–c), also it can be noticed that the extraction efficiency of the hemicelluloses was low for the 1-butanol under all tested conditions, 1-butanol also showed some degree of miscibility, especially in alkaline pH values. Figures 3. 6 (a–c) show the effects of the volume ratio (organic/aqueous) on the extraction hemicellulose. The change in solvent: hydrolyzate volume ratio led to a gradual increase in the hemicellulose extraction percent. The highest extraction percent was observed at 1:3 solvent: hydrolyzate volume ratio. It was shown that n-hexane and TBP could extract up to 71.03 and 72.34 %, respectively of the hemicellulose into the organic phase, while 1-butanol can extract 62.36% and 67.03 for toluene at a solvent: hydrolyzate volume ratio of 1:3. Overall, the optimum pH for extraction, phase ratio, and extraction time are at 4.3, 1:3 mL/mL and 30 min, respectively.

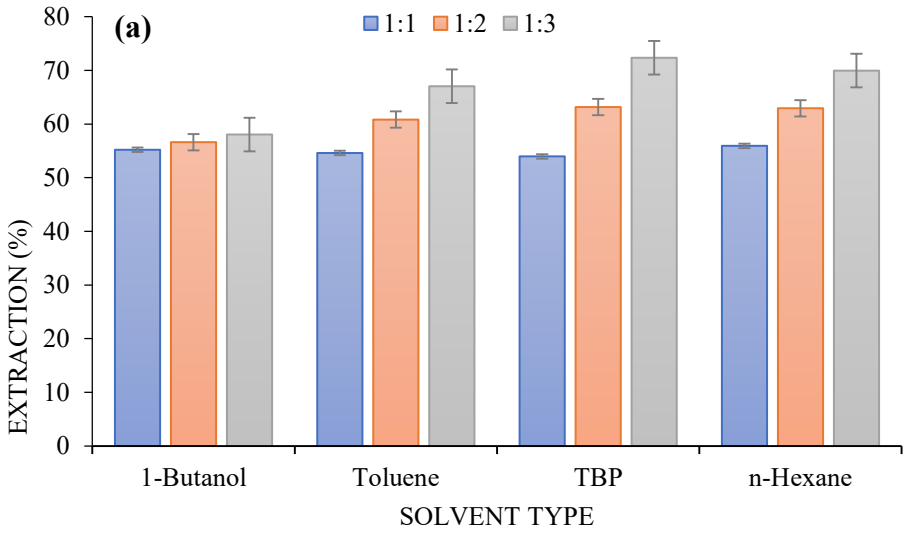

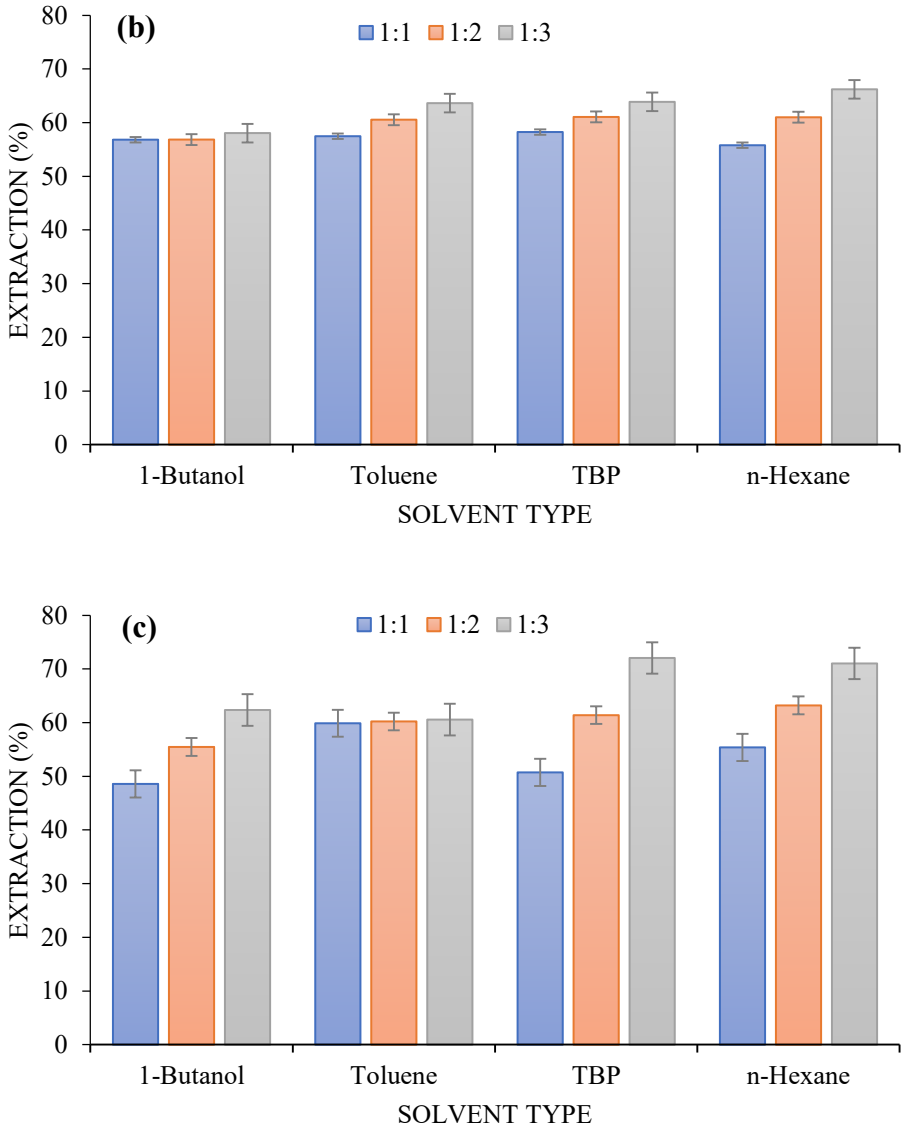

Figure 3.6: Extraction percent of hemicellulose of different solvents at pH values of 9.5 (Fig. **a**), 7.0 (Fig. **b**), and 4.3 (Fig. **c**). Note extraction conditions: solvent: hydrolyzate volume ratio (1:1–1:3), room temperature, and contact time=30min. Each data point indicates the average value of the measured samples.

3.4. Effect of pH on hemicellulose extraction

The liquid-liquid extractions of hemicellulose were performed at acidic (4.3), neutral (7) and alkaline (9.5) hydrolyzates conditions and room temperature for 30min in order to establish the effects of pH on the extraction efficiency. The pH value of the original process water is 4.3, and therefore it has been tested as it is. The effect of pH on extraction efficiency depends on the solvent tested (Figures 3. 4 and 5). The hemicellulose extraction efficiency of n-hexane was higher than the other selected solvents regardless of the pH used. However, for n-hexane, the highest

selectivity coefficients were measured at the lowest (4.3) and highest (9.5) pH values, with lower selectivity coefficients at neutral pH values (Figures 3. 4 and 5). Also, TBP has shown the same trend but with a minimal variation in selectivity coefficient. This experimental trend was similar to that reported by Cruz et al. (1999) for systems of phenolic compounds -water- diethyl ether operating at pH values of 3, 6.5 and 10 and by McPartland et al. (2012) for recovery of paclitaxel from plant cell cultures operating at pH values in the range of 4.0–8.0 using n-hexane and toluene. Also, liquid-liquid extraction data reported by Sheabar and Neeman (1988) for extraction of polyphenolics from the rape of olives using hexane, acetone, and ethanol operating at a pH value of 4 follow the same correlation with data given in this work.

For extractions in toluene, changing the pH had virtually no effect on selectivity, and selectivity coefficient values were between 2.3 and 3.2 for the entire pH range tested (Figure 3. 4 and 5). For 1-butanol, the selectivity coefficients were lower at the more acidic pH levels tested, with a measured value of 0.6, 0.9, and 1.04 for 1-butanol: hydrolyzate volume ratios of 1:1, 1:2, and 1:3, respectively. The varying selectivity coefficients are probably because of the change in extraction mechanisms (e.g., H-bonding or solvation), which are pH and solvent dependent. Figure 3. 5 shows the selectivity coefficient of n-hexane for hemicellulose from process water as a function of pH values.

3.5. Hemicellulose recovery

Figures 3. 7 (a–c) show the recovery of hemicellulose at different pH values. No significant difference was observed among tested solvents in the recovery of hemicellulose. Operating at a solvent: hydrolyzate volume ration of 1:3, the highest percent of hemicellulose recovery (71.9%) was achieved at a pH value of 4.3, in comparison with 68.6% at a pH value of 7 and 69.9% at a pH value of 9.5 for n-hexane. At the same volume ration, TBP achieved the highest percent of hemicellulose recovery (72.1%) at a pH value of 4.3, in comparison with 65.1% at a pH value of 7 and 72.2% at a pH value of 9.5. Of these results, it can be concluded that using an extraction system with multiple extraction stages may yield better results. The use of the extraction system with multiple extraction stages may also reduce the loss of extracted material, increase the extraction efficiency, and perhaps better extraction results can be achieved (McPartland et al., 2012; Gaddy and Clausen 1986). Figures 3. 8 (a–c) represent the percent of lignin concentration in the aqueous phase at different pH values.

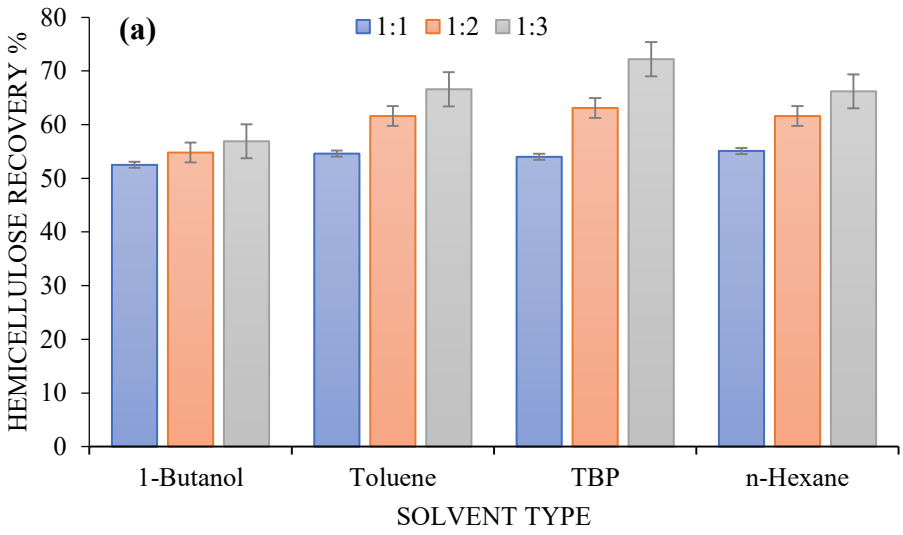
(a)
1:1
1:2
1:3
HEMICELLULOSE RECOVERY %
80
70
60
50
40
30
20
10
0
1-Butanol
Toluene
TBP
n-Hexane
SOLVENT TYPE

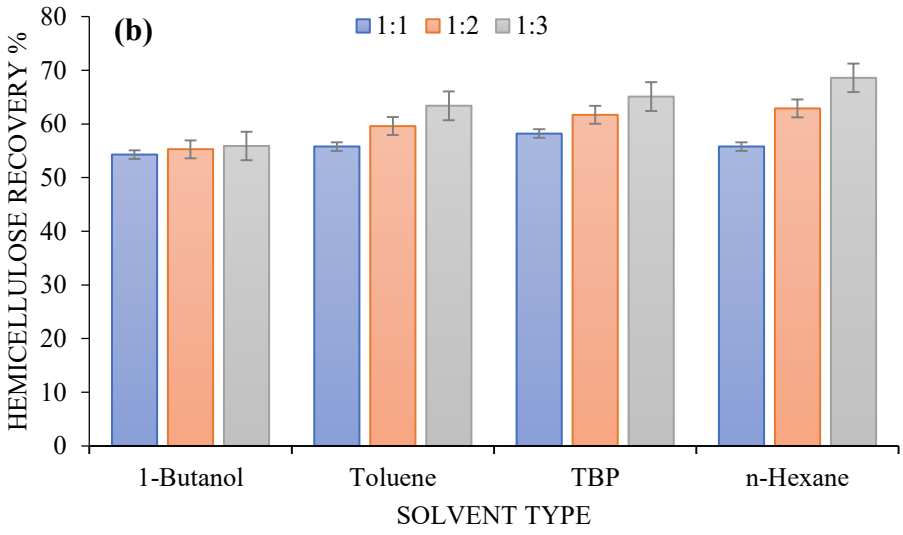
(b)
1:1
1:2
1:3
HEMICELLULOSE RECOVERY %
80
70
60
50
40
30
20
10
0
1-Butanol
Toluene
TBP
n-Hexane
SOLVENT TYPE

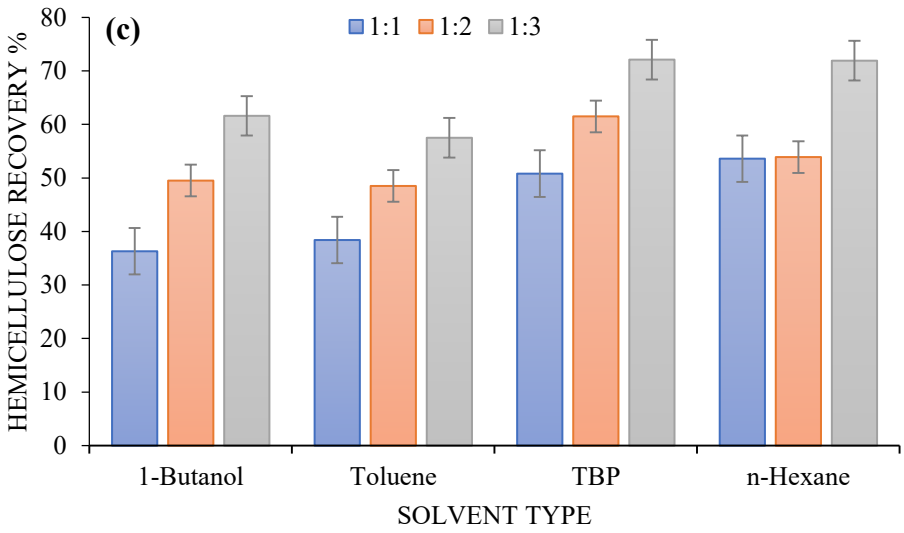

Figure 3.7: Hemicellulose recovery % of different solvents at pH values of 9.5 (Fig. **a**), 7.0 (Fig. **b**), and 4.3 (Fig. **c**). Initial feed concentration: 0.75±0.133 g/L, temperature: (approximately 24°C); extraction time: 30 min. Each data point is the average value of the measured samples.

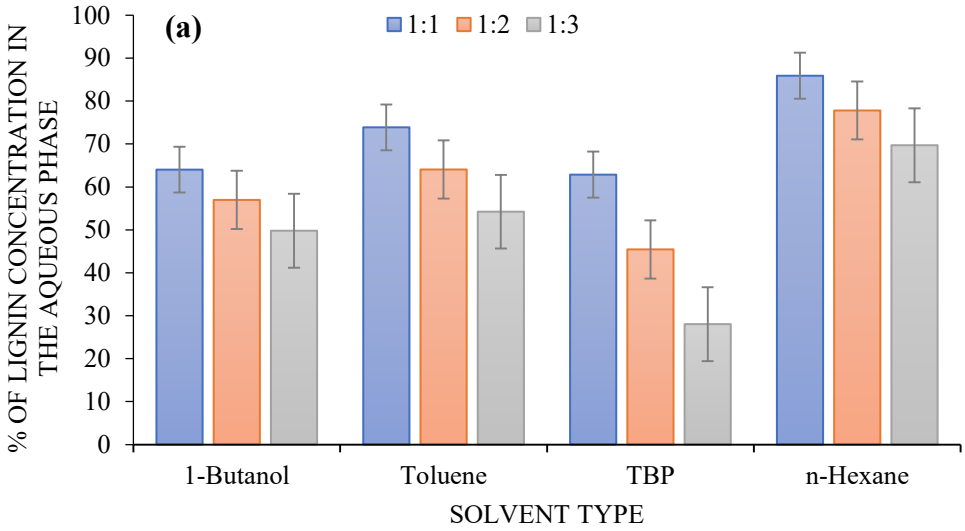

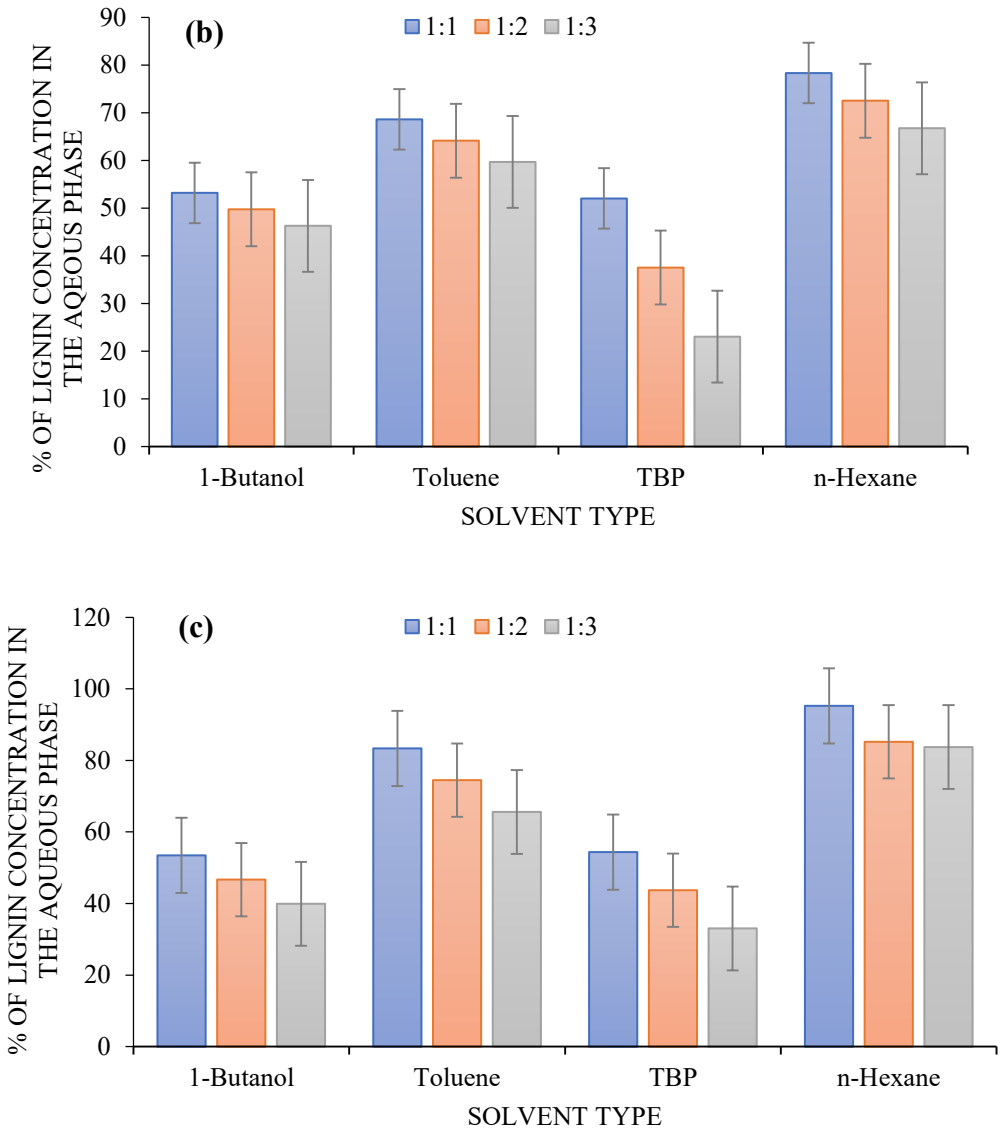

Figure 3.8: Percent of lignin concentration in the aqueous phase at pH values of 9.5 (Fig. **a**), 7.0 (Fig. **b**), and 4.3 (Fig. **c**). Note extraction conditions: solvent: hydrolyzate volume ratio (1:1–1:3), room temperature, and contact time=30min. Each data point indicates the average value of the measured samples.

4. Conclusions

The extraction potential of 1-butanol, toluene, TBP, and n-hexane were evaluated under a variety of operational conditions to determine their ability to extract hemicellulose from the process water of TMP. The liquid-liquid extractions were performed at different pH values (4.3, 7, and 9.5), at a room temperature of approximately 24°C and for 30min. Solvent: hydrolyzate volume ratios ranging from 1:1–1:6 were used. The tested solvents indicated different abilities to extract hemicellulose, and the effect of pH on hemicellulose extraction depends primarily on the solvent tested. For n-hexane, hemicellulose selectivity

coefficient of acidic and alkaline hydrolyzates was higher than the selectivity of the neutral hydrolyzate. Hemicellulose recovery showed relatively little increase with an increasing volume ratio of the aqueous phase. Among the solvents studied, the highest recovery percentages were obtained for n-hexane and TBP at 1:3 solvent: hydrolyzate volume ratio. Although tributyl phosphate (TBP) showed a high percentage of hemicellulose extraction, it was characterized by a low selectivity coefficient. To enhance the purity of hemicellulose, the selectivity of the extraction process can be improved by operating in a multistage process. Overall, the results indicate that n-hexane could be used as an extractant to separate hemicellulose from TMP process water because it gives not only the highest extraction rate but also the best selectivity.

Acknowledgments

This work was supported by the Ontario Graduate Scholarship (OGS) and the Natural Sciences and Engineering Research Council of Canada (NSERC). The helps of Dr. Pedram Fatehi and Dr. Weijue Gao at Lakehead University for hemicellulose and lignin measurements are highly appreciated.

References

[1] Pye, E.K., 2008. Industrial lignin production, and applications, in: Kamm, B., Gruber, P. R., Kamm M., (Eds.), Biorefineries-Industrial Processes and Products: Status Quo and Future Directions, Wiley-VCH Verlag GmbH, Weinheim, pp. 165–200. https://doi.org/10.1002/9783527619849.ch22.

[2] He, Y., Bagley, D.M., Leung, K.T., Liss, S.N., Liao, B.Q., 2012. Recent advances in membrane technologies for biorefining and bioenergy production, Biotechnol. Adv. 30, 817–858. https://doi.org/10.1016/j.biotechadv.2012.01.015.

[3] Norgren, M., Edlund, H., 2014. Lignin: recent advances and emerging applications, Curr. Opin. Colloid Interface Sci. 19, 409–416. https://doi.org/10.1016/j.cocis.2014.08.004.

[4] Bokhary, A., Liao B., Cui, L., Lin, H., 2017. A Review of membrane technology for integrated forest biorefinery, J. Membr. Sci. Res. 3, 120–141. https://doi:10.22079/JMSR.2016.22839.

[5] Saha, B.C., 2003. Hemicellulose bioconversion, J. Ind. Microbiol. Biotechnol. 30, 279–291. https://doi.org/10.1007/s10295-003-0049-x.

[6] Fišerová, M., Opálená, E., 2012. Hemicelluloses extraction from beech wood with water and alkaline solutions. Wood Res. 57, 505–514.

[7] Ji, X.J., Huang, H., Nie, Z.K., Qu, L., Xu, Q., Tsao, G.T., 2011. Fuels and chemicals from hemicellulose sugars. In: Bai, FW., Liu, CG., Huang, H., Tsao, G., (Eds.), Biotechnology in China III: Biofuels and Bioenergy. Advances in Biochemical Engineering Biotechnology, Springer, Berlin, Heidelberg, pp. 199-224. https://doi.org/10.1007/10_2011_124.

[8] Hongzhang, C., Liying, L., 2007. Unpolluted fractionation of wheat straw by steam explosion and ethanol extraction, Bioresour. Technol. 98, 666–676. https://doi.org/10.1016/j.biortech.2006.02.029.

[9] Mussatto, S.I., Fernandes, M., Roberto, I.C., 2007. Lignin recovery from brewer's spent grain black liquor, Carbohydr. Polym. 70, 218–223. https://doi.org/10.1016/j.carbpol.2007.03.021.

[10] Matsumoto, M., Ueba, K., Kondo, K., 2005. Separation of sugar by solvent extraction with phenylboronic acid and trioctylmethylammonium chloride, Sep. Purif. Technol. 43, 269–274. https://doi.org/10.1016/j.seppur.2004.11.010.

[11] Cruz, J.M., Domínguez, J.M., Domínguez, H., Parajó, J.C., 1999. Solvent extraction of hemicellulosic wood hydrolyzates: a procedure useful for obtaining both detoxified fermentation media and polyphenols with antioxidant activity, Food chem. 67, 147–153. https://doi.org/10.1016/S0308-8146(99)00106-5.

[12] Hameister, D., Kragl, K., 2006. Selective recovery of carbohydrates from aqueous solution facilitated by a carrier, Eng. Life Sci. 6, 187–192. https://doi.org/10.1002/elsc.200620906.

[13] Ouahid, S., Métayer, M., Langevin, D., Labbé, M., 1996. Sorption of glucose by an anion-exchange membrane in the borate form. Stability of the complexes and the facilitated transport of glucose, J. Membr. Sci. 114, 13–25. https://doi.org/10.1016/0376-7388(95)00162-X.

[14] Di Luccio, M., Smith, B.D., Kida, T., Borges, C.P., Alves, T.L.M., 2000. Separation of fructose from a mixture of sugars using supported liquid membranes, J. Membr. Sci. 174, 217–224. https://doi.org/10.1016/S0376-7388(00)00385-9.

[15] Olajire, A.A., 2010. CO_2 capture and separation technologies for end-of-pipe applications–a review, Energy, 35, 2610–2628. https://doi.org/10.1016/j.energy.2010.02.030.

[16] Liu, X., Fatehi, P., Ni, Y., 2011. Adsorption of lignocelluloses dissolved in prehydrolysis liquor of kraft-based dissolving pulp process on oxidized activated carbons, Ind. Eng. Chem. Res. 50, 11706–11711. https://doi:10.1021/ie201036q.

[17] Hassan, E.S.R., Mutelet, F., Moïse, J.C., 2013. From the dissolution to the extraction of carbohydrates using ionic liquids, RSC Adv. 3, 20219–20226. https://doi:10.1039/C3RA42640H.

[18] Mussatto, S.I., Santos, J.C., Ricardo Filho, W.C., Silva, S.S., 2005. Purification of xylitol from fermented hemicellulosic hydrolyzate using liquid-liquid extraction and precipitation techniques, Biotechnol. Lett. 27, 1113–1115. https://doi.org/10.1007/s10529-005-8458-8.

[19] McPartland, T.J., Patil, R.A., Malone, M.F., Roberts, S.C., 2012. Liquid-liquid extraction for recovery of paclitaxel from plant cell culture: solvent evaluation and use of extractants for partitioning and selectivity, Biotechnol. Prog. 28, 990–997. https://doi.org/10.1002/btpr.1562.

[20] Kontturi, A.K., Sundholm, G., 1986. The extraction and fractionation of lignosulfonates with long-chain aliphatic amines, Extraction, 40, 72–75. https://doi:10.3891/acta.chem.scand.40a-0121.

[21] Lisec, B., Radež, I., Žilnik, L.F., 2012. Solvent extraction of lovastatin from a fermentation broth, Sep. Purif. Technol. 96, 187–193. https://doi.org/10.1016/j.seppur.2012.06.006.

[22] Martins, S., Aguilar, C.N., Teixeira, J.A., Mussatto, S.I., 2012. Bioactive compounds (phytoestrogens) recovery from Larrea tridentata leaves by solvents extraction, Sep. Purif. Technol. 88, 163–167. https://doi.org/10.1016/j.seppur.2011.12.020.

[23] Li, M.F., Sun, S.N., Xu, F., Sun, R.C., 2012. Sequential solvent fractionation of heterogeneous bamboo organosolv lignin for value-added application, Sep. Purif. Technol. 101, 18–25. https://doi.org/10.1016/j.seppur.2012.09.013.

[24] Djas, M., Henczka, M., 2018. Reactive extraction of carboxylic acids using organic solvents and supercritical fluids: A review, Sep. Purif. Technol. 201, 106-119. https://doi.org/10.1016/j.seppur.2018.02.010.

[25] John Griffin, G., Shu, L., 2004. Solvent extraction and purification of sugars from hemicellulose hydrolyzates using boronic acid carriers, J. Chem. Technol. Biotechnol. 79, 505–511. https://doi.org/10.1002/jctb.1013.

[26] Ringena, O., Saake, B., Lehnen, R., 2005. Isolation and fractionation of lignosulfonates by amine extraction and ultrafiltration: A comparative study, Holzforschung, 59, 405–412. https://doi.org/10.1515/HF.2005.066.

[27] Birajdar, S.D., Rajagopalan, S., Sawant, J.S., Padmanabhan, S., 2015. Continuous predispersed solvent extraction process for the downstream separation of 2, 3-butanediol from fermentation broth, Sep. Purif. Technol. 151, 115-123. https://doi.org/10.1016/j.seppur.2015.07.037.

[28] Aziz, H.A., Kamaruddin, A.H., Bakar, M.A., 2008. Process optimization studies on solvent extraction with naphthalene-2-boronic acid ion-pairing with trioctylmethylammonium chloride in sugar purification using the design of experiments, Sep. Purif. Technol. 60, 190–197. https://doi.org/10.1016/j.seppur.2007.08.011.

[29] Bokhary, A., Esmat, M., Baoqiang, L., 2018. Ultrafiltration for hemicelluloses recovery and purification from thermomechanical pulp mill process waters, Desalin. Water Treat. 118, 103–112. https://doi.org/10.5004/dwt.2018.22641.

[30] Yang, G., Jahan, M.S., Ahsan, L., Ni, Y., 2013. Influence of the diluent on the extraction of acetic acid from the prehydrolysis liquor of kraft-based dissolving pulp production process by a tertiary amine, Sep. Purif. Technol. 120, 341–345. https://doi.org/10.1016/j.seppur.2013.10.004.

[31] Liu, Z., Fatehi, P., Jahan, M.S., Ni, Y., 2011. Separation of lignocellulosic materials by combined processes of pre-hydrolysis and ethanol extraction, Bioresour. Technol. 102, 1264–1269. https://doi.org/10.1016/j.biortech.2010.08.049.

[32] Krawczyk, H., Oinonen, P., Jönsson, A.S., 2013. Combined membrane filtration and enzymatic treatment for recovery of high molecular mass hemicelluloses from chemithermomechanical pulp process water, Chem. Eng. J. 225, 292–299. https://doi.org/10.1016/j.cej.2013.03.089.

[33] Kislik, V.S., 2012. Solvent extraction: classical and novel approaches, first ed., Elsevier, The Boulevard, Langford Lane, Kidlington, Oxford, UK.

[34] Sheabarand, F.Z., Neeman, I., 1988. Separation, and concentration of natural antioxidants from the rape of olives, J. Am. Oil Chem. Soc. 65, 990–993. https://doi.org/10.1007/BF02544526.

[35] Gaddy, J. L., Clausen, E. C., 1986. Method of separation of sugars and concentrated sulfuric acid, U.S. Patent No. 4,608,245. Washington, DC: U.S. http://www.freepatentsonline.com/4608245.html.

Chapter IV

Thermophilic anaerobic membrane bioreactor for pulp and paper primary sludge treatment: Effect of solids retention time on the biological performance

Abstract

Lignocellulosic biomass is a promising renewable feedstock for the production of bioenergy and platform chemicals; however, its use would not be economically viable without adopting effective transformation technologies. In this work, long-term anaerobic treatment (370 days) of pulp and paper primary sludge was performed by a thermophilic anaerobic membrane bioreactor (ThAnMBR) for the first time to investigate the effect of various solid retention times (SRTs) on biogas production and solids reduction ratios. The tested STRs (32-55 days) have shown varying biogas productivity, and it can be concluded that the longer the SRT, the higher is the biogas yield. At the optimum solids retention time of 55 d, an organic loading rate of 2.15±0.10 kg-TSS/L.d, and hydraulic retention time of 5 d, biogas yield of 153.8 m^3 biogas/ tonne $MLSS_{removed}$ was achieved with an average methane content of 56±4% and the solids reduction ratio ranged between 47% and 54.9%. Besides biogas yield, the quality of the permeates, solids reduction, and digestates characteristic/dewaterability changed by changing the SRT. The mixed liquor suspended solids concentrations and solids reduction increased with increasing SRT, while the effluent COD concentration and sludge dewaterability decreased. The Fourier Transform Infrared (FTIR) and X-ray photoelectron spectroscopy (XPS) findings exhibited that the digestate contains more lignin and cellulose than the other substances, while the nitrogen and carbon concentration decreased with increasing SRT.

Keywords: Pulp and paper primary sludge, Anaerobic digestion, Biogas production, Membrane bioreactor, thermophilic treatment.

---

1. Introduction

Due to population and economic growth, global energy demand is increasing rapidly. This demand is met by non-renewable fossil resources, which lead to higher greenhouse gas emissions to the atmosphere. Such a challenge entails adopting sustainable green energy, which requires a shift in the way we produce and use energy. Lately, lignocellulosic biomass has gained increased attention as a feedstock for the sustainable and feasible production of bioenergy and biomaterials. Several studies have focused on bioenergy production from lignocellulosic substrates (Sawatdeenarunat et al., 2015; Den et al., 2018) Lignocellulosic biomass contains carbohydrates that can be converted by biochemical processes into bioenergy. The structure of the lignocellulosic materials comprises chiefly of three polymers: cellulose, hemicelluloses, and lignin, along with a small portion of wood extractives. These polymers are not readily accessible by microorganisms of anaerobic degradation and fermentation processes due to their association with each other in a hetero matrix of various degrees. Therefore, a preprocessing step, to break the covalent bonds between them, de-polymerize lignin, and reduce cellulose crystallinity, is required (Bajpai 2016; Baruah et al., 2018). Among lignocellulosic materials, primary sludge from paper mills industry could have a high potential for bioenergy production due to its preprocessed biomass (pulping process), high content of organic substances (volatile solids), and water. Figure 4.1 shows the thermomechanical pulp mill production process and the subsequent wastewater treatment facility.

Among bioconversion processes, anaerobic digestion (AD), is very promising in terms of renewable energy production and reduced environmental footprint. AD technology is a commercial reality for a wide range of waste streams, including industrial, municipal, and agricultural waste. Various types of anaerobic bioreactors have been used such as an anaerobic filter, expanded granular sludge bed reactor (EGSB), up-flow anaerobic sludge blanket (UASB), and a modified anaerobic baffled reactor (MABR) (Bakraoui et al., 2020). Processes such as thermomechanical pulping use high temperatures during the wood processing, which can be recovered with a recovery boiler as clean steam, so AD operating at thermophilic temperature would be advantageous. Anaerobic treatment of pulp and paper (P&P) mill effluents could offer a broad spectrum of benefits from renewable energy production (biogas) to minimal emission of greenhouse gases if integrated into P&P biorefinery. Also, the produced digestate can be further processed to produce bioenergy or value-added products. However, the development of a suitable reactor design capable of effectively coping with recalcitrant biomass and selecting appropriate digestion conditions presents a major challenge in the digestion of the lignocellulosic material. Many researchers have investigated P&P sludge as a substrate for biogas generation for both types of sludges (primary/secondary sludges) and their mixture with or without pre-treatment (Bayr and Rintala 2012; Veluchamy and Kalamdhad 2017). However, reported results for anaerobic treatment of primary sludge (PS) are rare, and the use of PS as a bioenergy substrate is still in the research phase.

Karlsson et al. (2011) studied anaerobic degradation of dewatered P&P activated sludge under mesophilic conditions using CSTR reactors and reported CH_4 outputs of 120 m^3 CH_4/tVS for kraft pulping plant and180 m^3CH_4/t VS for the thermomechanical pulp (TMP) mill. Bayr and Rintala (2012) reported CH_4 yields in the range of 190–240 m^3CH_4/tVS_{fed} for primary sludge (PS) from a bleached kraft pulp plant, using CSTRs under OLRs of 1–1.4 kgVS/m^3 d and HRT of 16–32 d. Jokela et al. (1997) reported 45 m^3/t VS specific methane yield for PS from thermomechanical pulp mill by biochemical methane potential (BMP). Saha et al. (2011) achieved a methane yield of 0.05 ml/mg COD for co-digestion of (WAS) waste activated sludge and PS from bleached chemo–thermomechanical pulp (BCTMP) mill under thermophilic conditions using BMP. The methane potential of the pulp and paper sludges varied considerably depending on the mill pulping process, sludge types, and biogas production conditions. Also, these results indicated that the methane potentials of sludge produced in TMP, CTMP, and Kraft mills vary greatly. Literature survey indicates that most of the reported studies on anaerobic digestion of P&P mill sludges were carried out using BMP tests (batch assays) (Veluchamy and Kalamdhad 2017, Lopes et al., 2018; Bonilla et al., 2018) and very few studies were performed using conventional continuous stirred-tank reactors (CSTRs) (Bayr and Rintala 2012; Kinnunen et al., 2015; Ekstrand et al., 2016 ; Chatterjee et al., 2018).

In recent advances in the decoupling of HRT and SRT by incorporating a membrane into CSTRs reactors as AnMBRs have resulted in a significant advantage over conventional anaerobic treatment systems. This provided an opportunity to keep slow-growing anaerobic bacteria within the reactor, reducing the reactor footprint for subsequent treatment, and decrease HRT to a few days. Thus, AnMBR can play a major role in recovering energy from pulp and paper waste as it maintains the necessary biomass concentrations in the system and withstands fluctuations in organic loading rates (OLRs). AnMBRs have been operated either in the mesophilic or thermophilic range, and several findings have proven their high operational steadiness, high processing effectiveness, and firm biogas yield (Dvořák et al., 2016). Thermophilic membrane bioreactors were characterized by lower sludge yield and higher biodegradation kinetics [17]. However, due to limitations in reactor design and operating conditions, the use of AnMBRs in the P&P industry was restricted, as most of the currently installed anaerobic digestion reactors are designed to treat wastewater and not for lignocellulosic biomass (not solid-state digestion) (Paul et al., 2018). Adopting appropriate anaerobic reactor configuration and operating conditions could boost AD application in the P&P industry. In practice, OLR and SRT are the most frequently used parameters for dimensioning the reactor size of a CSTR Lin et al., 2011; Maleki et al., 2019). SRT adjustment has been shown to improve the biological performance of AnMBRs by controlling the concentrations of bacteria in the system, which is strongly correlated with the biodegradation kinetics. However, research needs to evaluate the impact of SRTs on the biological and membrane performance of AnMBRs remain. To the author's knowledge, there are no disseminated works on the treatment of P&P primary sludge using AnMBR, a relatively new technology. By carefully adjusting the SRT, among many other operating parameters, the anaerobic digestion may have the potential to enhance biogas production (Sawatdeenarunat et al., 2015) and reduce pulp and paper sludge.

The aims of this study were to evaluate the effect of SRTs on the biological performance of the thermophilic anaerobic membrane bioreactor (ThAnMBR) for P&P primary sludge treatment for biogas production and solids reduction. In particular, a long-term experiment was conducted to elucidate the influence of SRTs on biological and membrane performance during P&P primary sludge digestion. The biological performance of the ThAnMBR was the main focus of this study reported here.

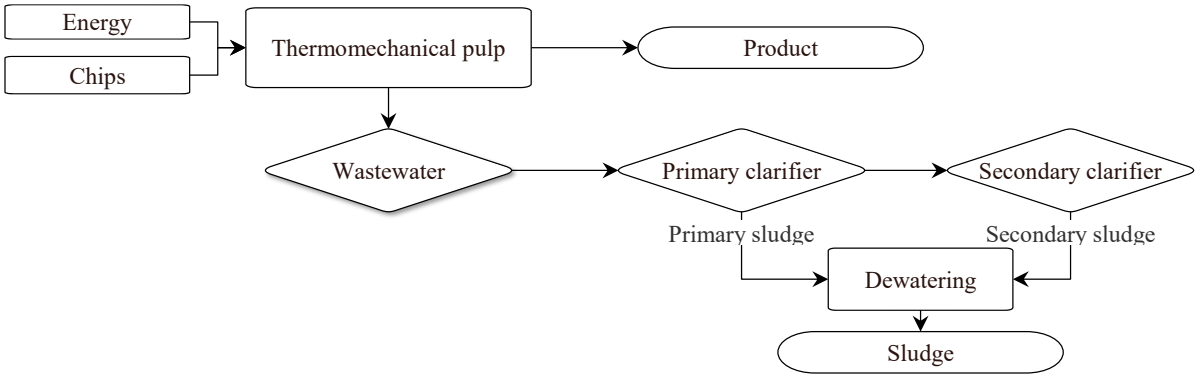

Figure 4.1: Material flow and wastewater treatment in the pulp and paper industry

2. Materials and methods

2.1. Feed and inoculum

Primary sludge from a primary clarifier of a local Canadian thermomechanical pulp mill was used as a substrate. Samples were collected in a 5-gallon plastic pail in the mill, after delivery to the laboratory, were stored at 4 °C before feeding the reactors. The sludge was mixed with a mixer (Sunbeam Corporation) after adding the required amount of tap water to facilitate the reactor feeding. A thermophilic inoculum was obtained from an anaerobic membrane bioreactor (AnMBR) treating P&P secondary sludge (Jiang 2018). Phosphorus and nitrogen were added to the feed in the form of dipotassium phosphate and ammonium chloride, in COD: N: P of 100:2.6:1 ratio to maintain nutrients concentration requirements for microorganisms' growth in an anaerobic digestion condition (Hamza et al., 2019; Lin et al., 2009). Pulp and paper sludges are generally characterized by low levels of trace minerals, nitrogen, and phosphorus, thus their biological treatment requires the addition of nutrients (Slade et al., 2004).

2.2. Laboratory scale submerged AnMBR setup and operation

Figure 4. 2 illustrates the experimental setup diagram used in this study. A submerged AnMBR comprising of a CSTR with a 6.5-liter active volume was operated in a semi-continuous fed laboratory-scale experiment to study the biogas production and solids reduction ratio from the P&P primary sludge. A PVDF (polyvinylidene fluoride) flat plate microfiltration (MF) membrane unit was employed in this study. It has an active surface area of 0.03 m^2 and a pore size of 0.1 μm (Shanghai SINAP Membrane Science & Technology Co., China). The membrane has two sides, and the dimensions of each side are 10cm x 15cm. The membrane unit consists of a plastic plate as support, two pieces of plastic mesh material as a barrier between the membrane and the plastic plate, and two rubber gaskets with two stainless steel frames to fasten the membrane and plate gasket together.

The reactor was operated at a thermophilic (50±1°C) temperature. The temperature was maintained by circulating hot water produced in an accompanying water bath (VWR international Inc. USA) through the bioreactor jacket. The Thermolyne Cimarec magnetic stirring instrument, Model S131435 (Barnstead

International, Iowa, USA) was placed at the bottom of the bioreactor to deliver the needed mixing that keeps biomass in suspension and maintains uniform reactor content. The reactor pH was maintained at 7.2 ± 0.1 using sodium hydroxide solution. The bioreactor was fed by a feed magnet pump (Iwaki co., LTD. Japan), and a constant slurry volume was maintained in the system by a water level sensor coupled with regulator device, as shown in the schematic diagram. A pressure gauge (Omega, spec. No.256099, Korea) was used to monitor the trans-membrane pressure (TMP). The system was purged with nitrogen gas for 5 minutes to establish an anaerobic environment after feeding it with the desired volume of inoculum and PS slurry. Also, nitrogen gas was utilized to get rid of the oxygen from the process at any time the bioreactor was opened to remove (at the end of phases) or to clean (when the TMP reaches a certain level) the membranes. Mixed liquor suspended solids (MLSS) samples were taken from the reactor through the lower sampling port for analysis and wasting.

Permeate from the system was withdrawn intermittently by a peristaltic pump (Masterflex C/L®, Cole-Parmer, Canada) and GraLab Timer model 451 (dimcogray.com, Ohio, USA), and it was gathered in its container for subsequent analysis. The timer was operated in 180 seconds on and 120 seconds off mode. To maintain the required permeability, the speed of effluent pump was accustomed, and calibration was performed as necessary. A 5 mL syringe was used for biogas sample injection in gas chromatography (Shimadzu, Model GC-2014) to determine biogas composition. The flat plate MF membrane module was submerged in the reactor, and its fouling was controlled by biogas sparging. This was achieved with a stainless steel tube distributor located below the membrane element on each side, and the produced gas was recirculated by two gas recirculation pumps (Masterflex Console Drive, Model 7520-40). The total biogas sparging rate of 3.76 ±0.08 L/min was fixed throughout investigations with the above-mentioned digital adjustable pump. To maintain the required SRT (32, 45, and 55 days), bioreactor sludge was withdrawn from the system once a day during the everyday measurements.

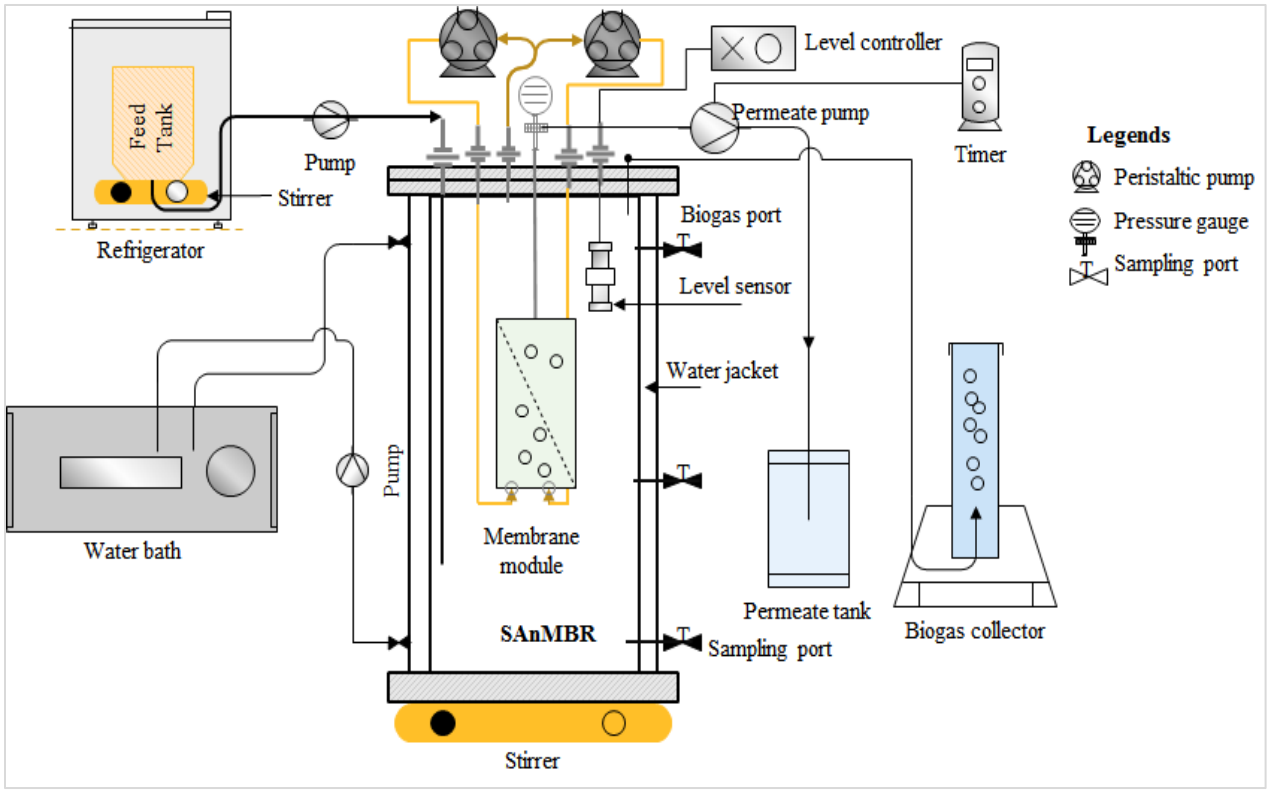

Figure 4.2: Schematic diagram of the SAnMBR process used in this study

2.3. Analytical methods

2.3.1. Primary sludge samples, reactor feeds, and inoculum

Table 4.1 exhibits the properties of PS and inoculum utilized in these studies. The amount of total solids (TS), volatile solids (VS), and fixed solids of the feed samples were measured based on the standard methods (Baird et al., 2017). Ash content of the oven-dry weight (ODW) of the sludge samples was determined after dry oxidation of the primary sludge at 575 °C by using a muffle furnace, equipped with a thermostat, as per standard biomass analytical methods (Sluiter et al., 2005). All measurements have done in triplicate and the outcomes were reported in relation to the oven-dried mass basis 105°C. pH was monitored by Oakton pH 700 benchtop meter (Singapore). Elemental analysis of carbon (C), hydrogen (H), nitrogen (N), oxygen (O), and sulfur (S) was performed by an elemental analyzer (Elementar Vario EL). Chemical oxygen demand (COD) was determined by HR COD test vials at high temperatures (using COD reactor, Hanna Instruments). The inoculum was evaluated for total solids, TSS, volatile solids, COD, ash, pH, and elemental component according to the beforehand determined protocols.

Table 4.1: Primary sludge and inoculum characteristics used in the digestion experiments.

Item	Unit	Primary sludge	Thermophilic inoculum
TSS	(g/L)	11.49±0.03	36.63±0.31
TS	(g/L)	11.68±0.63	39.62±0.43
VS	(%)	96.39±0.37	83.48±0.37
Ash	(%)	3.61±0.37	16.52±0.38
C	(%TS)	41.69±8.29	–
H	(%TS)	6.19±0.60	–
O	(%TS)	42.16±2.4	–
N	(%TS)	0.15±0.07	–
S	(%TS)	0.05±0.03	–
C/N		285.60	–
Feeding TCOD	(g/L)	19.99±1.82	47.66±1.04
Feeding sCOD	(g/L)	0.193±0.05	1.15±0.10
pH		7.2±1	6.99±0.030

2.3.2. Biogas production rate and composition measurements

The water displacement method was used to measure the biogas production rate. The biogas production rate was determined on a daily basis, while the biogas yield was calculated as weekly averages throughout the study period. For biogas composition analysis, 5 mL of biogas specimens were manually injected and analyzed for methane, carbon dioxide, and nitrogen content using gas chromatography (Shimadzu, GC-2014, Kyoto Japan). Specimens were withdrawn from the bioreactor headspace through the biogas sampling port and injected at room temperature for composition determination. The component of biogas (CH_4, N_2, and CO_2) was determined every two to three days during the experiment period.

2.3.3. Permeate quality and digestate characteristics measurements

The total COD of the effluent and feeding influent was determined per the standard procedures (Baird et al., 2017) using colorimetric approaches and COD test vials. The samples were quantified on a weekly basis. MLSS was analyzed to determine the total suspended solids concentration by passing the sample through a filter paper of 0.45 μm and drying it at a certain temperature for a specific time. Chemical element concentrations in the permeates were quantified by an inductively coupled plasma atomic emission spectroscopy (ICP-AES) elemental analyzer. The Bruker Tensor 37 FTIR (Fourier Transform Infrared) spectrophotometer and Axis Supra X-ray photoelectron spectroscopy (XPS) system (Kratos Analytical Ltd. Manchester, UK) was used to study structural changes and component decomposition of the PS after anaerobic treatment. The spectra of both XPS and FTIR were obtained from MLSS after freeze-drying of samples. In this study, spectra in the wavelength region between 4000 and 500 cm^{-1} were recorded by FTIR.

2.3.4. Digestate dewaterability

In the present study, the digestate dewatering was determined by Capillary Suction Time (CST), model 304 series (Triton Electronics Ltd., UK). All tests are performed according to the manufacturer's instructions, using Triton Electronics' CST filter and the 1cm sludge funnel. All tests were carried out in triplicate.

2.3.5 Statistical Analysis

The experimental results (MLSS, biogas composition, biogas produce, solids degradation ratios) from different SRTs were analyzed using Analysis of variance (ANOVA). The ANOVA test was done to find out the effects of the applied SRTs on the biological performance using alpha (α) = 0.05 for all statistical analysis carried out in this study.

3. Results and discussion

3.1. Biological performance

The biological performance of the system was studied by consideration of biogas yields, biogas composition, membrane permeate COD, and solids reduction. The tested SRTs were investigated under 5 days HRT. Table 4.2 displays the tested operating conditions of various phases of the SAnMBR.

Table 4.2: Operating conditions of SAnMBR

Phase	Duration (d)	Temperature (°C)	Average permeate flux L/m^2.hr.	Feed total COD (g/L)	Feed TS (g/L)	SRT (d)	HRT (d)	OLR (kg-TSS/L.d)
I	1 – 133	50±1	2.50±0.21	19.77±1.78	11.68±0.63	32	5	2.25±0.17
II	137 – 255	50±1	2.59±0.18	20.34±1.46	11.68±0.63	45	5	2.23±0.13
III	259 – 370	50±1	2.55±0.14	20.00±1.09	11.68±0.63	55	5	2.15±0.10

3.1.1. Biogas production and composition

Figure 4. 3 (a) - (d) shows the biogas production rate, biogas productivity based on the feed suspended solids, and cumulative (on a weekly basis) biogas yield based on MLSS removal, and biogas composition, respectively. Biogas productivity varied with the applied SRT, and from these results, it can be concluded that the longer the SRT, the higher is the biogas yield. Based on the ANOVA analysis, the differences in biogas yield were significant among the tested SRTs ($P<0.05$). Figure 4. 3-c displays biogas yield based on the MLSS removal over digestion time. The highest biogas production was 99.7 m^3 biogas/ tonne $MLSS_{removed}$ in the first phase, 134.2 m^3 biogas/ tonne $MLSS_{removed}$ in the second phase, and 153.8 m^3 biogas/ tonne $MLSS_{removed}$ in the third phase, corresponding to the SRTs of 32, 45, and 55 days, respectively. This indicates that changes in the SRT had a significant influence on biogas production. Treating primary sludge from the TMP mill, Jokela et al. (1997) reported a specific methane yield of 45 m^3/t VS_{added}. This difference can be attributed mainly to the membrane-CSTR integration that maintains a high concentration of microbes in the system. Under the applied SRTs, no major fluctuations in biogas yield were observed throughout the digestion period, indicating a stable biological performance and consistent biogas yield. After the

acclimatization period, biogas production was gradually increased, and the differences were pronounced clearly among the phases. When SRT increased from 32 days to 45 days, the biogas yield increased by 34.6% but when the SRT increased further to 55 days, the biogas production increased by only 14.6%. These results indicate that although a longer SRT normally gives enough time for microorganisms to digestate the substrate, there is an optimal SRT for improving biogas production.

Based on the literature, biogas production varies with different primary sludge sources. High biogas production was reported for the Kraft pulp process (KP), followed by CTMP, and TMP, respectively. Jokela et al. (1997) reported a CH_4 yield of 45 m^3/t VS $_{added}$ for the primary sludge from TMP in BMP. While Puhakka et al. (1988) achieved a biogas yield of 90 m^3/t VSS when studying the anaerobic treatment of a mixture of primary and secondary sludges from a CTMP mill under both mesophilic and thermophilic conditions in CSTR reactor experiments. Bayr and Rintala (2012) reported biogas production of 210-230 m^3 CH_4/t VS $_{added}$ for the primary sludge from a bleached kraft process in batch experiments, which is much higher than that reported in both CTMP and TMP sludge. This variation could be due to different pulping processes and digestion conditions. In TMP, wood chips are treated with pressurized steam before and during the refining process, where a reduced amount of woody material (2-5%) is dispersed as colloidal particles in the wastewater (Bokhary 2017). Whereas, the KP process involves cooking wood chips with white liquids, which consist of a hot mixture of water, NaOH, and Na_2S, as active ingredients. During cooking, part of the lignin and hemicelluloses are dissolved in the black liquor, and the wood fibers are liberated to form the solid pulp (around 50% by weight of the dry wood chips) (Ekstrand et al., 2013). CTMP works on the same basic principle as TMP but in CTMP, the refining phase is preceded by impregnation where the wood chips are chemically treated by sodium sulfite (Smook 2016). Consequently, increased methane production from kraft mill sludge can be explained by the fact that the sludge from KP mills mostly contains more dissolved substances, which are more easily digestible compared to CTMP and TMP sludge.

Compared to PS, waste activated sludge (WAS) of the P&P industry is likely more amenable to AD. Karlsson et al. (2011) studied methane production potential of WAS from different mills in batch experiments under mesophilic conditions (35 °C) and reported methane yields 89–197 m^3 CH_4/t VS_{added} for TMP mill and 145–188 m^3 CH_4/t VS_{added} for the kraft pulp mill. However, Bayr and Rintala (2012) reported a lower methane yield 50–100 m^3 CH_4/t VS_{added} for the Kraft mill WAS in batch experiments compared to primary sludge 210-230 m^3 CH_4/t VS $_{added}$. The lower biogas yield for WAS can be elucidated by the partial decomposition of the organic matter in the SS in the aerobic activated sludge process, along with the SS containing a large amount of lignin, a poorly biodegradable compound, and inhibitor of microorganisms on the other hand.

Figure 4. 3-d reveals biogas composition versus operating time. The biogas produced has a total average methane content of 56 ± 4%, a carbon dioxide content of 30.8 ± 3.6%, and nitrogen content of 12 ± 5.4%. No noteworthy differences in the biogas composition were detected amongst the phases during steady-state conditions. The average methane content was 54.2% in the first phase, 58.74% in the second phase, and 56.17% in the third phase. The value of the methane content in this study is to some extent identical to or in line with the value (56–57%) reported by Puhakka et al. (1992) for the activated sludge from a bleached kraft pulp mill. Similarly, Karlsson et al. (2011) reported methane content of around 56% for activated sludge from six different pulping processes. Given the heating value of approximately 22,400 kJ/m³ for the methane content of 60% resulting from anaerobic digestion (Turovskiy and Mathai 2006) the produced biogas can be used in one of two biogas uses heating and electrical generation.

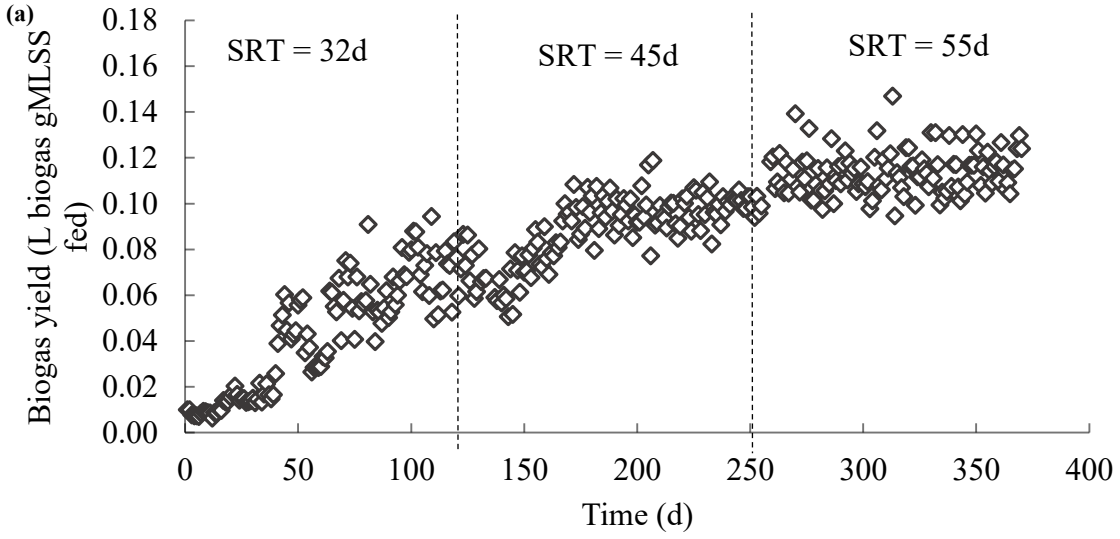

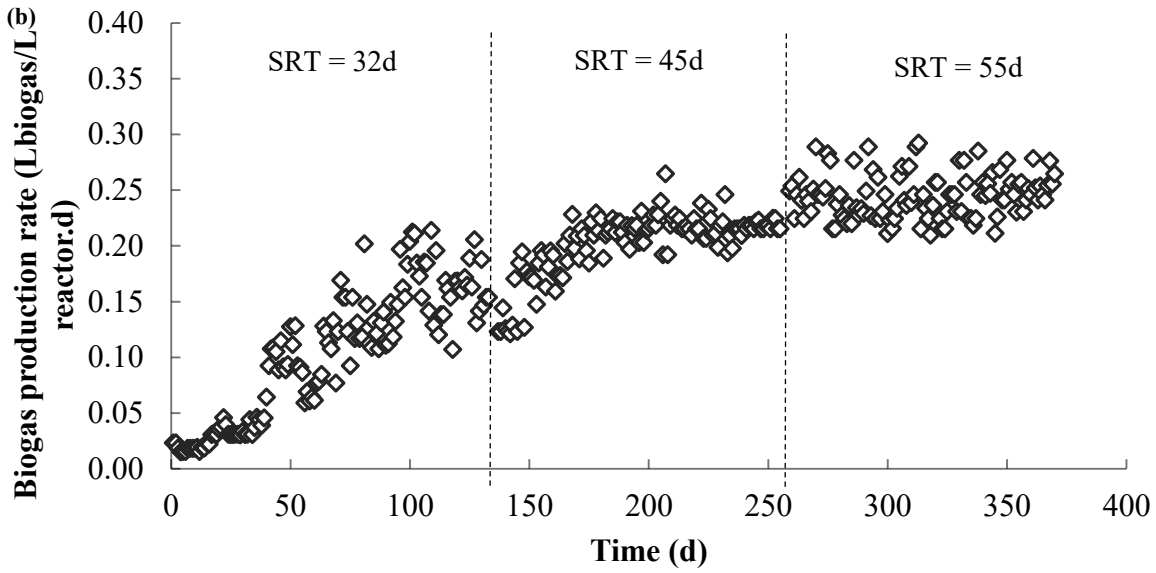
(b)
Biogas production rate (Lbiogas/L reactor.d)
0.40
0.35
0.30
0.25
0.20
0.15
0.10
0.05
0.00
SRT = 32d
SRT = 45d
SRT = 55d
0
50
100
150
200
250
300
350
400
Time (d)

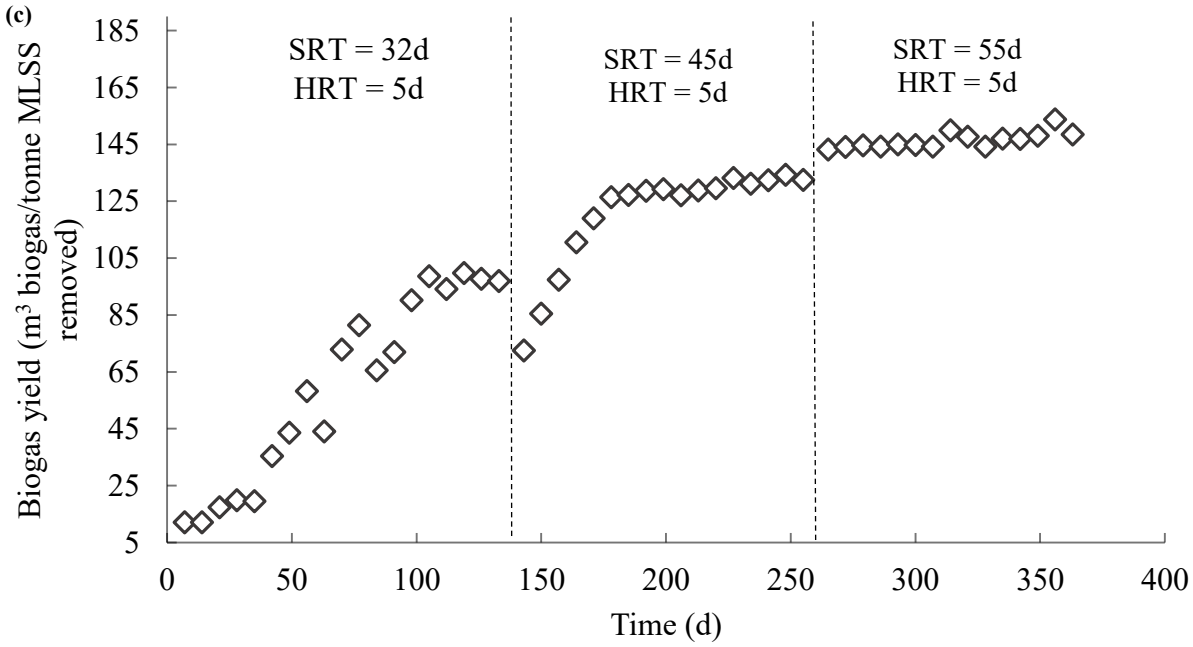
(c)
Biogas yield (m3 biogas/tonne MLSS removed)
185
165
145
125
105
85
65
45
25
5
SRT = 32d
HRT = 5d
SRT = 45d
HRT = 5d
SRT = 55d
HRT = 5d
0
50
100
150
200
250
300
350
400
Time (d)

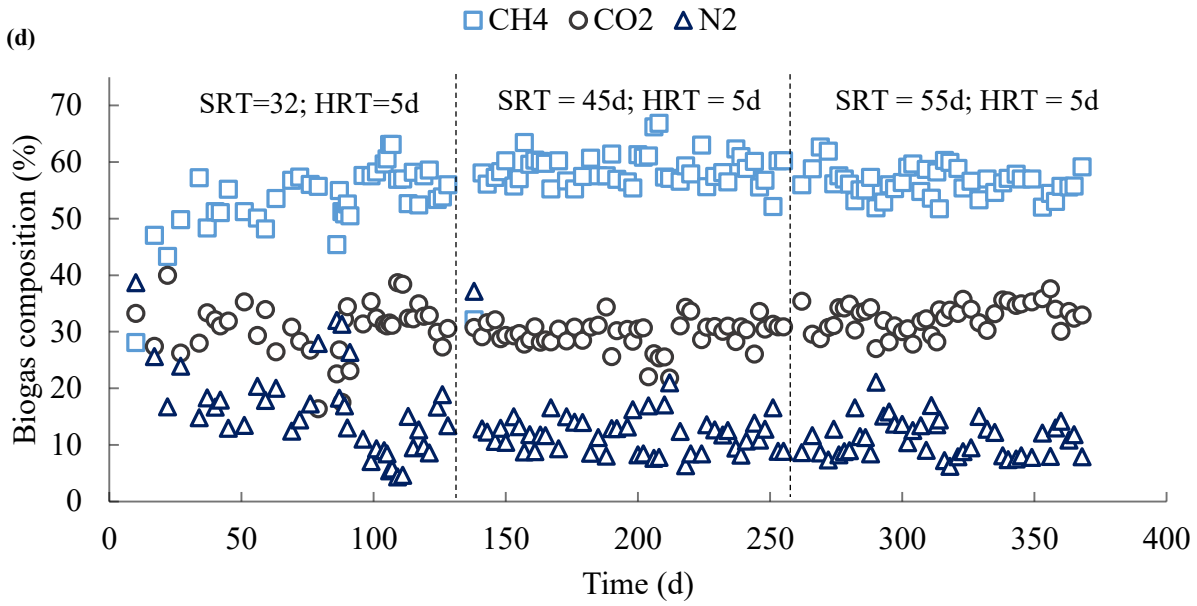

Figure 4.3: (a) daily biogas production rate (b) biogas yield based on the added feed suspended solids (c) biogas yield per m^3 MLSS removed (d) biogas composition over the operating time.

3.1.2. **Permeate quality and digestates characteristics**

3.1.2.1. Permeate quality

Figure 4. 4 displays effluent COD and pH value under the tested STRs during the digestion period. The average influent total COD concentration (including the primary sludge equivalent COD) was 19.99±1.82 g/L and the influent soluble COD (excluding the primary sludge) was around 192.8±47.4 mg/L, while (effluent) permeate COD value fluctuated between 2.40±0.79 g/L and 0.390±0.14 g/L. As can be seen in Fig.4.4, the effluent COD concentration decreased with increasing operating time, but, after phase I, the effluent COD became relatively stable for the rest of the experiment. This can be attributed to the increased cell concentration in the system and its acclimatization, which are associated with better biological performance and more organic materials degradation. Choo and Lee (1996) attributed COD's fluctuation in the early stage to inoculum acclimation to the new environment, but after the acclimatization period, the effluent SCOD remained fairly stable throughout the experiment period. On the other hand, this change can be attributed to the narrowing of the membrane pores over time as a result of the accumulation of some particles on them, which led to an enhanced rejection. Reduced pore size means less organic matter that passes through them, which decreases the permeated COD concentration. Many researchers have associated lower COD concentrations in the effluent with the narrowing of membrane pores due to fouling (Choi and Ng 2008).

The higher permeate soluble COD (0.39-2.4 g/L), as compared to the influent soluble COD (0.13-0.26 g/L), indicate that some lignocellulosic primary sludge was biologically hydrolyzed and released to the aqueous phase. However, some of the released compounds in the aqueous phase were not biodegradable or were recalcitrant compounds which contributed to the increase in permeate soluble COD. This is further evidenced by the color change of the permeate (Humpert et al., 2016), which suggests the presence of lignin from the hydrolyzed lignocellulosic primary sludge.

Table 4.3 displays the concentration of chemical elements in the effluent. As reported in Table 4.3, the permeates had much-reduced element concentrations and the values for most of the elements did not vary with operating conditions except phosphorus, sulfur, sodium, and potassium. The phosphorus concentration was higher in the first operating conditions compared to the second and the third conditions whose concentrations were very close. The sulfur concentration was close in the first and second phases but was very low in the last phase. Whereas sodium and potassium showed a similar trend, their concentrations were significantly low in the second and third phases compared to the first phase.

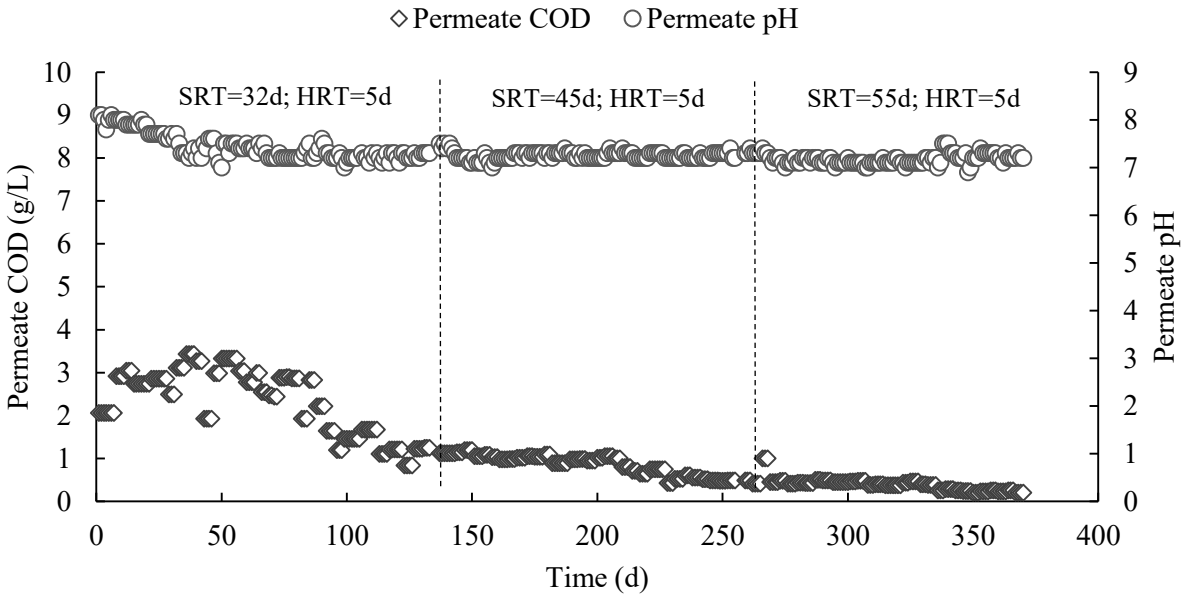

Figure 4.4: Effluent COD and pH over digestion time.

Table 4.3: Effluent characteristics at different SRTs

Description	Minimum detection limit (MDL)	Permeate characterization at different SRTs		
		32d	45d	55d
Macronutrients (mg/L)				
Phosphorus	0.05	166	74.53	78.8
Sulfur	0.3	37.37	32.77	6.3
Micronutrients (mg/L)				

Iron	0.005	0.046	0.048	0.085
Cobalt	0.002	0.0023	< 0.002	< 0.002
Nickel	0.03	< 0.03	< 0.03	< 0.03
Zinc	0.001	< 0.002	0.0017	0.0013
Copper	0.002	0.022	0.026	0.003
Manganese	0.001	0.02	0.039	0.045
Molybdenum	0.05	< 0.05	< 0.05	< 0.05
Selenium	0.05	< 0.05	< 0.05	< 0.05
Common cations (mg/L)				
Sodium	0.03	431.33	320.67	315.33
Potassium	0.5	300.33	124.67	114.53
Calcium	0.01	12.2	12.2	9.23
Magnesium	0.01	5.44	3.77	2.79
Lead	0.03	< 0.03	< 0.03	< 0.03
Aluminium	0.03	< 0.03	< 0.03	< 0.03
Barium	0.04	< 0.04	< 0.04	< 0.04
Chromium	0.002	< 0.002	< 0.002	< 0.002
Tin	0.05	< 0.05	< 0.05	< 0.05
Strontium	0.01	0.013	0.01	0.013
COD (mg/L)		2302±167	863±122	389.62±139
pH		7.4±0.3	7.3±0.08	7.2±0.1

3.1.2.2. Digestates characteristic

3.1.2.2.1. MLSS

Figure 4. 5 shows MLSS and feed suspended solids concentrations under different SRTs applied during digestion time. MLSS is a mixture of biologically active bacteria and a treatment substrate (primary sludge) and can, therefore, be reused to produce energy (e.g., biogas) or soil conditioner. In this study, the MLSS concentration was varied between phases. Based on the ANOVA analysis, there is a remarkable effect of SRT on MLSS concentrations (ANOVA, $p < 0.05$). The MLSS concentration increased with an increase in SRT and ranged between 18 and 29 g/L in the total experiment. In the first phase, 200 mL of sludge was wasted daily and the MLSS was maintained between 18–21.6 g/L at SRT of 32 days, while in the second phase, 144 mL of sludge was wasted daily and the MLSS was maintained between 21–26.5 g/L at SRT of 45 days. In phase 3, the MLSS was in the range of 26.4 – 29 g/L at SRT of 55 days and wasting amount of 118 mL. The increase in MLSS with an increase in SRT is expected, as less sludge is wasted at higher SRTs. It should be noted that all the phases were operated at a HRT of 5 days. In the literature, the reported MLSS concentration for the AnMBRs varies among the treated feed. However, compared to conventional reactors, AnMBRs have a higher MLSS concentration due to the retaining of the biomass by the membrane (Bokhary et al., 2020). High MLSS concentration may enhance the digestion process which could lead to improved effluent quality, reduced waste sludge production, and small bioreactors size (Bokhary et al., 2020). On the other hand, higher MLSS concentrations may cause reduce biogas sparging efficacy and membrane fouling.

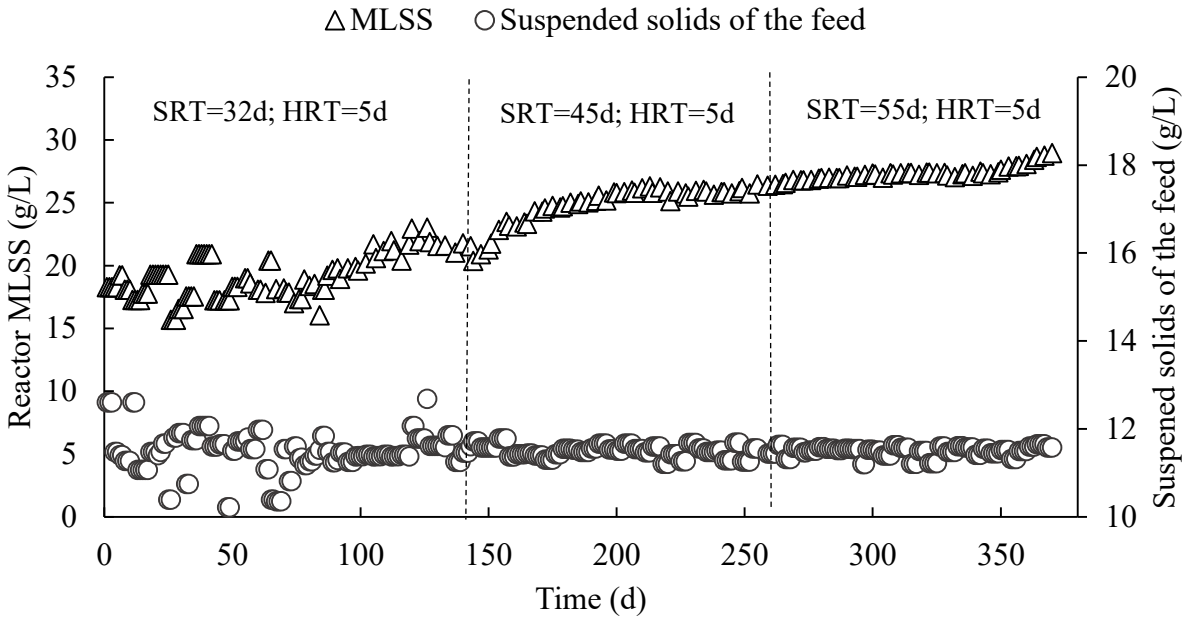

Figure 4.5: MLSS and feed suspended solids concentrations in different applied SRTs over operating time.

3.1.2.2.2. Digestate composition analysis

3.1.2.2.3. FTIR and XPS

FTIR was utilized to examine changes in cellulose structures and lignin properties after anaerobic digestion. Figure 4. 6 shows the variations of the FTIR spectra of feed and digestates of primary sludge at different SRTs. These results demonstrated that there was spectra variation around 3321 cm^{-1}, which represents a functional group of cellulose O-H, and about 1265 cm^{-1}, which represents a functional group C-O of lignin. Thus, these results indicate that the digestates contain more cellulose and lignin than the other compounds. This agreed with the previous studies. Elsayed et al. (2018) studied the structural changes of lignocellulosic material, attributing the peak near 3422 cm^{-1} to O–H stretching and linked it with the presence of cellulose in the samples. Whereas, Zhao et al. (2016) associated the band position at wavelength numbers of 3400 cm^{-1} with the O–H stretching of the cellulose functional group, whereas the band position at 1320 cm^{-1} and 1268 cm^{-1} linked to C-O stretch of guaiacyl and syringyl lignin, respectively. In this study, the intensity of these absorbance peaks increases at 3321 cm^{-1} with increased digestion time, possibly due to the digestion of other substances like hemicellulose, while the lignin remained as a result of its recalcitrant properties. Yue et al. (2010) reported that pretreated AD fiber (digestate) has better enzymatic digestibility compared to switchgrass, it produces 51 g/L glucose at a 90% conversion rate and has a 72% ethanol yield. This indicates that digestate of primary sludge can be a potential substrate for bio-ethanol production in light of recent developments in AD biorefinery due to its high cellulose content. Figure 4. 6 indicates C-O moved

from 0.96 to 0.90 and O-H moved from 0.99 to 0.97 compared with that of the feed. The above findings were proven by Lin et al. (2011), who reported 25% cellulose reduction efficiency and 5% lignin removal when co-digested PPM sludge and monosodium glutamate waste liquor under mesophilic conditions. Figure 4. 7 displays XPS spectra of the N, C, and O of MLSS samples and the binding energy. As can be seen from Fig.4. 7, the N concentration was significantly high in the first phase compared to the second and third phases. The nitrogen concentrations reduced with increasing digestion time possibly due to the increased concentration of microorganisms that consumed most of the available nitrogen. Also, the carbon was remarkably reduced in the third operating conditions compared to the first and second conditions, which may reflect the conversion of the organic carbon to biogas due to longer SRT.

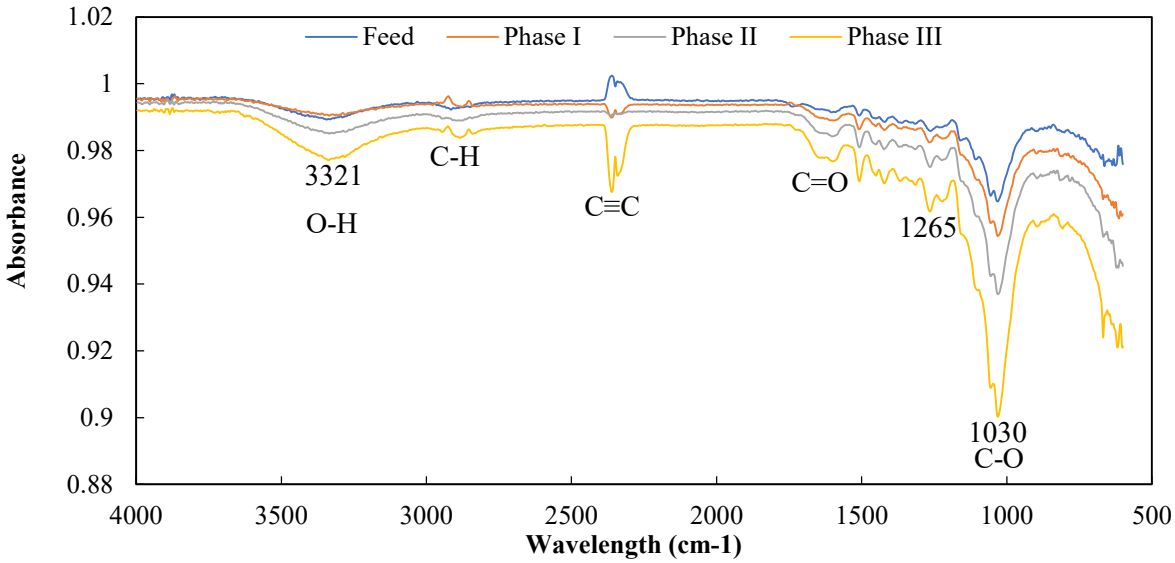

Figure 4.6: Fourier transform infrared spectroscopy spectra for the feed and digestate samples at different SRTs

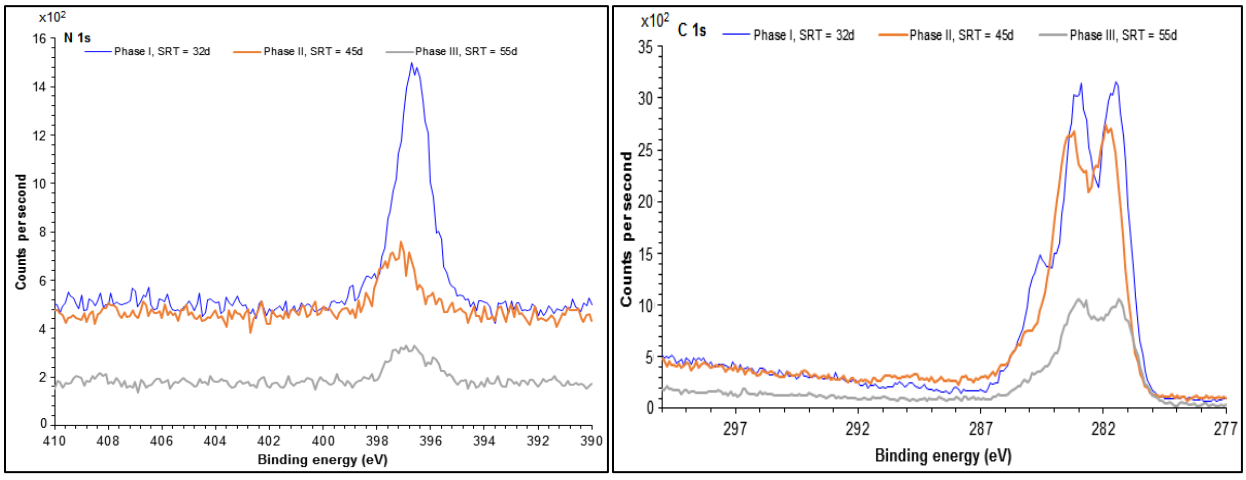

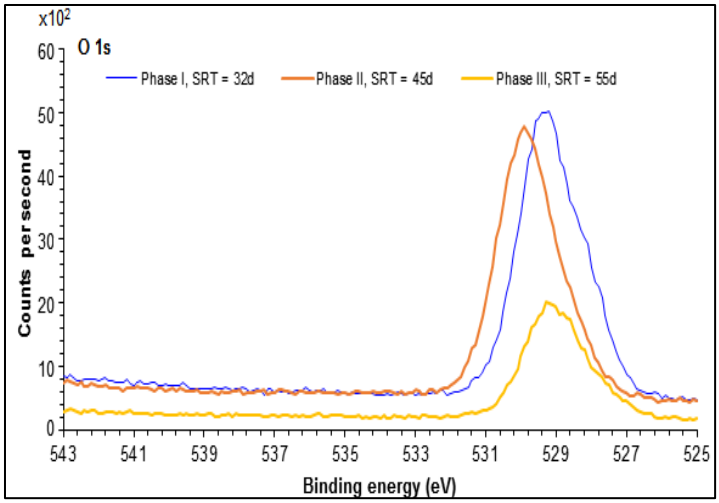

Figure 4.7: XPS spectra of the MLSS under different SRTs conditions.

3.1.2.2.4. Solids reduction ratio and sludge dewaterability under different SRTs

Solids reduction ratio and sludge dewaterability under different operating conditions are represented in Fig. 4. 8. Solids reduction (SR) is a process of breaking down primary sludge by microorganisms and recovery of organic carbon as biogas. In this study, the SR ranged between 47% and 54.9%. The differences in solids reduction percent are statically significant among the tested SRTs (ANOVA, $p < 0.05$). The longer SRT yielded the highest solids reduction compared to the shorter SRT. The low solids reduction ratio may indicate the recalcitrant nature of the primary sludge. Thus, pretreatment may be required to boost the overall organic matter reduction. Roy et al. (2016) reported 30%–40% solids removal for a refinery waste stream from a wastewater treatment plant. Whereas Bayr and Rintala (2011) achieved a 25–40% volatile solids (VS) removal for Kraft pulping primary sludge. The degradation of cellulose was significantly higher (70–73%) than hemicellulose (7–27%) while leaving lignin as non-degradable.

On the other hand, waste sludge needs to be dewatered before its further processing to ease its handling and minimize its overall volume. In wastewater treatment scenarios, many chemical coagulants are used to condition the sludge before the mechanical dewatering process (Yuan et al., 2019). In the forest industry, pulp and paper primary sludge (PS) is usually easily dewaterable than the bio-sludge, which can be mixed with PS to enhance its dewaterability (Meyer et al., 2018). However, it is generally believed that SRT affects the physical properties of sludge, by affecting the particle size distribution of the digested polymers and dewaterability (Halalsheh et al., 2005). On the other hand, lignocellulosic digestate contains partially digested materials besides microorganisms, which can be processed further for bioenergy (e.g., CH_4) or value-added biomaterials (e.g., fertilizer) production. Figure 4. 8 shows digestate dewaterability under different operating conditions. Dewaterability time varied with operation conditions, and it was 29.5±4.8

in phase I, 33.5±2.03 in phase II, and 49.6±5.9 in phase III. From this Figure, it can be seen that dewaterability decreased as anaerobic digestion proceeded. This could be attributed to the highest MLSS concentration in phase III (SRT=55 days), as a higher MLSS would reduce the dewaterability. Furthermore, this observation agrees with the results reported in the previous studies (Martínez et al., 2015). This indicates that although AD reduces the solids content of the treated sludge, however, the sludge dewaterability may not be enhanced. It was found that digestates from anaerobic digestion were more difficult to dewater than primary or activated sludge. Sludge dewaterability was found to be affected by sludge particle size distribution, cationic content, type, and quantity of EPS (extracellular polymeric substances) (Meyer et al., 2018).

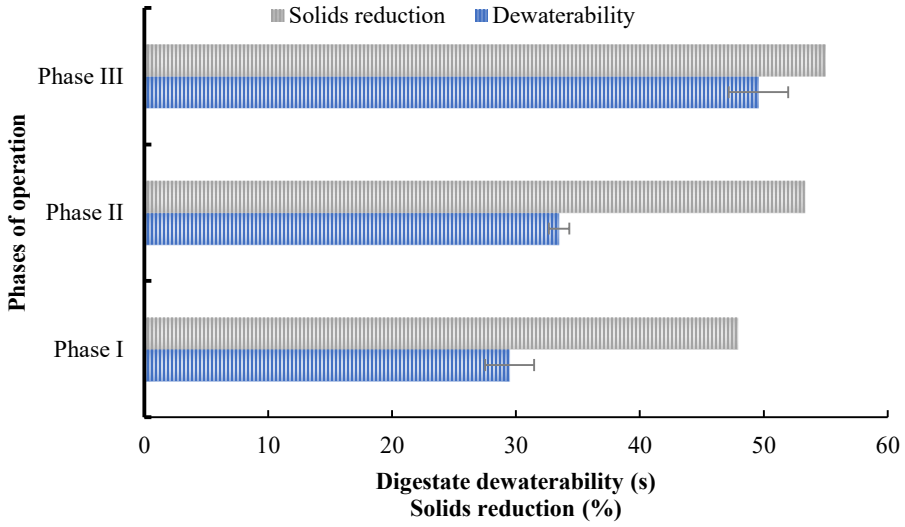

Figure 4.8: Solids reduction ratio and digestate dewaterability under different operating conditions (phase I - 32d SRT/18.9 g/L MLSS; phase II - 45d SRT/24.6 g/L MLSS; phase III - 55d SRT/27.3 g/L MLSS).

4. Conclusion

In this research, the effect of different SRTs on pulp and paper primary sludge anaerobic digestion was investigated and compared in a long-term study (370 days). Moreover, permeate and digestate characteristics were evaluated, and digestate dewaterability was determined. The tested STRs demonstrated different biogas productivity, and it can be concluded that the longer the SRT period, the more biogas production will be. Biogas production ranged from 99.7 to 153.8 m^3 biogas/ tonne $MLSS_{removed}$. The solid retention time of 55 d, organic loading rate of 2.15±0.10 kg-TSS/L.d, and hydraulic retention time of 5 d were considered optimal, they resulted in biogas production of 153.8 m^3 biogas/ tonne $MLSS_{removed}$. Digestates concentration and dewaterability were varied between the applied SRTs. The solids reduction ratio ranged from 47 % to 54% for the SRT of 32, 45, and 55 days. FTIR data showed that the peak intensity of O-H at 3400 cm^{-1} increased significantly due to hemicellulose digestion while leaving cellulose and

lignin in AD slurry. Overall, primary sludge is a feasible substrate for biogas production using a thermophilic membrane bioreactor. However, the anaerobic digestion of primary sludge requires long retention times and sufficient nutrients for bacterial growth. Further, a techno-economic analysis is needed to help beneficiaries evaluate whether dealing with pulp and paper sludges through anaerobic digestion using ThAnMBR is feasible or not.

Acknowledgements

This research was financially supported by Ontario Graduate Scholarship (OGS) and Natural Sciences and Engineering Research Council of Canada (NSERC).

References

[1] Baird, R. B., Eaton, A. D., Rice, E. W., 2017. Standard methods for the examination of water and wastewater, American Public Health Association, American Water Works Association, Water Environment Federation, 23rd ed. Washington, DC, https://doi.org/10.2105/SMWW.2882.216.

[2] Bajpai, P., 2016. Pretreatment of lignocellulosic biomass for biofuel production, Springer, Singapore, 1st ed., https://doi.org/10.1007/978-981-10-0687-6.

[3] Bakraoui, M., Karouach, F., Ouhammou, B., Aggour, M., Essamri, A., El Bari, H., 2020. Biogas production from recycled paper mill wastewater by UASB digester: Optimal and mesophilic conditions, Biotechnol. Rep. 25, e00402. https://doi.org/10.1016/j.btre.2019.e00402.

[4] Baruah, J., Nath, B.K., Sharma, R., Kumar, S., Deka, R.C., Baruah, D.C., Kalita, E., 2018. Recent trends in the pretreatment of lignocellulosic biomass for value-added products, Front. Energy Res. 1-19. https://doi.org/10.3389/fenrg.2018.00141.

[5] Bayr, S., Rintala, J., 2012. Thermophilic anaerobic digestion of pulp and paper mill primary sludge and co-digestion of primary and secondary sludge, Water Res. 46, 4713-4720. https://doi.org/10.1016/j.watres.2012.06.033.

[6] Bokhary, A., Maleki, E., Hong, Y., Hai, F.I., Liao, B., 2020. Anaerobic membrane bioreactors: Basic process design and operation. In: Ngo, H. H., Guo, W., Ng, H. Y., Mannina, G., Pandey, A., (Eds.), Current developments in biotechnology and bioengineering, Elsevier, Amsterdam, p. 25-54. https://doi.org/10.1016/B978-0-12-819852-0.00002-6.

[7] Bokhary, A.M.A., 2017. Advanced ultrafiltration technology for lignocelluloses recovery and purification from thermomechanical pulp (TMP) mills process waters, Dissertation, Lakehead University. http://knowledgecommons.lakeheadu.ca:7070/handle/2453/4102.

[8] Bonilla, S., Choolaei, Z., Meyer, T., Edwards, E.A., Yakunin, A.F., Allen, D.G., 2018. Evaluating the effect of enzymatic pretreatment on the anaerobic digestibility of pulp and paper biosludge, Biotechnol. Rep. 17, 77-85. https://doi.org/10.1016/j.btre.2017.12.009.

[9] Chatterjee, P., Lahtinen, L., Kokko, M., Rintala, J., 2018. Remediation of sedimented fiber originating from pulp and paper industry: Laboratory scale anaerobic reactor studies and ideas of scaling up, Water Res. 143, 209-217. https://doi.org/10.1016/j.watres.2018.06.054.

[10] Choi, J.H., Ng, H.Y., 2008. Effect of membrane type and material on performance of a submerged membrane bioreactor, Chemosphere, 71, 853-859. https://doi.org/10.1016/j.chemosphere.2007.11.029.

[11] Choo, K.H., Lee, C.H., 1996. Membrane fouling mechanisms in the membrane-coupled anaerobic bioreactor, Water Res. 30, 1771-1780. https://doi.org/10.1016/0043-1354(96)00053-X.

[12] Den, W., Sharma, V.K., Lee, M., Nadadur, G., Varma, R.S., 2018. Lignocellulosic biomass transformations via greener oxidative pretreatment processes: access to energy and value-added chemicals, Front. Chem. 6, 1 - 23. https://doi.org/10.3389/fchem.2018.00141.

[13] Duncan, J., Bokhary, A., Fatehi, P., Kong, F., Lin, H., Liao, B., 2017. Thermophilic membrane bioreactors: A review, Bioresour. Technol. 243, 1180-1193. https://doi.org/10.1016/j.biortech.2017.07.059.

[14] Dvořák, L., Gómez, M., Dolina, J., Černín, A., 2016. Anaerobic membrane bioreactors—a mini review with emphasis on industrial wastewater treatment: applications, limitations and perspectives, Desalination Water Treat. 57, 19062-19076. https://doi.org/10.1080/19443994.2015.1100879.

[15] Ekstrand, E.M., Karlsson, M., Truong, X.B., Björn, A., Karlsson, A., Svensson, B.H., Ejlertsson, J., 2016. High-rate anaerobic co-digestion of kraft mill fibre sludge and activated sludge by CSTRs with sludge recirculation, J. Waste Manag. 56, 166-172. https://doi.org/10.1016/j.wasman.2016.06.034.

[16] Ekstrand, E.M., Larsson, M., Truong, X.B., Cardell, L., Borgström, Y., Björn, A., Ejlertsson, J., Svensson, B.H., Nilsson, F., Karlsson, A., 2013. Methane potentials of the Swedish pulp and paper industry–A screening of wastewater effluents. Appl. Energy. 112, 507-517. https://doi.org/10.1016/j.apenergy.2012.12.072.

[17] Elsayed, M., Abomohra, A.E.F., Ai, P., Wang, D., El-Mashad, H.M., Zhang, Y., 2018. Biorefining of rice straw by sequential fermentation and anaerobic digestion for bioethanol and/or biomethane production: comparison of structural properties and energy output, Bioresour. Technol. 268, 183-189. https://doi.org/10.1016/j.biortech.2018.07.130.

[18] Halalsheh, M., Koppes, J., Den Elzen, J., Zeeman, G., Fayyad, M., Lettinga, G., 2005. Effect of SRT and temperature on biological conversions and the related scum-forming potential, Water Res. 39, 2475-2482. https://doi.org/10.1016/j.watres.2004.12.012.

[19] Hamza, R.A., Zaghloul, M.S., Iorhemen, O.T., Sheng, Z., Tay, J.H., 2019. Optimization of organics to nutrients (COD: N: P) ratio for aerobic granular sludge treating high-strength organic wastewater. Sci. Total Environ. 650, 3168-3179. https://doi.org/10.1016/j.scitotenv.2018.10.026.

[20] Humpert, D., Ebrahimi, M., Czermak, P., 2016. Membrane technology for the recovery of lignin: A review. Membranes, 6, 42. https://doi.org/10.3390/membranes6030042.

[21] Jiang, S., 2018. Thermophilic anaerobic membrane bioreactor for pulp and paper sludge treatment, Dissertation, Lakehead University. http://knowledgecommons.lakeheadu.ca:7070/handle/2453/4207.

[22] Jokela, J., Rintala, J., Oikari, A., Reinikainen, O., Mutka, K., Nyrönen, T., 1997. Aerobic composting and anaerobic digestion of pulp and paper mill sludges, Water Sci. Technol. 36, 181-188. https://doi.org/10.1016/S0273-1223(97)00680-X

[23] Karlsson, A., Truong, B., Gustavsson, J., Svensson, B.H., Nilsson, F., Ejlertsson, J., 2011. Anaerobic treatment of activated sludge from Swedish pulp and paper mills–biogas production potential and limitations, Environ. Technol. 32, 1559-1571. https://doi.org/10.1080/09593330.2010.543932.

[24] Kinnunen, V., Ylä-Outinen, A., Rintala, J., 2015. Mesophilic anaerobic digestion of pulp and paper industry biosludge–long-term reactor performance and effects of thermal pretreatment, Water Res. 87, 105-111. https://doi.org/10.1016/j.watres.2015.08.053.

[25] Lin, Y., Wang, D., Li, Q., Huang, L., 2011. Kinetic study of mesophilic anaerobic digestion of pulp & paper sludge. Biomass Bioener. 35, 4862-4867. https://doi.org/10.1016/j.biombioe.2011.10.001.

[26] Lin, Y., Wang, D., Li, Q., Xiao, M., 2011. Mesophilic batch anaerobic co-digestion of pulp and paper sludge and monosodium glutamate waste liquor for methane production in a bench-scale digester, Bioresour. Technol. 102, 3673-3678. https://doi.org/10.1016/j.biortech.2010.10.114.

[27] Lin, H.J., Xie, K., Mahendran, B., Bagley, D.M., Leung, K.T., Liss, S.N., Liao, B.Q., 2009. Sludge properties and their effects on membrane fouling in submerged anaerobic membrane bioreactors (SAnMBRs). Water Res. 43, 3827-3837. https://doi.org/10.1016/j.watres.2009.05.025.

[28] Lopes, A.D.C.P., Silva, C.M., Rosa, A.P., de Ávila Rodrigues, F., 2018. Biogas production from thermophilic anaerobic digestion of kraft pulp mill sludge, Renew. Energy. 124, 40-49. https://doi.org/10.1016/j.renene.2017.08.044.

[29] Maleki, E., Bokhary, A., Leung, K., Liao, B.Q., 2019. Long-term performance of a submerged anaerobic membrane bioreactor treating malting wastewater at room temperature (23±1° C), J. Environ. Chem. Eng. 7, 103269. https://doi.org/10.1016/j.jece.2019.103269.

[30] Martínez, E.J., Rosas, J.G., Morán, A., Gómez, X., 2015. Effect of ultrasound pretreatment on sludge digestion and dewatering characteristics: Application of particle size analysis, Water, 7, 6483-6495. https://doi.org/10.3390/w7116483.

[31] Meyer, T., Amin, P., Allen, D.G., Tran, H., 2018. Dewatering of pulp and paper mill biosludge and primary sludge, J. Environ. Chem. Eng. 6, 6317-6321. https://doi.org/10.1016/j.jece.2018.09.037.

[32] Paul, S., Dutta, A., 2018. Challenges and opportunities of lignocellulosic biomass for anaerobic digestion, Resour. Conserv. Recycl. 130, 164-174. https://doi.org/10.1016/j.resconrec.2017.12.005.

[33] Puhakka, J.A., Alavakeri, M., Shieh, W.K., 1992. Anaerobic treatment of kraft pulp-mill waste activated-sludge: gas production and solids reduction, Bioresour. Technol. 39, 61-68. https://doi.org/10.1016/0960-8524(92)90057-5.

[34] Puhakka, J.A., Viitasaari, M.A., Latola, P.K., Määttä, R.K., 1988. Effect of temperature on anaerobic digestion of pulp and paper industry wastewater sludges, Water Sci. Technol. 20, 193-201. https://doi.org/10.2166/wst.1988.0022.

[35] Roy, R., Haak, L., Li, L., Pagilla, K., 2016. Anaerobic digestion for solids reduction and detoxification of refinery waste streams, Process Biochem. 51, 1552-1560. https://doi.org/10.1016/j.procbio.2016.08.006.

[36] Saha, M., Eskicioglu, C., Marin, J., 2011. Microwave, ultrasonic and chemo-mechanical pre-treatments for enhancing methane potential of pulp mill wastewater treatment sludge, Bioresour. Technol. 102, 7815-7826. https://doi.org/10.1016/j.biortech.2011.06.053.

[37] Sawatdeenarunat, C., Surendra, K. C., Takara, D., Oechsner, H., Khanal, S. K., 2015. Anaerobic digestion of lignocellulosic biomass: challenges and opportunities, Bioresour. Technol. 178, 178-186. https://doi.org/10.1016/j.biortech.2014.09.103.

[38] Slade, A.H., Ellis, R.J., Van den Heuvel, M., Stuthridge, T.R., 2004. Nutrient minimisation in the pulp and paper industry: an overview, Water Sci. Technol. 50, 111-122. https://doi.org/10.2166/wst.2004.0175.

[39] Sluiter, A., Hames, B., Ruiz, R., Scarlata, C., Sluiter, J., Templeton, D., 2005. Determination of ash in biomass (NREL/TP-510-42622), National Renewable Energy Laboratory, Golden.

[40] Smook, G. A., 2016. Handbook for pulp & paper technologists, 4th ed. TAPPI Press.

[41] Turovskiy, I.S., Mathai, P.K., 2006. Wastewater sludge processing, John Wiley & Sons, Hoboken, New Jersey.

[42] Veluchamy, C., Kalamdhad, A.S., 2017. Biochemical methane potential test for pulp and paper mill sludge with different food/microorganisms ratios and its kinetics. Int. Biodeterior. Biodegradation. 117, 197-204. https://doi.org/10.1016/j.ibiod.2017.01.005.

[43] Yuan, T., Cheng, Y., Zhang, Z., Lei, Z., Shimizu, K., 2019. Comparative study on hydrothermal treatment as pre-and post-treatment of anaerobic digestion of primary sludge: Focus on energy balance, resources transformation and sludge dewaterability, Appl. Energy. 239, 171-180. https://doi.org/10.1016/j.apenergy.2019.01.206.

[44] Yue, Z., Teater, C., Liu, Y., MacLellan, J., Liao, W., 2010. A sustainable pathway of cellulosic ethanol production integrating anaerobic digestion with biorefining, Biotechnol. Bioeng. 105, 1031-1039. https://doi.org/10.1002/bit.22627.

[45] Zhao, C., Shao, Q., Ma, Z., Li, B., Zhao, X., 2016. Physical and chemical characterizations of corn stalk resulting from hydrogen peroxide presoaking prior to ammonia fiber expansion pretreatment, Ind. Crops Prod. 83, 86-93. https://doi.org/10.1016/j.indcrop.2015.12.018.

Chapter V

Thermophilic anaerobic digestion of pulp and paper primary sludge using a submerged AnMBR: Effect of solids retention time on the membrane performance.

Abstract

This study focused on the membrane performance of a thermophilic anaerobic membrane bioreactor (ThAnMBR) treating primary sludge from a thermomechanical pulping mill. The ThAnMBR was operated for 370 days, and various solids retention times (SRTs) (32, 45, 55 days) were tested. Membrane filtration performance in terms of permeate flux, membrane fouling rate, and membrane resistance was evaluated, and surface properties of both sludge and membrane were characterized. Various characterization techniques were used including scanning electron microscope (SEM), energy-dispersive X-ray spectroscopy (EDX), X-ray photoelectron spectroscopy (XPS), FTIR (Fourier Transform Infrared) spectroscopy, particle size distributions (PSD), zeta potential analyzer, and contact angle analysis. The results indicate that the membrane had stable performance and that the primary sludge showed low tendencies for membrane fouling. However, the degree of fouling increases with increasing SRT, and mixed liquor suspended solids (MLSS) concentration was the predominant factor affecting membrane performance. The formation of a loose gel layer on the module surfaces was determined as the predominant mechanism of membrane fouling during primary sludge treatment by ThAnMBR and accounts for most of the total resistance. The smaller particle showed a higher tendency towards deposition on the membrane surfaces than the big particles. The EDX, XPS, and FTIR analysis suggests that the foulants deposited on the membrane surface have varied compositions of organic and inorganic materials and that the increase of SRT not only increases in the concentration of sludge in the system but also leads to the accumulation of chemical elements which in turn increases the filtration resistance of the membrane. Overall, this study could assist in gaining a better elucidation of the membrane filtration performance, fouling behavior, and foulants origins during the treatment of lignocellulosic sludge by AnMBR.

Keywords: Membrane performance; SRT; fouling; primary sludge, anaerobic digestion; membrane bioreactor.

---

1. Introduction

Anaerobic membrane bioreactors (AnMBRs) have been developed to retain microorganisms in the system and allow operation at high concentrations of biomass with long solids retention times (SRTs), facilitating higher volume conversion rates, which in turn lead to a smaller footprint (less sludge production) (Dvořák et al., 2016). When operating at a longer SRT, the microorganisms will have more time to degrade the substrate and hydrolyze slowly decomposable COD. Thus, the outcomes of MBRs would be translated into higher biogas production, better effluent (permeate) quality acceptable for reuse in various applications and the reactor could be smaller in size than conventional anaerobic reactors (CAR) (Padmasiri et al., 2007). The CAR design always relies on empirical values of the SRT and hydraulic retention time (HRT) parameters that often lead to oversized digester due to their coupling (SRT is equal to HRT) (Orhon et al., 2016). However, in AnMBR, the integration of the membrane unit with the digester enables the separation of the SRT from HRT and system resizing, thus reducing the high capital cost associated with a large bioreactor. On the other hand, AnMBR has been found to withstand fluctuations in organic loading rates (OLRs) compared to a conventional activated sludge (CAS) process and provides an opportunity to maintain a viable OLR at a similar or longer SRT. Currently, there are two MBR configurations in place, submerged and external, and both polymeric and ceramic materials are used in AnMBR. There is a growing demand for MBR due to the requirement for high-quality effluent and energy neutral.

Despite MBRs are widely used in domestic and high-strength wastewater treatment, and many reviews have been published (Liao et al. 2006; Lin et al., 2013), their applications in organic sludge treatment are still in their infancy. Of the limited studies dealing with this topic (Pollice et al., 2008; Xu et al., 2011; Yu et al., 2016; Abdelrahman et al., 2020), most of them were conducted on the treatment of waste activated sludge (WAS) from municipal wastewaters treatment facilities, and there is a large knowledge gap in the literature. Pileggi and Parker (2017) compared conventional anaerobic digester and AnMBR when treating mixed municipal sludges under different temperatures (25, 35, and 55 °C) at the pilot scale. AnMBR surpassed the traditional anaerobic digester in terms of solids reduction, biogas production, and net energy balance. Meabe et al. (2013) compared the biodegradability of sewage sludge under thermophilic and mesophilic conditions using AnMBRs and reported better performance for the thermophilic system, but they observed more irreversible fouling at the thermophilic temperature. Dagnew et al. (2012) treated WAS with AnMBR and reported that the effects of anaerobic sludge concentration were dependent on the applied flux. Most of this work has focused on sludge digestibility with a very limited investigation of membrane performance. Also, reportedly, thermophilic temperatures allow higher digester throughputs, low sludge yield, and higher biodegradation kinetic (Duncan et al., 2017), but their impact on the membrane performance is not documented. Membrane fouling is a complex phenomenon caused by several factors including process conditions (e.g., pH, temperature, transmembrane pressure, flux, OLR, and SRT), treated sludge source and type (e.g., particle dimensions and concentrations), and membrane properties (surface chemistry, pores size, morphology, and hydrophobicity) (Bokhary et al., 2018). Thus, the effect of each substrate and its digestion conditions, on the performance of the membrane should be individually investigated and membrane fouling problems under such environmental conditions elucidated.

Due to the integrated membrane module, AnMBRs can operate at longer SRTs and higher mixed liquid suspended solids (MLSS) concentrations, which is not the case for conventional anaerobic digesters such as up-flow anaerobic sludge blanket (UASB) (Bokhary et al., 2020). Longer SRTs retain slow-growing anaerobic microorganisms within the AnMBR, increase biogas yield (Smith et al., 2012), and may reduce the influence of ammonia inhibition due to adequate biomass acclimatization (Meabe et al., 2013). However, the high MLSS concentration was shown to negatively affect the membrane performance of AnMBRs due to cake layer formation and reduced membrane permeability (Wang et al., 2018). SRT is known to affect both the biochemical and physical properties of sludge, which in turn may impact the performance of the membrane. It has been reported that the characteristics of the particle size distribution of sludge, MLSS concentration, soluble microbial products (SMPs) quantity, and extracellular polymeric substances (EPSs) content in the system can directly be affected by the applied SRT (Luna et al., 2014; Bokhary et al., 2020). Thus, the SRT should be adjusted to the optimal level to ensure improved membrane performance while obtaining the necessary biological performance (Smith et al., 2012; Ng et al., 2020).

Huang et al. (2011) reported an increased rate of membrane fouling at the longer SRT when treating low-strength wastewater by AnMBR due to the higher carbohydrate and protein content in SMP, and they also observed reduced particles flocculation at the longer SRT resulting from lower EPS, which exacerbated the fouling. Baek et al. (2010) detected a diminution in EPS concentration at longer SRTs when treating dilute municipal wastewater by AnMBR. In aerobic MBR, Ahmed et al. (2007) observed increased bound-EPS when SRT decreased to 20 days, resulting in elevated trans-membrane pressure but no significant reduction in bound EPS was observed when SRT increased over 60 days. These results indicate that an optimal solid retention time may exist to reduce the membrane fouling by decreasing the accumulation of SMP and EPS in the system. However, the interrelationship between SRT and the membrane fouling rate is not well defined and understood in the reported literature of AnMBR (Smith et al., 2012).

Although MBRs are used extensively in municipal wastewater treatment with a growing list of full-scale plants with a detailed investigation on membrane performance, their applications in primary sludge are still limited and there is an insufficiency of practical information on the impacts of different operating strategies and sludge characteristics on the membrane performance under thermophilic anaerobic conditions. To our knowledge, no study investigated the effect of SRT on the membrane performance of AnMBR treating pulp and paper primary sludge from a thermomechanical pulping. This research aims to fill some gaps in this regard by evaluating the effect of SRT on the membrane performance of the thermophilic AnMBR.

2. Materials and methods

2.1. Substrate and inoculum

The primary sludge was collected from a local Canadian thermomechanical pulp mill. The mill utilizes a mix of soft and hardwood as feedstocks to produce the pulp. Samples were stored at 4 ° C upon their delivery for further use. The inoculum for the reactor for seeding was obtained from an AnMBR that handles pulp and paper secondary sludge and is located at Lakehead University (Jiang, 2018). Phosphorous and nitrogen were added to the feed in the form of dipotassium phosphate (K_2HPO_4) and ammonium chloride (NH_4Cl), in a COD: N: P ratio of 100: 2.6: 1 to preserve the nutrients needed for microbial growth in AnMBR (Lin et al., 2009; Hamza et al., 2019).

2.2. Experimental setup

Digestion was performed in a thermophilic submerged anaerobic membrane bioreactor (ThSAnMBR) with a working volume of 6.5 liters. The process temperature was sustained at 50±1°C by circulating the hot water from the water-bath through the reactor case. A magnetic stirrer plate was used to gently mix the bioreactor and keep the system components suspended. The pH of the prepared sludge substrate was close to neutral. The pH of the reactor was maintained at about 7.2 ± 0.1 by adjusting the feed pH using NaOH solution. After installing the membrane unit and closing the reactor head, the system was purged with

nitrogen gas for 5 minutes to form an anaerobic atmosphere and the same process was performed when required (e.g., during a phase termination and starting up of a new phase or system opening for membrane cleaning). The membrane performance was investigated under three different solids retention times (32, 45, 55 d). The HRT was maintained at 5 d during the entire experiment. The reactor was fed intermittently by a sludge slurry using a magnetic pump, equipped with a controller and a water level sensor (Fig. 5.1). Excess digested sludge was withdrawn from the systems daily to sustain the required SRT. The biogas production rate was determined by liquid displacement technique using a graduated measuring cylinder while the biogas composition was quantified by the gas chromatography instrument (Shimadzu, GC-2014, Japan).

A flat plate microfiltration (MF) membrane unit with a working filtration area of 0.03 m^2 and a pore size of 0.1 µm was used in this study. The module has two effective filtration sides, and the dimensions of each side are 0.1 x 0.15 m. The membrane was made of polyvinylidene fluoride (PVDF) material. The produced biogas was used to sparge the membrane unit and reduce the foulants deposition on it during the operation. The gas of headspace was recirculated at a total flow rate of 3.76 ±0.08 L/min by Masterflex pumps equipped with two stainless steel tubes located under the module on each side. A peristaltic pump (Masterflex C/L®, Cole-Parmer, Canada), was used to withdraw the permeate from the reactor. The permeate pump was equipped with a timer, that runs for three minutes and stops for two minutes in order to reduce the fouling process. The needed flux was sustained by controlling the peristaltic pump speed, and calibration and adjustment were performed as required. Transmembrane pressure was monitored by a pressure vacuum gauge (Omega, Korea), which was attached to the membrane unit at the top of the reactor and the suction pump of the permeate. Figure 5. 1 shows the process flow diagram of ThSAnMBR.

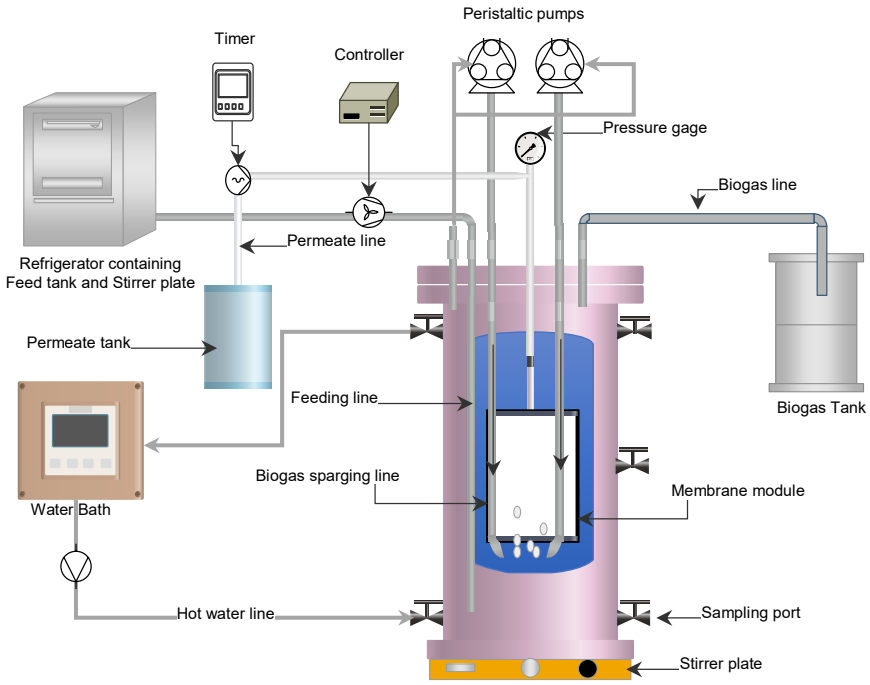

Figure 5.1: Process flow diagram of the TSAnMBR process used in this study.

2.3. Analytical methods

2.3.1. Primary sludge samples, reactor feeds, and inoculum

The volatile solids content, total solids (TS), the ash content of inoculum, and sludge substrate were evaluated in accordance with the standard techniques (Baird et al., 2017). The pH values of inoculum and sludge substrate were determined by Oakton pH 700 benchtop meter. The particle size of the prepared substrate was determined by a Malvern Mastersizer 2000 system. The carbon (C), hydrogen (H), nitrogen (N), oxygen (O), and sulfur (S) contents were determined using an elemental analyzer (Elementar Vario EL). Total chemical oxygen demand (TCOD), and soluble chemical oxygen demand (SCOD) for primary sludge and inoculum was quantified using HR COD test vials (K-7365, 0–1500 ppm) and high temperature (using COD reactor, Hanna Instruments), followed by measuring absorbance with a colorimeter (Hach DR 2800 Spectrophotometer).

2.3.2. Analysis of membrane resistance and permeability

Darcy's law was used for membrane resistance analysis. By viewing the resistances as being connected in series, Darcy's law can be employed in calculating individual resistances and the extent of their contributions to total resistance as given by the equation (eqn) below (Di Bella and Di Trapani 2019).

$$R_{tot} = R_m + R_C + R_p = \frac{\Delta P_T}{\eta x J} \qquad (1)$$

In eqn [1], R_t is the total hydraulic resistance of the membrane, R_m is the resistance of the new membrane, R_c is the resistance of the cake/gel layer, R_p is the resistance of the pore blockage, ΔP_T is the trans-membrane

pressure (Pa), η represents the dynamic viscosity of the pure water (Pa.s), and J is the measured membrane flux (cubic centimeters per second). As a new membrane was used at each phase, each phase began by determining the hydraulic resistance of the new membrane unit by performing a permeability test. The permeability test was also performed at the end of each phase and after each membrane cleaning cycle. Whereas the total resistance was computed from the final flux and its corresponding trans-membrane pressure at the end of the phase (Mahmoud and Liao, 2017).

After each cleaning cycle (physical, NaClO, and $C_6H_8O_7$ cleaning), the resistance of the organic, inorganic, and permanent fouling was determined using the equation below as it has been measured by other researchers (Keller et al., 2017; Mahmoud and Liao, 2017).

$$R_P = R_{organic} + R_{inorganic} + R_{permanent} \quad (2)$$

Since the temperature is among the influencing factors of the membrane permeability coefficient where when the temperature increases the viscosity decreases, the following equation was used to determine the temperature corrected permeability.

$$K_{20\,°C} = \frac{J.e^{(-0.0239\,(T-20)}}{\Delta P} \quad (3)$$

Where $K_{20\,°C}$ is the membrane permeability (L/m^2.hr. kPa) at 20 °C; J is the membrane flux (L/m^2.hr) at temperature T (°C); T is the water temperature at which the permeability was measured in °C, and ΔP is transmembrane pressure (kPa).

2.3.3. SEM-EDX

Scanning electron microscope (SEM) and energy-dispersive X-ray spectroscopy (EDX) were used in tandem to produce both the surface image of the membranes and analyze the elemental composition of the prepared specimens. In this study, representative samples of the membrane module were taken at the end of each operating condition and soaked in liquid nitrogen for 10 min. Specimens were then prepared, fixed on a metal support, and coated with carbon using a sputter coater (Model 12560, Fullam, USA) to enhance heat conduction and prevent the sample from being burned or charged. Finally, surface and cross-sectional images were taken from coated samples at the desired magnification using SEM (SU-70, Hitachi, Japan), while the spectrums of the elemental composition were determined by EDX analysis.

2.3.4. XPS

The elemental composition of mixed liquor suspended solids (MLSS) and employed membranes were characterized by Axis Supra X-ray photoelectron spectroscopy (XPS) system (Kratos Analytical Ltd. Manchester, UK). XPS spectra were obtained from MLSS and membrane samples after freeze-drying of samples at the end of each phase conditions (Liao et al, 2011).

2.3.5. FTIR

After the physical and chemical cleaning of the used membranes, Bruker Tensor 37 FTIR (Fourier Transform Infrared) spectroscopy (Bruker Co., Ltd.) was used to detect the foulants deposited on the membrane surfaces by obtaining detailed information on the functional groups of the foulants (Puspitasari et al., 2010; Hu et al., 2016). FTIR measurements were carried out on freeze-dried employed membrane specimens and new membrane using Labconco Freeze dryer.

2.3.6. Surface properties of MLSS and membrane

The zeta potential of the MLSS was measured using a ZetaPALS zeta potential analyzer (Brookhaven, Holtsville, NY, USA). Due to the large particles of MLSS, MLSS supernatant, containing fine colloidal particles and macromolecules, was used to determine the surface charge of MLSS. A permeate solution from the reactor was utilized to provide the background electrolyte. The contact angle of MLSS and membranes was measured by Dropometer M-3 (Droplet Smart Tech Inc. Canada). The pure water was used as a probe fluid for measuring purposes, about 3 μL of the water droplet was dispensed with a micropipette on the surface of the specimens. At the end of the measurements, an average contact angle value was calculated for each tested specimen.

2.3.7. Particle size distributions (PSD)

The PSDs of the MLSS specimens were routinely monitored with the Malvern Mastersizer 2000 system. The instrument entails an optical bench (for primary data collection), dispersion parts (for specimen delivery), and a computer unit running Malvern software. The machine utilizes laser diffraction and measures particles in the range of 0.02 – 2000 micrometers. This system measures every individual sample three times automatically and calculates the average (Mahmoud and Liao, 2017).

2.3.8. Soluble microbial products (SMP) measurement

The SMP samples were prepared from the mixed liquor, which was withdrawn from the bioreactor at the end of each phase conditions. The mixed liquor samples were centrifuged at 1900 g force and passed through a 0.45 μm membrane, and SMP was measured in the filtrates. Protein (PN) and carbohydrates (CH) were determined colorimetrically using Hach DR 2800 Spectrophotometer, and Anthrone and Folin as reagents. While bovine serum albumin (BSA) and glucose were employed for protein and carbohydrate standard curve preparation (Richards et al., 2020).

3. Results and discussion

3.1. Material characterization

Characteristics of the feedstock and inoculum were tested in this study. The mean volatile matter of the primary sludge was approximately 96.39±0.37 (%TS). The main components of primary sludge are cellulose, hemicellulose, lignin, inorganic, and woody extractives, most of which are considered to be

degradable (Bayr and Rintala 2012). The mean volatile solids (VS) concentration of the inoculum was about 83.48±0.37 (%TS), while the ash content of the feed substrate and the inoculum were 3.61±0.37 and 16.52±0.38 %, respectively. The total COD of the feed substrate and the inoculum were 19.99±1.82 and 47.66±1.04 (g/L), respectively. The values of elemental analysis of the primary sludge were 41.69±8.29%, 6.19±0.60%, 0.05±0.03%, and 0.15±0.07 % for carbon, hydrogen, sulfur, and nitrogen, respectively, with 285.60 carbon to nitrogen ratio (C/N). These values were in similarity to those given in the literature for biomass materials. For example, values of 42.43% carbon, 6.43% hydrogen, and 0.16% nitrogen were reported by dos Reis Ferreira et al. (2020) for sugarcane straw. While the reported values for the kraft primary sludge (PS) were 44.10 % C, 6.04 % H, 0.06 % N, and 0.40 % S (Lopes et al., 2018). The total solids of the treated feed were approximately 11.7 g/L, while its pH was 7.2.

3.2. Long-term operation of ThSAnMBR

The research was conducted in three different digestion conditions (3 phases) and lasted for 370 days. Table 5.1 illustrates the operating conditions of AnMBR treating primary sludge from a thermomechanical pulping. Phases I, II, and III were run at SRT of 32d, 45d, and 55d, respectively. The HRT was constant for all phases at 5 days. The OLR of all phases ranged between 3.8±0.27 and 3.9±0.43 kg-COD/m^3d as can be seen in Fig. 5.2. While the average effluent flux for the three phases ranged between 2.50±0.21 and 2.59±0.18 L/m^2.hr. Gas sparging rate was kept at (3.76 ±0.08 L/min) to minimize foulants deposition on the surface of the membrane. The permeate COD concentrations varied 2.30 g/L and 0.39 g/L, reflecting excellent effluent quality. This may indicate that, with increasing SRT, the microorganisms had more time to hydrolyze the primary sludge. The effluents of the various phases contained very low elemental concentrations, and the tested operating conditions showed no significant influence on the concentration of the element.

Table 5.1: AnMBR digestion conditions of the primary sludge.

Parameters	Phase I	Phase II	Phase III
Duration (d)	1 – 133	137 – 255	259 – 370
Temperature (°C)	50±1	50±1	50±1
Average permeate flux (L/m^2.hr.)	2.50±0.21	2.59±0.18	2.55±0.14
Average transmembrane pressure (kPa)	9.8±5.2	16.8±8.2	17.2±10.5
Feed concentration (g/L)	11.68±0.63	11.68±0.63	11.68±0.63
Feed COD (g/L)	19.77±1.78	20.34±1.46	20.00±1.09
Feed TSS (g/L)	11.49±0.466	11.5±0.14	11.46±0.66
SRT (d)	32	45	55
HRT (d)	5	5	5
OLR (kg-COD/m^3d)	3.9±0.43	3.9±0.36	3.8±0.27
Biogas sparging rate (L/min)	3.76 ±0.08	3.76 ±0.08	3.76 ±0.08
Mixed liquor suspended solids (MLSS) (g/L)	16.55 – 23.02	20.38 – 26.18	26.36 – 28.96

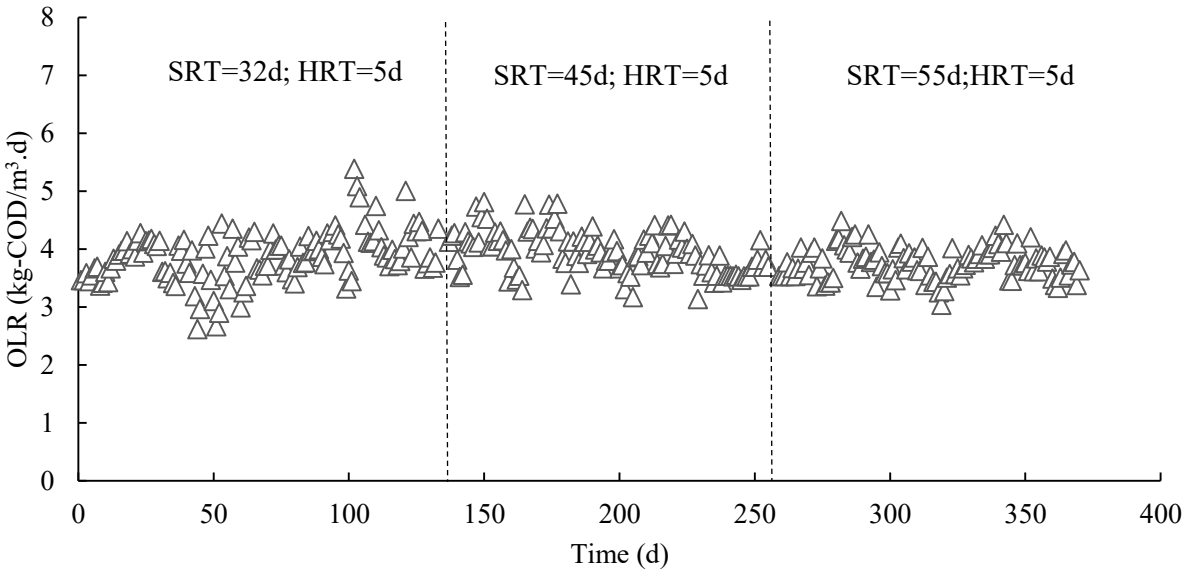

Figure 5.2: Solid loading rate versus operating time.

3.3. Membrane flux and transmembrane pressure

Figure 5.3 shows the profiles of permeate flux and transmembrane pressure versus operating time during primary sludge treatment. In this study, AnMBR was operated at constant flux, and a steady-state flux with an average value of 2.55±0.05 L/m^2.hr was maintained. The behavior of the transmembrane pressure can be directly related to the membrane fouling rate when operating at a constant permeable flow rate. During the course of operation, the required permeate flux was sustained by daily amending the pump speed, and no significant deterioration in membrane performance was observed. This can be explained by operating the AnMBR at low membrane flux as shown in Fig. 5. 3, and the application of biogas sparging and intermittent filtration. However, to sustain this flux, a three-stage transmembrane pressure profile has occurred in each operating condition, starting with an initial increase stage followed by an incremental increase, then a rapid rise. In the first phase, the transmembrane pressure ranged between 5 and 28.8 kPa with slight fluctuation, while the transmembrane pressure in the second and third phases ranged between 4.1 and 30.5 kPa, and 3.4 and 36.6 kPa, respectively. The increase in transmembrane pressure may be explained by pore blockage and gel layer formation during filtration and could also be attributed to more SMP release due to high temperature. The average fouling rate of the ThAnMBR at an SRT of 32, 45 and 55 days was 0.27, 0.40, and 0.39 kPa/day, respectively. The second and third phases have more fouling rates than the first phase, and this may be due to increased sludge age and the release of extracellular polymeric substances (EPS) and SMP. More soluble microbial products (SMP) and biopolymer clusters were observed in the thermophilic SAnMBR treating Kraft evaporator condensate (Lin et al., 2009). Also, the results suggest that the fouling rate increased with an increase in SRT. The total SMP obtained in this

work was ranging from 30.8 and 49.7 mg/L. An increase in transmembrane pressure could also be associated with increased MLSS concentrations, as a higher MLSS concentration could increase the potential for membrane clogging and reduce biogas sparing efficiency. In this study, the MLSS concentration increased progressively from 18g/L to 23 g/L in phase I, from 20g/L to 26.5 g/L in phase II, and from 26.4g/L to 28.8 g/L in phase III. The third phase had a higher transmembrane pressure (36.6 kPa) compared to the first (28.8 kPa) and the second (30.5 kPa) phases despite its less operating time (110 days versus 133 days, phase I and 115 days, phase II). The increase in the transmembrane pressure could also be linked to an increase in MLSS with operating time.

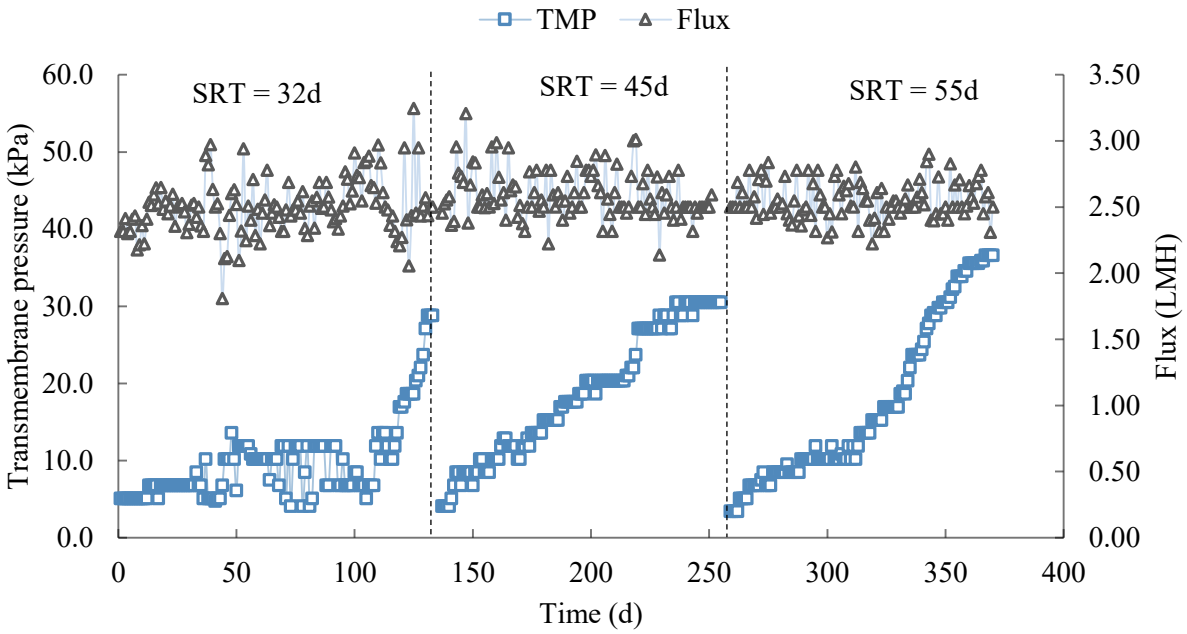

Figure 5.3: The profile of permeate flux and transmembrane pressure versus operating time.

3.4. Membrane fouling characterization

At end of each operating condition, membrane cleaning was performed, and membrane permeability and resistance were determined to evaluate the membrane fouling behavior. Visual inspection of membrane modules (Fig. 5. 3) at the end of each operating conditions suggests that gel layer, rather than cake layer, was the prevailing mechanism of membrane fouling. The contribution of each resistance and membrane permeability are shown in Fig. 5.4. As can be seen from Fig. 5.4 -a, the gel layer resistance (R_c) in the three phases ranged between about 98.6% and 98.8%. This reflects that R_c is the predominant fouling mechanism during primary sludge treatment by AnMBR and accounts for most of the total resistance. Thus, the physical cleaning was able to recover about 80 - 89 % of the membrane permeability (Fig. 5. 4-b). This result also indicates that the gel layer, which partially covers the membrane, cannot be removed easily by biogas sparging turbulence and requires physical cleaning. While the fouling resistance due to pore blocking (R_p)

ranged between 0.15% and 0.28% under the tested conditions indicating a minimal contribution of R_p to the membrane fouling. It is worth mentioning that the total hydraulic resistance increases with increasing SRT, and this may be partly explained by the higher MLSS in the longer SRT. These results correspond to the findings of other studies (Lin et al., 2009; Mahmoud and Liao 2017), where the dominance of the gel layer is the main fouling type during the operation of SAnMBRs. Lin et al. (2009) reported that the involvement of the cake layer in membrane fouling is more severe in the thermophilic SAnMBR than mesophilic SAnMBR. After removing the gel layer by physical cleaning, the membrane permeability was restored by about 84% on average representing that gel layer formation is the predominant type of membrane fouling. However, after cleaning the membrane with NaClO, the permeability was not improved significantly, and the recovery percent was only around 86% on average, but it increased further to about 88 % when the citric acid cleaning was performed. From these results, it can be concluded that the gel layer is the predominant fouling mechanism during primary sludge treatment by AnMBR, and organic ($R_{organic}$) and inorganic ($R_{inorganic}$) fouling had no significant effect on membrane performance.

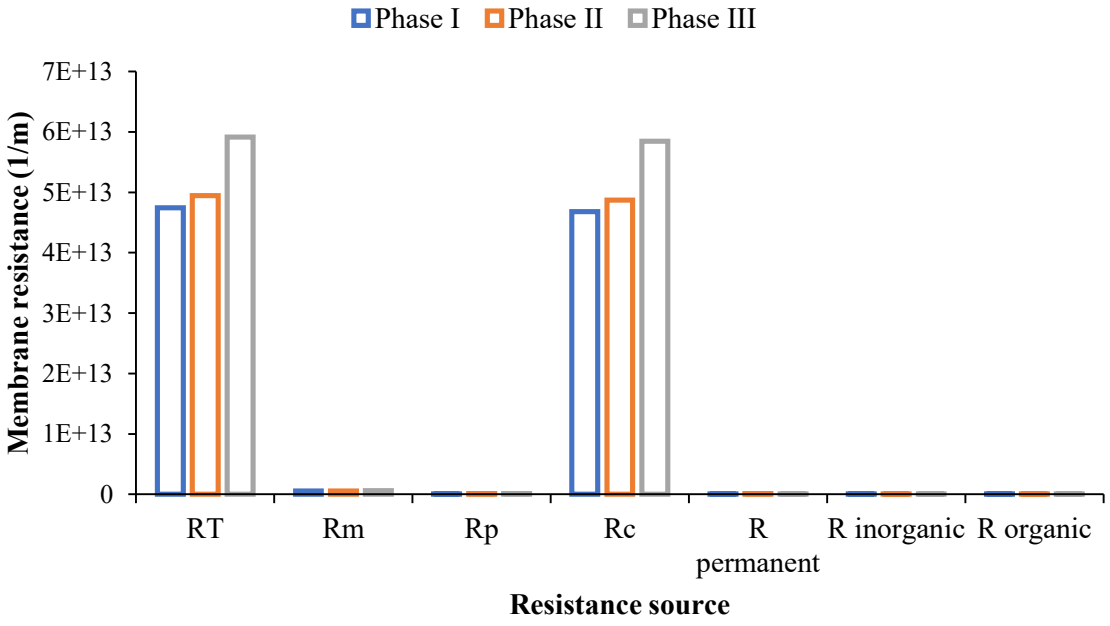

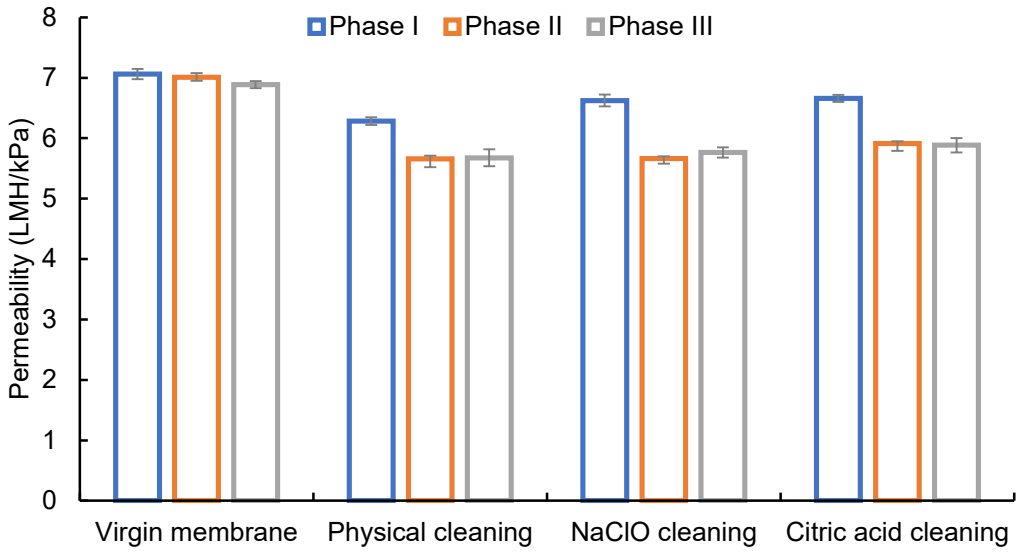

Figure 5.4: (a) membrane resistance and (b) membrane permeability under various tested conditions.

3.5. Surface properties of the membranes

3.4.1. SEM-EDX analysis

Scanning electron microscopy (SEM) was used in combination with energy dispersive X-ray analysis (EDX) to study the membrane surface morphology under various conditions and to examine the physical and chemical interactions between the fouling components and the membrane surface. The SEM images and elemental composition of the virgin and used membrane surfaces are presented in Figs. 5. 5 and 6, respectively. It should be noted that SEM-EDX tests were conducted after performing all the cleaning cycles for the used membranes. As can be seen from Fig. 5. 5, the pore structure of the new membrane was clearly visible compared to the membranes used. While based on the 3D surface plot data of the ImageJ, the surface of the fresh membrane was smoother compared to the used membranes. It was also observed that the pore size of the used membranes has shifted towards a larger size especially those larger than 25 nm due to the thermophilic conditions (high temperature) (data are not shown). This result is in agreement with the other findings (Masselin et al., 2001; Dang et al., 2014; Tikka et al., 2019). The EDX spectra of all the membranes showed that all the membranes had a high content of carbon and fluorine, which represents the membrane materials. It is evident from Fig. 5. 6 that the element composition of the used and fresh membrane is significantly different indicating the deposition of foulants on the surface of the used membrane. From this figure, it can also be seen that the deposition of foulants on the surface of the membrane in the first phase was less than in the later phases, and this could be partly due to the rise in the MLSS concentration with the increase in the runtime and SRT, which enhances the fouling potentiality. It can be observed from Fig. 5. 6, only the peaks of C, F, and O were detected in the first phase but more elemental peaks like Mg, Si, N, Na, S, and Cl were detected in the subsequent phases. Additionally, a high

ferric (Fe) peak was detected in some samples of the used membrane. This indicates that the foulants on the surfaces of the membranes include not only organic materials but also inorganic substances. It was found that the peak of O was increased with increasing SRT and MLSS concentration.

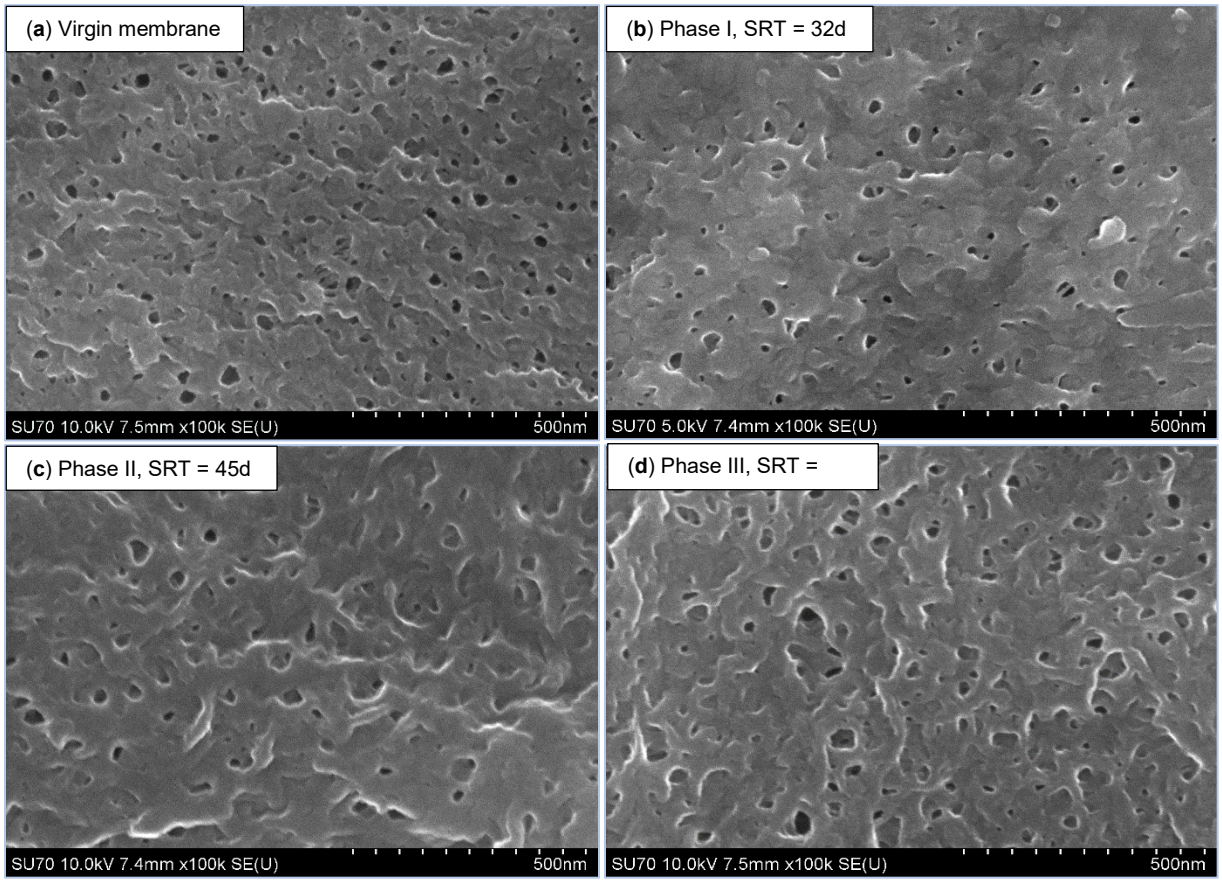

Figure 5.5: SEM images of the surfaces of the virgin and used PVDF membranes under different SRTs.

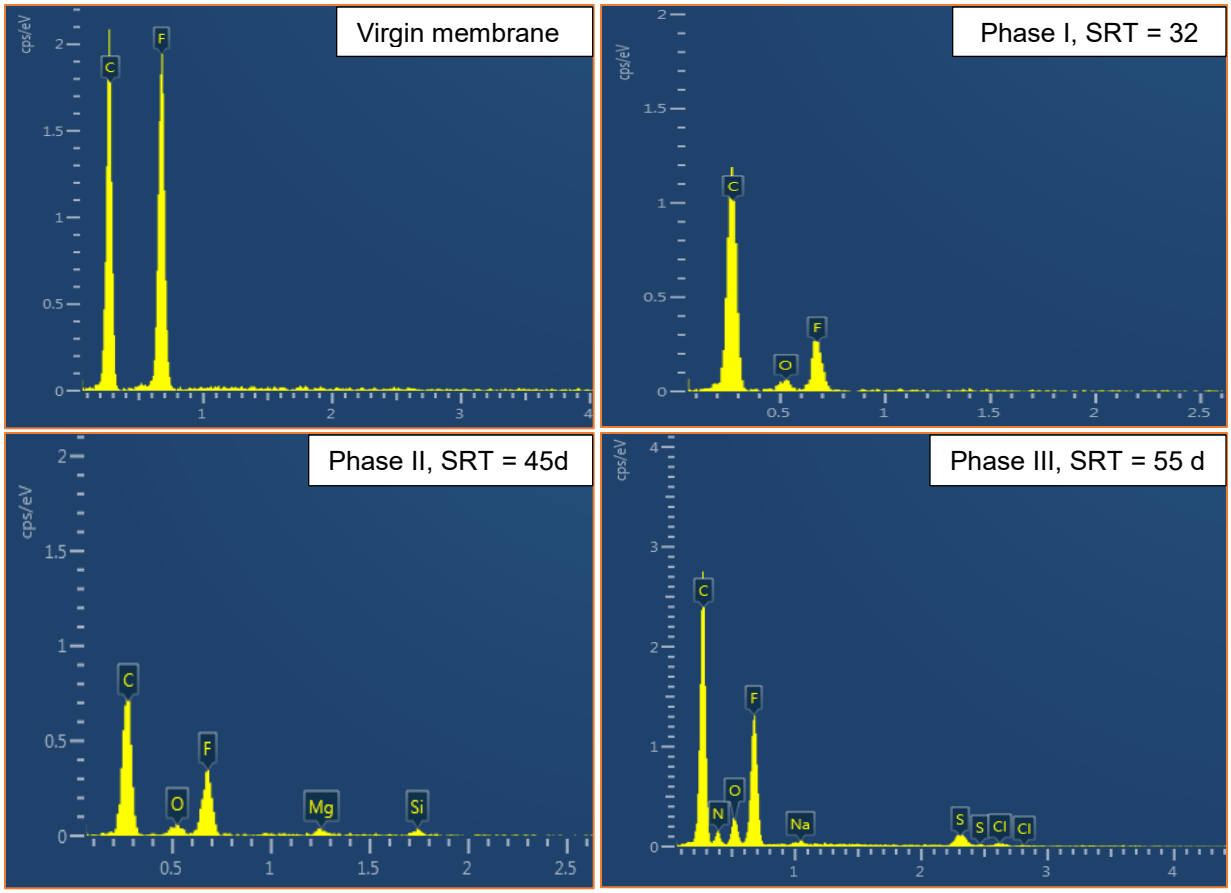

Figure 5.6: EDX elemental analysis of the virgin and used PVDF membranes under various SRTs.

3.4.2. FTIR spectra of virgin and used membranes

FTIR was utilized to describe the chemical nature of the fouling substances that remained on the membrane surface after the cleaning cycles. The FTIR spectra of the new and used membranes are presented in Fig. 5. 7. As presented in Fig. 5. 7, the used and virgin membranes exhibit roughly the same spectral pattern with little difference in intensity in some regions, indicating that the applied cleaning protocol was able to remove most of the fouling material deposited on the membrane surfaces. All membranes (used and virgin) exhibited four large peaks at roughly around 1712, 1240, 1090, and 723 cm^{-1}, which could be attributed to the fingerprints/bands of the PVDF membrane. Puspitasari et al. (2010) assigned peak values between 975 and 1069 to PVDF fingerprint, peak at 1729 to carbonyl peak, and peak at 764 PVDF skeletal bending. However, the used membranes showed an additional large peak at about 2300 cm^{-1} which is markedly different from the spectrum of the virgin membrane. This peak increased with the increase in SRT, which could be credited to the existence of foulants on the surface of the membrane. The absorption peak at a wavelength close to 2300 cm^{-1} has been assigned to the presence of polysaccharides or polysaccharide-like substances (Hu et al., 2016). Also, the intensity of the peak around 723 cm^{-1} was different between the virgin and used membranes, which may indicate that some foulants still remaining on the membranes. It is

evident from these results that the cleaning regime cannot remove all foulants, and these foulants could be counted towards irreversible fouling type. The increased peak intensity with increasing SRT could be attributed to the increased concentration of solids in the reactor due to longer SRT. On the other hand, the virgin membrane has a peak at approximately around 2920 cm^{-1}, this peak is not visible or to an inconspicuous degree in the used membranes, which may indicate deformation of these functional groups of the membrane materials as a result of digestion conditions.

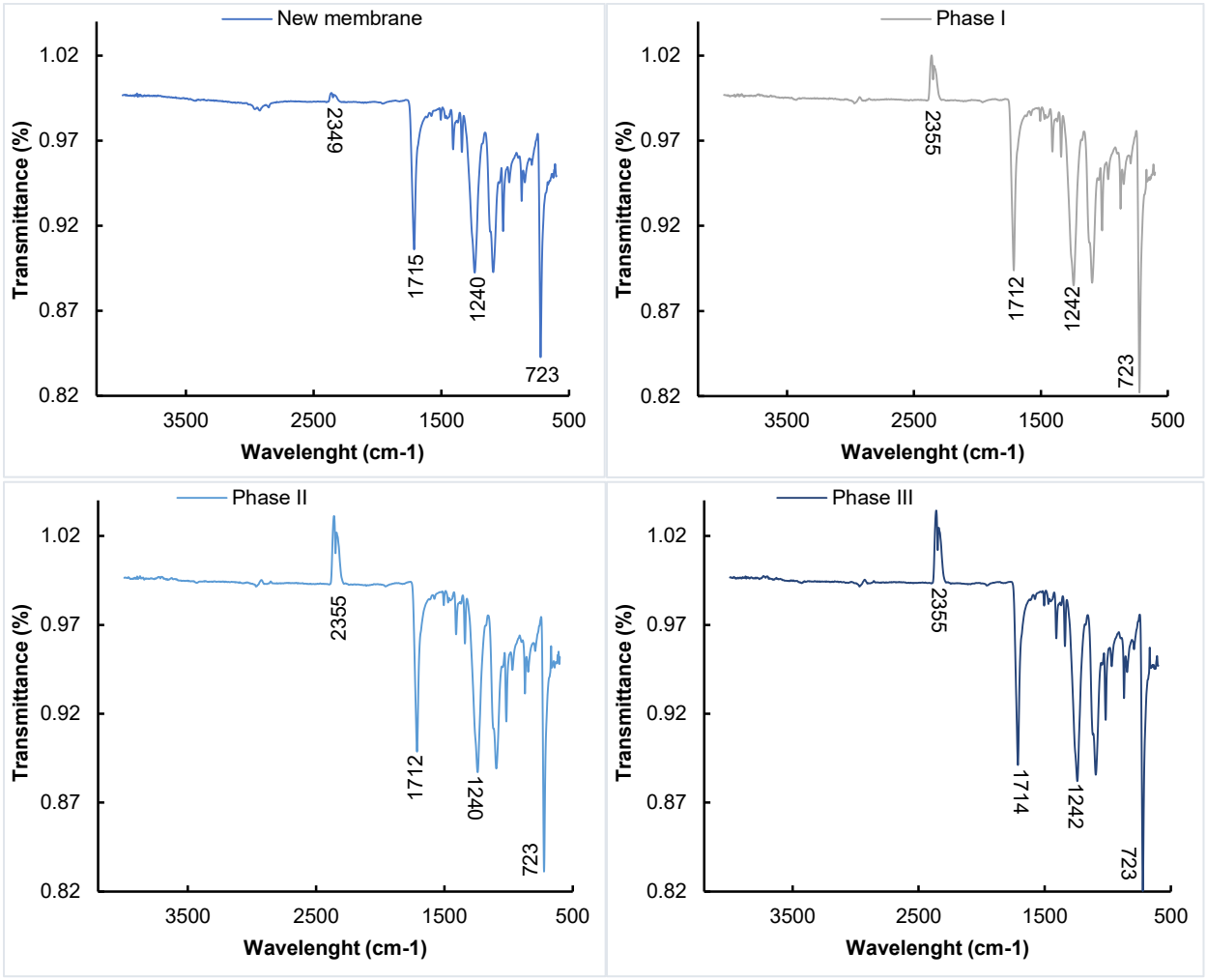

Figure 5.7: FTIR spectra of virgin membrane and membrane used in different phases.

3.6. MLSS properties

3.6.1. Particle size distributions (PSDs)

Particle size distributions (PSDs) of the mixed liquor of the reactor and the membrane loosed gel layer under different operating conditions for AnMBR are shown in Fig. 5. 8 –a-b. The particle size distribution of the MLSS ranged between 0.4 and 1000 µm with a predominant peak at 30.3 µm, while the loose gel layer of the membrane had a similar range of the particle size distribution but peaked at 24 µm and contained

few large size particles. Phase II and III had more large particles (>100 m) compared to phase I. This could be attributed to flocs formation with increased digestion time. Also, the formation of the floc seems to increase progressively with increased SRT (Fig. 5. 8 -a). Most of the gel layer particles lie between 10 and 100 µm with fewer particles less than 10 µm and greater than 100 µm. These results may indicate the tendency of the smaller particle towards deposition on the membrane surfaces. This finding is in agreement with the observations reported by Wang et al. (2008), who found that fine particles in the mixed liquid have a strong deposition tendency on membrane surfaces compared to large particles. It can also be seen that all membranes were fouled with gel layers and the gel layer particles had almost the same shape and size regardless of the applied SRT. This reduced variation might be due to the similarity of biogas sparging intensity among the phases. It can be seen in Fig. 5. 4-a, that 98% of the membrane resistance was induced by these gel layers in all phases tested, reflecting their major role in the fouling mechanism in AnMBR. It should be noted that the particle sizes of MLSS and gel layer are larger than the pores of the employed membrane, which reduces the possibility of membrane fouling due to pore blockage. From this finding, it can be concluded that changing the SRT does not lead to a significant change in the particle size distribution of the MLSS despite its increased concentration with increased SRT. PSD analysis showed that nearly all MLSS and gel layers had sizes greater than 0.4 µm, which correspond to a low pore-clogging potential.

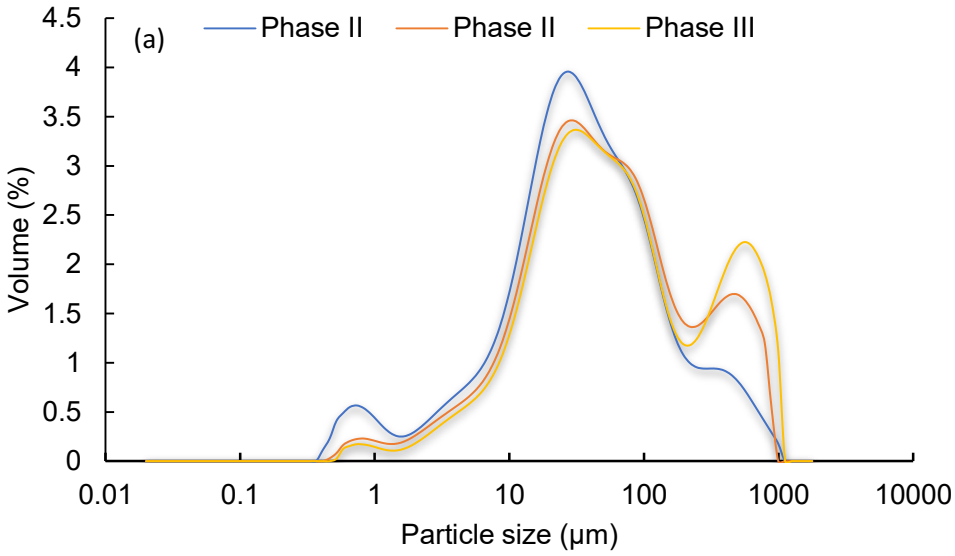

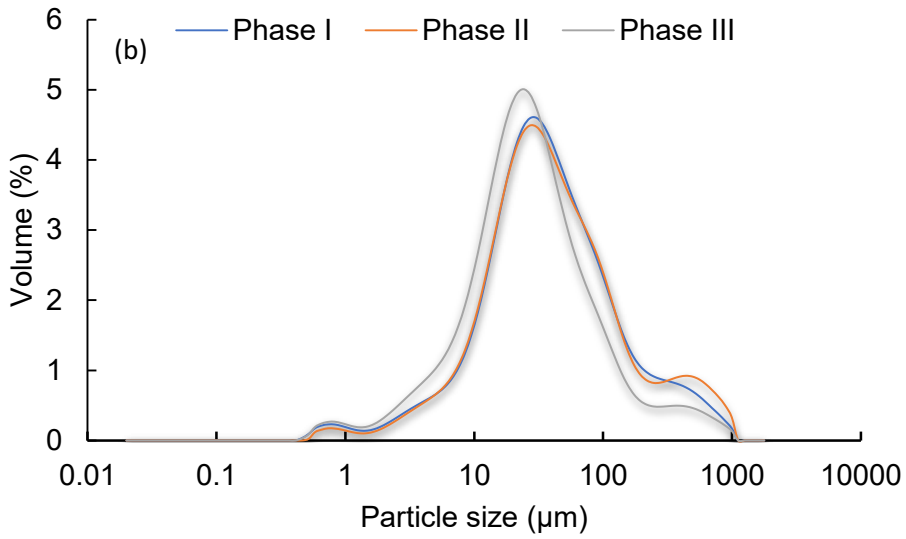

Figure 5.8: Particle size distributions of the reactor mixed liquor and membrane loose gel layer.

3.6.2. Surface properties of MLSS

The effect of sludge retention time (SRT) on the MLSS physicochemical properties (hydrophobicity, dewaterability, and surface charge) was studied. The surface properties and dewaterability of the mixed liquors particles under different SRTs are listed in Table 5.2. It has been reported that surface charge controls the stability of fine particle suspensions (Liao et al., 2001) and the degree to which they are attached to the membrane surfaces (Meng et al., 2006). An increase in the surface charge of reactor sludge can lead to severe membrane fouling (Meng et al., 2006). In this study, the surface charge of sludge ranges from −20 to − 29 mV. The sludge surfaces were more negatively charged in the higher SRTs (45 and 55d) than in the lower SRT (32d). Sabouhi et al. (2020) attributed the increased surface charge of the sludge with increased digestion time to sludge aging and filamentous bacterial growth. This result can explain the deposition of more foulants on the surface of the membrane in phase II and III compared to phase I (Fig. 5. 6). Sludge surfaces were less hydrophobic (smaller contact angle) in the higher SRTs (45 and 55d) than in the lower SRT (32d) (Table 5.2). Other researchers also observed the same trend as sludge at lower SRTs was more hydrophobic than those at higher SRTs (Liao et al., 2001; Yang et al., 2018). Several researchers have linked the hydrophobicity and surface charge of the sludge to the composition and properties of EPS, which is among the main fouling substances in MBR (Liao et al., 2001; Meng et al., 2006). In this study, the MLSS concentration ranged between 17-29 g/L depending on the applied SRT, and the variation of MLSS in the reactor as a function of SRT is shown in Table 5.2. It was found that resistance of membrane fouling increases with increasing MLSS concentration, which increases with increasing SRT. Also, increased MLSS concentration has resulted in more foulants deposition (organic and inorganic) on the membrane surface (Fig. 5. 6). This may be due to the presence of more sludge particles, colloids, and particulate matter.

In this study, sludge dewaterability was also associated with the applied SRTs. The higher SRT has resulted in reduced sludge dewatering capacity and vice versa. The sludge dewaterability ranged between 30 and 49 s in this study, and the higher MLSS concentration at longer SRT and sludge aging may explain the reduced sludge dewaterability.

Table 5.2: Influence of SRT on surface properties and dewaterability of the mixed liquors particles

Items	Phase I	Phase II	Phase III
Zeta-potential (mV)	-20.098±1.71	-27.65±1.56	-29.00±2.18
Contact angle (°)	49.3 – 62.4	28.2 – 42.3	19.1 – 26.7
Dewaterability (s)	29.48±1.98	33.48±0.38	48.57±2.39
MLSS conc. (g/L)	16.55 – 23.02	20.38 – 26.18	26.36 – 28.96

3.6.3. Comparison of SMP

The influence of various SRTs on SMPs content was investigated. The SMP concentrations at the tested conditions are shown in Fig. 5. 9. The total SMP concentration ranged between 30.8 and 49.7 mg/L, while the protein and carbohydrate concentrations were in the range of 20 – 33 mg/L and 10 – 19 mg/L, respectively. The carbohydrate concentration was significantly lower than that of protein. As can be seen from Fig. 5. 9, SMP accumulation in the reactor was more pronounced in the short SRT than in the long SRT. This finding agrees with Duan et al. (2014) who found a greater accumulation of carbohydrates and proteins at short SRT compared to long SRT, but they investigated shorter SRTs (3–10 days) compared to this study (32–55d). Similarly, Liang et al. (2007) observed increased concentrations of SMP as SRT shortened when they studied the effect of different SRTs (10, 20, and 40 days) on the accumulation and composition of SMP. Duan et al. (2014) attributed the increased accumulation of SMP at short SRT to the higher biomass activity in the reactor.

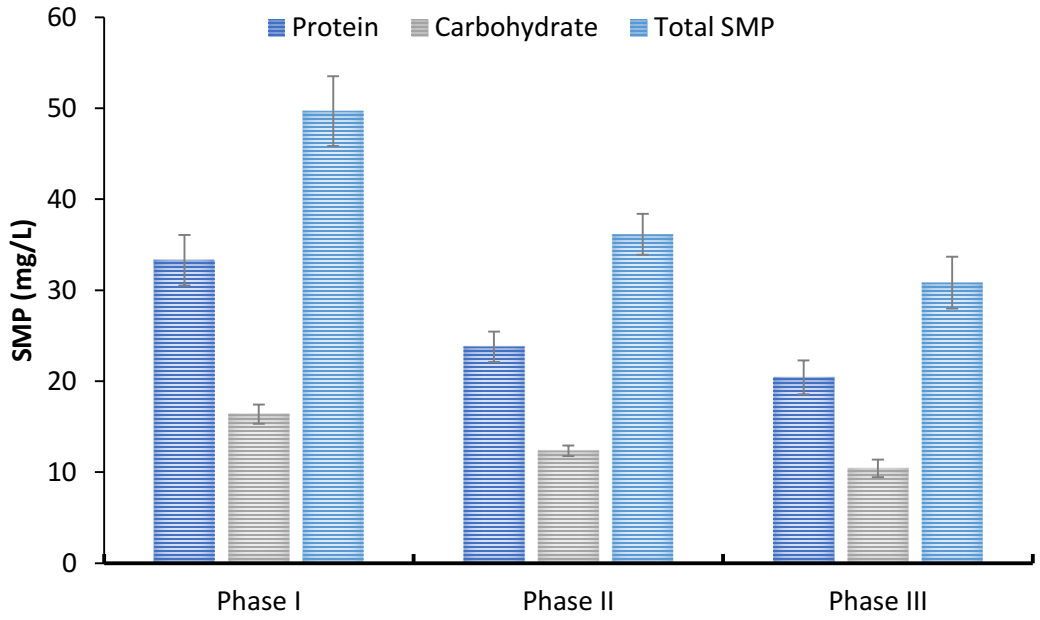

Figure 5.9: Protein, carbohydrate, and total SMP fraction under the tested conditions

3.5.4. Surface analysis by XPS

X-ray photoelectron spectroscopy (XPS) analysis was performed to define the changes in chemical speciation of the used membranes and MLSS in the course of tested conditions. XPS spectra of the membranes and MLSS as well as the binding energy and corresponding mass concentration are presented in Fig. 5.10. The concentration of some elements on the surface of the membrane increased with increasing operating time and lifetime of the sludge in the reactor. For instance, the Si concentration increased by 8.5 % in the first phase and 10.6 % in the second phase, while it was 78.7 % in the last phase. Calcium showed the same pattern, but at different concentrations and percentage changes (6.3 – 93.7 %). Moreover, Zn appeared only in the last phase compared to the other phases. The pattern of XPS data is in agreement with the data pattern presented in Fig. 5. 6 for EDX analysis, where the concentration of both organic and inorganic elements on the surface of the employed membranes increased with increasing operating time and SRT. In respect of MLSS spectra, more elements appeared in the MLSS with increasing SRT and sludge age, reflecting the increased elemental concentration on the membrane surfaces. For example, the elements like Al, Si, Rh, and Na appeared only in the second and third phases, compared to the first phase, which contained a small number and lower proportions of elements. The appearance of more elements with increasing operating time may also explain the increased fouling resistance in the higher SRTs, as shown in Fig. 5. 4. It can be concluded that the longevity of the SRT leads not only to an increase in the concentration of sludge in the system but also to the accumulation of chemical elements that in turn increase the filtration resistance of the membrane.

(a)

Element	Si 2p	S 2p3/2	C 1s	Ca 2p3/2	N 1s	O 1s	F 1s	Na 1s
BE [eV]	100	164	284	346	398	531	686	1070
Mass conc. [%]	0.47	0.07	48.48	0.16	1.75	7.43	41.4	0.25

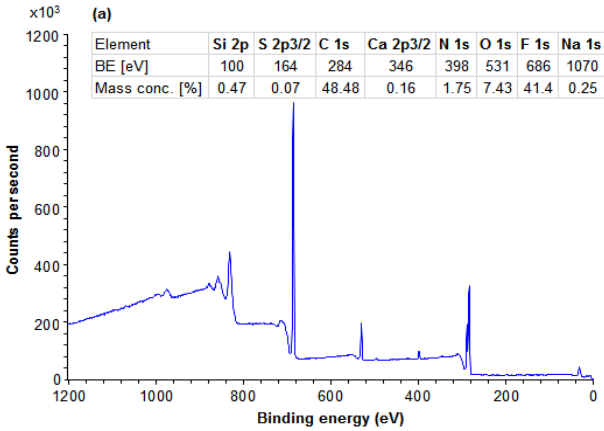

(b)

Element	Si 2p	Cl 2p	C 1s	Ca 2p3/2	N 1s	O 1s	F 1s	Na 1s
BE [eV]	101	197	284	346	399	531	686	1070
Mass conc. [%]	0.51	0.31	46.33	0.27	1.21	6.91	44.16	0.3

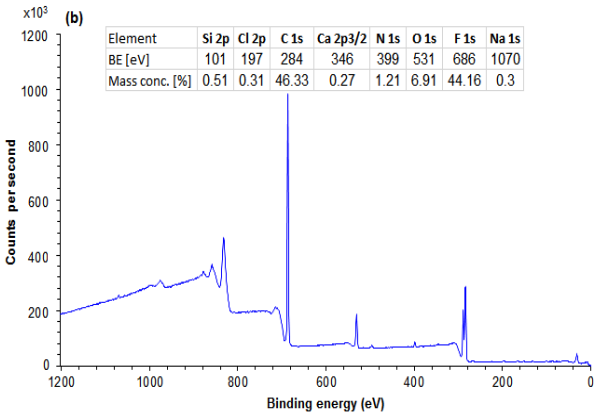

(c)

Element	Si 2p	S 2p	Cl 2p	C 1s	Ca 2p	N 1s	O 1s	F 1s
BE [eV]	101	166	199	284	346	399	531	686
Mass conc. [%]	0.52	0.26	0.44	48.66	0.17	1.46	7.71	40.78

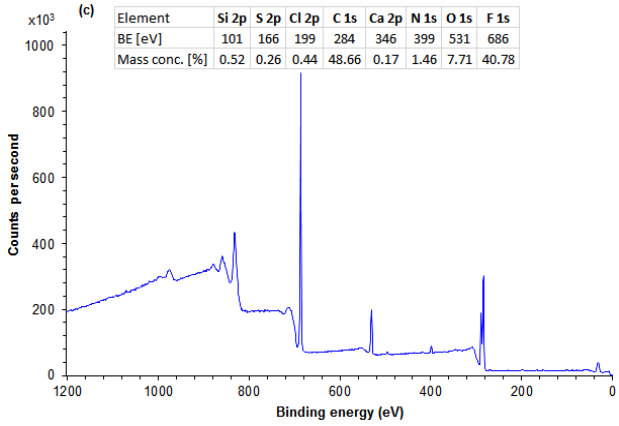

(d)

Element	Si 2p	S 2p	Cl 2p	C 1s	Ca 2p3/2	N 1s	O 1s	F 1s	Zn 2p3/2
BE [eV]	100	167	198	284	346	398	531	686	1021
Mass conc. [%]	0.84	0.73	0.39	50.17	0.31	1.99	10.6	34.56	0.41

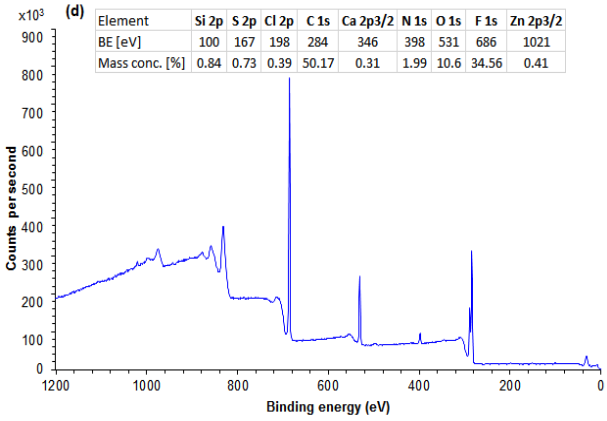

(1)

Element	O 1s	N 1s	Ca 2p	C 1s	S 2p
Binding energy [eV]	532.4	399.4	349.4	285.4	168.4
Mass conc. [%]	1.37	61.90	0.38	6.63	29.72

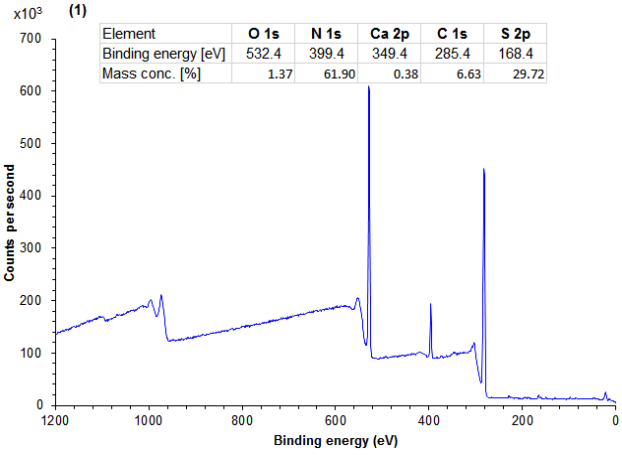

(2)

Element	Al 2s	P 2p	S 2p	Cl 2p	C 1s	Ca 2p	N 1s	O 1s	Na 1s
BE [eV]	119.2	133.2	163.2	198.2	285.2	347.2	399.2	532.2	1071.2
Mass conc. [%]	1.25	2.29	0.96	0.99	58.15	1.80	2.01	31.88	0.69

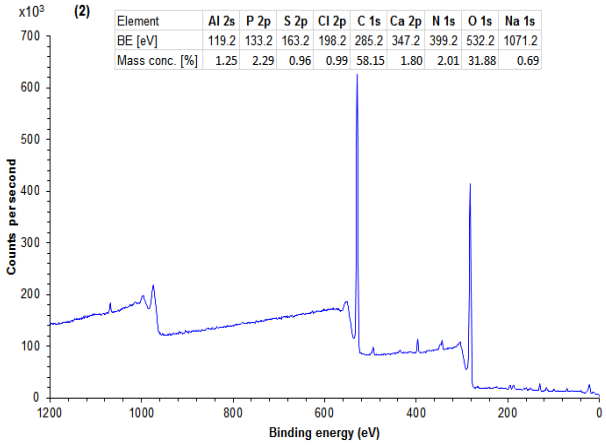

(3)

Element	Si 2p	Al 2s	P 2p	S 2p	Cl 2p	C 1s	Rh 3d	Ca 2p	N 1s	O 1s	Na 1s
BE [eV]	102.6	118.6	132.6	162.6	199.6	284.6	305.6	346.6	399.6	531.6	1071.6
[%]	1.15	1.06	1.05	0.72	0.09	55.05	6.52	1.14	2.31	30.65	0.27

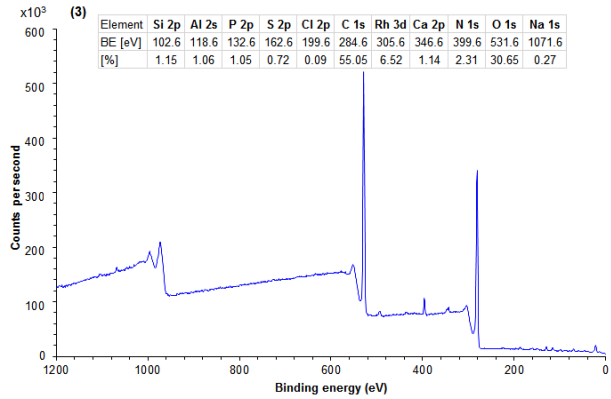

Figure 5.10: XPS spectra of the new membrane (a), used membranes (b-d), and MLSS (1-3) under tested conditions.

4. Conclusion

In this study, long-term anaerobic digestion of primary sludge from a thermomechanical pulping process was performed in a thermophilic submerged anaerobic membrane bioreactor (ThSAnMBR). Different SRTs were investigated, and membrane performance was evaluated. The membrane showed stable performance through the course of this study. The study showed that it is operationally feasible to use AnMBR for primary sludge treatment. MLSS concentration was the predominant factor affecting membrane performance, where there were more fouling species deposited on the surface of the membrane module as the MLSS concentration increased. Also, sludge surface charges increased with increasing sludge age. The smaller particle showed a higher tendency towards deposition on membrane surfaces than the larger particles. Membrane fouling resistance had a strong correlation with MLSS concentration, which increased with increasing SRT. The formation of a loose gel layer on the surfaces of the membrane unit was identified as the predominant type of membrane fouling during the treatment of primary sludge from the pulp and paper industry by AnMBR and accounts for most of the total resistance. EDX, XPS, and FTIR analysis indicate that the foulant materials deposited on the surface of the membrane have diverse compositions of inorganic and organic materials, and the longevity of the SRT leads not only to an increase in the concentration of sludge in the system but also to the accumulation of chemical elements that in turn increase the filtration resistance of the membrane.

References

[1] Abdelrahman, A.M., Ozgun, H., Dereli, K., Isik, O., Ozcan, O.Y., van Lier, J.B., Ozturk, I. Ersahin, M.E., 2020. Anaerobic membrane bioreactors for sludge digestion: Current status and future perspectives. Crit. Rev. Environ. Sci. Technol. 1-39. https://doi.org/10.1080/10643389.2020.1780879.

[2] Ahmed, Z., Cho, J., Lim, B.R., Song, K.G. Ahn, K.H., 2007. Effects of sludge retention time on membrane fouling and microbial community structure in a membrane bioreactor. J. Membr. Sci. 287, 211-218. https://doi.org/10.1016/j.memsci.2006.10.036.

[3] Baek, S.H., Pagilla, K.R. and Kim, H.J., 2010. Lab-scale study of an anaerobic membrane bioreactor (AnMBR) for dilute municipal wastewater treatment. Biotechnol. Bioprocess Eng. 15, 704-708. https://doi.org/10.1007/s12257-009-0194-9.

[4] Baird, Rodger B. Eaton, Andrew D. Rice, Eugene W. 2017. Standard Methods for the Examination of Water and Wastewater, 23rd Edition, American Public Health Association, American Water Works Association, Water Environment Federation, Washington, DC.

[5] Bayr, S., Rintala, J., 2012. Thermophilic anaerobic digestion of pulp and paper mill primary sludge and co-digestion of primary and secondary sludge, Water Res. 46, 4713-4720. https://doi.org/10.1016/j.watres.2012.06.033.

[6] Bokhary, A., Maleki, E., Hong, Y., Hai, F.I., Liao, B., 2020. Anaerobic membrane bioreactors: Basic process design and operation. In: Ngo, H., H., Guo, W., Ng, H., Y., Mannina, G., Pandey A. (Eds.), Current Developments in Biotechnology and Bioengineering. Elsevier. 25-54.

[7] Bokhary, A., Tikka, A., Leitch, M. Liao, B., 2018. Membrane fouling prevention and control strategies in pulp and paper industry applications: A review. J. Membr. Sci. Res. 4, 181-197. DOI: 10.22079/jmsr.2018.83337.1185.

[8] Dagnew, M., Parker, W., Seto, P., 2012. Anaerobic membrane bioreactors for treating waste activated sludge: Short term membrane fouling characterization and control tests. J. Membr. Sci. 421, pp.103-110. https://doi.org/10.1016/j.memsci.2012.06.046.

[9] Dang, H.Q., Price, W.E., Nghiem, L.D., 2014. The effects of feed solution temperature on pore size and trace organic contaminant rejection by the nanofiltration membrane NF270. Sep. Purif. Technol. 125, 43-51. https://doi.org/10.1016/j.seppur.2013.12.043.

[10] Di Bella, G., Di Trapani, D., 2019. A brief review on the resistance-in-series model in membrane bioreactors (MBRs). Membranes, 9, no 2:24. https://doi.org/10.3390/membranes9020024.

[11] dos Reis Ferreira, R.A., da Silva Meireles, C., Assunção, R.M.N., Barrozo, M.A.S., Soares, R.R., 2020. Optimization of the oxidative fast pyrolysis process of sugarcane straw by TGA and DSC analyses. Biomass Bioenerg. 134, p.105456.

[12] Duan, L., Song, Y., Yu, H., Xia, S., Hermanowicz, S.W., 2014. The effect of solids retention times on the characterization of extracellular polymeric substances and soluble microbial products in a submerged membrane bioreactor. Bioresour. Technol. 163, 395-398. https://doi.org/10.1016/j.biortech.2014.04.112.

[13] Duncan, J., Bokhary, A., Fatehi, P., Kong, F., Lin, H., Liao, B., 2017. Thermophilic membrane bioreactors: A review. Bioresour. Technol. 243, 1180-1193. https://doi.org/10.1016/j.biortech.2017.07.059.

[14] Dvořák, L., Gómez, M., Dolina, J., Černín, A., 2016. Anaerobic membrane bioreactors—a mini review with emphasis on industrial wastewater treatment: applications, limitations and perspectives, Desalination Water Treat. 57, 19062-19076. https://doi.org/10.1080/19443994.2015.1100879.

[15] Hamza, R.A., Zaghloul, M.S., Iorhemen, O.T., Sheng, Z., Tay, J.H., 2019. Optimization of organics to nutrients (COD: N: P) ratio for aerobic granular sludge treating high-strength organic wastewater. Sci. Total Environ. 650, 3168-3179. https://doi.org/10.1016/j.scitotenv.2018.10.026.

[16] Hu, Y., Wang, X.C., Yu, Z., Ngo, H.H., Sun, Q., Zhang, Q., 2016. New insight into fouling behavior and foulants accumulation property of cake sludge in a full-scale membrane bioreactor. J. Membr. Sci. 510, 10-17. https://doi.org/10.1016/j.memsci.2016.02.058.

[17] Huang, Z., Ong, S.L., Ng, H.Y., 2011. Submerged anaerobic membrane bioreactor for low-strength wastewater treatment: effect of HRT and SRT on treatment performance and membrane fouling. Water Res. 45, 705-713. https://doi.org/10.1016/j.watres.2010.08.035.

[18] Jiang, S., 2018. Thermophilic anaerobic membrane bioreactor for pulp and paper sludge treatment (Master dissertation), Lakehead University Knowledge Commons.

[19] Keller, M., Panglisch, S., Gimbel, R., 2017. Measuring hydraulic layer resistance and correlated effects in colloidal fouling of salt-retaining membranes. Water Science and Technology: Water Supply, 17, 985-997. https://doi.org/10.2166/ws.2016.181.

[20] Liang, S., Liu, C., Song, L., 2007. Soluble microbial products in membrane bioreactor operation: behaviors, characteristics, and fouling potential. Water Res. 41, 95-101. https://doi.org/10.1016/j.watres.2006.10.008.

[21] Liao, B.Q., Allen, D.G., Droppo, I.G., Leppard, G.G., Liss, S.N., 2001. Surface properties of sludge and their role in bioflocculation and settleability. Water Res. 35, 339-350. https://doi.org/10.1016/S0043-1354(00)00277-3.

[22] Liao, B.Q., Kraemer, J.T., Bagley, D.M., 2006. Anaerobic membrane bioreactors: applications and research directions. Crit. Rev. Environ. Sci. Technol. 36, 489-530. https://doi.org/10.1080/10643380600678146.

[23] Liao, B.Q., Lin, H.J., Langevin, S.P., Gao, W.J. and Leppard, G.G., 2011. Effects of temperature and dissolved oxygen on sludge properties and their role in bioflocculation and settling. Water Res. 45, 509-520. https://doi.org/10.1016/j.watres.2010.09.010.

[24] Lin, H., Peng, W., Zhang, M., Chen, J., Hong, H., Zhang, Y., 2013. A review on anaerobic membrane bioreactors: applications, membrane fouling and future perspectives. Desalination, 314, 169-188. https://doi.org/10.1016/j.desal.2013.01.019.

[25] Lin, H.J., Xie, K., Mahendran, B., Bagley, D.M., Leung, K.T., Liss, S.N., Liao, B.Q., 2009. Sludge properties and their effects on membrane fouling in submerged anaerobic membrane bioreactors (SAnMBRs). Water Res. 43, 3827-3837. https://doi.org/10.1016/j.watres.2009.05.025.

[26] Lin, H.J., Xie, K., Mahendran, B., Bagley, D.M., Leung, K.T., Liss, S.N., Liao, B.Q., 2009. Sludge properties and their effects on membrane fouling in submerged anaerobic membrane bioreactors (SAnMBRs). Water Res. 43, 3827-3837. https://doi.org/10.1016/j.watres.2009.05.025.

[27] Lopes, A.D.C.P., Silva, C.M., Rosa, A.P., de Ávila Rodrigues, F., 2018. Biogas production from thermophilic anaerobic digestion of kraft pulp mill sludge. Renew. Energy. 124, 40-49. https://doi.org/10.1016/j.renene.2017.08.044.

[28] Luna, H.J., Baeta, B.E.L., Aquino, S.F.D., Susa, M.R., 2014. EPS and SMP dynamics at different heights of a submerged anaerobic membrane bioreactor (SAMBR). Process Biochem. 49, 2241-2248. https://doi.org/10.1016/j.procbio.2014.09.013.

[29] Mahmoud, I., Liao, B., 2017. Effects of sludge concentration and biogas sparging rate on critical flux in a submerged anaerobic membrane bioreactor. J. Water Process. Eng. 20, 51-60. https://doi.org/10.1016/j.jwpe.2017.09.012.

[30] Masselin, I., Chasseray, X., Durand-Bourlier, L., Lainé, J.M., Syzaret, P.Y., Lemordant, D., 2001. Effect of sonication on polymeric membranes. J. Membr. Sci. 181, 213-220. https://doi.org/10.1016/S0376-7388(00)00534-2.

[31] Meabe, E., Déléris, S., Soroa, S., Sancho, L., 2013. Performance of anaerobic membrane bioreactor for sewage sludge treatment: Mesophilic and thermophilic processes. J. Membr. Sci. 446, 26-33. https://doi.org/10.1016/j.memsci.2013.06.018.

[32] Meng, F., Zhang, H., Yang, F., Zhang, S., Li, Y., Zhang, X., 2006. Identification of activated sludge properties affecting membrane fouling in submerged membrane bioreactors. Sep. Purif. Technol. 51, 95-103. https://doi.org/10.1016/j.seppur.2006.01.002.

[33] Ng, T.C.A., Xu, B., Ng, H.Y., 2020. Challenges and opportunities for anaerobic membrane bioreactors. In Current Developments in Biotechnology and Bioengineering (pp. 55-77). Elsevier.

[34] Orhon, D., Sözen, S., Teksoy Basaran, S., Alli, B., 2016. Super fast membrane bioreactor—transition to extremely low sludge ages for waste recycle and reuse with energy conservation. Desalin. Water. Treat. 57, 21160-21172. https://doi.org/10.1080/19443994.2015.1127781.

[35] Padmasiri, S.I., Zhang, J., Fitch, M., Norddahl, B., Morgenroth, E., Raskin, L., 2007. Methanogenic population dynamics and performance of an anaerobic membrane bioreactor (AnMBR) treating swine manure under high shear conditions. Water Res. 41, 134-144. https://doi.org/10.1016/j.watres.2006.09.021.

[36] Pileggi, V., Parker, W.J., 2017. AnMBR digestion of mixed WRRF sludges: Impact of digester loading and temperature. J. Water Process. Eng. 19, 74-80. https://doi.org/10.1016/j.jwpe.2017.07.011.

[37] Pollice, A., Laera, G., Saturno, D., Giordano, C., 2008. Effects of sludge retention time on the performance of a membrane bioreactor treating municipal sewage. J. Membr. Sci. 317, 65-70. https://doi.org/10.1016/j.memsci.2007.08.051.

[38] Puspitasari, V., Granville, A., Le-Clech, P., Chen, V., 2010. Cleaning and ageing effect of sodium hypochlorite on polyvinylidene fluoride (PVDF) membrane. Sep. Purif. Technol. 72, 301-308. https://doi.org/10.1016/j.seppur.2010.03.001.

[39] Richards, C., O'Connor, N., Jose, D., Barrett, A. and Regan, F., 2020. Selection and optimization of protein and carbohydrate assays for the characterization of marine biofouling. Anal. Methods, 12, 2228-2236. DOI: 10.1039/D0AY00272K.

[40] Sabouhi, M., Torabian, A., Bozorg, A., Mehrdadi, N., 2020. A novel convenient approach toward the fouling alleviation in membrane bioreactors using the combined methods of oxidation and coagulation. J. Water Process. Eng. 33, p.101018. https://doi.org/10.1016/j.jwpe.2019.101018.

[41] Smith, A.L., Stadler, L.B., Love, N.G., Skerlos, S.J., Raskin, L., 2012. Perspectives on anaerobic membrane bioreactor treatment of domestic wastewater: a critical review. Bioresour. Technol. 122, 149-159. https://doi.org/10.1016/j.biortech.2012.04.055.

[42] Tikka, A., Gao, W., Liao, B., 2019. Reversibility of membrane performance and structure changes caused by extreme cold water temperature and elevated conditioning water temperature. Water Res. 151, 260-270. https://doi.org/10.1016/j.watres.2018.12.047.

[43] Wang, K.M., Martin Garcia, N., Soares, A., Jefferson, B., McAdam, E.J., 2018. Comparison of fouling between aerobic and anaerobic MBR treating municipal wastewater. H_2Open Journal. 1, 131–159. https://doi.org/10.2166/h2oj.2018.109.

[44] Wang, Z., Wu, Z., Yin, X., Tian, L., 2008. Membrane fouling in a submerged membrane bioreactor (MBR) under sub-critical flux operation: membrane foulant and gel layer characterization. J. Membr. Sci. 325, 238-244. https://doi.org/10.1016/j.memsci.2008.07.035.

[45] Xu, M., Wen, X., Yu, Z., Li, Y., Huang, X., 2011. A hybrid anaerobic membrane bioreactor coupled with online ultrasonic equipment for digestion of waste activated sludge. Bioresour. Technol. 102, 5617-5625. https://doi.org/10.1016/j.biortech.2011.02.038.

[46] Yang, L., Ren, Y.X., Chen, N., Cui, S., Wang, X.H., Xiao, Q., 2018. Organic loading rate shock impact on extracellular polymeric substances and physicochemical characteristics of nitrifying sludge treating high-strength ammonia wastewater under unsteady-state conditions. RSC Advances, 8, 41681-41691. DOI: 10.1039/C8RA08357F.

[47] Yu, H., Wang, Z., Wu, Z., Zhu, C., 2016. Enhanced waste activated sludge digestion using a submerged anaerobic dynamic membrane bioreactor: performance, sludge characteristics and microbial community. Sci. Rep. 6, 20111. https://doi.org/10.1038/srep20111.

Chapter VI

Effect of Organic Loading Rate on the Biological Performance of the Thermophilic Anaerobic Membrane Bioreactor Treating Pulp and Paper Primary Sludge

Abstract

Waste-to-energy or value-added products have been increasingly considered in many pulp and paper mills (PPMs) worldwide. However, developing appropriate conversion technologies is a major challenge in transforming PPMs wastes into biofuels or value-added biomaterials. In the present study, a long term (320 d) anaerobic digestion of primary sludge of a thermomechanical pulp mill (TMP) was carried out for the first time in a thermophilic anaerobic membrane bioreactor (ThAnMBR). Effect of organic loading rate (OLR) in the range of 2.5–6.8 kg-COD/m^3 d and hydraulic retention times (HRT) of 3–8 d on the process performance was investigated. Under various OLRs, stable biogas productions were obtained, and the best results were achieved with lower OLR (2.5 kg-COD/m^3 d) and higher HRT (8 d), at biogas yields of 189 L biogas/kg MLSS fed. However, it was found that the biogas production and sludge biomass degradation decrease when the organic loading rate increases. The proportion of sludge reduction ranged from 28.9 to 46.7% depending on the applied OLRs. Despite varying OLRs, stable membrane performance was obtained, where the required membrane flux was easily maintained during the reactor operation. In this study, also the properties of digestate and membrane permeates were studied under different operating conditions, and they fluctuated to some extent with OLR. ThAnMBR is a promising new technology for pulp and paper mill primary sludge treatment.

Keywords: Biogas production; biological performance; primary sludge, anaerobic digestion; membrane bioreactor.

---

1. Introduction

Pulp and paper mill sludge (PPMS) represents a large part of the industrial waste and contains a high portion of the organic matter (Elliott and Mahmood, 2012). Sludge waste is produced from both virgin and recycled paper production processes (Simão et al., 2018). However, this substrate is usually undesirable and needs to be treated or disposed of in an environmentally acceptable manner. The common handling strategies of the waste sludge are landfilling, incineration, and recycling in the paper making process. The first two practices place a significant financial burden on the forestry industry because of the high capital expenses and high energy required to dry large amounts of water before burning the waste sludge (Meyer et al., 2018). Reportedly, sludge disposal takes a large part of the wastewater treatment facility budget (≈ $30 per wet ton), which may reach approximately 60% of the total cost (Elliott and Mahmood 2012; Park et al. 2012). In addition to the high expenses, these traditional handling approaches have been characterized by several problems such as air (incineration) and water (landfill leachate) pollution. Conversely, PPM sludge contains valuable molecules (25–75% carbohydrate). For example, Kraft PPM primary sludge is composed of woody materials such as cellulose (58 wt%), hemicelluloses (12 wt%), and lignin (20 wt%), along with inorganic materials that have been used in the pulping process (Bayr and Rintala 2012).

Bokhary, A., Leitch, M. and Liao, B., 2021. Effect of Organic Loading Rate on the Biological Performance of the Thermophilic Anaerobic Membrane Bioreactor Treating Pulp and Paper Primary Sludge. Journal of clean technologies and environmental policy.

While, the secondary sludge is composed of microbial biomass, cellulose (36–50 wt%), and non-degradable lignin's compounds (19–44 wt%) (Likon and Trebše 2012; Kinnunen et al. 2015). The quantity of sludge production varies depending on the pulping processes, but primary sludge represents the majority of the total solids compared to secondary sludge (Bajpai, 2015). The application of traditional sludge treatment processes leads to the loss of these precious resources accompanied by environmental pollution (Bayr et al., 2013; Hazarika and Khwairakpam, 2018).

Several technologies, including direct combustion (Manwatkar et al., 2012; Pio et al 2020a), pyrolysis (Yin et al., 2021), gasification (Pio et al., 2020b), hydrothermal liquefaction (Zhang et al., 2021), processes have evolved to convert sludge waste into fuels. Besides power generation, these technologies were characterized by reducing the volume of sludge, destroying harmful pathogens, and stabilizing heavy metals (Liew et al., 2012). However, the high initial investment cost and requirements for the pre-dewatering process hamper their wide application (Liew et al., 2012). Among the treatment alternatives, one strategy that has been recognized worldwide as a feasible option to improve the energy efficiency of PPM sludge is anaerobic digestion (AD). Anaerobic digestion (AD) offers a promising alternative relative to the above-mentioned options due to its reduced environmental footprint, small reactor size, and requires no sludge dewatering, where sludge dewatering represents a considerable economic burden. Also, the residual organic matter and nutrients that are retained in effluents (digestate) can be returned and reused for different applications (Veluchamy and Kalamdhad, 2017a).

The substrate's content of sugar, fat, and protein controls its anaerobic digestion potential and energy production; accordingly, PPM sludge appears an appropriate substrate for AD due to high carbohydrate and high-water content. Also, one of the attractive features of PPM sludge is that the raw material cost is zero, no excessive pre-treatment is required due to previously processed biomass, and the possibility of using the existing pulp or paper mill equipment (Gurram et al. 2015). AD has been applied extensively and for a wide range of organic substrates. Nonetheless, the literature shows very limited studies treating PPM sludge as an anaerobic digestion substrate. Yet, studies on PPM sludge digestion are in their infancy and no industrial application has been reported to date. This may be due to long residence times (20–60 d), low yield of bio-methane and bio-hydrogen because of its low degradability (30–50%) (Lin et al. 2009; Kinnunen et al. 2015), plus the biomass separation problems of the traditional anaerobic digestion processes (Dereli et al., 2012). Additionally, effluent quality from anaerobic treatment is usually poorer than that from aerobic treatment and needs further polishing. This defect might limit the application of anaerobic technology, especially in places that require wastewater reclamation and reuse, such as an integrated forest biorefinery (IFB), where the resulting wastes and by-products are recycled and utilized as a resource.

Compared to traditional anaerobic digestion, the anaerobic membrane bioreactor (AnMBR) a combination of anaerobic digestion and membrane filtration, is a relatively new technology for the treatment of municipal and industrial wastes but has demonstrated its superiority over conventional anaerobic biological processes in terms of higher effluent quality for reuse/reclamation, recovery of the most of potential energy in biodegradable waste streams, and decoupling of solids retention time (SRT) from hydraulic retention time (HRT) (Bokhary et al. 2020). By integrating the membrane process for microbial biomass retention, anaerobic microorganisms can proliferate without being washed out of the system. This leads to higher biomass concentration in AnMBR, which may enhance biogas yield compared to conventional processes. Also, decoupling the HRT and SRT in AnMBRs can achieve a significant reduction in reactor volumes, thereby reducing capital costs. Thus, AnMBR could be a promising option for primary sludge digestion. However, to the authors' knowledge, no study has ever been reported on the treatment of pulp and paper primary sludge using thermophilic anaerobic membrane bioreactor (ThAnMBR) technology. Of the few experimental studies involving conventional anaerobic digestion of PPM sludge, only two studies tested PPM primary sludge (Jokela et al. 1997; Bayr and Rintala 2012), while other studies focused on the treatment of secondary sludge, or sludge mixtures (Karlsson et al. 2011; Lin et al. 2011; Saha et al. 2011; Bayr and Rintala 2012). Most PPM sludge studies have been conducted at mesophilic temperatures using batch assays, but few have been conducted in thermophilic conditions (Teghammar et al. 2012; Lopes et al. 2018). Bayr and Rintala (2012) examined AD of kraft mill primary sludge under thermophilic conditions using a semi-continuous bioreactor (CSTR) but at relatively long HRTs and low OLRs. OLR is an essential parameter and limited information is available about the steady-state performance of the ThAnMBR for biogas production under high OLRs.

Taking into account all the advantages of AnMBR mentioned above, the current research program focuses on the application of a relatively new ThAnMBR technology for biogas production from primary sludge of thermomechanical pulp (TMP) aiming for improving biogas yield and solids reduction and reducing HRT without the risk of washing out the microbial population. This study aimed to investigate the possibility of performing AD of TMP primary sludge at low HRT and high OLRs. Of interest is elucidating an optimal organic loading rate that maximizes bio-methane production and solids reduction, minimizes membrane fouling propensity, and produces permeate with suitable quality for reuse in a pulp and paper biorefinery.

2. Materials and methods

2.1. Feed and inoculum

PPM sludge was obtained from a local Canadian thermomechanical pulp mill. Sludge received from this mill was dewatered sludge from a primary clarifier. The mill uses a mixture of hardwood and softwood as raw materials for pulp production. After delivered to the laboratory, the collected PPMS was stored in the

refrigerator at 4°C before being prepared and used as a substrate. Primary sludge was mixed with tap water to create a slurry with a certain concentration as a feeding substrate. As primary sludges are relatively low in nitrogen and phosphorus (Hagelqvist 2013), ammonium chloride and dipotassium phosphate were added in COD: N: P of 100:2.6:1 ratio to improve its nutrients content. Table 6.1 shows the characteristics of the primary sludge and inoculum used in this study. The inoculum was collected from a thermophilic anaerobic membrane bioreactor operated for one year by a member of our research group (Jiang, 2018), and the system was treating secondary sludge from the local pulp and paper mill.

2.2. Laboratory scale submerged AnMBR setup and operation

The submerged AnMBR setup consists of a CSTR reactor with an active volume of 6.5 L and a flat sheet microfiltration (MF) membrane module with an active surface area of 0.03 m^2 (10 cm × 15 cm on each side of the module) and pore size of 0.1µm. The membrane material was a polyvinylidene fluoride (PVDF) (DAFU Membrane Technology Co., P.R. China). The bioreactor temperature was maintained at 50±1°C by circulating the warm water from an adjustable water bath through the water jacket of the reactor. The pH of the bioreactor was controlled at 7.2 ± 0.1 using a NaOH solution. For reactor feeding, the sludge was pumped into the bottom of the bioreactor by a feeding pump (Iwaki Magnet Pump, Iwaki co., LTD. Tokyo Japan). The pump was controlled by a water level sensor (Madison Co., USA), and controller (Flowline, USA) to maintain a constant liquid level in the bioreactor. Figure 6. 1 shows a schematic diagram of the ThAnMBR setup used in this study. After feeding the reactor with the required amount of inoculum and primary sludge, it was flushed with nitrogen gas for 5 min to create anaerobic conditions. Permeate was withdrawn from the system using a peristaltic pump (Masterflex C/L®, Cole-Parmer, Montreal, Canada), and collected in its tank for further analysis. The peristaltic pump was controlled by a timer that operated in three minutes on and two minutes off mode. Transmembrane pressure was monitored with a pressure gauge (Omega, model 656201BA4CD3ACD1. Korea). To sustain the required SRT, reactor sludge was taken out from CSTR once a day during the daily measurement of the biogas production rate, reactor pH, and TSS of digestate.

For fouling control, the membrane was sparged by biogas. This was accomplished using a stainless-steel pipe diffuser placed below the membrane unit on each side, and the biogas was recirculated by two gas recycling pumps (Masterflex Console Drive, Model 7520-40, Thermo Fisher Scientific, USA). The biogas sparging rate was fixed at 3.76 ±0.08 L/min during the experiments by adjusting the digital pump speeds. At the bottom of the reactor, a gentle mixing was applied using a magnetic stirrer blade (Barnstead Thermolyne, Cimarec Plate Stirrer, Dubuque, IA, USA) to keep the reactor in suspension. For biogas composition measurement, the biogas samples were taken from the top reactor's port, while the biogas produced was collected in a graduated cylinder using a water displacement method. The reactor was

operated at OLRs between 2.5 and 6.8 kg-COD/m^3 d and hydraulic retention times (HRTs) in the 3–8 d range.

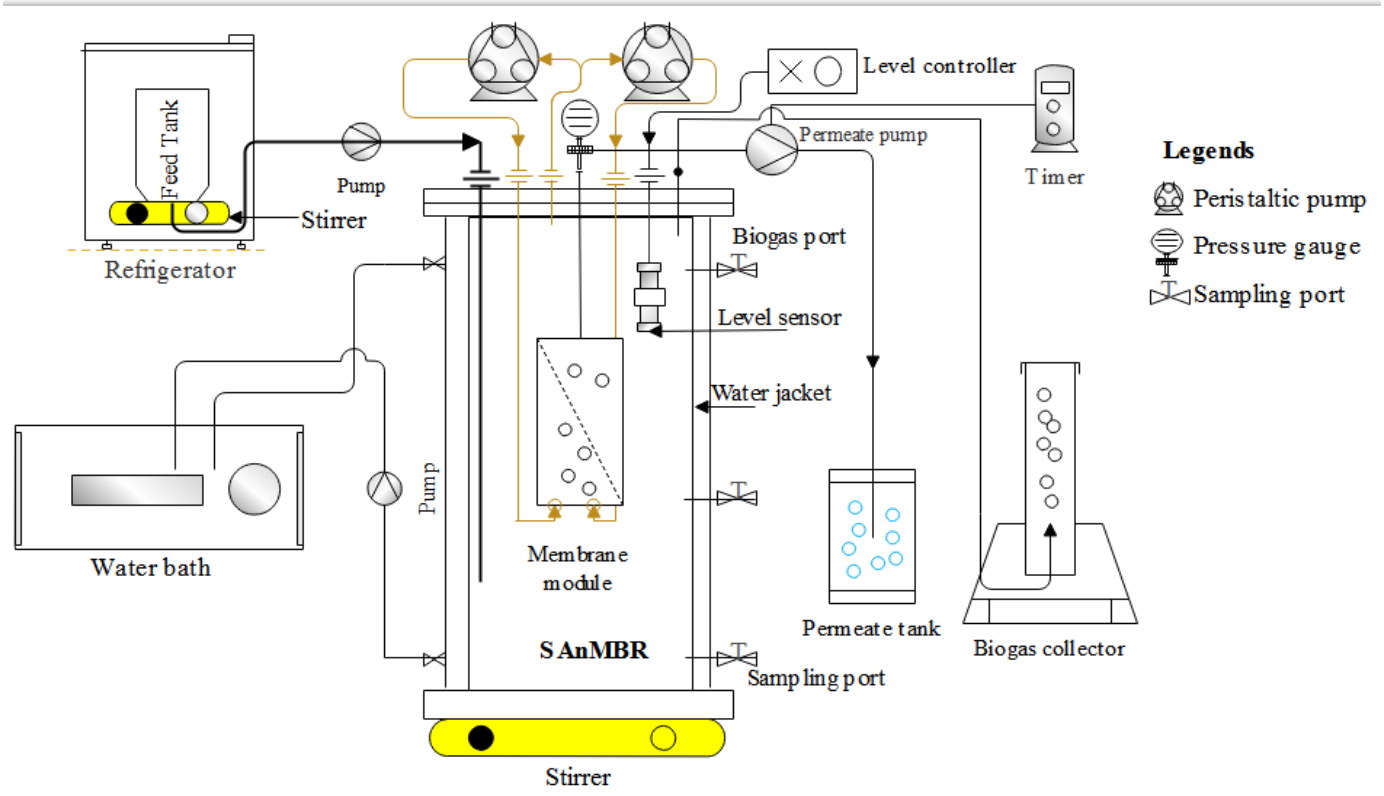

Figure 6.1: a schematic diagram of the SAnMBR setup

2.3. Analytical methods

2.3.1. Primary sludge samples, reactor feeds, and inoculum

Primary sludge was characterized for total solids (TS), total suspended solids (TSS), and volatile solids (VS) according to standard methods (Baird et al. 2017). TSS of the reactor feed and digestate was analyzed three times a week, while pH was monitored daily. Total COD of the permeate and feed were analyzed every alternate week, using HR COD test vials (K-7365, 0–1500 ppm) and a COD reactor (Hanna Instruments), followed by absorbance measurement using a colorimeter (Hach DR 2800 Spectrophotometer). Ash content in the sludge sample was measured after dry oxidation of PS at 575 °C using a muffle furnace, according to standard methods for biomass analysis (Cai et al., 2017). The pH was measured using Oakton pH 700 benchtop meter. Elemental composition (C, N, H, S, and O) was measured by an elemental analyzer (Elementar Vario EL). The inoculum was analyzed for TS, TSS, VS, COD, ash, pH, and elemental content as per the methods mentioned previously. Table 6.1 shows the results of the primary sludge, feed, and inoculum characterization. Air dry primary sludge contains 96.32±0.28 % total solids, 93.93±0.24% volatile solids, and 6.07±0.244 % fixed solids. The reduction of TSS and VSS is

usually used as an indicator of the biodegradation efficiency of sludge. There is a linear relationship between SCOD solubilization and VSS reduction (Zhang et al., 2013). Where the high the solubilization of COD, the higher is the reduction of VSS.

Table 6.1: Characteristics of the primary sludge and thermophilic inoculum used in this study.

Item	Unit	Primary sludge	Thermophilic inoculum
TSS	(g/L)	11.54±0.42	36.63±0.31
TS	(g/L)	11.80±0.65	39.62±0.43
VS	(%TS)	93.93±0.24	83.48±0.37
C	(%TS)	41.69±8.29	43.66±0.60
H	(%TS)	6.19±0.60	5.82±0.29
O	(%TS)	42.16±2.4	–
N	(%TS)	0.15±0.07	3.25±0.10
S	(%TS)	0.05±0.03	1.02±0.11
C/N		285.60	13.43
TCOD	(g/L)	20.078±1.865	47.66±1.04
Soluble COD	(g/L)	0.194±0.010	1.150±0.100
Ash	(%)	3.61±0.37	16.52±0.38
pH		7.2±1	6.99±0.030

– = indicates not measured values

2.3.2. Biogas production and composition

The biogas production rate was measured daily throughout the experimental period using the water displacement method and graduated cylinder, and then the biogas yields were calculated as weekly averages. Whereas biogas composition (methane, nitrogen, and carbon dioxide) was measured by a gas chromatography system (Shimadzu, GC-2014, Kyoto Japan). The biogas samples were taken from the headspace of the bioreactor using a 5 ml syringe and injected in the GC system equipped with a thermal conductivity detector (room temperature + 10°C to 400°C), a silica gel packed column, and injectors. Helium was used as an equipment carrier gas at a flow rate of 30 mL min $^{-1}$ (digital setting by electronic flow controller (AFC)). Samples were injected at room temperature via a single packed injector to determine the composition. The composition was measured every two days throughout the experimental period.

2.3.3. Permeate quality and digestate properties

COD of the permeate was measured according to the standard protocols (APHA, 2005) every other week. MLSS was measured three times a week and monitored throughout the experimental period. Elemental composition (C, N, H, S, O) of digestates were analyzed by Elementar Vario EL (GmbH, Hanau, Germany). Chemical element concentrations of the permeate were measured by the ICP-AES (Inductively coupled plasma atomic emission spectroscopy) elemental analyzer. NanoBrook Zeta PALS Analyzer (Brookhaven Instruments Corp, USA) was used to analyze the zeta potential of digestates suspension. Structural changes and degradation of primary sludge components after anaerobic digestion were studied by Bruker Tensor 37

Fourier Transform Infrared (FT-IR) Spectrophotometer. Digestates dewaterability was measured by Capillary Suction Time (CST) (Triton Electronics Ltd., Bigods Hall, Dunmow, UK), using CST filter paper and a 1cm sludge funnel. Some measurements were performed throughout the experimental period, others were made in triplicate, and results were reported as means ± standard deviations.

2.3.4. Particle size distributions

Mastersizer 2000 Particle Size Analyzer (Malvern Instruments Ltd. Worcestershire, UK) was used for the measurement of the particle size distributions of the mixed liquor and feed samples. It consists of an optical bench (to collect raw data), dispersion units (for sample preparation/delivery), and a standalone computer unit that runs Malvern software. This instrument uses laser diffraction or low light angle scattering and can measure particle sizes in the range of 0.02 to 2000 microns using a single optical measurement path. The mastersizer detects the scattered light, which is a combination of two light sources, by a detector that is used to measure across the particle size range and converts a signal to size. This device measures each sample three times automatically and calculates the average.

3. Results and discussion

3.1. Effect of OLR on biological performance and stability

The biological performance was determined in this study based on biogas productivity/composition, permeate quality/digestate properties, and solids reduction. Table 6.2 shows the operating conditions of ThAnMBR. The experiment was divided into three phases as shown in Table 6.2. Phase I was operated at HRT of 5 d and OLR of 3.7 kg-COD/m^3 d, while phases II and III were operated at HRTs of 3 and 8 d and OLRs of 6.8 and 2.59 kg-COD/m^3 d, respectively. This study aims to test the feasibility of the primary sludge digestion under relatively higher organic loading rates and lower HRTs. Regarding the primary sludge studies, Bayr and Rintala (2012) studied primary sludge digestion under hydraulic retention times (HRT) in the range of 16-32 d, which is relatively high compared to the current study. Likewise, Veluchamy and Kalamdhad (2017b) investigated pulp and paper mill sludge digestion under HRT of 45 d.

All phases of this study were run at a constant solid retention time of 32 d. In all phases, the primary sludge was introduced as a sole substrate to examine its biogas potential and solids reduction. At the end of each phase, the reactor was shut down, and the membrane was taken out for characterization. To initiate each phase, the reactor was mixed, and a new membrane module installed, then, the required HRT and OLR were set up. Each phase lasted for more than 3 months, once the reactor biogas production and MLSS concentration were stable, the reactor was shifted into the next operating conditions, as shown in Figure 6. 2 (a–c). The system was operated in three different organic loading environments by changing the HRT (flow rate) while maintaining a constant SRT for the process.

Table 6.2: Digestion conditions of the primary sludge in AnMBR.

Phase	Duration (d)	Temperature (°C)	Average permeate flux L/m^2.hr.	Feed COD (g/L)	Feed TS (g/L)	SRT (d)	HRT (d)	OLR (kg-COD/m^3 d)
I	1 – 94	50±1	2.43±0.20	19.39±1.22	11.57±0.74	32	5	3.73±0.35
II	99 – 206	50±1	4.59±0.28	20.61±1.49	11.59±0.30	32	3	6.84±0.89
III	212 – 323	50±1	1.48±0.11	19.76±1.01	11.48±0.14	32	8	2.55±0.19

3.1.1. Biogas production and composition

Reportedly, optimal biogas yield is a result of appropriate reactor design and enhanced growth of methanogens forming bacteria, which in turn depends on the favorable operating environment (e.g., the optimal amount of feedstock (OLR), temperature, and HRT). Biogas production and percentage of biogas composition of different operating conditions studied are presented in Figure 6. 2 (a–c). Reactor performance was studied at different OLR ranges from 2.5 to 6.8 kg-COD/m^3 d. The best results were obtained at higher HRTs and lower organic loading rates. At the beginning of each phase, a slight decrease in biogas yield was observed but the system soon recovered and adapted to new conditions over time. The average biogas production rate of the reactor for loading rates of 3.7±0.4, 6.8±0.9, and 2.5±0.1 kg COD/ m^3 d was observed as 0.96, 1.14, and 1.6 L/d, respectively (Figure 6. 2 a). Best biogas productivity was achieved at OLR 2.5 kg COD/ m^3 d and HRT 8 d. The biogas production at 2.5 kg COD/ m^3 d OLR was about two times higher than that at 3.7 kg COD/m^3 d OLR. The system showed a decrease in biogas production with an increased loading rate. The increased solids content can be outside the capacity of microorganisms to handle it due to the recalcitrant nature of the primary sludge. A decrease in biogas production with an increase in OLR is observed in many previous findings. For example, Gou et al. (2014) observed an approximately 43% decrease in CH_4 yield when the OLR increased from 1 to 6 g VS/L/day, during the co-digestion of waste activated sludge with food waste in a thermophilic system. Hassan et al. (2015) reported a similar result when anaerobically treated recycled paper mill effluent by a hybrid baffled reactor. The biomass degradation was also decreased as OLR increased. Several studies have shown similar findings. For example, Mel et al. (2015) reported a reduced COD degradation as the organic loading increased. This can be attributed to the recalcitrant property of the primary sludge, which requires a longer residence time, and the overloading of the system. These results illustrate that it is not feasible to operate the system under the high solids rate of the primary sludge, and OLR 2.5 kg COD/m^3 d and HRT 8 d may be consider optimum and can be suggested as design criteria for PS treatment. Different optimal OLRs are reported for anaerobic digestion of organic wastes, but this result is similar to results obtained by Liu et al. (2017) when they treated food waste under a thermophilic condition and an optimum OLR of 2.5 was reported. Figure 6. 2b shows biogas yield based on the amount of the feed suspended solids added. The

average biogas production obtained during phase I at OLR of 3.7 kg COD/m^3 d was approximately 53 L biogas/kg MLSS fed, however when the OLR increased to 6.8 kg COD/m^3 d in phase II this resulted in a decreased biogas production of 45 L biogas/kg MLSS fed. However, when OLR was reduced to 2.5 kg COD/m^3 d in phase III this resulted in an improved biogas production of 155 L biogas/kg MLSS fed. The biogas production at phase II is corresponding to biogas production of 45 m^3/t $VS_{removed}$, which is reported by Jokela et al. (1997) for primary sludge from the TMP mill using the Biochemical Methane Potential (BMP) test. For comparison, the reported biogas yield for Kraft pulp mill primary sludge under the same operating temperature (thermophilic conditions) was higher than the biogas yield from the thermomechanical pulp mill reported in this study. For example, Bayr and Rintala (2012) reported 190–230 m^3CH_4/tVS_{fed} methane yields for primary sludge from bleached Kraft mill under OLR of 1–1.4 kgVS/m^3 d and HRT of 16–32 d using CSTR. The OLR used in this study showing excellent biogas production rate was 2-2.5 times of the OLR used in the study of Bayr and Rintala (2012), demonstrating the advantages of the THAnMBR, as compared to conventional CRTR. Differences in biogas production can be attributed to the different pulping conditions between the Kraft and TMP plants, as well as the resulting sludge. In the TMP process, the fibers are produced by thermal treatment followed by mechanical refining, while the kraft process involves treating the wood chips with a hot mixture containing water, NaOH, and Na_2S, known as white liquor. Hence, kraft fiber is flexible and easily degradable fiber compared to TMP fiber. Also, the surface of the kraft fibers contains less amounts of lignin and extractives than the TMP fibers, and the wood extractives are well known inhibitory compounds for biological processes.

Under the steady-state, the methane content of the biogas was around 55.5± 5.78%, while, carbon dioxide and nitrogen content were 31.3±6.3 and 13.2±5.6, respectively (Figure 6. 2c). No significant change in the methane content was observed with the change in the solid loading rate, but the profile of the biogas production rate was different. The methane content achieved in this study was close to the results of most lignocellulosic treatment studies. It has been reported that the percentage of methane and carbon dioxide in biogas is largely dependent on the feedstock processed as well as the duration and extent of bio-methanation over the retention period (Kavuma 2013). The relatively high CO_2 content in the produced biogas of this study can be a result of the presence of acidifying microorganisms in methanogens, which causes the accumulation of volatile fatty acids in the process (Wijekoon et al., 2011; Franke-Whittle et al., 2014). Usually, a high VFAs concentration reduces the pH value in the reactor and prevents methane formation due to the inhibition of the methanogenesis process.

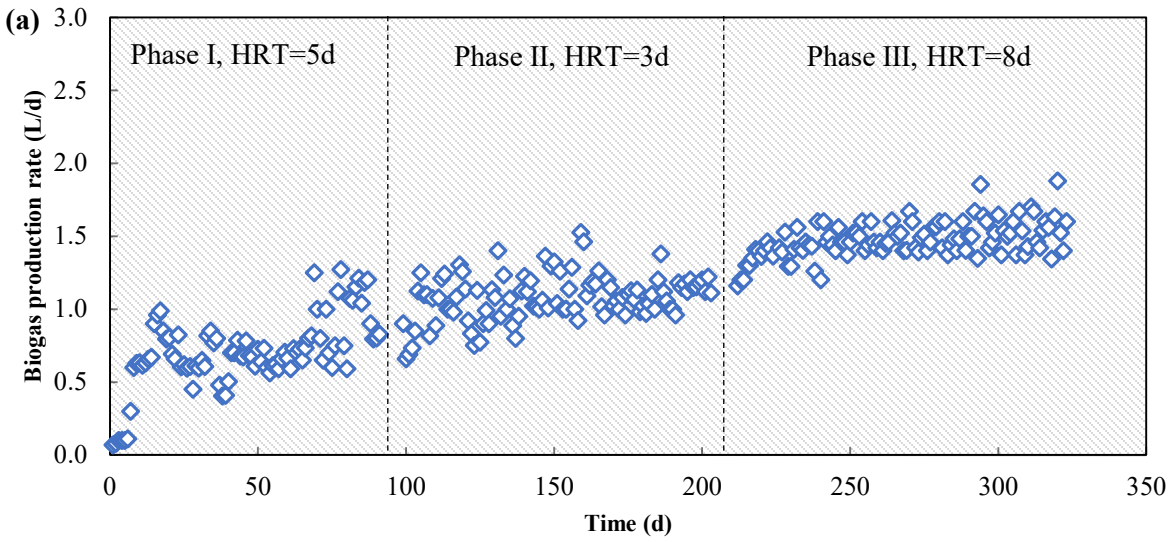
(a)
Phase I, HRT=5d
Phase II, HRT=3d
Phase III, HRT=8d
Biogas production rate (L/d)
3.0
2.5
2.0
1.5
1.0
0.5
0.0
0
50
100
150
200
250
300
350
Time (d)

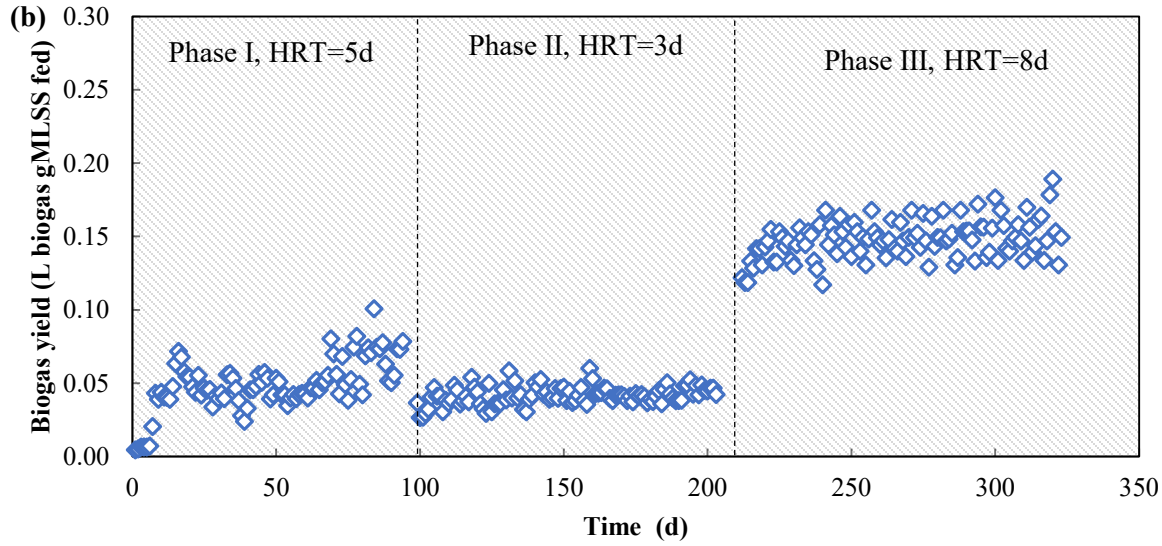
(b)
Phase I, HRT=5d
Phase II, HRT=3d
Phase III, HRT=8d
Biogas yield (L biogas gMLSS fed)
0.30
0.25
0.20
0.15
0.10
0.05
0.00
0
50
100
150
200
250
300
350
Time (d)

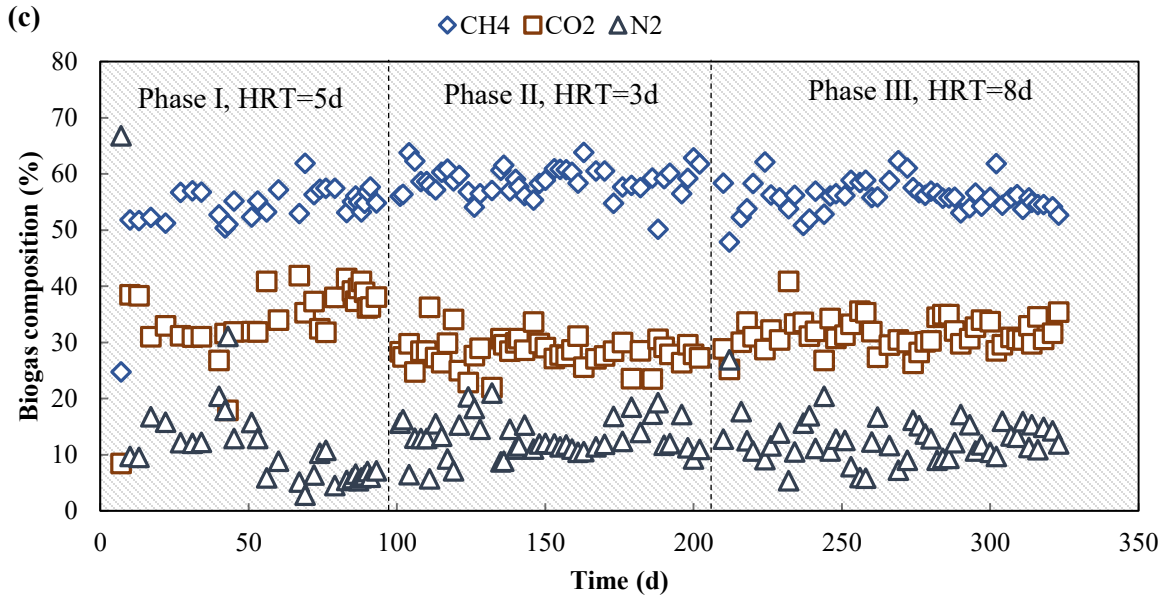

Figure 6.2: (a) Biogas production rate (b) biogas yield based on the amount of the feed suspended solids added (c) percentage of biogas composition at different organic loading rates over digestion time.

3.1.2. Permeate quality.

The effect of OLRs on effluent (permeate) characteristics was evaluated in this study. The effluent properties were analyzed in terms of COD concentration, pH, and chemical element concentrations. Effluent COD and chemical element concentrations have fluctuated to some extent with OLRs in the experiment. In the first phase, the average effluent COD was 1.67±0.46 g/L at OLR of 3.7 kg-COD/m^3 d while the average concentration of the COD in the second and third phases were 0.70±0.34 and 0.32±0.11 g/L at OLRs of 6.8 and 2.59 kg-COD/m^3 d, respectively. As can be seen from Figure 6. 3, the COD of the effluent fluctuated slightly in the first phase, which could be due to the beginning of the acclimatization of microorganisms to the new environment and the addition of the inoculation substance (inoculum). Thereafter, the COD concentration stabilized and varied between 0.16 g/L and 0.6 g/L throughout the experimental period. This trend has also been reported in other studies, for example, Lin et al. (2011) reported a high COD value (800 mg/L) in the initial start-up period and a low COD value (425 mg/L) during the stable-state process of the submerged anaerobic membrane reactor (SAnMBR). A similar pattern was observed by Hafuka et al. (2019), they reported a gradual decrease in the effluent COD concentration in the range of 840 – 240 mg/L. Sato et al. (2016) reported COD values in the effluent in the range of 510 - 251 mg/L for a membrane bioreactor treating sludge biomass. Hafuka et al. (2019) attributed the high COD concentration of the membrane filtrate in early operating time to the high concentration of soluble-COD of the seed sludge. The soluble COD of inoculum (seed sludge) was 1.2 g/L in this study, which could also be linked to the high COD concentration in the first phase. COD concentration decreased with increasing

operating time can also be attributed to an increase in biological activity in the reactor (high degradation rate).

On the other hand, the OLR has shown some influence on the effluent COD, where the lower OLR was associated with a lower COD concentration. This may indicate that the high solid loading rate is not fully digested by the reactor microorganisms. It is worth noting that the COD of the effluent at the lower OLR was to a certain extent stable compared to the higher OLRs. Higher effluent COD with higher OLRs was also reported in other research works. For example, Boonyungyuen et al. (2014) reported 132.0±4.3 mg/L effluent COD concentration for OLR of 0.52 kg/m^3 d compared to 84.4±10.2 mg/L for OLR of 0.13 kg/m^3 d, when they treated textile wastewater by MBR. Wijekoon et al. (2011) attributed the higher permeate concentration to the increased generation of volatile fatty acid (VFA) on the reactor with increased OLR, and they achieved VFA removal efficiency in descending order of 96%, 94%, and 82% for OLRs of 5, 8, and 12 kg COD/m^3 d, respectively. In this study, the pH of the effluent ranged from 7.2 to 7.4, which is in the methanogenic range indicating the stability of the system. Concentrations of chemical elements differed slightly between the tested conditions (Table 6. 3), where the permeates of the shorter HRTs had more concentrations of phosphorus, copper, sodium, and potassium, compared to the longer HRT permeate. However, the remaining elements did not differ greatly between the varied operating conditions.

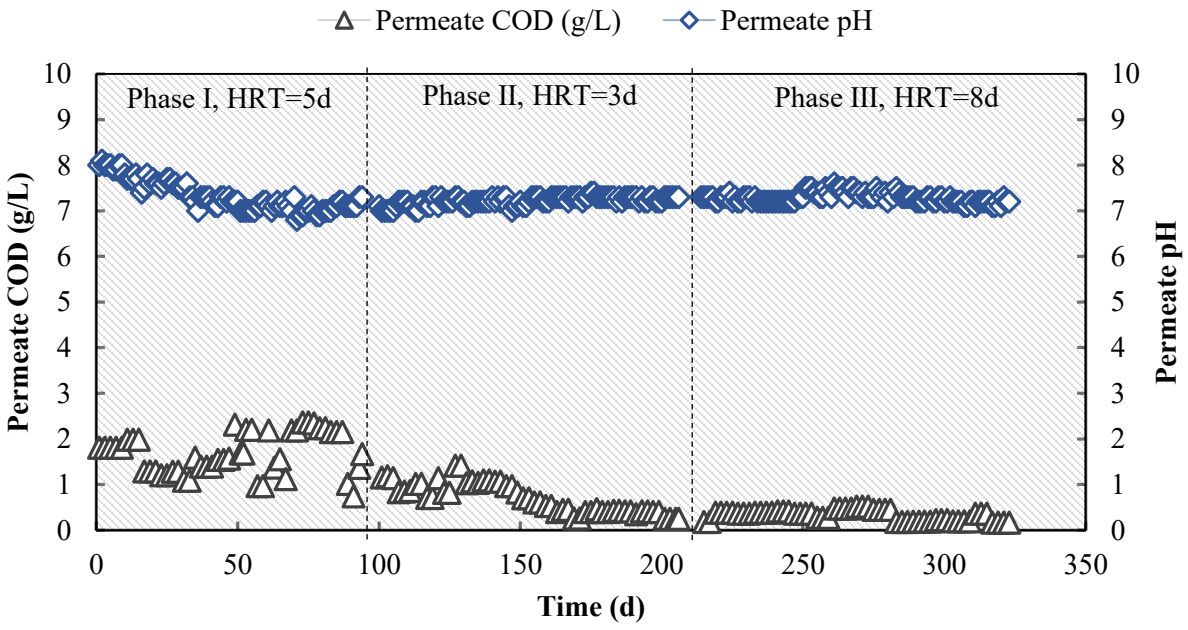

Figure 6.3: Permeate COD and pH under the tested conditions over digestion time.

Table 6.3: Effluent characteristics under different SRTs

Description	Minimum detection limit (MDL)	Permeate properties at different HRTs		
		5d	3d	8d
Macronutrients (mg/L)				
Phosphorus	0.05	100.5	100.7	73.83
Sulfur	0.3	34.27	50.4	70.93
Micronutrients (mg/L)				
Iron	0.005	0.039	0.044	0.084
Cobalt	0.002	< 0.002	< 0.002	< 0.002
Nickel	0.03	< 0.03	< 0.03	< 0.03
Zinc	0.001	0.0023	0.0023	< 0.001
Copper	0.002	0.0073	0.0043	<0.0027
Manganese	0.001	0.034	0.040	0.057
Molybdenum	0.05	<0.05	<0.05	<0.05
Selenium	0.05	<0.05	<0.05	<0.05
Common cations (mg/L)				
Sodium	0.03	505	403.33	346.67
Potassium	0.5	167	145	117.33
Calcium	0.01	11.99	9.10	12.23
Magnesium	0.01	3.16	2.92	3.49
Lead	0.03	< 0.03	< 0.03	< 0.03
Aluminum	0.03	< 0.03	< 0.03	< 0.03
Barium	0.04	< 0.04	< 0.04	< 0.04
Chromium	0.002	0.0053	< 0.002	< 0.003
Tin	0.05	< 0.05	< 0.05	< 0.05
Strontium	0.01	0.023	< 0.01	0.017
COD (mg/L)		**1.7±0.46**	**0.70±0.34**	**0.32±0.11**
pH		**7.3±0.3**	**7.2±0.1**	**7.3±0.1**

3.1.3. Digestates properties

The performance of the system was assessed also by taking into consideration the digestate properties under different operating conditions of ThAnMBR. Figure 6. 4 shows the concentrations of MLSS (mixed liquor suspended solids), FSS (Feed suspended solids), and reactor pH upon changing of different OLRs in the reactor. The MLSS concentrations for the reactor ranged from 16 to 28 g/L. The first phase showed fluctuation in MLSS concentration, which could be due to microorganisms' acclimatization (Fig. 6. 4). In the second phase, the MLSS concentration increased from 20 to 24 g/L due to the increased organic loading rate (from 3.7 to 6.8 kg COD/m^3 d) and stabilized at about 26 g/L throughout the phase time. However, when the OLR was reduced to 2.5 kg COD/m^3 d in the third phase, the MLSS concentration remained stable and high. The reason for this was the accumulation of sludge on the wall of the reactor at the liquid and biogas interface in the second phase, the falling of the accumulated headspace sludge on the bioreactor at the end of the second phase resulted in a higher MLSS concentration in the following phase (third phase). The sludge accumulated in the headspace of the reactor in the second phase due to the high OLR coupled with reactor sparging by biogas for fouling control. The latter blow-out the sludge into the reactor headspace

and then the sludge accumulates on the headspace and between the fittings. Although a drop in MLSS concentrations was expected due to reduced OLR, the MLSS concentration in the third phase ranged between 25 and 26.5 g/L because of the aforesaid reasons, and no major fluctuation was seen, as shown in Figure 6. 4.

In this study, the total solids of the treated sludge were 11.80±0.65, and NH_4Cl and K_2HPO_4 were added as nutrients to the feed to meet the COD:N:P ratio of 100:2.6:1. At this concentration, the bioreactor can be easily fed with the sludge substrate using a magnetic drive centrifugal pump (Iwaki magnetic pump). It has been reported that there is an optimal concentration of TS content in raw materials and usually ranges between 1–10% and that the volume of the produced biogas diminishes by reducing and increasing the TS concentration portion below and above the optimum value (Yavini et al. 2014; Dhar et al. 2016). The pH profile of the reactor during the experimental time is shown in Figure 6. 4. The pH of the system ranged between 7.2 and 7.5 in this study. Reportedly, the pH values and temperature regime have a direct impact on biogas production. Methanogens have been reported to grow better in the pH range 6.8-7.5, which is favorable for biogas production. However, the anaerobic digester process can tolerate a range of 6.5 to 8.0 (Cioabla et al. 2012). On the other hand, lower pH levels may lead to a complete reactor failure by inhibiting the CH_4-forming bacteria.

Table 6.4 shows the properties of digestate under different operating conditions. The average soluble COD for digestates was 0.188, 0.326, and 0.153 g/L in phase I, II, and III, respectively. The soluble COD of the digestate was higher in the third phase compared to the first (HRT, 5 d) and second (HRT, 8 d) phases. This may be due to the short HRT (3 d), which corresponds to the highest OLR (6.8 kgCOD/m^3 d). Elemental composition (C, N, H, and S) was analyzed by an elemental analyzer. As can be seen from Table 6.4, there is no significant difference in C, N, H, and S concentrations between the tested OLRs. However, nitrogen concentration decreased slightly with increasing digestion time. It can be concluded from Table 6.4 that digestates contain high carbon sources and low nutrient sources. Thereby, for the further valorization of this digestate via bioconversion processes, the value of these two crucial elements needs to be optimized for improved microorganisms' growth and degradation rate. As indicated in Table 6.4, the weekly average of the biogas yield ranged between 0.061 and 0.095 L biogas/g $MLSS_{removed}$ in the first phase and ranged between 0.045 and 0.059 in the second phase. Whereas the biogas yield in the third phase was in the range of 0.316 – 0.339 095 L biogas/g $MLSS_{removed.}$

Solid's reduction ratio is an important parameter in anaerobic digestion of sludge. The reduction of the sludge biomass ranged from 28.9 to 46.7 % in this study, depending on the applied OLRs. Sludge biomass degradation efficiency decreased with increasing OLR. Sludge biomass reduction was 45.5% at the OLR of 3.7 kg COD/m^3 d but was markedly reduced to 28.9 % when the OLR increased to 6.8 kg COD/m^3 d.

While the solids reduction in the reactor varied between 46.13 and 46.7% for the OLR of 2.5 kg COD/m^3 d. This result was in similarity to the previously reported results for MBRs. For example, Sato et al. (2016) achieved about 47.4% sludge biomass reduction when reduced the OLR from 0.45 to 0. 225 kg COD/m^3 d, using pilot-scale MBR. Using conventional bioreactors, Lin et al. (2009) reported cellulose degradation efficiency in the range of 21.8 to 65% for pulp and paper sludge, but no pronounced change was observed for lignin degradation even after NaOH pretreatment, indicating the low degradability of the lignin. Bayr and Rintala (2012) achieved cellulose removal efficiency in the range of 70–73% after anaerobic digestion of pulp and paper primary sludge with overall volatile solids (VS) removal between 25 and 40% (similar to the results from this study), but hemicellulose did not degrade much compared to cellulose with a degradation efficacy between 7 and 27%. Kinnunen et al. (2015) reported VS removal between 11 and 26% for pulp and paper industry bio-sludge, which is similar to the finding (9–23% VS removal) reported by Saha et al. (2011) for pulp and paper mill secondary sludge. Thus, for improved organic matter degradation, pretreatment of the sludge substrate could be recommended.

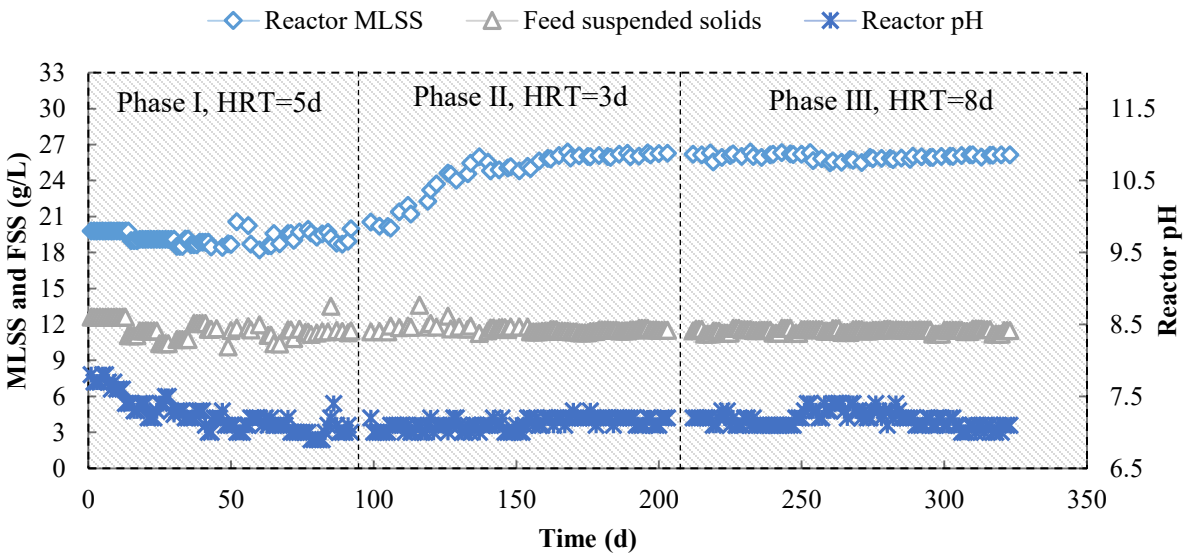

Figure 6.4: Mixed liquor suspended solids (MLSS) and pH of the digester and the suspended solids of the feeding substrate (FSS).

Table 6.4: Digestates properties under different operating conditions of anaerobic digestion of pulp and paper mill primary sludge in thermophilic AnMBR.

Component	Digestate characteristics at different phases		
	Phase I	Phase II	Phase III
Days	1 – 94	99 – 206	212 – 323
OLR (kgCOD/m^3d)	3.7	6.8	2.5
HRT (d)	5	3	8
SRT (d)	32.5	32.5	32.5

Nitrogen addition [a]	yes	yes	yes
Phosphorus addition [b]	yes	yes	yes
VS (%)	90.18±0.39	92.83±1.2	92.35±0.64
Fixed solids (%)	9.82±0.38	7.17±1.2	7.65±0.65
SCOD (g/l)	0.188±0.007	0.326±0.009	0.153±0.058
Biogas yield (L biogas/g MLSS $_{removed}$)	0.095	0.059	0.334
Average methane conc. (%)	55	58.7	56
Solid reduction (%)	45.5±0.74	28.9±0.02	46.13±0.95
C (%)	45.22±1.26	45.59±0.70	45.07±1.20
H (%)	5.98±0.50	5.94±0.15	6.01±0.48
N (%)	0.86±0.18	0.79±0.24	0.75±0.15
S (%)	0.29±0.08	0.25±0.06	0.24±0.07
C/N	52.58	57.71	60.09
pH	7.2±0.10	7.2±0.05	7.2±0.09

[a] NH_4Cl
[b] KH_2PO_4

3.1.4. Particle size distribution

The particle size distribution (PSD) measurement of the digestates is shown in Fig. 6. 5. The PSD of the digestates did not vary greatly with different operating conditions (OLRs), as they ranged between 1 and 1000 microns. The second phase contained larger particles (peaked at about 500 microns) than the other phases, possibly due to the higher loading rate (OLR, 6.8 kg COD/m^3 d). The other phases had OLRs in the range of 2.5 – 3.7 kg COD/m^3 d. All phases showed a similarly low amount of small particles, which peaked at about 0.8 μm. The average size of the digestates of the different phases was around 30 μm. On the other hand, the size of the digestates molecules did not appear to have any clear effect on the membrane pores blocking, and this may be due to their large sizes. The employed membrane has a pore size of 0.1μm, and it is well known that when the pore size is relatively small, fouling may result mainly from the foulants adsorption. It has been reported that when foulants are similar or smaller than the pores of the membrane, adsorption and pore-blocking mechanisms occur; however, when the foulants are greater than the pores of the membrane, a cake layer will likely form on the surface of the membrane (Bokhary et al. 2018).

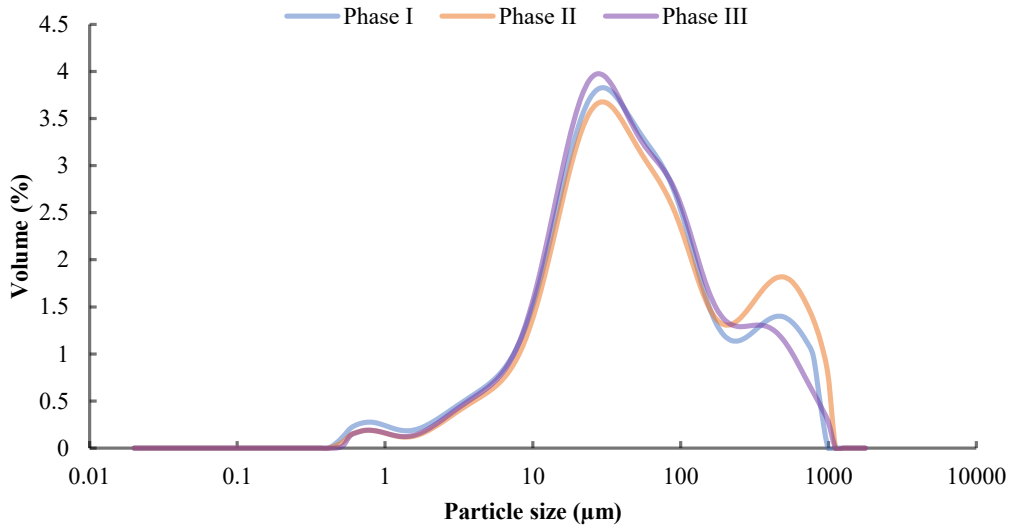

Figure 6.5: Particle size distribution of the mixed liquor suspended solids in the four tested conditions.

4. Conclusion

In this study, thermophilic anaerobic digestion of primary sludge of a thermomechanical pulp mill in a relatively new type of bioreactor (ThAnMBR) was studied for the first time. In particular, the variations of OLRs with operational parameters and their interrelations were investigated. The results of this study showed that the primary sludge of the TMP mill can be satisfactorily treated with a ThAnMBR. The reactor showed stable performance and biogas production in the range of 0.059 – 0.334 L biogas/g MLSS $_{\text{removed}}$ was achieved. Lower OLRs and higher HRTs have been associated with higher biogas production compared to higher OLR and shorter HRT, and OLR of 2.5 kg COD/m^3 d and HRT 8 d could be considered optimum and can be suggested as design criteria for PS treatment. The reduction of the sludge biomass ranged from 28.9 to 46.7 % depending on the applied OLRs. Sludge biomass degradation efficiency decreased with increasing OLR. Also, changing the OLRs has shown some influence on the effluent COD, where the lower OLR was associated with a lower COD concentration. Similarly, digestate properties have fluctuated with OLRs, for instance, SCOD increased with increased organic loading rate but C/N ratio has decreased. Regardless of OLRs, membrane performance was stable, and the required membrane flux was easily maintained during the operation. The results demonstrated that ThAnMBR is a promising new technology for pulp and paper mill primary sludge treatment and has many advantages as compared to conventional bioreactors.

Acknowledgements

This research was financially supported by Ontario Graduate Scholarship (OGS) and Natural Sciences and Engineering Research Council of Canada (NSERC).

References

[1] Baird, R.B., Eaton, A.D., Rice, E.W., 2017. Standard methods for the examination of water and wastewater, 23rd Edition, American Public Health Association, American Water Works Association, Water Environment Federation, Washington DC.

[2] Bajpai P (2015) Management of pulp and paper mill waste. Springer International Publishing.

[3] Bayr S, Kaparaju P, Rintala J (2013) Screening pretreatment methods to enhance thermophilic anaerobic digestion of pulp and paper mill wastewater treatment secondary sludge. Chem Eng J 223: 479–486. https://doi.org/10.1016/j.cej.2013.02.119

[4] Bayr, S., Rintala, J., 2012. Thermophilic anaerobic digestion of pulp and paper mill primary sludge and co-digestion of primary and secondary sludge. Water Res. 46, 4713–4720. https://doi.org/10.1016/j.watres.2012.06.033.

[5] Bokhary, A., Maleki, E., Hong, Y., Hai, F.I., Liao, B., 2020. Anaerobic membrane bioreactors: Basic process design and operation. In: Ngo, H., Guo, W., Ng, H., Mannina, G., Pandey, A., (ed) Current Developments in Biotechnology and Bioengineering, 1st edn. Elsevier, pp. 25-54. https://doi.org/10.1016/B978-0-12-819852-0.00002-6.

[6] Bokhary, A., Maleki, E., Liao, B., 2018. Ultrafiltration for hemicelluloses recovery and purification from thermomechanical pulp mill process waters. Desalin. Water Treat. 118, 103–112. https://doi.org/10.5004/dwt.2018.22641.

[7] Bokhary, A., Tikka, A., Leitch, M., Liao, B., 2018. Membrane fouling prevention and control strategies in pulp and paper industry applications: A review. J. Membr. Sci. Res. 4, 181–197. https://doi.org/10.22079/jmsr.2018.83337.1185.

[8] Boonyungyuen, W., Wonglertarak, W., Wichitsathian, B., 2014. Effect of organic loading rate on the performance of a membrane bioreactor (MBR) treating textile wastewater. In Proceedings of the International Conference on Chemical, Environment and Biological Sciences, Kuala Lumpur, Malaysia.

[9] Cai J, He Y, Yu X, Banks SW, Yang Y, Zhang X, Yu Y, Liu R, Bridgwater AV, (2017) Review of physicochemical properties and analytical characterization of lignocellulosic biomass. Renewable Sustainable Energy Rev. 76: 309–322. https://doi.org/10.1016/j.rser.2017.03.072.

[10] Cioabla, A.E., Ionel, I., Dumitrel, G.A., Popescu, F., 2012. Comparative study on factors affecting anaerobic digestion of agricultural vegetal residues. Biotechnol. Biofuels. 5, 1–9. https://doi.org/10.1186/1754-6834-5-39.

[11] Dereli R, K, Ersahin M.E, Ozgun H, Ozturk I, Jeison D, van der Zee F, van Lier J, B (2012) Potentials of anaerobic membrane bioreactors to overcome treatment limitations induced by industrial wastewaters. Bioresour Technol 122: 160–170. https://doi.org/10.1016/j.biortech.2012.05.139.

[12] Dhar, H., Kumar, P., Kumar, S., Mukherjee, S., Vaidya, A.N., 2016. Effect of organic loading rate during anaerobic digestion of municipal solid waste. Bioresour. Technol. 217, 56–61. https://doi.org/10.1016/j.biortech.2015.12.004.

[13] Elliott, A., Mahmood, T., 2012. Comparison of mechanical pretreatment methods for the enhancement of anaerobic digestion of pulp and paper waste activated sludge. Water Environ. Res. 84, 497–505. https://doi.org/10.2175/106143012X13347678384602.

[14] Elliott A., Mahmood T., 2012. Comparison of mechanical pretreatment methods for the enhancement of anaerobic digestion of pulp and paper waste activated sludge. Water Environ. Res. 84: 497–505. https://doi.org/10.2175/106143012X13347678384602.

[15] Franke-Whittle, IH, Walter, A, Ebner, C, Insam, H., 2014. Investigation into the effect of high concentrations of volatile fatty acids in anaerobic digestion on methanogenic communities. J. Waste Manag. 34: 2080–2089. https://doi.org/10.1016/j.wasman.2014.07.020.

[16] Gou, C., Yang, Z., Huang, J., Wang, H., Xu, H., Wang, L., 2014. Effects of temperature and organic loading rate on the performance and microbial community of anaerobic co-digestion of waste activated sludge and food waste. Chemosphere. 105, 146–151. https://doi.org/10.1016/j.chemosphere.2014.01.018.

[17] Gurram, R.N., Al-Shannag, M., Lecher, N.J., Duncan, S.M., Singsaas, E.L., Alkasrawi, M., 2015. Bioconversion of paper mill sludge to bioethanol in the presence of accelerants or hydrogen peroxide pretreatment. Bioresour. Technol. 192, 529–539. https://doi.org/10.1016/j.biortech.2015.06.010.

[18] Hafuka, A., Mashiko, R., Odashima, R., Yamamura, H., Satoh, H., Watanabe, Y., 2019. Digestion performance and contributions of organic and inorganic fouling in an anaerobic membrane bioreactor treating waste activated sludge. Bioresour. Technol. 272, 63–69. https://doi.org/10.1016/j.biortech.2018.09.147.

[19] Hagelqvist A, (2013) Sludge from pulp and paper mills for biogas production: Strategies to improve energy performance in wastewater treatment and sludge management (Doctoral dissertation, Karlstads universitet).

[20] Hassan, S.R., Zaman, N.Q., Dahlan, I., 2015. Effect of organic loading rate on anaerobic digestion: Case study on recycled paper mill effluent using Modified Anaerobic Hybrid Baffled (MAHB) reactor. KSCE J. Civ. Eng. 19, 1271–1276. https://doi.org/10.1007/s12205-015-0746-9.

[21] Hazarika J, Khwairakpam M., 2018. Evaluation of biodegradation feasibility through rotary drum composting recalcitrant primary paper mill sludge. Waste Manag 76: 275–283. https://doi.org/10.1016/j.wasman.2018.03.044.

[22] Jokela, J., Rintala, J., Oikari, A., Reinikainen, O., Mutka, Nyrönen, T., 1997. Aerobic composting and anaerobic digestion of pulp and paper mill sludges. Water Sci. Technol. 36, 181–188. https://doi.org/10.1016/S0273-1223(97)00680-X.

[23] Jiang, S., 2018. Thermophilic anaerobic membrane bioreactor for pulp and paper sludge treatment. Dissertation, Lakehead University Knowledge Commons.

[24] Karlsson, A., Truong, X.B., Gustavsson, J., Svensson, B.H., Nilsson, F., Ejlertsson, J., 2011. Anaerobic treatment of activated sludge from Swedish pulp and paper mills–biogas production potential and limitations. Environ. Technol. 32, 1559–1571. https://doi.org/10.1080/09593330.2010.543932.

[25] Kavuma C., 2013. Variation of methane and carbon dioxide yield in a biogas plant. Dissertation, Royal Institute of Technology.

[26] Kinnunen, V., Ylä-Outinen, A., Rintala, J., 2015. Mesophilic anaerobic digestion of pulp and paper industry biosludge–long-term reactor performance and effects of thermal pretreatment. Water Res. 87, 105–111. https://doi.org/10.1016/j.watres.2015.08.053.

[27] Mel M, Mohd Suhuli N, Ihsan SI, Ismail AF, Yaacob S., 2015. Effect of organic loading rate (OLR) of slurry on biogas production quality. In Advanced Materials Research 1115: 325-330. https://doi.org/10.4028/www.scientific.net/AMR.1115.325

[28] Liew CS, Kiatkittipong W, Lim JW, Lam MK, Ho YC, Ho CD, Ntwampe SK, Mohamad M, Usman A., 2021. Stabilization of heavy metals loaded sewage sludge: Reviewing conventional to state-of-the-art thermal treatments in achieving energy sustainability. Chemosphere, 277: 130310. https://doi.org/10.1016/j.chemosphere.2021.130310

[29] Likon, M., Polonca, T., 2012. Recent advances in paper mill sludge management. In: Show KY, Xinxin G (ed) Industrial waste. InTech, pp. 73–90. https://doi.org/10.5772/37043.

[30] Lin, H., Liao, B.Q., Chen, J., Gao, W., Wang, L., Wang, F., Lu, X., 2011. New insights into membrane fouling in a submerged anaerobic membrane bioreactor based on characterization of cake sludge and bulk sludge. Bioresour. Technol. 102: 2373–2379. https://doi.org/10.1016/j.biortech.2010.10.103.

[31] Lin, Y., Wang, D., Wu, S., Wang, C., 2009. Alkali pretreatment enhances biogas production in the anaerobic digestion of pulp and paper sludge. J. Hazard. Mater. 170, 366–373. https://doi.org/10.1016/j.jhazmat.2009.04.086.

[32] Liu, C., Wang, W., Anwar, N., Ma, Z., Lium, G., Zhangm R., 2017. Effect of organic loading rate on anaerobic digestion of food waste under mesophilic and thermophilic conditions. Energ. Fuel. 31, 2976–2984. https://doi.org/10.1021/acs.energyfuels.7b00018.

[33] Lopes, A.D.C.P., Silva, C.M., Rosa, A.P., de Ávila, Rodrigues, F., 2018. Biogas production from thermophilic anaerobic digestion of kraft pulp mill sludge. Renew. Energy. 124, 40–49. https://doi.org/10.1016/j.renene.2017.08.044.

[34] Manwatkar P, Dhote L, Pandey RA, Middey A, Kumar S., 2021. Combustion of distillery sludge mixed with coal in a drop tube furnace and emission characteristics. Energy, 221: 119871. https://doi.org/10.1016/j.energy.2021.119871.

[35] Meyer T, Amin P, Allen DG, Tran H., 2018. Dewatering of pulp and paper mill biosludge and primary sludge. J. Environ. Chem. Eng 6: 6317–6321. https://doi.org/10.1016/j.jece.2018.09.037.

[36] Park, N.D., Helle, S.S., Thring, R.W., 2012. Combined alkaline and ultrasound pre-treatment of thickened pulp mill waste activated sludge for improved anaerobic digestion. Biomass Bioenergy. 46: 750–756. https://doi.org/10.1016/j.biombioe.2012.05.014.

[37] Pio DT, Tarelho LAC, Nunes TFV, Baptista MF, Matos MAA., 2020a. Co-combustion of residual forest biomass and sludge in a pilot-scale bubbling fluidized bed. J Clean Prod 249: 119309. https://doi.org/10.1016/j.jclepro.2019.119309.

[38] Pio DT, Tarelho LAC, Pinto PR., 2020b. Gasification-based biorefinery integration in the pulp and paper industry: A critical review. Renewable Sustainable Energy Rev 133: 110210. https://doi.org/10.1016/j.rser.2020.110210.

[39] Saha, M., Eskicioglu, C., Marin, J., 2011. Microwave, ultrasonic and chemo-mechanical pretreatments for enhancing methane potential of pulp mill wastewater treatment sludge. Bioresour. Technol. 102,7815–7826. https://doi.org/10.1016/j.biortech.2011.06.053.

[40] Sato, Y., Hori, T., Navarro, R.R., Naganawa, R., Habe, H., Ogata, A., 2016. Effects of organic-loading-rate reduction on sludge biomass and microbial community in a deteriorated pilot-scale membrane bioreactor. Microbes Environ. 31, 361–364. https://doi.org/10.1264/jsme2.ME16015.

[41] Simão L, Hotza D, Raupp-Pereira, F, Labrincha JA, Montedo ORK., 2018. Wastes from pulp and paper mills-a review of generation and recycling alternatives. Cerâmica, 64: 443–453. https://doi.org/10.1590/0366-69132018643712414.

[42] Teghammar, A., Castillo, M.D.P., Ascue, J., Niklasson, C., Sárvári, H., 2012. Improved anaerobic digestion by the addition of paper tube residuals: pretreatment, stabilizing, and synergetic effects. Energ. Fuel. 27, 277–284. https://doi.org/10.1021/ef301633x

[43] Veluchamy C, Kalamdhad AS., 2017a. Influence of pretreatment techniques on anaerobic digestion of pulp and paper mill sludge: A review. Bioresour. Technol 245: 1206-1219. https://doi.org/10.1016/j.biortech.2017.08.179.

[44] Veluchamy C, Kalamdhad AS., 2017a. Biochemical methane potential test for pulp and paper mill sludge with different food/microorganisms ratios and its kinetics. Int. Biodeterior 117: 197-204. https://doi.org/10.1016/j.ibiod.2017.01.005.

[45] Wijekoon, K.C., Visvanathan, C., Abeynayaka, A., 2011. Effect of organic loading rate on VFA production, organic matter removal and microbial activity of a two-stage thermophilic anaerobic membrane bioreactor. Bioresour. Technol. 102, 5353–5360. https://doi.org/10.1016/j.biortech.2010.12.081.

[46] Yavini, T.D., Chia, A.I., John, A., 2014. Evaluation of the effect of total solids concentration on biogas yields of agricultural wastes. Int. Res. J. Environ. Sci. 3, 70–75.

Chapter VII

Thermophilic submerged anaerobic membrane bioreactor for pulp and paper primary sludge treatment: Membrane performance and fouling characteristics.

Abstract

The effect of organic loading rates (OLRs) on membrane performance and mixed-liquor suspended solids (MLSS) characteristics was investigated in this study for the first time using a laboratory-scale thermophilic submerged anaerobic membrane bioreactor (ThSAnMBR) for lignocellulosic materials treatment. Membrane performance was evaluated by monitoring its flux and corresponding transmembrane pressure. Changes in membrane chemical and physical properties resulting from operating conditions were investigated using Fourier transform infrared (FTIR), scanning electron microscopy (SEM), contact angle, energy-dispersive X-ray analyzer (EDX), and pore size measurement. While MLSS properties are analyzed by X-ray photoelectron spectroscopy (XPS), zeta potential, and particle size distribution (PSD) analysis. Membrane performance and MLSS properties were studied at different OLRs ranging from 1.5 to 3.9 kg-MLSS/m^3d, and hydraulic retention times (HRTs) of 3–8 d.

This study showed that the increased OLR reduced the membrane performance and degradation of the primary sludge, as well as the biogas yield. This result indicates that OLR of less than 1.5 kg MLSS/m^3d, HRT of 8d, and solids retention time (SRT) of 32d should be maintained to achieve stable membrane performance and better biogas production. Also, results showed that important changes occurred on the membrane morphology and MLSS characteristics under the tested operating conditions. High-resolution SEM images reveal distinct differences in the pore morphology between the virgin and used membranes indicating the effect induced by the operating conditions. Overall, the primary sludge from pulp and paper mills can be treated successfully by ThSAnMBR for methane production with stable membrane performance and high treatment efficiency.

Keywords: Membrane performance; OLR; biogas yield; primary sludge, anaerobic digestion; membrane bioreactor.

---

1. Introduction

Global production of paper and paperboard was estimated at more than 420 million metric tons in 2018, and the industry will continue to grow despite the fundamental transformation that is going through (from a single product (pulp) to a multi-product biorefinery system). In Canada, the pulp and paper industry represents one of the main pillars of Canadian industry and economy with a GDP contribution of C$7.84 billion in 2018. Based on statistics in Canada, the production of wood pulp was 16 thousand metric tons, while the production of paper and newsprint collectively was 6 thousand metric tons in the same year. The manufacturing of pulp and paper is always accompanied by the generation of large quantities of sludge as a by-product. The sludge considers waste and requires proper management. It is usually disposed of in landfills or incinerated. This practice places a huge burden on the pulp and paper industry. Alternatively, pulp and paper mill sludge (PPMS) can be used to produce biogas which is considered economically feasible in various studies. Approximately 240 m^3 CH_4/ton VS can be produced from primary sludge of Kraft mill (Bayr and Rintala, 2012) and approximately 180 m^3 CH_4/ton VS can be produced from secondary sludge (Karlsson et al., 2011). About 26-27 TWh per year of biogas can be produced in a medium-sized Kraft plant that annually produces 327,000 tons of air-dry pulp (Larsson et al., 2015).

Anaerobic digestion of energy-rich substrates such as animal manure, sewage sludge, PPMS, and food waste is usually performed by conventional stirred tank reactors (CSTR) and upflow anaerobic sludge beds (UASBs). However, due to excess sludge production, frequent biomass washout, and identical hydraulic retention time (HRT) and sludge retention time (SRT), conventional anaerobic digestion processes require further improvement (Yu et al., 2016). Thus, anaerobic membrane bioreactors (AnMBR) were proposed as an alternative. AnMBRs have received considerable attention in recent years in both industrial and municipal wastewater treatment. Owing to the fact that the development of AnMBR has combined the merits of traditional anaerobic digestion and membrane filtration. Membrane incorporation into completely stirred tank reactors (CSTRs) ensures effective biomass retention within the system, high effluent quality, and low sludge yield. Also, AnMBRs enable the decoupling of hydraulic and solids retention time compared to conventional CSTRs, which results in reduced reactor volumes and flexibility in maintaining high biomass concentration in the reactor and SRT extension (Bokhary et al., 2020; Lutze and Engelhart, 2020). Although AnMBRs are a very attractive alternative to wastewater treatment, their applications in organic sludge substrates are limited, and very few studies were reported in the literature (Dagnew et al., 2012; Yu et al., 2016; Pileggi and Parker, 2017; Dagnew and Parker, 2020). Due to the above-mentioned advantages, AnMBR might be a favorable choice for organic sludge treatment. However, membrane fouling is the major obstacle for the applications of membrane technology in organic sludge treatment.

Fouling causes reduced membrane flux, increased membrane cleaning frequency, and shorter membrane life, leading to higher operating expenses and the need for membrane replacement (Bokhary et al., 2018). In the AnMBR operation, both inorganic (e.g., dissolved inorganic materials) and organic (e.g., extracellular polymeric substances (EPSs)) foulants were observed and the cake layer was the core fouling mechanism (Meng et al., 2017). Although substantial research efforts are devoted to addressing membrane fouling, fouling control still hampers the financial viability of both aerobic membrane bioreactor (AeMBR) and AnMBR. Several researchers have linked the membrane fouling to operating parameters such as temperature, SRT, sludge age, MLSS concentration, organic loading rate (OLR), and feed substances (Bokhary et al., 2018). Forest product streams have been described as having a high tendency to cause membrane fouling as they contain various substances such as carbohydrates (cellulose and hemicellulose), wood extractives (lipid and phenolic extracts), and lignin and its degradation products (Bokhary et al., 2017). While the thermophilic temperature was found to induce more SMP release and increased EPS production compared to mesophilic temperature (Liao et al., 2011; Lin et al., 2013). On the other hand, it has been found that a high OLR can cause the build-up of volatile fatty acid (VFA) in the system (Wijekoon et al., 2011) and uneven distribution of the slurry during stirring, which jeopardizes both biogas production and membrane performance (Bokhary et al., 2020).

Thus, the rate of addition of feedstock to the AnMBR digestion system should be adjusted to the optimum level not only for a better performance of methanogen bacteria but also for improved membrane operation. In this study, the influence of changing the OLR on the membrane performance and mixed liquor suspended solids (MLSS) characteristics was investigated using a thermophilic submerged anaerobic membrane bioreactor (ThSAnMBR). In particular, the relationship between OLR and MLSS properties and their effect on PVDF membrane performance was studied to understand the fouling of a SAnMBR treating thermomechanical pulp primary sludge as a sole substrate for the first time using various membrane visualization and characterization techniques as well as hydraulic measurements.

2. Materials and methods

2.1. Feed and inoculum

The slurry was prepared from a primary sludge (PS) from a Canadian pulp plant using tap water. The main components of the PS were cellulose, hemicellulose, and lignin. The primary sludge, after being received in a 5-gallon plastic pail, was saved in a cold room at 4 °C to prevent biological decomposition. The primary sludge was mixed with faucet water homogeneously to 1−1000 μm with a mixer (Sunbeam Corporation) to facilitate the reactor feeding. NH_4Cl and K_2HPO_4 were added (in COD:N:P ratio of 100:2.6:1) to boost the nutrient content of the sludge. The total suspended solids and COD of the feed were 11.54±0.42 g/L and 20.078±1.865 g/L, respectively. The inoculum for seeding was obtained from AnMBR digesting secondary sludge from the paper industry.

2.2. Experimental setup

Thermophilic submerged anaerobic membrane bioreactor (ThSAnMBR) is made of polyvinyl chloride (PVC) and consisting of a continuous stirring tank reactor (CSTR) with an active volume of 6.5 liters and a flat plate membrane unit. The reactor was operated under thermophilic conditions, and the process temperature was controlled at 50±1 °C by passing hot water from the water bath continuously via the reactor casing. The bioreactor was mixed mechanically by a magnetic stirrer blade (Barnstead Thermolyne, Cimarec Plate Stirrer, USA), which is located at the bottom of the reactor to keep the system sludge liquor in suspension. The pH of the reactor was maintained at around 7.2 ± 0.1 and adjusted as needed by the NaOH solution. The experimental setup of ThSAnMBR is shown in Fig. 7. 1. The system was operated in three different hydraulic retention times (5, 3, and 8d) to make three OLR conditions of 2.2, 3.9, and 1.5 kg-MLSS/m^3 d while maintaining a constant SRT (32 d) during the whole experiment. The loading rate was increased by decreasing the HRT (increasing inflow to the reactor) and vice versa. ThSAnMBR was operated in three different OLRs starting at 2.2±0.16 kg MLSS/m^3d and was followed by loading rates of 3.9±0.19 and 1.5±0.10 kg MLSS/m^3d, and the experiment was lasted for over 280 days. After the membrane was installed and the reactor sealed, the system was purged with nitrogen gas for 5 minutes to form an

anaerobic atmosphere. A magnetic pump, controlled by a controller and a water level sensor, was used to feed the reactor by the sludge substrate intermittently. The excess digested sludge was removed from the systems on a daily basis to maintain a SRT of 32 d.

Flat sheet microfiltration (MF) membrane modules made out of polyvinylidene fluoride (PVDF) was used in this study, each module has a working filtration area of 0.03 m^2 (the dimensions of each side were 100 mm × 150 mm) and pore size of 0.1 µm (DAFU Membrane Technology Co., P.R. China). As shown in Fig. 7. 1, the membrane module is constructed from a plastic sheet as support, plastic mesh on each side, two pieces of PVDF flat sheet membrane, and two stainless steel frames with rubber for fastening. During the operation, the membrane module was sparged by the biogas produced to control the fouling by preventing solids deposition over the surface of the membrane module. The biogas was transported by stainless steel tubes positioned to both sides of the membrane module using Masterflex pumps. The effluent was removed from the reactor using a peristaltic pump and kept in its container for upcoming measurements. A Gralab 451 timer was used to control the peristaltic pump, and it was set to run for three minutes and off for two minutes in order to sluggish down the fouling development. The required flux was maintained by controlling the peristaltic pump speed, and calibration and adjustments were made as needed. An omega analog pressure gauge was utilized for trans-membrane pressure monitoring.

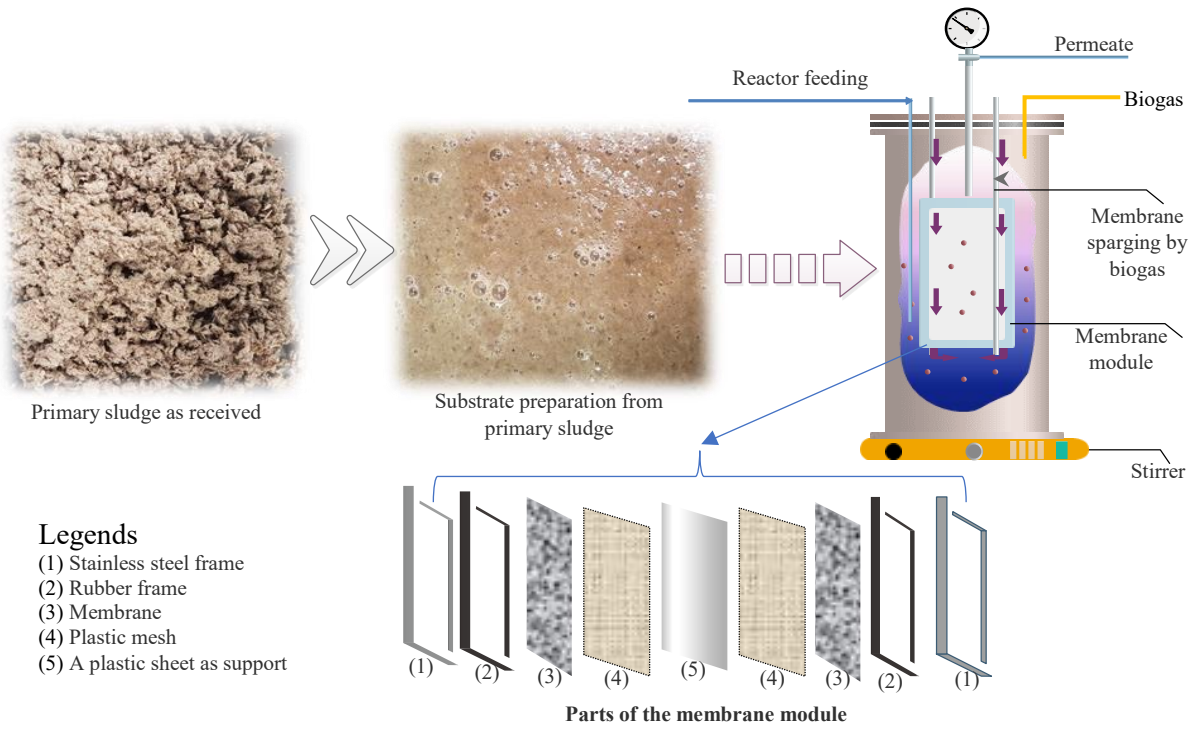

Figure 7.1: Schematic of submerged anaerobic membrane bioreactor and membrane module configuration used in this study.

2.3. Analytical methods

2.3.1. Primary sludge, reactor feed, and inoculum

Total solids (TS), total suspended solids (TSS), volatile solids (VS), total chemical oxygen demand (TCOD), and soluble chemical oxygen demand (SCOD) of the primary sludge, inoculum, and reactor digestates were tested per standard protocols. The pH value was determined using Oakton pH 700 benchtop meter. Elemental substances (C, H, N, and S) of the digestates were analyzed using an elemental analyzer (Vario El Cube, Germany). The chemical element concentrations for permeates were analyzed by an ICP-OES (inductively coupled plasma - optical emission spectroscopy) elemental analyzer. The biogas generation rate was quantified by water displacement technique using a graduated measuring cylinder and the composition was determined 3-4 times a week by a gas chromatograph machine (GC-2014, Japan). The chromatograph was equipped with an analytic column of silica gel, and helium was employed as a carrier gas at constant pressure and flow rate.

2.3.2. Membrane resistance and permeability measurement

Before starting the reactor operation, the permeability and resistance of the virgin membranes were obtained to approximate the amount of foulant, (R_F), later in each operating condition. When the reactor reached the end of its specified operating period, the membrane was removed from the system and its cleaning was performed following the defined cleaning regimes (physical/chemical). Following every cleaning phase, the permeability of the module was performed using clean water (tap water) and a permeability graph was generated for the membrane fluxes versus corresponding transmembrane pressures. The physical cleaning stage included removing the loose gel layer by a damp sponge and rinsing the module with water. After the physical cleaning, two chemical cleaning steps were performed. The first step involved immersing the membrane in a NaClO solution (200 ppm) for two hours, followed by rinsing it with water, while the second stage involved immersing the module in a $C_6H_8O_7$ solution (2000 ppm) for two hours and rinsing it with tap water. The resistance of the membrane was determined using the resistance-in-series model and Darcy's law, while the temperature-corrected permeability was measured with the following equation as the changes in the permeate viscosity directly affect the transmembrane pressure.

$$K_{20\,^{\circ}C} = J.exp^{(-0.0239(T-20))}/\Delta P$$

Where $K_{20\,^{\circ}C}$ is the permeability (L/m^2.hr. kPa) at 20 °C; J is the module flux (L/m^2.hr) at temperature T (°C); T is the water temperature at which the permeability was measured in °C; ΔP is transmembrane pressure (kPa).

2.3.3. SEM-EDX and ImageJ analysis

Scanning electron microscope (SEM) and energy-dispersive x-ray spectroscopy (EDX) were utilized in conjunction to produce membrane surface images and analyze the elemental composition. SEM yields high-

resolution imageries of a specimen by scanning the surface with a highly focused ray of electrons. In this investigation, representative segments of the membrane module were taken at the end of each operating condition and soaked in liquid nitrogen for 10 min. Specimens were then prepared and coated with carbon using a sputter coater (Model 12560, Fullam, USA) to enhance heat conduction and prevent burning or charging of the specimen. Finally, the surface and sectional images were taken from coated samples at the desired magnification using SEM (SU-70, Hitachi, Japan).

ImageJ processing software version 1.51p was utilized to determine the pore size, surface porosity, and pore size distribution (PSD) of the virgin and used membranes from SEM micrographs. It has been proven that SEM technology delivers reliable evidence on the pore size of the PVDF membrane (Tikka et al., 2019). In this study, a total of 700 pores were measured for the virgin and used membranes at the end of each phase to represent a major part of the porosity and was deemed sufficient for the current investigation. After converting the SEM images to 8-bit binary images, ImageJ, an open-source software, was used to extract the required data.

2.3.4. Surface analysis by XPS

X-ray photoelectron spectrometer (XPS) was utilized to characterize the detailed element composition of MLSS and membranes. XPS is a powerful surface analysis technology, it measures the elemental composition to the highest depth 1-10 nm from the surface area providing insights into the surface chemistry of materials with high surface sensitivity. The signals measured in XPS are based on the photoelectric effect that can recognize elements within the material through the reflection of photoelectrons by the sample. XPS spectra of the MLSS samples were obtained at the end of each operating condition.

2.3.5. FTIR

Bruker Tensor 37 FTIR (Fourier Transform Infrared) spectroscopy (Bruker Co., Ltd.) and windows-based spectroscopy software were used to detect the foulants deposition on the membrane surfaces by obtaining detailed information on the functional groups of the foulants, and the membranes. The wavelength of all measured spectra ranged between 4000 and 400 cm^{-1}. The FTIR analysis of used membranes was performed at the end of all cleaning regimes.

2.3.6. Surface properties and dewaterability of MLSS

Zeta potential of the mixed liquor suspended solids (MLSS) was measured during the experiment using a ZetaPALS zeta potential analyzer (Brookhaven, Holtsville, NY, USA). Due to the large particles of MLSS, MLSS supernatant, containing fine colloidal particles and macromolecules, was used to determine the surface charge of MLSS. A permeate solution from the reactor was utilized to provide the background electrolyte. The digestate dewaterability was determined by Capillary Suction Time (CST), model 304 series (Triton Electronics Ltd., UK). All tests were carried out per the manufacturer's instructions, using

Triton Electronics' CST filter paper and the 1cm sludge funnel. The contact angle of MLSS was measured by using Dropometer M-3 (Droplet Smart Tech Inc. Canada), and the pure water was used as a probe fluid for the contact angle measurement.

2.3.7. Particle size distributions

Particle size distribution (PSD) of feed samples and MLSS samples were determined by a Malvern Mastersizer instrument (Malvern Instruments Ltd., UK). The instrument comprises of optical bench and sample dispersion units and sizes the particles by using laser diffraction, which takes measurements over a wider range of angles. It accurately measures particles from 0.02 to 2000 μm. This device measures every specimen three times automatically and calculates the average. In this study, PSDs were routinely monitored and throughout the operation.

3. Results and discussion

3.1. Characteristics of the feedstock and inoculum

The properties of the primary sludge and inoculum were examined in this study. The mean volatile solids were 93.93 ± 0.24 (%TS) for the feeding substrate and it was 83.48 ± 0.37 (% TS) for the used inoculum. The ash content in the primary sludge was 3.61 ± 0.37%, while the ash content in the inoculum was 16.52 ± 0.38%. The pH was 7.2 for the primary sludge, and it was 6.9 for inoculum. The feed total solids in the three phases (I–III) were approximately 11.8 g/L, while their total COD concentrations ranged between 19.39±1.22 and 20.61±1.49 g/L. The feed contained around 0.194±0.010 g/L soluble COD. The total solids for inoculum were found to be 39.62±0.43 g/L with 1.150±0.100 g/L soluble COD. The total suspended solids (TSS) were 11.54±0.42 and 36.63±0.31 g/L for the feed substrate and inoculum, respectively. While the carbon to nitrogen ratio (C/N) was 285.60 and 13.43 for the feed substrate and inoculum, respectively.

The results of the biological performance of the ThAnMBR suggest that the thermomechanical mill PS can be satisfactorily digested by a thermophilic submerged anaerobic membrane bioreactor, and organic loading rate of 2.5 kg COD/m^3 d and hydraulic retention time 8 d could be considered optimal, suggesting ThAnMBR is a capable new technology for PS (lignocellulosic materials) digestion for bioenergy production and solids reduction. The article presented here would focus on the membrane performance of this novel ThAnMBR system for lignocellulosic materials treatment for the first time.

3.2. Long-term operation of ThSAnMBR

The AnMBR system was operated on a lab scale for approximately 350 days for primary sludge from thermo-mechanical pulping treatment. AnMBR demonstrated excellent biological and membrane performance. Table 7.1 summarizes the operating conditions of ThSAnMBR. The system was run in three different digestion environments. In the first phase, the average organic loading rate was 2.2 kg-MLSS/m^3d, while in the second and third phases, the OLRs were 3.9 and 1.5 kg-MLSS/m^3d, respectively. The

membrane flux was maintained around 2.43±0.20 L/m^{2}hr in the first operating condition (phase I) and was 4.59±0.28 and 1.48±0.11 L/m^{2}hr in the second and third conditions (phase 2 and 3), respectively. The temperature of the system was maintained at 50±1 °C. All phases ran at a constant 32-day SRT, and the hydraulic retention times (HRTs) were 5 (phase 1), 3 (phase 2), and 8 (phase 3) days (Table 7.1). The concentrations of permeates (effluents) COD and chemical elements varied somewhat with the organic loading rates, where the average effluent COD in the first phase being 1.67±0.46 g/L whilst the typical concentration of effluents COD in the second and third operating conditions was 0.70 ± 0.34 and 0.32 ± 0.11 g/l respectively. The element concentrations in the effluents did not vary significantly among the different operating environments. At the end of each operating condition, the reactor was terminated, and the membrane was taken out for permeability measurement and characterization after fouling cleaning. Biogas production and solid material degradation were found to reduce when the OLR increased. The average biogas yield was about 53 L/kg MLSS $_{fed}$ in the first phase at OLR of 2.2 kg MLSS/m^{3}d, but once the organic loading raised to 3.9 kg MLSS/m^{3}d in the second phase, it decreased the production of biogas at 45 L/kg MLSS $_{fed}$. Though, once the OLR was decreased again to 1.5 kg MLSS/m^{3}d in the third phase, this significantly increased biogas production at 155 liters of biogas/kg of MLSS $_{fed}$. Methane contents ranged between 52 – 60% and the patterns were roughly similar between the tested OLRs.

Table 7.1: Digestion conditions of the primary sludge in AnMBR for each phase.

Parameters	Phase I	Phase II	Phase III
Duration (d)	1 – 94	99 – 206	212 – 323
Temperature (°C)	50±1	50±1	50±1
Average permeate flux (L/m^2.hr.)	2.43±0.20	4.59±0.28	1.48±0.11
Average transmembrane pressure (kPa)	8.2±3.3	16.5±9.1	7.3±1.98
Feed concentration (g/L)	11.80±0.65	11.88±0.17	11.85±13
Feed COD (g/L)	19.39±1.22	20.61±1.49	19.76±1.01
Feed TSS (g/L)	11.57±0.74	11.59±0.30	11.48±0.14
SRT (d)	32	32	32
HRT (d)	5	3	8
OLR (kg-MLSS/m^{3}d)	2.2±0.16	3.9±0.19	1.5±0.10
Biogas sparging rate (L/min)	3.76 ±0.08	3.76 ±0.08	3.76 ±0.08
Mixed liquor suspended solids (MLSS) (g/L)	16.57 – 20.55	24.04 – 26.24	25.54 – 26.14

3.3. Membrane flux and transmembrane pressure

The permeate flux is usually correlated with membrane fouling tendency, and as a result of this relationship, the conception of the critical flux was presented. It is commonly known that working under the critical flux region reduces the foulants deposition, but it is not sufficient to obtain zero fouling rates. Several factors influence the critical flux such as OLR, MLSS concentrations, and gas sparging ferocity (Mahmoud and Liao, 2017). Membrane fluxes under different tested OLRs are given in Fig. 7. 2. In this study, AnMBR

was operated on the constant permeate flux mode, in which the permeate volume was adjusted when required by tweaking the speed of the peristaltic pump. While the corresponding changes in transmembrane pressure were monitored. At the end of each operating condition, a new membrane was used to study its performance. The mean permeates fluxes in the first, second, and third operating conditions were 2.43±0.20, 4.59±0.28, and 1.48±0.11 LMH, respectively. Due to the reduced OLRs and the longer HRTs in the first (2.2 kg-MLSS/m^3d and 5d) and the third (1.5 kg-MLSS/m^3d and 8d) phases, the required permeate fluxes were maintained without difficulty compared to the second phase with a shorter hydraulic retention time of 3 days and OLR of 3.9 kg-MLSS/m^3d. During phase II operation, as the OLR was raised from 2.2 to 3.9 kg-MLSS/m^3d, the transmembrane pressure rapidly increased and reached 40.5 kPa in less than 50 days. Thus, the process was stopped, and the membrane unit was removed from the system for cleaning. After the physical and chemical cleaning, the permeability of the membrane was almost fully restored, and the module was reused to complete the operation of the phase. It can be concluded from these results that the fouling effect on MBR operation is negligible at longer HRTs, but detrimental at lower HRTs. The reduced fouling can be attributed to two main reasons: the formation of the fibrous balls scouring the cake layer and the operation of the system under the critical flux region. However, lower fluxes should be considered within the economic viability of anaerobic membrane bioreactors.

Notably, no differences were observed in the transmembrane pressure in the first and third phases, with transmembrane pressure ranged between 3.4 – 11.9 kPa in each. However, the transmembrane pressure of phase II was significantly different, ranging between 3.4 – 40.6 kPa. These results indicate that the operating of AnMBRs under lower fluxes (longer HRTs) would be advantageous due to reduced membrane fouling. Regardless of OLRs, a typical three-stage transmembrane pressure profile was observed in phase I and II, beginning with (I) a sudden rise in transmembrane pressure from 3.4 to 5.1 kPa presumed due to pore blockage, (II) followed by a prolonged period of progressive transmembrane pressure rise from 5.1 to 10.2 kPa, and (III) ended with a decrease in transmembrane pressure from 10.2 to 8.5 kPa possibly due to collapse of the cake layer and then started to level up again. This phenomenon has been reported frequently in other studies of MBR systems (Zhang et al., 2006; Gao, et al., 2011). In this study, the digested primary sludge formed fibrous balls of approximately 0.5 – 2 cm in diameter, as shown in Fig. 7. 3. These spheres can be effective in controlling the AnMBR fouling due to their contact with the membrane module and removing the cake layer. Hence, this phenomenon should be considered among the flux decline minimization strategies because these balls may help in reducing the intensity of the membrane sparging.

At the end of each operating condition, the permeability and resistance of the membrane were measured. In the first phase, a slight increase in the permeability of the used membrane (7.2 L/m^2kPa) was observed compared to the virgin membrane (6.6 L/m^2kPa). The permeability difference can be attributed to the

enlargement of the membrane pores due to the operation of the system at high temperature and the small age of the sludge. On increasing the OLR in the second phase, the situation was different, the membrane permeability was recovered by 98.5% after chemical cleaning, and the resistance of the gel layer was 96.87%. The third phase had similar results as the second phase where the membrane permeability was restored with 97.8% after chemical cleaning, and the resistance of the gel layer was 96.9%.

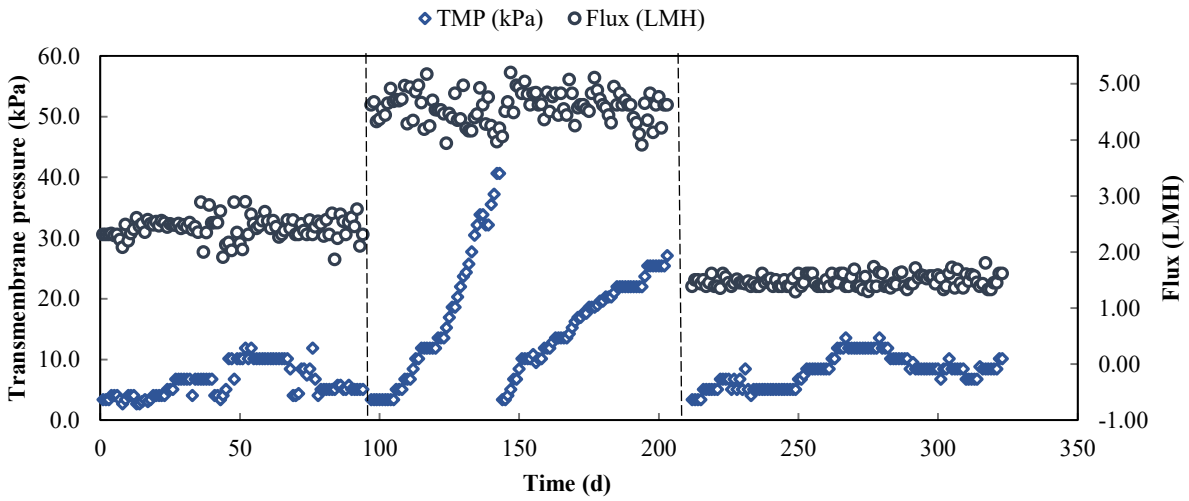

Figure 7.2: Membrane flux under different conditions versus operating time.

Figure 7.3: Fibrous balls formed during the primary sludge digestion, which are taken at the end of phase 3

3.4. Morphology and pore sizes of membranes

3.4.1. SEM-EDX system and ImageJ analysis

The SEM images of (a) the new membranes, (b) used membrane phase I, (c) used membrane phase II, and (d) used membrane phase III are shown in Fig. 7. 4. As can be seen from images of surface topography, which have been taken at a 500 nm scale, pore sizes, shapes, and pore size distribution vary greatly between the virgin and the membranes used. Although the employed membranes were exposed to physical and chemical cleaning regimes before taking the images with SEM, the pores were more visible in the virgin membrane than the used membranes, especially the small pores. To confirm these differences in pore morphology, the pore size was subsequently measured by ImageJ processing software to define nominal pore size and surface porosity. From Fig. 7. 4, there is a clear difference between the pore and the solid surface. Fig 7. 5 depicts the distribution of pore sizes for the virgin and used membranes that have been measured by ImageJ. There is a shift in the pore size distribution (PSD). The pore size shifted towards a larger size especially those greater than 25 nm. This shift can be attributed to the operation of the system at a high temperature (thermophilic condition 50±1°C). These results are comparable to those obtained by Masselin et al. (2001) when they studied the effect of ultrasonic irradiation on polymeric membranes where the distribution of the pores of the treated membrane underwent some modification as smaller pores (radius 1 – 4 nm) became less frequent in distribution and at the same time, the large pores (radius> 4 nm) become more frequent. Dang et al. (2014) also detected an increase in the pore radius of 0.39 to 0.44 nm for the polyamide nanofiltration membrane when the temperature was increased from 68 to 104 °F. This fact was proved once again by Tikka et al., 2019, who observed more portions of large pores (>30 nm) when the membranes were conditioned at 35 °C compared to 23 °C. The change in pore morphology may explain the lower transmembrane pressure in this study, as the increased pores due to high temperature have preserved the permeate flux from the sharp decrease that occurs due to membrane fouling. This result is consistent with the results of Masselin et al., (2001), who obtained increased membrane flux and permeability due to an increase in mean pore radius (30% increase) when they treated polymeric membranes with ultrasonic irradiation. Worth noting here, the range of pore size measured by ImageJ is smaller than that reported by the membrane supplier. Comparatively, the pore shift or increase can also be linked to the local applied hydraulic pressure and permeated flux. Van der Marel et al. (2010) detected a similar change in the pore structure of the PVDF membrane, where pore size increased from the skin towards the permeate side.

Interestingly, the frequencies of large pores (>35 nm) in the second phase were lower than those of the large pores in the first and third phases (Fig. 7. 5). This difference can be explained by shorter (3d) HRT and

higher OLR (3.9 kg-MLSS/m^3d) where a large volume of permeate needs to be withdrawn from the system, which may cause pores narrowing by the foulants. This is for the reason that both big suspended substances and small colloidal materials can be rapidly trapped on the surface of the membrane, due to the rise in the applied flow rate (Bokhary et al., 2018). It has often been spotted that large pores are far susceptible to fouling than smaller pore sizes. The lower frequencies of large pores in the second phase may also explain the sharp increase in transmembrane pressure.

Fig. 7. 6 shows a three-dimensional (3D) graph of the membrane surface structure before and after utilization. These 3D profiles of ImageJ are based on the brightness level of the topographies on the membrane surface where black areas represent pores and grey/white regions indicate the solid surfaces. Thus, the 3D surface plot tool in ImageJ visualizes the surface structure of the membranes by detecting the variations in brightness degrees in the SEM images taken from the surface of the specimens (AlMarzooqi et al., 2016). From these surface plots, it can be concluded that the topography of the membrane surface differs between the virgin and the used membranes, where the virgin membrane exhibited more pores compared to used membranes. The small pores were distinctively visible in the virgin membrane compared to the membranes used (Fig. 7. 4). These variations could have been related to the combined effect of OLR, HRT, and high temperature.

In this study, the elemental composition of the surface of the PVDF microfiltration membrane was identified by EDX. EDX spectra of the new and employed membranes were presented in Fig. 7. 7. As revealed in Fig. 7. 7, large quantities of C and F were spotted by the SEM-EDX system in the virgin membrane, which considers part of the membrane construction. However, in addition to C and F, a small amount of O was detected in the employed membrane, compared to the new membrane. Detection of a small fraction of O may indicate the occurrence of reduced organic fouling on the membrane. Also, this result indicates the absence of the inorganic fouling during the operation of the SAnMBR or that chemical cleaning was effective in removing inorganic elements from the membrane. The absence of inorganic elements may explain also the non-formation of the cake layer on the membrane surface during operation. It has been found that the inorganic elements may aid in the build-up of the cake layer through neutralizing the charge, bridging of metal clusters and metal ions, and concentration polarization (Gao et al., 2011).

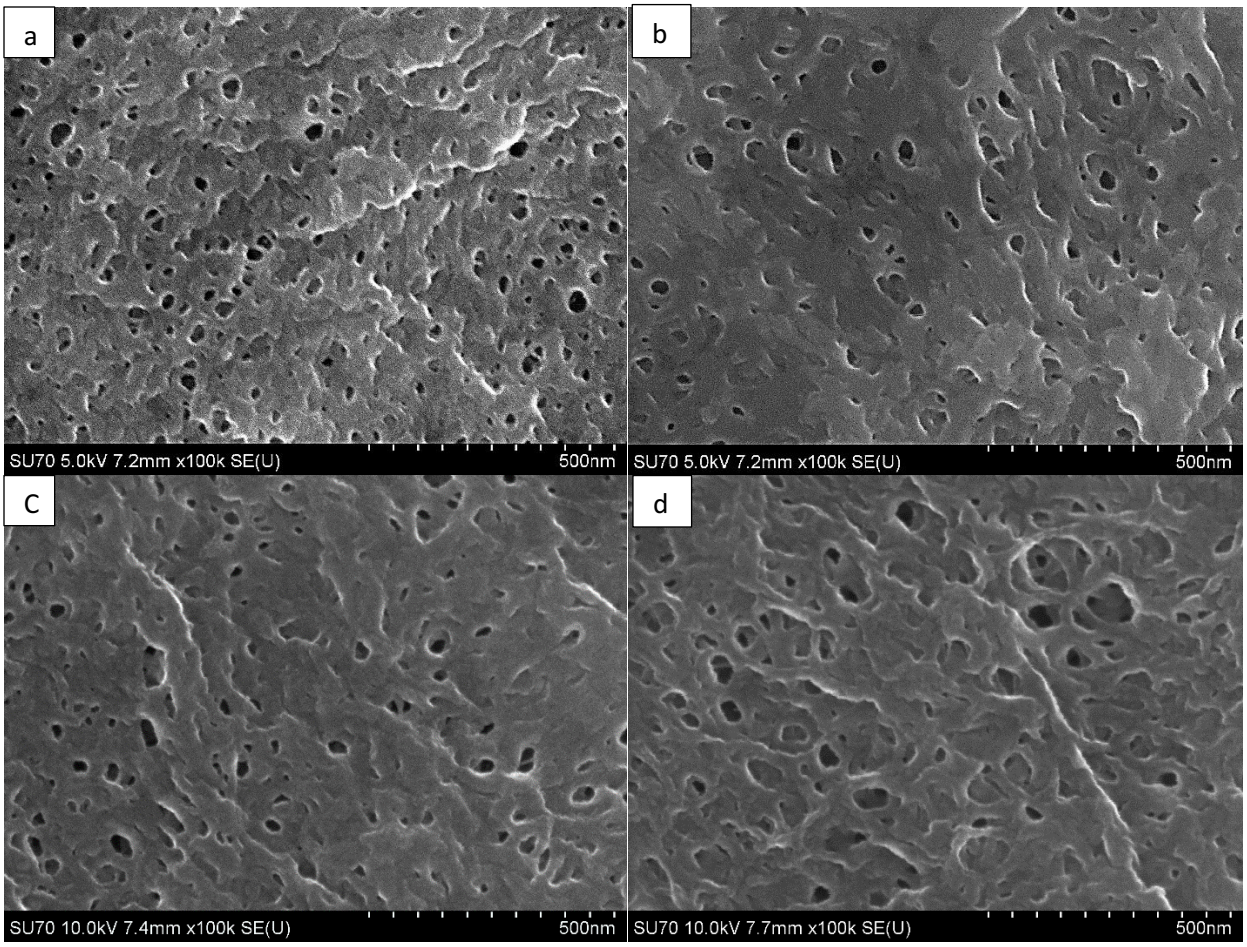

Figure 7.4: Scanning electron microscope (SEM) images of (a) new membrane, (b) used membrane phase I, (c) used membrane phase II, and (d) used membrane phase III, using PVDF membrane after chemical cleaning.

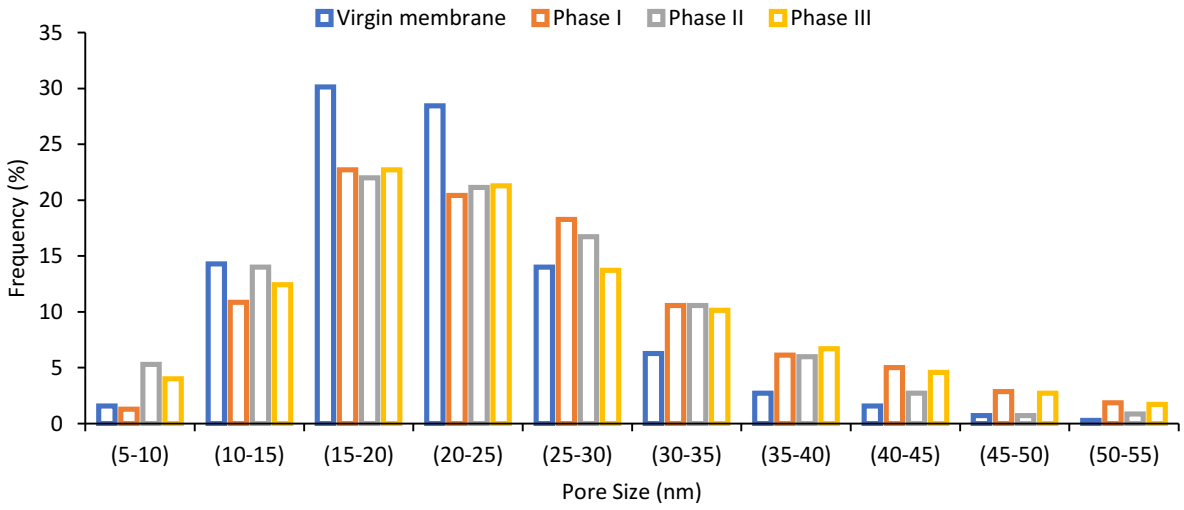

Figure 7.5: Pore sizes distribution of the virgin and used membranes (after chemical cleaning) in various operating conditions.

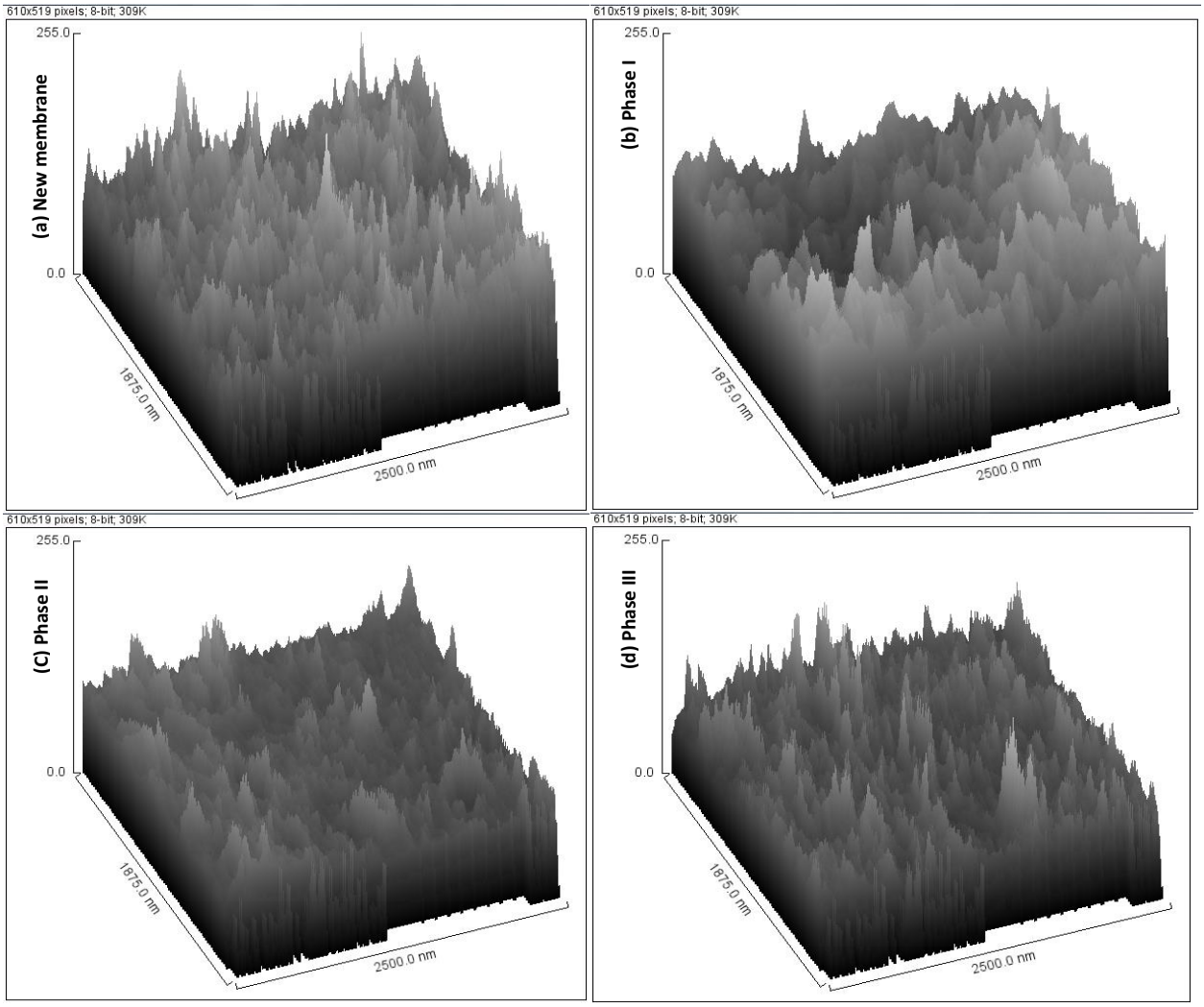

Figure 7.6: Surface plot of (a) virgin membrane, (b) used membrane phase I, (c) used membrane phase II, and (d) used membrane phase III.

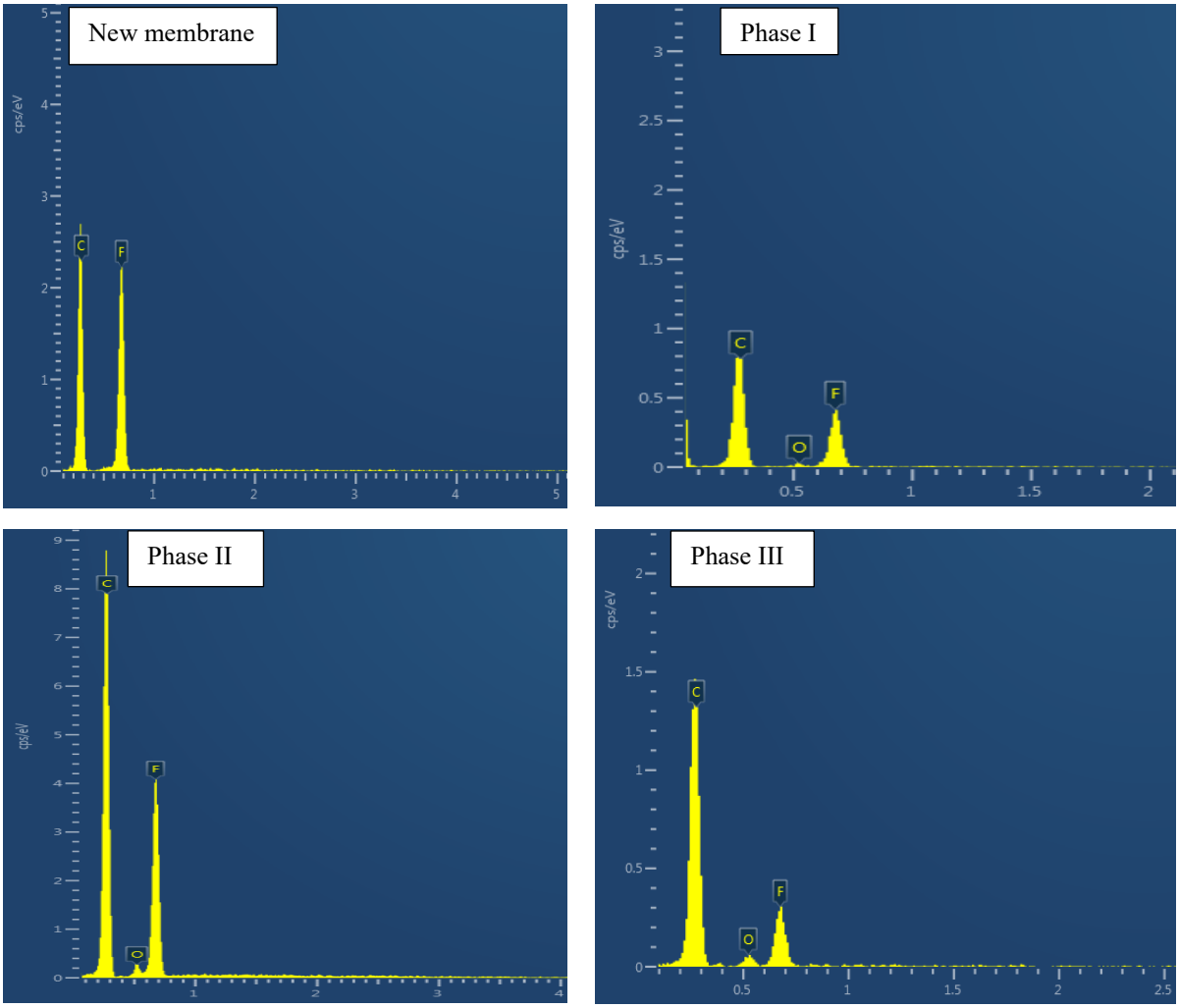

Figure 7.7: Energy-dispersive X-ray spectroscopy (EDX) analysis of the virgin and used membranes in different operating conditions.

3.4.2. FTIR spectra of virgin and used membranes

The FTIR spectrum of the virgin and used PVDF flat sheet membranes after chemical cleaning were depicted in Fig. 7. 8. Each peak demonstrates a particular type of molecular vibration (e.g., symmetric, asymmetric, twisting, wagging, bending, deformation, or rocking) and some of which is a spectrum that precisely characterizes the skeleton of PVDF (e.g., $–CH_2$ and $–CF_2$ groups) (Puspitasari et al., 2010). FTIR analysis showed chemical changes in the functional groups of the PVDF membrane, indicating a possible foulants deposition on the membrane surfaces. The absorption peaks at 975–1069 cm^{-1} were linked to the PVDF fingerprint, while the peak at 1402 cm^{-1} was accredited to the CH_2 wagging vibration (Puspitasari et al., 2010). The peaks at around 1018 cm^{-1} and 840 cm^{-1} were assigned to the C–C and C–C–C bands of PVDF membranes, respectively, while the vibration spectra at around 1632 cm^{-1} were given to the bending vibration of absorbing H–O–H groups (Gu et al., 2010; Bai et al., 2012). From Fig. 7. 8, the spectra of the utilized membranes were distinctly different from those of the virgin membrane, except for some peaks.

Whereas the used membranes exhibited nearly identical spectral profiles. These peak shifts in the spectra may indicate some foulants deposition on the used membrane surfaces. For instance, the change in weak hydroxyl peak observed at roughly 2300 cm^{-1} (stretching of the O–H bond) (Fig. 7. 8), which only appeared at the used membranes, most likely indicates the presence of polysaccharides (Ding et al., 2015). This hydroxyl peak was clearly pronounced for higher OLR compared to lower OLRs, and this may be related to the combined effect of increased OLR and lower HRT, which have accumulated more polysaccharides on the surface of the membrane (Fig. 7. 8). Also, the peak intensity of about 723 cm^{-1} was significantly different between the virgin and the membranes used showing a major increase in the higher tested OLR compared to the lower OLR, which suggests foulants deposition on the membrane. In addition, there is a clear vibration in peak centered on 1712 cm^{-1} (stretching shaking of C=O and C–N), which are the characteristic bands for proteins secondary structure (amide I and amide II), indicating the presence of some organic foulants (Gao et al., 2011). Furthermore, there is a peak shift in the fingerprint spectra between 1409 and 1095 cm^{-1} for the used membrane, and this may indicate deformation of these functional groups, which in some cases is associated with an increase in the membrane's hydrophobicity (Puspitasari et al., 2010). These spectral bands' differences between the fouled membranes and virgin membranes were also attributed to the presence of foulant materials like fatty acid (Ding et al., 2015). From the results of FTIR, it can be ensured that chemical cleaning cannot fully remove foulant materials from the membranes, and proteins, polysaccharides, and fatty acids are evidently among the substances that exist in the membrane surfaces.

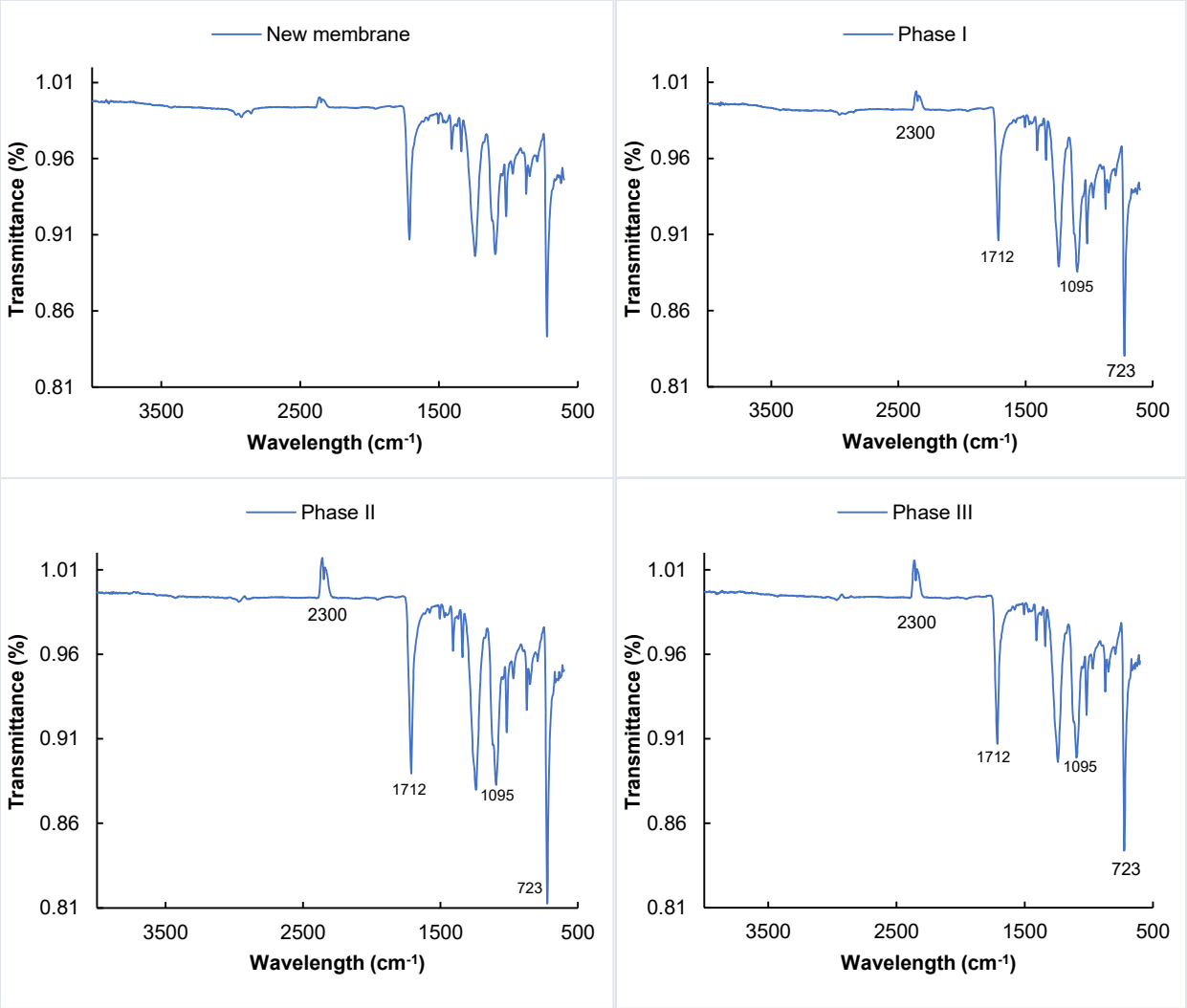

Figure 7.8: FTIR spectrum: (a) of virgin membrane and membranes used under various digestion conditions.

3.5. MLSS properties

3.5.1. Particle size distributions (PSDs)

The PSDs of the suspended solids in the mixed liquid ranged from 0.1 – 1000 µm. Most of the particles were centered between 10 and 100 microns, with a tiny fraction whose size was less than 1 micron and greater than 100 microns as can be seen in Fig. 7. 9–a. The PSD did not vary much between the tested OLRs, except for the first phase that contained fewer molecules with a size greater than 100 microns and slightly more particles with a size lower than 1 micron. The large particles in the second and third phases are most likely due to flocs formation with the digestion time. Also, the reduced variation in the PSD of MLSS among the phases can be attributed to the slow digestion of PS molecules due to their recalcitrant nature, which demands a longer digestion time. The particle size distributions of the loose gel layer formed on the membrane surface ranged from 0.5 – 100 µm as shown in Fig. 7. 9–b. Most of the gel layer particles were between 10 and 100 microns, with a small fraction ranging in size from 0.5 – 1 micron, which is in

similarity to the MLLS particles. However, the molecules larger than 100 microns were only observed in the MLSS compared to the loose gel layer particles. This result indicates that the tendency of small particles to deposit on the membrane surface is larger than that of large particles. Similar observations were obtained by several researchers as the smaller particles have a higher propensity to accumulate on the surface of the membrane compared to the large ones (Lin et al., 2011; Gao et al., 2011; Hu et al. 2016). It ought to be noted here that most of the particles in the MLSS and the loose gel layer are larger than the membrane pore sizes (Fig. 7. 9 – a and b). The membranes utilized in this study have a pore size of around 0.1 µm, while most of the MLSS and gel layer sizes are between 10 and 100 µm. Thus, pore-blocking is not the dominant mechanism of membrane fouling. Also, the large particle size of the MLSS and the loose gel layer, which could not penetrate and block the membrane pores, may explain the lower transmembrane pressure obtained in this study. Compared to the large particle, small particles, which are similar or lesser than the membrane pore size, can easily enter the membrane pores and cause fouling (Bokhary et al., 2018).

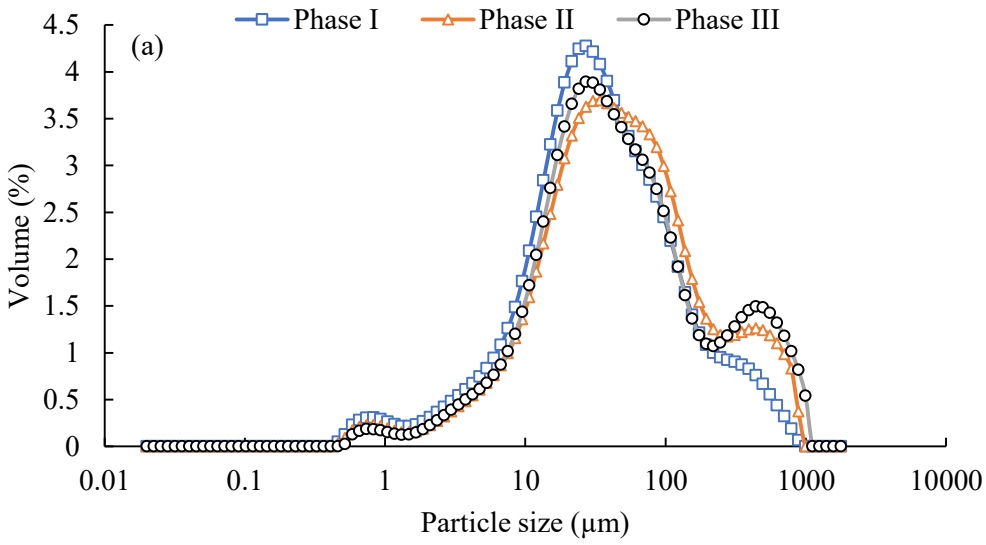

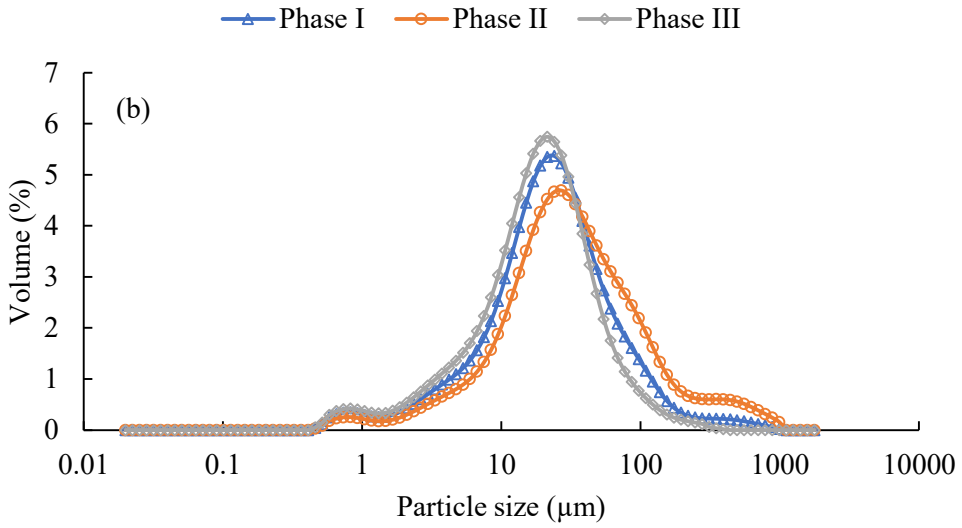

Figure 7.9: Particle size distributions (PSDs) of (a) mixed liquors and (b) gel layer in the tested conditions.

3.5.2. Surface properties and dewaterability of MLSS

Table 7.2 lists the zeta potential, contact angle, and dewaterability of the MLSS. The surface charge property of the sludge, which can be obtained by measuring the zeta-potential, is an essential indicator of membrane fouling. During the operation period, the zeta potential of sludge was increased with increased digestion time and changed from – 20.9 (mV) in phase I to – 29 (mV) in phase III. The absolute value of the zeta potential of the third phase was 38% greater than that of the first phase. While it was 12% higher in the second phase than the first phase. The increase in the zeta potential of the sludge can be partly explained by the aging of the sludge and the growth of filamentous bacteria (Sabouhi et al., 2020). As can be seen from Table 7.2, MLSS dewaterability decreased with increasing operating time and ranged between 29 and 37 s. Dewaterability decreased by 17% in the second phase and decreased by 25% in the third phase. This decline can be attributed to the aging of sludge and the accumulation of EPSs in the system. This decrease could also be related to the varied concentrations of MLSS among the phase, where MLSS concentration was to some extent higher in the third phase (26 g/L) than the second (24 g/L) and first phase (20 g/L). No evident effect was spotted on dewaterability due to the change in the OLR.

The contact angle of the mixed liquors ranged between 24 and 64° and decreased as operating time increased. As evidenced in Table 7.2, the highest contact angle was 64.3±3.2° at the first phase with the OLR of 2.2±0.16 kg-MLSS/m^3d, but when the OLR increased to 3.9±0.19 kg-MLSS/m^3d, the contact angle decreased significantly to 24.6±3.04°. However, the hydrophobicity recovered then back with the decrease of OLR to 1.5±0.10 kg-MLSS/m^3d at a contact angle of 43.5±5.8°. A similar phenomenon has been noted

by other researchers (Liao et al., 2001; Yang et al., 2018). Soluble microbial products (SMP) followed the same hydrophobic trend, with the highest SMP concentration observed at the lower OLR and vice versa.

The concentration of the MLSS was fairly stable in the different tested OLRs except for the first phase in which the MLSS witnessed a slight fluctuation which could be attributed to the beginning of the organism's adaptation to the new conditions. Regardless of the OLR, MLSS ranges from 16 to 29 g/L in the system. MLSS concentrations ranged between 16 and 20 g/L for OLR of 2.2 kg MLSS/m^3d and between 20 and 24 g/L for OLR of 3.9 kg MLSS/m^3d, and its concentration averaged 26 g/L for OLR of 1.5 kg MLSS/m^3d. Though the increased concentration of mixed liquor suspended solids gives some sign of the fouling tendency, the effect of mixed liquor suspended solids on membrane performance was not evident in this study.

Table 7.2: Surface properties and dewaterability of the mixed liquors particles.

Items	Phase I	Phase II	Phase III
Zeta-potential (mV)	-20.92±0.89	-23.52±1.02	-28.98±3.24
Dewaterability (s)	29.95±1.59	32.58±0.97	37.40±1.56
Contact angle (°)	64.3±3.2	24.6±3.04	43.5±5.8
SMP (mg/L)	25.15±1.90	13.42±1.38	38.64± 5.36
MLSS conc. (g/L)	18.6±1.25	25.6±0.71	25.98±0.23

3.5.3. Surface analysis by XPS

XPS analysis was performed to identify MLSS elemental composition that might interact with the membrane and cause its fouling. Fig. 7. 10 (1 – 3) represents the XPS spectra of the elemental composition of MLSS for the different phases. XPS signals of ~ 532 eV in the O 1s sone, ~ 399 eV in the N 1s zone, and ~ 284 eV in the C 1s area were predominant and were observed by XPS in all three phase samples. Every peak matches a specific chemical bond. The peak at 284 eV was given to C–H, while peaks at around 532 eV and 399 eV were allocated to OH–C/C–O–C and N=C, respectively, which further linked to the protein-like (e.g., C=N bond and C–N bond) and carbs-like (e.g., C–OH bond and C–H bond) substances (Li et al., 2018). Also, other elements like Al (119 eV), P (133 eV), S (163 eV), Na (1071 eV), CL (199 eV), and Ca (347 eV) were detected by this technique but at a low mass concentration. Their mass concentration (%) ranged between 0.38 and 2.61%, while the mass concentration of C, O, and N was in the range of 38.9 – 59.9%, 30.2 – 44.8%, and 1.7 – 11.6%, respectively. However, the N mass concentration was significantly high in the first phase compared to the second and third phases, it reduced by 64.6 % in the second phase and 85.4 % in the third phase. From Figures 7. 10. (1 – 3) below, a decline in the intensity of the vertex corresponding to the ~ 399 eV signal of the N 1s region can be seen, where the concentration of nitrogen appears to decrease as the digestion time increases. This could be attributable to the fact that the concentration of microorganisms increased with increasing digestion time, which led to the consumption

of the available nitrogen. The C1s spectra show the distinct peaks of the hydroxyl groups including C–OH, C–O, and CF_2 (Zhang et al., 2020).

Regarding membrane surface chemistry, Figure 7. 10 (a – d) shows XPS spectra of the new and used membranes. XPS spectroscopy was performed on the used membranes after chemical cleaning and cleaned virgin membranes. XPS analysis of the membranes showed four distinct peaks including fluorine (F 1s) (~ 686 eV), oxygen (O 1s) (~ 530 eV), carbon (C 1s) (~ 284 eV), and nitrogen (N 1s) (~ 398 eV), other elements were also found but at a low concentration. Compared to the new membrane, there is a peak broadening of O 1s in XPS for the used membranes. C 1s core spectra were assigned the characteristic peaks of hydroxyl groups and PVDF, including C–OH, C–O, CH2-CF2, and CF2 (Zhang et al., 2020). Whereas the F 1s peak detected at 686 eV was attributed to the XPS spectrum of PVDF (Meng e al., 2019). Compared to the MLSS result, some elements were only detected in the membranes, which could be assigned to the membrane materials, however, other elements like Al, P, Na, and Ca were detected in both MLSS and used membranes, which may reflect the fouling of the membranes. Furthermore, more elements were detected at a higher OLR (Fig. 7. 10 – c) than at lower OLRs (Fig. 7. 10 – b and d). Also, La was only detected in higher OLR compared to lower OLRs. This result may indicate that the high loading rate increases the tendency of membrane fouling, and the cleaning regime with its different stages is unable to completely remove the fouling materials.

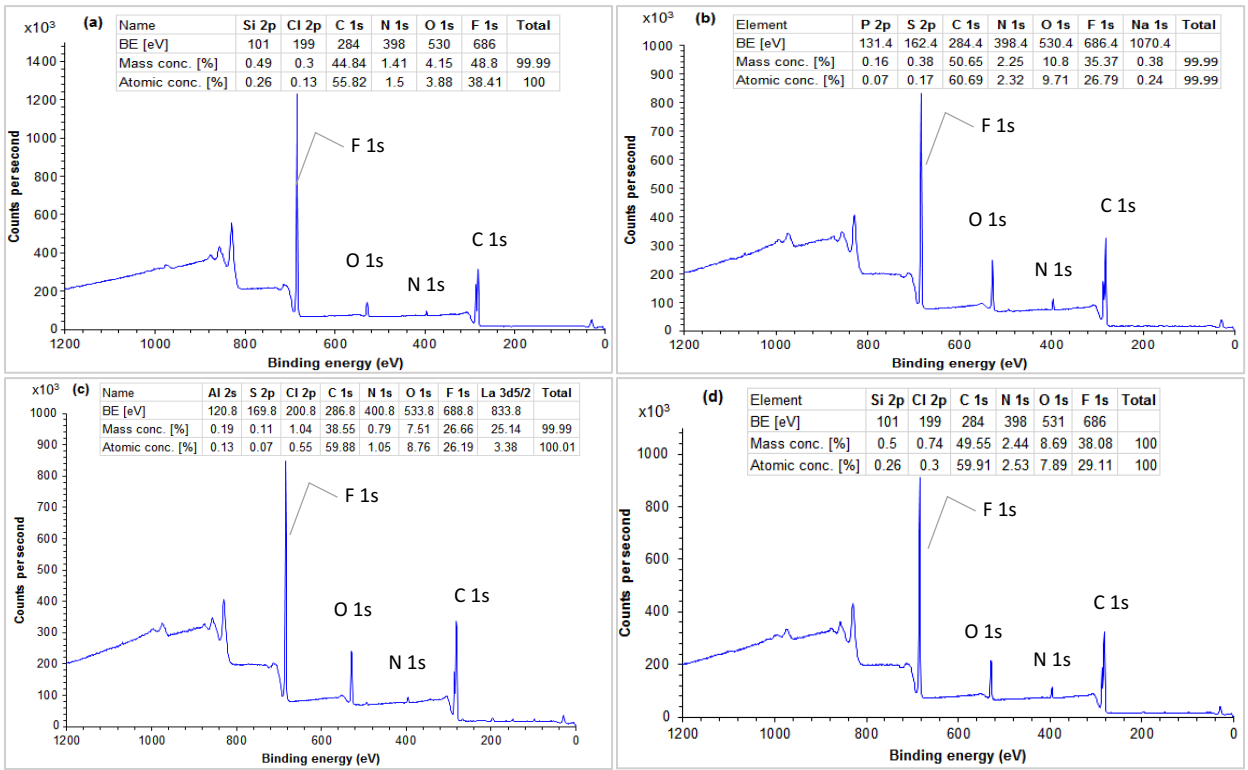

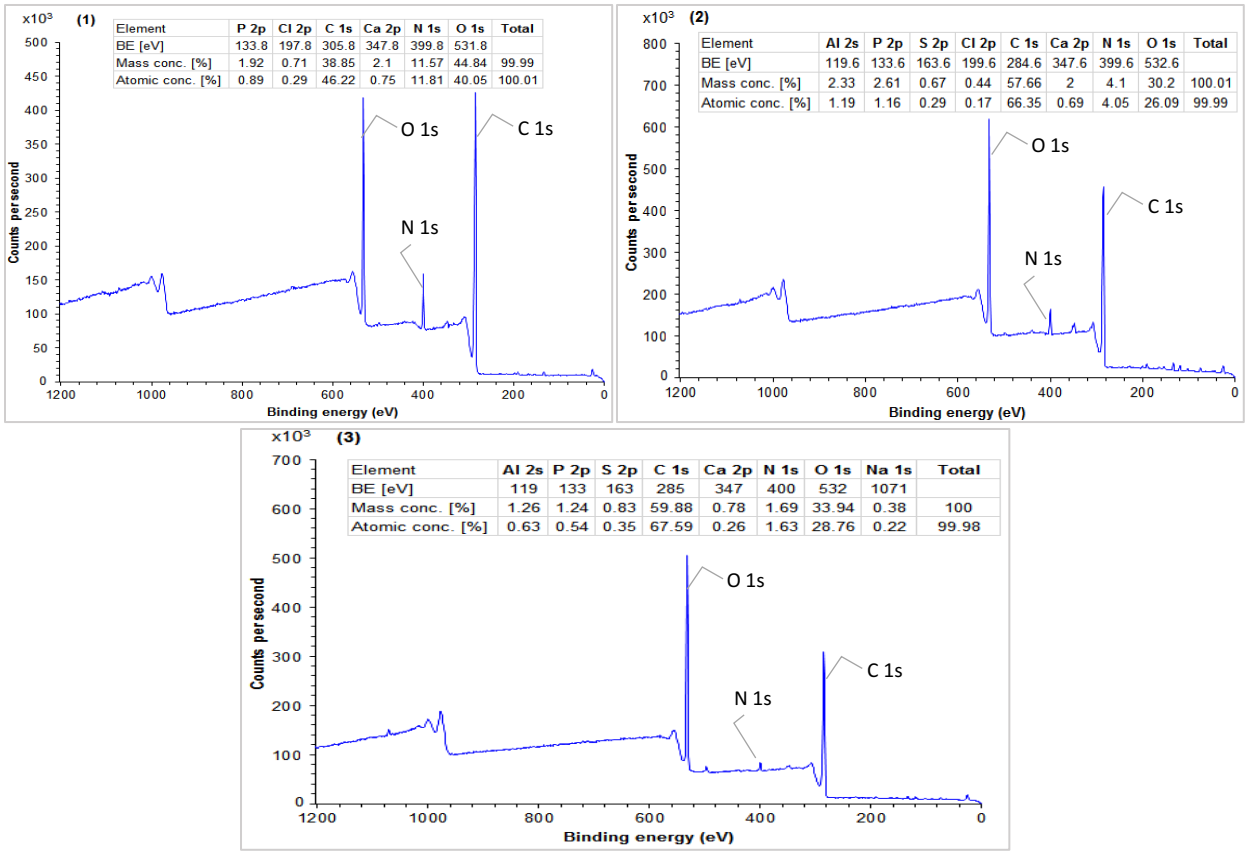

Figure 7.10: XPS spectra of the elemental composition of ((a) new) and used membranes: ((b) phase I), ((c) phase II), ((d) phase III), and MLSS ((1) phase I), ((2) phase II), and ((3) phase III) under various digestion conditions.

4. Conclusion

The goal of this research was to investigate membrane performance and MLSS characteristics when operating at different primary sludge (PS) loading rates. Membrane performance was assessed by observing its flux and corresponding transmembrane pressure as well as changes in its chemical and physical properties resulting from operating conditions using FTIR, SEM, EDX, contact angle, and pore size measurement, while MLSS properties characterized by XPS, zeta potential, and particle size distribution. Results showed that important changes occurred on the membrane morphology and MLSS characteristics under the tested three phases operating environments. From this study, we can conclude that digestion of primary sludge from thermomechanical pulping using SAnMBR does not cause significant membrane fouling, and this was attributed to the nature of the digested materials and the formation of fibrous balls that scour the surface of the membrane and remove the foulants layer. High-resolution SEM images reveal distinct differences in pore morphology between the virgin and used membranes indicating the effect induced by the operating conditions particularly the thermophilic temperature (50±1°C). An increase in temperature (50±1°C) led to an expansion of membrane pores. Gel layer formation was the predominant fouling mechanism. FTIR and XPS results indicate foulants' presence on the surfaces of the used membranes after chemical cleaning, and this implicates that there are chemical foulants that cannot be removed by chemical cleaning.

References

[1] AlMarzooqi, F.A., Bilad, M.R., Mansoor, B., Arafat, H.A., 2016. A comparative study of image analysis and porometry techniques for characterization of porous membranes. J. Mater. Sci. 51, 2017-2032. DOI: 10.1007/s10853-015-9512-0.

[2] Bai, H., Wang, X., Zhou, Y. and Zhang, L., 2012. Preparation and characterization of poly (vinylidene fluoride) composite membranes blended with nano-crystalline cellulose. Prog. Nat. Sci. Materials International, 22, 250-257. https://doi.org/10.1016/j.pnsc.2012.04.011.

[3] Bayr, S., Rintala, J., 2012. Thermophilic anaerobic digestion of pulp and paper mill primary sludge and co-digestion of primary and secondary sludge. Water Res. 46, 4713-4720. https://doi.org/10.1016/j.watres.2012.06.033.

[4] Bokhary, A., Liao, B., Cui, L., Lin, H., 2017. A Review of membrane technology for integrated forest biorefinery. J. Membr. Sci. Res. 3,120-141. https://doi.org/10.22079/JMSR.2016.22839.

[5] Bokhary, A., Maleki, E., Hong, Y., Hai, F.I., Liao, B., 2020. Anaerobic membrane bioreactors: Basic process design and operation. In: Ngo, H., H., Guo, W., Ng, H., Y., Mannina, G., Pandey A. (Eds.), Current Developments in Biotechnology and Bioengineering. Elsevier. pp. 25-54. https://doi.org/10.1016/B978-0-12-819852-0.00002-6.

[6] Bokhary, A., Tikka, A., Leitch, M., Liao, B., 2018. Membrane fouling prevention and control strategies in pulp and paper industry applications: A review. J. Membr. Sci. Res. 4,181-197. https://doi.org/ 10.22079/jmsr.2018.83337.1185.

[7] Dagnew, M., Parker, W., 2020. Impact of AnMBR operating conditions on anaerobic digestion of waste activated sludge. Water Environ. Res. https://doi.org/10.1002/wer.1361.

[8] Dagnew, M., Parker, W., Seto, P., 2012. Anaerobic membrane bioreactors for treating waste activated sludge: Short term membrane fouling characterization and control tests. J. Membr. Sci. 421, 103-110. https://doi.org/10.1016/j.memsci.2012.06.046.

[9] Dang, H.Q., Price, W.E., Nghiem, L.D., 2014. The effects of feed solution temperature on pore size and trace organic contaminant rejection by the nanofiltration membrane NF270. Sep. Purif. Technol. 125, 43-51. https://doi.org/10.1016/j.seppur.2013.12.043.

[10] Ding, Y., Tian, Y., Li, Z., Zuo, W., Zhang, J., 2015. A comprehensive study into fouling properties of extracellular polymeric substance (EPS) extracted from bulk sludge and cake sludge in a mesophilic anaerobic membrane bioreactor. Bioresour. Technol. 192, 105-114. https://doi.org/10.1016/j.biortech.2015.05.067.

[11] Gao, W.J., Lin, H.J., Leung, K.T., Schraft, H., Liao, B.Q., 2011. Structure of cake layer in a submerged anaerobic membrane bioreactor. J. Membr. Sci. 374,110-120. https://doi.org/10.1016/j.memsci.2011.03.019.

[12] Gu, S., He, G., Wu, X., Hu, Z., Wang, L., Xiao, G., Peng, L., 2010. Preparation and characterization of poly (vinylidene fluoride)/sulfonated poly (phthalazinone ether sulfone ketone) blends for proton exchange membrane. J. Appl. Polym. Sci. 116, 852-860. https://doi.org/10.1002/app.31547.

[13] Lin, H., Peng, W., Zhang, M., Chen, J., Hong, H., Zhang, Y., 2013. A review on anaerobic membrane bioreactors: applications, membrane fouling and future perspectives, Desalination. 314, 169-188. https://doi.org/10.1016/j.desal.2013.01.019.

[14] Hu, Y., Wang, X.C., Yu, Z., Ngo, H.H., Sun, Q. and Zhang, Q., 2016. New insight into fouling behavior and foulants accumulation property of cake sludge in a full-scale membrane bioreactor. J. Membr. Sci. 510, 10-17. https://doi.org/10.1016/j.memsci.2016.02.058.

[15] Karlsson, A., Truong, X.B., Gustavsson, J., Svensson, B.H., Nilsson, F., Ejlertsson, J., 2011. Anaerobic treatment of activated sludge from Swedish pulp and paper mills–biogas production potential and limitations. Environ. Technol. 32, 1559-1571. https://doi.org/10.1080/09593330.2010.543932.

[16] Larsson, M., Jansson, M., Grönkvist, S., Alvfors, P., 2015. Techno-economic assessment of anaerobic digestion in a typical Kraft pulp mill to produce biomethane for the road transport sector. J. Clean. Prod. 104, 460-467. https://doi.org/10.1016/j.jclepro.2015.05.054.

[17] Li, X., Mei, Q., Yan, X., Dong, B., Dai, X., Yu, L., Wang, Y., Ding, G., Yu, F., Zhou, J., 2018. Molecular characteristics of the refractory organic matter in the anaerobic and aerobic digestates of sewage sludge. RSC Advances, 8, 33138-33148. DOI: 10.1039/C8RA05009K.

[18] Liao, B.Q., Allen, D.G., Droppo, I.G., Leppard, G.G., Liss, S.N., 2001. Surface properties of sludge and their role in bioflocculation and settleability. Water Res. 35, 339-350. https://doi.org/10.1016/S0043-1354(00)00277-3.

[19] Liao, B.Q., Lin, H.J., Langevin, S.P., Gao, W.J., Leppard, G.G., 2011. Effects of temperature and dissolved oxygen on sludge properties and their role in bioflocculation and settling. Water Res. 45, 509-520. https://doi.org/10.1016/j.watres.2010.09.010.

[20] Lin, H., Liao, B.Q., Chen, J., Gao, W., Wang, L., Wang, F., Lu, X., 2011. New insights into membrane fouling in a submerged anaerobic membrane bioreactor based on characterization of cake sludge and bulk sludge. Bioresour. Technol. 102, 2373-2379. https://doi.org/10.1016/j.biortech.2010.10.103.

[21] Lutze, R., Engelhart, M., 2020. Comparison of CSTR and AnMBR for anaerobic digestion of WAS and lipid-rich flotation sludge from the dairy industry. Water Resour. Ind. 23, 100122. https://doi.org/10.1016/j.wri.2019.100122.

[22] Mahmoud, I., Liao, B., 2017. Effects of sludge concentration and biogas sparging rate on critical flux in a submerged anaerobic membrane bioreactor. J. Water Process. Eng. 20, 51-60. https://doi.org/10.1016/j.jwpe.2017.09.012.

[23] Masselin, I., Chasseray, X., Durand-Bourlier, L., Lainé, J.M., Syzaret, P.Y., Lemordant, D., 2001. Effect of sonication on polymeric membranes. J. Membr. Sci. 181, 213-220. https://doi.org/10.1016/S0376-7388(00)00534-2.

[24] Meng, F., Zhang, S., Oh, Y., Zhou, Z., Shin, H.S., Chae, S.R., 2017. Fouling in membrane bioreactors: an updated review. Water Res. 114, 151-180. https://doi.org/10.1016/j.watres.2017.02.006.

[25] Meng, X., Ji, Y., Yu, G., Zhai, Y., 2019. Preparation and Properties of Polyvinylidene Fluoride Nanocomposited Membranes based on Poly (N-Isopropylacrylamide) Modified Graphene Oxide Nanosheets. Polymers, 11, 473. https://doi.org/10.3390/polym11030473.

[26] Pileggi, V., Parker, W.J., 2017. AnMBR digestion of mixed WRRF sludges: Impact of digester loading and temperature. J. Water Process. Eng. 19, 74-80. https://doi.org/10.1016/j.jwpe.2017.07.011.

[27] Puspitasari, V., Granville, A., Le-Clech, P., Chen, V., 2010. Cleaning and ageing effect of sodium hypochlorite on polyvinylidene fluoride (PVDF) membrane. Sep. Purif. Technol. 72, 301-308. https://doi.org/10.1016/j.seppur.2010.03.001.

[28] Sabouhi, M., Torabian, A., Bozorg, A., Mehrdadi, N., 2020. A novel convenient approach toward the fouling alleviation in membrane bioreactors using the combined methods of oxidation and coagulation. J. Water Process. Eng. 33, 101018. https://doi.org/10.1016/j.jwpe.2019.101018.

[29] Tikka, A., Gao, W. and Liao, B., 2019. Reversibility of membrane performance and structure changes caused by extreme cold water temperature and elevated conditioning water temperature. Water Res. 151, 260-270. https://doi.org/10.1016/j.watres.2018.12.047.

[30] van der Marel, P., Zwijnenburg, A., Kemperman, A., Wessling, M., Temmink, H., van der Meer, W., 2010. Influence of membrane properties on fouling in submerged membrane bioreactors. J. Membr. Sci. 348, 66-74. https://doi.org/10.1016/j.memsci.2009.10.054.

[31] Wijekoon, K.C., Visvanathan, C., Abeynayaka, A., 2011. Effect of organic loading rate on VFA production, organic matter removal and microbial activity of a two-stage thermophilic anaerobic membrane bioreactor. Bioresour. Technol. 102, 5353-5360. https://doi.org/10.1016/j.biortech.2010.12.081.

[32] Yang, L., Ren, Y.X., Chen, N., Cui, S., Wang, X.H., Xiao, Q., 2018. Organic loading rate shock impact on extracellular polymeric substances and physicochemical characteristics of nitrifying sludge treating high-strength ammonia wastewater under unsteady-state conditions. RSC Advances, 8, 41681-41691. DOI: 10.1039/C8RA08357F.

[33] Yu, H., Wang, Z., Wu, Z., Zhu, C., 2016. Enhanced waste activated sludge digestion using a submerged anaerobic dynamic membrane bioreactor: performance, sludge characteristics and microbial community. Sci. Rep. 6, 20111. https://doi.org/10.1038/srep20111.

[34] Zhang, J., Chua, H.C., Zhou, J., Fane, A.G., 2006. Factors affecting the membrane performance in submerged membrane bioreactors. J. Membr. Sci. 284, 54-66. https://doi.org/10.1016/j.memsci.2006.06.022.

[35] Zhang, Y., Wang, Y., Cao, X., Xue, J., Zhang, Q., Tian, J., Li, X., Qiu, X., Pan, B., Gu, A.Z., Zheng, X., 2020. Effect of carboxyl and hydroxyl groups on adsorptive polysaccharide fouling: A comparative study based on PVDF and graphene oxide (GO) modified PVDF surfaces. J. Membr. Sci. 595, 117514. https://doi.org/10.1016/j.memsci.2019.117514.

Chapter VIII

Conclusions and future perspectives

1. Conclusions

In the first project, the extraction potential of various solvents including 1-butanol, toluene, tributyl phosphate (TBP), and n-hexane under a wide range of operating conditions (pH values 4.3, 7, and 9.5; room temperature; 1:1–1:6 solvent:hydrolyzate volume ratios, different min extraction time) was assessed to identify their capacity to extract hemicellulose from the process water of thermomechanical pulp and synthetic hydrolyzate. Among the solvents examined, n-hexane and TBP achieved the highest recovery ratios at the solvent:hydrolyzate volume ratio of 1:3, and the influence of the pH value on the separation of hemicellulose was mainly dependent on the type of solvent. TBP exhibited the highest hemicellulose extraction but was characterized by a lower separation factor, while n-hexane accomplished the uppermost selectivity coefficient.

The results obtained in the second project reveal that the TMP mill primary sludge can be satisfactorily treated with thermophilic AnMBR. Lower OLRs and higher HRTs have been associated with higher biogas production compared to higher OLR and shorter HRT, and OLR of 2.5 kg COD/m^3 d and HRT 8d could consider optimum and can be proposed as design criteria for primary sludge treatment. The degradation efficiency of the sludge biomass decreased with the increase in OLR, while the digestate characteristics fluctuated with the OLR as well. Moreover, the results of this study ascertained that the increased organic loading reduces the performance of the membranes due to the high membrane susceptibility to fouling.

On the other hand, the longer the SRT, the higher is the biogas yield. Also, the mixed liquor suspended solids (MLSS) concentration and solids reduction increased with increasing SRT. The Fourier Transform Infrared (FTIR) and X-ray photoelectron spectroscopy (XPS) results showed that the digestate contained more lignin and cellulose than the other substances, while the nitrogen and carbon concentration decreased with increasing SRT. Membrane performance was contingent on SRT, where the degree of fouling increased with increasing SRT. The mixed liquor suspended solids (MLSS) concentration was the predominant factor affecting membrane performance and was dependent on the applied SRT.

Loose gel layer formation on membrane surfaces was identified as the predominant mechanism of membrane fouling during primary sludge treatment by AnMBR and accounts for most of the overall resistance.

The fouling characterization results indicated that the primary sludge from the thermomechanical pulp pulp did not have a high fouling tendency. Loose gel layer formation on membrane surfaces was identified as the main mechanism of membrane fouling during primary sludge treatment by AnMBR and accounts for

most of the overall resistance. The smaller particle exhibited a higher propensity towards deposition on the membrane surfaces than the large particles. EDX, XPS, and FTIR analysis shows that the foulants deposited on the surface of the membrane have mixed compositions of organic and inorganic materials.

Overall, the primary sludge from pulp and paper mill could be successfully processed by ThSAnMBR for methane production with excellent membrane performance and high processing efficiency.

2. Future perspectives

Although liquid-liquid extraction shows promise in separating hemicellulose and lignin from the process water, many challenges remain and need to be tackled. A solvent with a high capacity for the partitioning of the pulping effluents coupled with high selectivity for the target product over other constituents still calls for research. The present market values of the extractants are very high, and therefore finding affordable solvents, especially for products with a relatively lower market value (lignin/hemicellulose) compared to metal prices, requires further research and development. Also, a move towards green solvents is required because most of the solvents used today are toxic to both humans and the environment.

Anaerobic Membrane Bioreactor (AnMBR) is a comparatively new technology and can be considered long-term solutions for the valorization of pulp and paper mill sludge (PPMS) compared to the currently available conventional processes because it can simultaneously function as a method of waste management and resource recovery. However, its current state requires further retrofitting and development to targeting more efficient yield, reduced production cost, and minimal environmental impacts. All studies on anaerobic digestion of pulp and paper sludge have been at the lab-scale and pilot-scale level and no full-scale application has yet been reported, thus this process needs to be brought up to the commercial level. For the compensation for the nutrient deficiency faced by the mono digestion of primary sludge, it is recommended that co-digestion of pulp and paper plant sludge with other nutrient-rich non-paper mill substrates. Moreover, due to the recalcitrant structure of the primary sludge, a dedicated initial treatment method before the anaerobic digestion may be recommended to enhance further the biogas productivity. Furthermore, anaerobic digestion can be engineered as a biorefinery approach for multiple product generations like methane, carboxylic acids, and volatile fatty acids (VFAs) production. Finally, the use of the membrane with the reactor requires watchfulness (in terms of membrane selection and the use of proper cleaning protocol) because the fouling of the membrane reduces the efficiency of the process performance, causing an increase in the costs of the process operation and maintenance.